

# The genetic basis of sexual antagonism in *Drosophila melanogaster*

*Mark Stephen Hill*

A dissertation submitted in partial fulfillment  
of the requirements for the degree of  
**Doctor of Philosophy**  
of  
**University College London.**

Department of Genetics, Evolution and Environment  
University College London

October 2, 2017

I, Mark Stephen Hill, confirm that the work presented in this thesis is my own. Where information has been derived from other sources, I confirm that this has been indicated in the work.

Signature.....

October 2, 2017

# Thesis abstract

The divergent reproductive roles of males and females generate sexually antagonistic selection, with different trait values favoured in each sex. Responses to these selective pressures are however constrained by the sexes' shared genome, leading to 'sexual antagonism, where, at a given locus, opposing alleles are favoured in males and females. Sexual antagonism is a taxonomically widespread and evolutionarily important phenomenon, but the identity and characteristics of the genetic loci underlying it remain almost entirely unknown. This thesis combines experimentation, bioinformatics and theory to identify, characterise, and explore the evolution of sexually antagonistic loci. In the introduction (chapter 1), I review the literature and integrate underlying theory and key empirical findings. I then identify the first putative antagonistic variants across the *Drosophila melanogaster* genome by comparing the sequences of haplotypes with contrasting sex-specific fitness profiles (chapter 2). I find a substantial excess of candidate SNPs, beyond the null expectation, and show that these SNPs are a non-random subset of the genetic variation in the LH<sub>M</sub> population. In chapter 3, I characterise the functional properties of antagonistic loci using a suite of bioinformatic analyses. Here, a prominent role of gene regulation emerges. I further describe an evolve-and-resequence experiment conducted to investigate the evolution of sexually antagonistic loci under sex-limited selection (chapter 4). Here, I was able to verify a subset of the sexually antagonistic loci identified in chapter 2. In chapter 5, I build a theoretical model to investigate when and where sexually antagonistic alleles invade in gene regulatory cascades. I find sexually antagonistic polymorphism can be displaced to higher levels of the regulatory hierarchy from where it initially arises. In the general discussion (chapter 6), I place these findings into context and provide a perspective on future research prospects.

# Impact statement

The focus of the work detailed here is sexual antagonism, a phenomenon whereby alternative alleles, at a given locus, are favoured in each sex. This is widespread in populations of animals and plants and is known to have important evolutionary consequences. However, until now our understanding of sexual antagonism came mainly from quantitative genetic studies. Thus, we had little understanding of its underlying genetic basis. This was a critical shortcoming as without knowledge of the identity and characteristics of sexually antagonistic loci, we cannot fully understand the general biological processes encapsulated in sexual antagonism nor its evolutionary dynamics. In this thesis I describe the first genome-wide identification of putative sexually antagonistic SNPs in any organism, filling this vital knowledge gap. Through a series of analyses of these loci and by developing new theory related to my primary findings, I have been able to offer new insights into this important evolutionary phenomenon. Within the academic community, the work documented in this thesis has been disseminated at both national (London) and international (Lausanne, Roscoff, Groningen, Michigan) conferences. In terms of dissemination in scientific journals, a paper containing work from this thesis is currently in review, another is in preparation and I anticipate several more to be prepared in the near future.

Beyond the immediate academic benefits of this research in the field of evolutionary biology, there are also broader implications. For example, sexual antagonism generates strong balancing selection and therefore could be very important in human medical contexts. Thus, alleles that increase disease susceptibility in one sex can be favoured by selection if they engender a net fitness benefit in the other sex. This means that sexually antagonistic selection will maintain such alleles within a population for longer than if they had symmet-

ric deleterious consequences in the two sexes. Indeed, a recent empirical study suggests that sexual antagonism is important for the maintenance of polycystic ovary syndrome risk alleles in human populations. In cases such as these, our understanding of how disease risk alleles are maintained will depend critically on our knowledge of sexual antagonism. This can only be gained through detailed study of the genetic basis of sexual antagonism and my thesis provides some of the first insights on this topic. I expect that my findings will be of clear value in the mid- and longer term to clinicians, health professionals and public policy makers.

# Acknowledgements

First and foremost my gratitude extends to my supervisors, Max Reuter and Kevin Fowler, who have provided a constant source of guidance and support throughout my PhD. I would also like to thank Alex Stewart, my collaborator for chapter 5. His mentorship has greatly enriched my overall understanding and appreciation of theoretical approaches in evolutionary biology.

My thanks also go to the members of the Reuter and Pomiankowski laboratories who have provided help, intellectual stimulation, and friendship over the past four years: Sara Fuentes, Filip Ruzicka, Florencia Camus, Lara Meade, James Howie, Sam Finnegan, and Rebecca Finlay.

Thanks to my parents who have helped more than just financially over my extended 'student' period and to Christofer Åkerlund, my partner since the very early stages of the PhD, who never wavers in his support.

Finally, a generic thank you to all I have interacted with over the past four years. It's not always possible to pin down how specific interactions have helped me develop as a scientist and as a person, but their overall effect is well pronounced.

# Contents

<b>1</b>	<b>General Introduction</b>	<b>14</b>
1.1	Sex-specific selection and sexual dimorphism . . . . .	15
1.2	Sexual antagonism . . . . .	16
1.3	Theoretical studies of sexual antagonism . . . . .	18
1.4	Empirical studies of sexual antagonism . . . . .	21
1.5	Evolutionary consequences of sexual antagonism . . . . .	24
1.6	Major outstanding gaps in knowledge . . . . .	26
1.7	Thesis structure . . . . .	29
1.7.1	Chapter 2 . . . . .	30
1.7.2	Chapter 3 . . . . .	31
1.7.3	Chapter 4 . . . . .	31
1.7.4	Chapter 5 . . . . .	32
1.7.5	Chapter 6 . . . . .	33
1.7.6	Appendix A . . . . .	33
1.7.7	Appendix B . . . . .	33
1.7.8	Appendix C . . . . .	34
<b>2</b>	<b>Genome-wide identification of sexually antagonistic loci in</b>	
	<b><i>Drosophila melanogaster</i></b>	<b>35</b>
2.1	Abstract . . . . .	36
2.2	Introduction . . . . .	37
2.3	Materials and Methods . . . . .	42
2.3.1	Hemiclonal haplotypes . . . . .	42
2.3.2	DNA extraction, sequencing and initial processing of haplotype sequencing reads . . . . .	43
2.3.3	Identification of informative and candidate SNPs . . . . .	44

2.3.4	Distribution of candidate loci . . . . .	45
2.3.5	Assessing the contribution of false positives to the number of SA SNPs . . . . .	45
2.3.6	Characterisation of sexually antagonistic loci . . . . .	46
2.3.7	Statistical analysis and plotting . . . . .	47
2.4	Results . . . . .	47
2.4.1	Identification and distribution of sexually antagonistic candidate SNPs . . . . .	47
2.4.2	Characteristics of SA loci . . . . .	49
2.5	Discussion . . . . .	50
2.6	Tables and Figures . . . . .	58

**3 Elucidating the functional properties of sexually antagonistic loci in *Drosophila melanogaster* 63**

3.1	Abstract . . . . .	64
3.2	Introduction . . . . .	65
3.3	Materials and Methods . . . . .	68
3.3.1	Sexually antagonistic SNP data . . . . .	68
3.3.2	Functional roles of SA loci . . . . .	69
3.3.3	Regulatory functions of SA loci . . . . .	69
3.3.4	Sex-biased gene expression . . . . .	70
3.3.5	Expression of genes across tissues and developmental stages . . . . .	71
3.3.6	Statistical analysis and plotting . . . . .	72
3.4	Results . . . . .	72
3.4.1	Functional roles of candidate loci . . . . .	72
3.4.2	Regulatory functions of SA loci . . . . .	73
3.4.3	Sex-biased gene expression . . . . .	74
3.4.4	Expression of genes across tissues and life stages . . . . .	75
3.5	Discussion . . . . .	75
3.6	Tables and Figures . . . . .	84

<b>4</b>	<b>Verifying putative sexually antagonistic loci using experimental sex-limited selection</b>	<b>92</b>
4.1	Abstract . . . . .	93
4.2	Introduction . . . . .	94
4.3	Materials and Methods . . . . .	98
4.3.1	Experimental evolution protocol . . . . .	98
4.3.2	DNA extraction and sequencing of the experimental populations . . . . .	99
4.3.3	Inferring selection coefficients from the evolve-and-resequence data . . . . .	101
4.3.4	Selection on female-beneficial alleles under sex-limited selection . . . . .	102
4.3.5	Selection response index . . . . .	102
4.3.6	Estimating effective population size . . . . .	102
4.3.7	Statistical analysis and plotting . . . . .	103
4.4	Results . . . . .	104
4.4.1	Overall response to sex-limited selection . . . . .	104
4.4.2	Selection on female-beneficial alleles under sex-limited selection . . . . .	105
4.4.3	Properties of validated SA SNPs . . . . .	106
4.5	Discussion . . . . .	106
4.6	Tables and Figures . . . . .	113
<b>5</b>	<b>Sexual antagonism and displaced polymorphism in gene regulatory cascades</b>	<b>118</b>
5.1	Abstract . . . . .	119
5.2	Introduction . . . . .	120
5.3	Methods . . . . .	122
5.3.1	Biophysical model of transcription factor binding . . . . .	122
5.3.2	Gene regulation under weak mutation . . . . .	124
5.3.3	Sexual antagonism and weak mutation . . . . .	125

5.3.4	Evolutionary dynamics of a binding site under SA selection	126
5.3.5	Conditions for polymorphism . . . . .	127
5.3.6	Simulations . . . . .	128
5.4	Results . . . . .	129
5.4.1	Polymorphism at a single binding site . . . . .	130
5.4.2	Polymorphism in a gene regulatory cascade . . . . .	131
5.5	Discussion . . . . .	132
5.6	Tables and Figures . . . . .	138
<b>6</b>	<b>General Discussion</b>	<b>142</b>
6.1	Overview . . . . .	143
6.2	Functional basis of sexual antagonism . . . . .	145
6.3	Evolutionary dynamics of sexual antagonism . . . . .	147
6.4	Avenues for future research . . . . .	151
6.5	Conclusion . . . . .	153
	<b>References</b>	<b>153</b>
	<b>Appendices</b>	<b>171</b>
<b>A</b>	<b>Sexually antagonistic SNPs in the fruitfly reveal persistent constraints on sex-specific development</b>	<b>172</b>
<b>B</b>	<b>Rapid evolution of the inter-sexual genetic correlation for fitness in <i>Drosophila melanogaster</i></b>	<b>200</b>
<b>C</b>	<b>Evolving plastic responses to external and genetic environments</b>	<b>216</b>

# List of Figures

<b>Chapter 1</b>	<b>14</b>
1.1 The intersexual genetic correlation ( $r_{MF}$ ) . . . . .	17
1.2 Diagrammatic representation of sexual antagonism . . . . .	18
<b>Chapter 2</b>	<b>35</b>
2.1 Clustering of antagonistic candidate SNPs along chromosomes .	58
2.2 Relative distribution of antagonistic candidate SNPs across the genome . . . . .	59
2.3 Distributions of antagonistic candidate SNPs across major chromosome arms . . . . .	60
2.4 Comparison of the number of antagonistic candidate SNPs to the null expectation . . . . .	61
2.5 Association of candidate genes with previous analyses of sexual antagonism . . . . .	62
<b>Chapter 3</b>	<b>63</b>
3.1 Enriched Gene Ontology terms of candidate genes . . . . .	89
3.2 Genetic consequences of antagonistic candidate SNPs . . . . .	89
3.3 Expression bias of non-candidate and candidate genes . . . . .	90
3.4 Tissue specificity index of non-candidate and candidate genes . .	90
3.5 Life stage specificity index of non-candidate and candidate genes	91
3.6 Expression of non-candidate and candidate genes across life stages	91
<b>Chapter 4</b>	<b>92</b>
4.1 Experimental design used to restrict selection to a single sex . .	113

4.2	Site response index . . . . .	114
4.3	Selection on autosomal female-beneficial variants under sex-limited selection . . . . .	115
4.4	Direction of antagonistic response as a function of the site response index . . . . .	116
4.5	Antagonistic axis of allele frequency change . . . . .	117
<b>Chapter 5</b>		<b>118</b>
5.1	Biophysical model of transcription factor binding . . . . .	138
5.2	When SA polymorphism arises at a binding site . . . . .	139
5.3	Pairwise mutation-selection plot for an evolving binding site . .	140
5.4	Antagonistic polymorphism across a regulatory network . . . . .	141
5.5	General displacement of polymorphism over time . . . . .	141

# List of Tables

<b>Chapter 3</b>	<b>63</b>
3.1 Results from GO cluster analysis. Shown are top five annotation clusters. . . . .	84
3.2 Frequency of different variant consequences for all SNPs covered in the haplotype sequencing. . . . .	84
3.3 Enriched motifs upstream of candidate genes . . . . .	84
3.4 Enriched motifs in sequences flanking (+/- 20bp) candidate SNPs.	88

## Chapter 1

# General Introduction

## 1.1 Sex-specific selection and sexual dimorphism

Across the majority of sexual species, males and females exhibit fundamentally different gametic investments, a phenomenon known as anisogamy. Females generally invest in few, large, and energetically expensive gametes, while males produce many smaller, cheaper gametes. This asymmetry means that male and female fitness is necessarily maximised through different life history strategies (Trivers 1972). While the manifestation of these contrasting selection pressures have long been informally documented, the first empirical work to explicitly illustrate these sex-specific roles was conducted by Bateman (1948). This landmark study measured reproductive success of both male and female *Drosophila melanogaster* and uncovered three important distinctions: (i) that male reproductive success is more variable than female reproductive success, (ii) that female reproductive success was not limited by the ability to attract a mate (unlike male reproductive success), and (iii) that male reproductive success increased with successive matings, whereas female reproductive success did not. Overall, these early findings suggested that female fitness is primarily limited by gamete production, while male fitness is mainly limited by the ability to acquire matings.

These contrasting sex roles mean that males and females will often be subject to divergent selection pressures on homologous traits. For example, Long and Rice (2007) correlated adult locomotory activity and fitness in fruitflies and found strong and opposing selection gradients in each sex. Specifically, in males they found that as locomotory activity increased, fitness also increased whereas the opposite trend was found in females. Similar findings have been reported for other traits in different species, including bill colour in zebra finches (*Taeniopygia guttata*, Price and Burley 1993) and horn structure in Soay sheep (*Ovis aries*, Robinson et al. 2006).

Responses to these divergent selection pressures move males and females closer towards their respective phenotypic optima. At the same time, they re-

sult in greater phenotypic differences between the sexes, i.e., increased sexual dimorphism (SD). SD occurs across taxa (Cox and Calsbeek 2009) and covers a range of scales, from conspicuous differences in morphology and colouration to subtle variation in patterns of gene expression. For example, sexual dimorphism in body size is broadly observed across taxa (Cox and Calsbeek 2009). In peafowl, male peacocks are brightly coloured and have enlarged tail feathers to attract mates. In contrast, peahens do not have enlarged tail feathers and have much duller plumage. Patterns of gene expression also typically vary between males and females, indeed a recent study in humans suggests that up to 60% of autosomal genes are sexually dimorphic in their expression patterns (Chen et al. 2016).

## 1.2 Sexual antagonism

The incidence of SD across such a wide and diverse range of taxa might suggest that responding to divergent selection pressures and evolving towards sex-specific phenotypic optima is straightforward. However, efficiently responding to selection and actually attaining these divergent optima is complicated by the largely shared genome of males and females. Thus, many homologous traits have high and positive intersexual genetic correlations ( $r_{mf} \approx 1$ , see Figure 1.1). This shared genetic architecture means that if selection on a homologous trait in males and females is divergent, one sex moving closer towards an optimal trait value will result in the other sex being displaced from its optimal value (Lande 1980). This is visualised in Figure 1.2, which shows a population with a monomorphic trait distribution where males and females express similar trait values on average. The sexes are, however, under opposing selection pressures (as shown by the overlaid male and female fitness functions), with smaller trait values favoured in males and larger ones in females. Assuming a strongly positive genetic correlation between male and female traits ( $r_{mf} \approx 1$ ) mutant alleles will have essentially identical effects in both sexes, and either increase or decrease the trait value in both males and females. Due to the opposing

slopes of the fitness functions, mutations will therefore also have opposing fitness consequences on males and females and be ‘sexually antagonistic’. Thus, alleles that decrease the trait value will be favoured in males but detrimental in females, and alleles that increase the trait value will be favoured in females but detrimental in males. The sexual antagonism of alleles can ultimately prevent either sex from reaching their respective phenotypic optima (Rice 1984; Bonduriansky and Chenoweth 2009; Cox and Calsbeek 2009; Pennell and Morrow 2013).

The intersexual genetic correlation ( $r_{MF}$ ) estimates the similarity of the additive effects of alleles in males and females. Thus, an  $r_{MF} \approx 1$  suggests that allelic effects are almost identical in each sex and that the genetic architecture of the trait in question is equivalent in males and females. Overall,  $r_{MF}$  is typically large and positive (Poissant et al. 2010), reflecting the largely shared genomes of males and females.

$r_{MF}$  is calculated as the ratio of additive genetic covariance between the sexes ( $COV_{mf}$ ) to the geometric average of additive genetic variances in males and females ( $\sigma_{a,m}^2$  and  $\sigma_{a,f}^2$ ),

$$r_{MF} = \frac{COV_{mf}}{\sqrt{\sigma_{a,m}^2} \sqrt{\sigma_{a,f}^2}}.$$

One way of documenting ongoing sexual antagonism is to show a negative  $r_{MF}$  for fitness. This would suggest that the average additive effects of alleles on fitness in a population are sexually antagonistic, with alleles that increase fitness in one sex, decreasing it in the other. Indeed, this way of inferring sexual antagonism has been used in many studies to date (e.g., Chippindale et al. 2001; Delcourt et al. 2009; Innocenti and Morrow 2010; Collet et al. 2016).

**Figure 1.1:** The intersexual genetic correlation ( $r_{MF}$ )

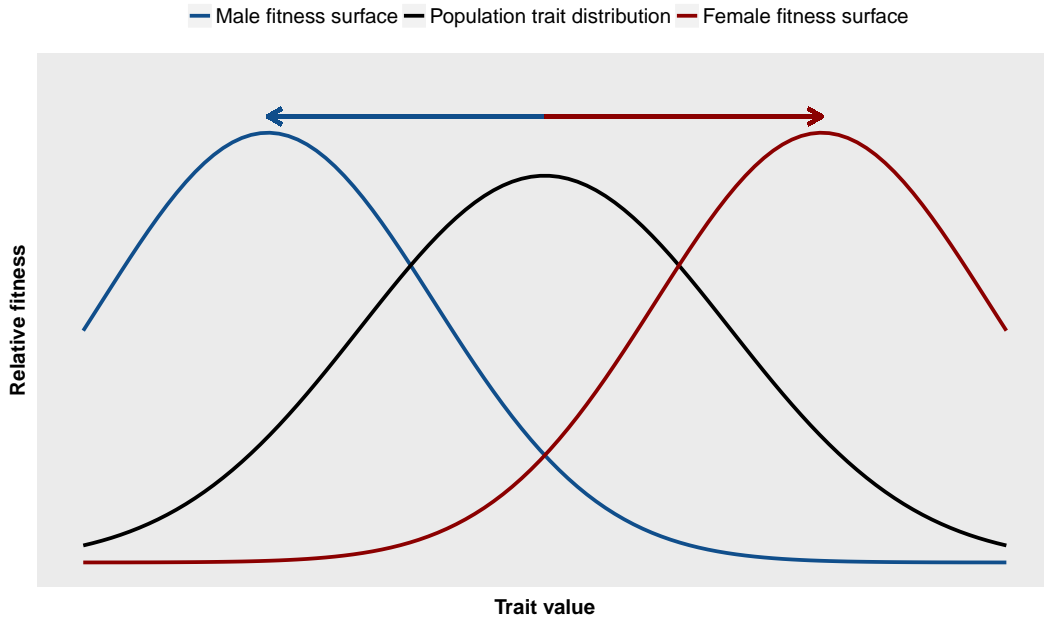


**Figure 1.2: Diagrammatic representation of sexual antagonism.** Shown is a hypothetical trait distribution (black) with sex-specific fitness functions for males (blue) and females (red) respectively. Coloured arrows indicate the displacement of males and females within the population from their respective fitness optima. This is the case of ongoing sexual antagonism, where both males and females are constrained from attaining sex-specific phenotypic optima by shared genetic architecture. Figure adapted from Cox and Calsbeek (2009).

### 1.3 Theoretical studies of sexual antagonism

A body of theoretical work has examined the conditions necessary for the invasion and maintenance of SA alleles. At a basic level, an autosomal SA variant is expected to invade if the benefit it confers to one sex (S) is greater than the cost it imposes on the other (T):

$$S > T,$$

i.e., when there is a net positive fitness effect when summed across the sexes. If that variant is to be maintained by selection, the benefit it confers to one sex must not be so great as to drive one allele to fixation (Gavrilets and Rice

2006), or

$$T > \frac{S}{1 + 2S}.$$

Building on these simple inequalities, a body of theory has explored the factors that may influence the invasion and maintenance of SA alleles. For example, initial single locus models suggested that linkage with major sex chromosomes (X or Z) is an important consideration. Specifically, Rice (1984) suggested that conditions for invasion were less stringent for the X chromosome than for autosomes. This is because X-linked alleles reside in females for 2/3 of the time as opposed to for 1/3 of the time in males. Thus X-linked, female-beneficial, dominant alleles can increase in frequency even when they are more costly to males than they are beneficial to females. Likewise, X-linked, recessive male-beneficial alleles are shielded from selection in females but expressed in hemizygous males, meaning they can increase in frequency even when more costly to females than beneficial to males. These considerations lead to the prediction that the X chromosome should be a hotspot for the accumulation of SA alleles. However, this prediction relies critically on the assumption of equal dominance in the two sexes (Fry 2010). When this assumption is relaxed then autosomes are more permissive of invasion than are X/Z chromosomes.

Other, more recent, models have gone on to examine the consequences of factors such as epistasis (Arnqvist et al. 2014), linkage disequilibrium (Patten et al. 2010), sex-specific recombination rate (Wyman and Wyman 2013), and genetic drift (Mullon et al. 2012; Connallon and Clark 2012) on the invasion and maintenance of SA alleles. For example, Patten et al. (2010) showed that linked loci support stable antagonistic polymorphism over a greater range of parameter space than a single isolated locus. Moreover, linkage disequilibrium that builds up between any two antagonistic loci generates excess fitness variance.

While sexually antagonistic selection favours the invasion of antagonistic alleles, we also expect selection for mechanisms that decouple intersexual ge-

netic correlations and reduce the deleterious fitness effects of SA alleles when residing in the sex they harm. The ubiquity of SD suggests that it is possible to resolve sexual antagonism and for the sexes to approach or reach their respective phenotypic optima, but currently we have a poor understanding of how this occurs and over what timescale. One mechanism that could resolve sexual antagonism and that has received some theoretical attention is gene duplication followed by sex-specific regulation of the paralogues (Proulx and Phillips 2006; Connallon and Clark 2011). If alternative protein isoforms are favoured in males and females, a gene duplication event would allow the paralogues to evolve independently towards male and female specific genes. If these are later coupled to sex-specific regulators, such that the male beneficial protein isoforms are expressed only in males and female beneficial isoforms in females, then conflict at this locus could be effectively resolved. However, this is a complex multi-step process and theoretical work has shown that conditions favouring the invasion and maintenance of gene duplicates under sexual antagonism are highly sensitive to a number of factors, including dominance relationships of alleles and ancestral levels of polymorphism (Connallon and Clark 2011).

Similarly, sex-specific splicing of antagonistic genes would allow for the uncoupling of male and female phenotypes (Pennell and Morrow 2013). As with the case of gene duplicates though, unless a SA gene already has the ability to respond to a sex signal the evolution of both a novel splice site as well as regulatory sequences that can respond to a sex signal is likely very slow (Stewart et al. 2010). Other mechanisms of resolution have also been suggested, for example, genomic imprinting (Day and Bonduriansky 2004), and sex-dependent dominance of antagonistic alleles (Kidwell et al. 1977; Barson et al. 2015). Overall, our understanding of the dynamics of sexual antagonism remains in its infancy and requires further empirical and theoretical attention.

## 1.4 Empirical studies of sexual antagonism

Empirical evidence for the existence of SA alleles only started to accumulate several decades after the initial theoretical studies. The first of a series of early landmark studies subjected an autosomal eye-colour variant in *D. melanogaster* to opposing sex-specific selection (Rice 1992). Each generation, females carrying the variant were selected, while males carrying the variant were discarded. Accordingly, the region harbouring these alleles effectively acted as a novel sex-determining locus. If SA alleles were segregating in the population, one would expect positive linkage disequilibrium to build up between the 'female-determining' allele at the eye-colour locus and nearby female-beneficial/male-detrimental (FBMD) alleles. To demonstrate this, after 29 generations of selection Rice (1992) expressed these female-determining loci in males and measured the change in fitness. Consistent with the accumulation of FBMD alleles over the course of the experiment, males expressing the evolved region had significantly reduced fitness, although the expected mirrored increase in female fitness was not statistically significant. While overall this constitutes strong evidence for the accumulation of SA alleles, the asymmetry suggests that the variation that did accumulate caused a much stronger fitness disadvantage to males than a fitness benefit to females.

A series of subsequent studies made use of hemiclonal analysis. This is a system developed for *D. melanogaster* which enables one to randomly sample genomes from a population and express them in a random genetic background, generating many individuals with the same haplotype. More specifically, male flies from the focal population are crossed with a so called 'clone-generator' (CG) female. CG females contain two linked X-chromosomes, a set of marked translocated autosomes (II & III) and a Y chromosome (in *Drosophila* sex is determined by the X:autosome ratio rather than the presence of a Y chromosome). This system effectively forces male transmission of the X chromosome to male offspring (the opposite of the natural case). Thus, F1 males will contain a haploid genome derived from the focal population and a haploid genome

derived from the CG female. Taking a single F1 male from this initial cross and subsequently backcrossing it with multiple CG females amplifies the haploid genome sampled from the focal population. These haploid genomes can then be maintained in males over long periods owing to a lack of male recombination in *Drosophila*. From here it is possible to express the focal genome in either males or females through other crosses. For full details of the system see Abbott and Morrow (2011).

Using this methodology, Rice (1998) forced male-limited transmission of a sampled haploid genome for 41 generations. As expected, males with the evolved haploid genome had higher fitness than control males. Again, however, the effect in females was not so clear, with no significant effects other than retarded development observed. A more recent study replicated this experiment on a larger scale with additional measures of female fitness and confirmed the earlier finding of increased male fitness. Crucially however, they also observed the expected reduction in female fitness (Prasad et al. 2007).

As well as facilitating experiments where a single haploid genome is transmitted through a single sex for several generations, hemiclonal analysis also makes it possible to take a snapshot of standing genetic variation within a population at a single time-point and to evaluate the fitness effects of each sampled genome in males and females. Chippindale et al. (2001) took this approach to sample and characterise 40 haploid genomes. They found significant variation in both male and female fitness, as well as a significant negative genetic correlation  $r_{mf}$  for adult fitness. Thus, on average, genomes with high fitness in one sex had low fitness in the other, the hallmark of sexual antagonism.

Collectively the results of these early studies suggest that there is substantial segregating SA variation in the LH<sub>M</sub> laboratory population of *D. melanogaster*. It could, however, be argued that these findings in a laboratory adapted population are not representative of other populations and species, particularly in the wild. This is because the relatively constant environmental conditions experienced in the laboratory will tend to reduce total fitness vari-

ation relative to wild populations where environmental conditions are much more variable. The consequence of reduced total fitness variance is that we likely overestimate the contribution of SA alleles to total fitness variation.

Nevertheless, to date an abundance of studies of both laboratory and wild populations has documented sexual antagonism across a diversity of taxa including: mammals (Foerster et al. 2007; Mainguy et al. 2009; Mokkonen et al. 2011), birds (Tarka et al. 2014), reptiles (Svensson et al. 2009), insects (Rice 1992; 1998; Berger et al. 2014), fish (Roberts et al. 2009; Barson et al. 2015), and plants (Delph et al. 2011). Overall, studies that document sexual antagonism fall in to two major categories, (i) those that show global antagonistic fitness effects, and (ii) those that identify specific SA traits. A consequence of this is that we still have a rather limited view of the types of traits that contribute towards sexual antagonism. The studies that show global effects do not capture the action of individual traits, only their collective impact. In contrast, trait-focused approaches can only be informative about the specific trait measured, thus their representation is biased by ease of study. Despite these shortcomings the number of studies that identify specific SA traits is steadily increasing with examples including morphology (Abbott et al. 2010), immune response (Svensson et al. 2009), colouration (Roberts et al. 2009), and locomotory activity (Long and Rice 2007), to name but a few (see Cox and Calsbeek (2009) for review). A classic example of a SA trait is testosterone production in bank voles (*Myodes glareolus*). In males increased testosterone is associated with increased mating rates but in females higher levels of testosterone decrease the number of mating partners (Mokkonen et al. 2011). Mokkonen et al. (2011) also showed that mating rates were positively correlated with fitness in both sexes, conclusively documenting testosterone production as a SA trait in this species.

## 1.5 Evolutionary consequences of sexual antagonism

It is clear from a wealth of empirical studies that many populations across a broad range of species harbour substantial SA variation. Accordingly, sexual antagonism can be considered to reflect a major constraint to sex-specific adaptation that acts as a significant source of maladaptation, or ‘gender load’. Indeed, harbouring SA genetic variation is expected to have extensive evolutionary consequences.

Fundamentally, sexual antagonism generates strong balancing selection where male- and female-beneficial alleles can be maintained at intermediate frequencies. As a consequence, it is a mechanism that can maintain not only genetic variation for specific traits but also for fitness itself. This is somewhat paradoxical as we expect directional selection to remove additive variation for fitness within populations. In line with widespread sexual antagonism, accumulating evidence shows that substantial amounts of genetic variation for fitness remains in natural populations (Hill and Zhang 2009). Historically, mutation-selection balance was invoked to explain this apparent paradox, but theoretical predictions of equilibrium fitness variance under mutation-selection balance were much lower than observed (Turelli and Barton 2004). In contrast, recent theoretical work found that a significant amount of fitness variance at equilibrium could be maintained by sexual antagonism (Patten et al. 2010).

This balancing selection generated by sexual antagonism could also be important in medical contexts (Gilks et al. 2014; Mokkonen and Crespi 2015). Thus, alleles that increase disease susceptibility in one sex can be favoured by selection if they engender a net fitness benefit in the other sex (note that the favoured sex may also experience increased disease risk, as long as this is compensated by a larger, pleiotropic beneficial effect). Antagonistic selection will maintain such alleles within a population for longer than if they had symmetric deleterious consequences. To date the idea that sex-specific selection and sexual antagonism are important in determining the evolutionary dynam-

ics of disease-causing variants is understudied, although theory predicts that among disease-causing alleles, those under sex-specific or sexually antagonistic selection should be overrepresented (Morrow and Connallon 2013). In addition, a recent empirical study found that sexual antagonism may contribute to the observed geographic patterns in risk allele frequencies for polycystic ovary syndrome in human populations (Casarini and Brigante 2014). Unfortunately, measuring the fitness consequences of individual alleles in contemporary human populations is almost impossible. That said, we may be able to infer their effects from the ever increasing amount of available population genomic data.

Sexual antagonism also has potentially broader evolutionary consequences, both as a constraining or driving force of adaptive evolution. For example, 'good gene' benefits, often invoked to explain the evolution of female preference for honest signals of male quality, may be eroded by sexual antagonism (Pischedda et al. 2006). This is because, under sexual antagonism, the fittest males will sire low-fitness daughters. This is compounded further if much of the fitness variation is X-linked and therefore cannot be transmitted from father to son at all. In this situation, females will accrue no genetic benefits from choosing high-quality mates through sons, while suffering a genetic cost through low-fitness daughters. Indeed, empirical work in *D. melanogaster* has shown that not only can sexual antagonism reduce the benefits of sexual selection but it can in fact completely reverse them (Pischedda et al. 2006).

There are a number of other potential consequences of sexual antagonism that have been suggested in the literature, but many of these currently lack sufficient theoretical and empirical exploration. These include: the acceleration of population extinction through the imposed gender-load (Kokko and Brooks 2003) and the acceleration of speciation owing to coevolution between SA and sex-limited genes (Rice and Chippindale 2002). In addition, it has been suggested that sexual antagonism can open up of new areas of a fitness landscape, through the gender-load pulling a population to the bottom of a fitness valley and into the basin of attraction of new fitness peaks (Lande and

Kirkpatrick 1988; Rowe and Day 2006).

## 1.6 Major outstanding gaps in knowledge

The preceding sections have laid out the wealth of studies that has now established sexual antagonism as a taxonomically ubiquitous and evolutionarily important phenomenon, but major knowledge gaps remain. Notably, we still have little understanding of the biological mechanisms underlying this conflict and virtually no empirical data on the identity, characteristics, and evolutionary dynamics of antagonistic alleles. This paucity of information is a major constraint to our understanding of the limits on the evolution of sexual dimorphism and sex-specific adaptation.

One major outstanding question regards the identity of SA loci. Establishing the identity of SA loci on a large scale is the first step towards understanding the fundamental properties of these loci. Indeed, without this knowledge we will be unable to fully understand either the general biological processes encapsulated in sexual antagonism, or the evolutionary dynamics of SA variation. To date, studies which identify even a single antagonistic locus remain exceptionally rare, with only a few documented examples to date. One such study uncovered the genetic basis of a pigmentation trait in Lake Malawi Cichlids (Roberts et al. 2009). In this system, male colouration has been under strong sexual selection owing to intense competition for females, resulting in brightly coloured and conspicuous males. In comparison, females are usually drab and brown in colour. However, a variant phenotype characterised by black blotches against an orange background and known as the orange-blotch (OB) phenotype is known to segregate. The OB colour pattern provides camouflage benefits to females against the lake bed, but disrupts male nuptial pigmentation patterns, resulting in decreased male fitness. Thus, this can be considered a sexually antagonistic trait. Roberts et al. (2009) investigated the genetic basis of the OB phenotype and found that it is due to a cis-regulatory mutation in the *pax7* gene. Interestingly, this gene was found

to be in tight linkage with a dominant female-determining locus. Accordingly, the frequency of the OB phenotype is much higher in females than males and conflict is predominantly resolved at this locus.

Another good example of a SA locus comes from *D. melanogaster*. Around the middle of the 20th century, DDT (dichlorodiphenyltrichloroethane) was a widely used agricultural pest control agent. This resulted in the rapid evolution of an insecticide resistance allele known as DDT-R. Resistance is the result of a single transposable element insertion in the promoter region of the *Cyp6g1* gene (Daborn et al. 2002). In the presence of DDT, the DDT-R allele provides substantial fitness benefits to both sexes. Interestingly however, even in the absence of DDT, this allele increases female fecundity and offspring survival. In contrast, recent work has documented deleterious fitness effects in males from the Canton-S (CS) *D. melanogaster* laboratory strain when not exposed to pesticide. Smith et al. (2011) found that CS males which carried an introgressed DDT-R allele achieved only 22% of matings when in competition with wildtype CS males. The authors also note that DDT-R-carrying CS males were smaller than their non-resistant counterparts. Given that male size negatively correlates with mating success in *D. melanogaster* (Partridge and Farquhar 1983), it is possible that male size is the driving mechanism of DDT-R's male-deleterious effect. Overall, this means that in the absence of the selective pressure imparted by the now widely disused pesticide, this region acts as a sexually antagonistic locus.

While collectively these and a few other studies (e.g., Barson et al. 2015) have identified a small number of individual SA loci in disparate taxa, they are of limited use for elucidating the general biological properties of antagonistic loci. Thus, studies that identify antagonistic loci on a genome-wide scale are essential. To this end, one previous transcriptomic study has associated antagonistic fitness effects with patterns of gene expression in *D. melanogaster* (Innocenti and Morrow 2010). This study used hemiclinal analysis of fitness, as described earlier, to extract and measure male and female fitness of 100

genomic haplotypes. Consistent with previous analyses of the same laboratory population (Chippindale et al. 2001) they found a significant negative  $r_{mf}$  for fitness. Building on their quantitative analysis of fitness, the authors took ten of their haplotypes with the most extreme sex-specific fitness effects (five male-beneficial / female-detrimental and five female-beneficial / male detrimental) as well as 5 with intermediate fitness profiles (haplotypes with equivalent fitness when expressed in either sex) and performed a microarray gene expression analysis. Combining data from the fitness assays with the gene expression analysis, they then identified transcripts with sexually antagonistic expression patterns. This was achieved by fitting a regression model to examine gene expression variation as a function of the interaction between sex and fitness. A significant interaction term for a given transcript would indicate a different relationship between expression and fitness in each sex. Using this methodology, the authors identified 1,478 transcripts with a significant sex-by-fitness interaction term, corresponding to 1,292 putative SA genes. This was the first study to provide a genome-wide list of candidate SA loci in any organism. However, this approach can only describe sexual antagonism in terms of gene expression and thus may not actually identify the causal SA loci. This is because antagonistic patterns of gene expression may just reflect the action of upstream cis- and distant trans-regulatory variants that are the true causal loci.

Owing to the paucity of information on the identity of SA loci, we also have little idea of the biological roles and general functional properties of loci underlying sexual antagonism. One study which may hint towards some of the functional roles of SA loci documents the apparent resolution of sexual antagonism in a replicate of the LH<sub>M</sub> *D. melanogaster* population, discussed earlier. In this study, the authors compared two replicate populations, one which had a significant negative  $r_{mf}$  for fitness and the other where  $r_{mf}$  was not significantly different from zero (thus antagonism is apparently resolved) (Collet et al. 2016). They identified regions of extreme allele frequency differentia-

tion between these two populations and were able to associate these regions with the previously described transcriptomic analyses of sexual antagonism. The loci associated with the resolution of antagonism were predominately involved in development, pointing towards sexual antagonism being rooted in anatomical differences between the sexes. Interestingly they also found several sex-determination and -differentiation genes among the candidates. However, while these are interesting hints, care should be taken when interpreting these results in the context of the genetic basis of sexual antagonism. This is because the association is an indirect one. For example, changes in allele frequency are not necessarily the cause of resolution but may occur in response to a resolution event. If the latter is predominantly true these loci may not accurately reflect properties of causal antagonistic loci.

As well as the lack of information on the identity and characteristics of SA loci, there is an incongruence between theoretical expectations and the empirically observed abundance of SA fitness variation. Classic population genetic models predict that the conditions which favour the invasion of SA alleles are somewhat restrictive. This is particularly the case under weak selection, where — without additional mechanisms such as linkage between loci (Patten et al. 2010) or dominance reversal (Fry 2010; Connallon and Clark 2011) — SA alleles are not expected to invade at all. Given that previous models have effectively dealt with the major drivers of frequency change, this discrepancy suggests that current theory fails to adequately capture the biological properties of antagonistic loci. To address this, more biologically informed models built on realistic fitness landscapes are needed. This will allow a more detailed investigation, offering more specific predications about when and where we would expect SA to invade and be maintained.

## 1.7 Thesis structure

In light of the major shortcomings detailed above, this thesis focuses on first identifying SA loci across the genome of *D. melanogaster*. Following on from

the initial identification, I conduct a series of analyses to characterise and verify these loci. Motivated by some of my findings and previous work by others, I go on to generate a population genetic model to explore the invasion of SA alleles in gene regulatory networks. Finally, I discuss all of my findings in context and provide a look to future studies of sexual antagonism. Below I summarise, in more detail, each of the thesis chapters.

This PhD project was funded by a UCL IMPACT PhD studentship and was performed under the supervision of Dr Max Reuter and Prof. Kevin Fowler. All experiments and analyses were performed by myself, with help from members of the Reuter Laboratory when needed. Chapter 5 was a collaboration between Dr Alex Stewart, Dr Max Reuter, and myself.

### **1.7.1 Chapter 2**

In this first empirical chapter of the thesis I focus on identifying putative antagonistic SNPs across the *D. melanogaster* genome. To do this I sequenced 9 of the 10 most antagonistic haplotypes first isolated in Innocenti and Morrow (2010). This allowed me to define the genetic sequences that come from each haplotype and are thus associated with the sex-specific fitness profiles of interest. I then compared the sequences of female-beneficial / male-detrimental (FBMD) and male-beneficial / female-beneficial (MBFD) haplotypes. Antagonistic loci were identified as those where each haplotype within each fitness class was fixed for the same allele while being different to all lines comprising the alternative fitness class. Using this approach I identified 6,275 antagonistic SNP loci across the *D. melanogaster* genome. I found that my approach identified many more antagonistic candidate SNPs than expected by chance. Further, these SNPs were enriched in genic regions and non-randomly distributed across the genome. Interestingly, and in contrast to some early theoretical work, I found antagonistic loci to be significantly underrepresented on the X chromosome. Finally, the loci that I identified significantly overlapped with those identified in other, previous, analyses of sexual antagonism.

*Material from this chapter was included in a manuscript, submitted to Nature Ecology and Evolution, with me as first author—see Appendix A. All of the analyses presented in this chapter were included in the manuscript.*

### **1.7.2 Chapter 3**

Here, I characterise the functional properties and elucidate the biological roles of the SA loci identified in chapter 2. For this, I combined my candidates with a number of publicly available datasets that detail, for example, the location of annotated regulatory elements in the *D. melanogaster* genome, or the expression of genes throughout development. My results suggest that sexual antagonism is rooted in developmental regulation and associated with a number of specific cis-regulatory elements. Interestingly, I found multiple associations with sexual differentiation, the most notable being that a number of SNPs mapped to *fruitless*, a gene at the core of sex-specific development. I found little evidence to support pleiotropy as an important mechanism for maintaining SA variation. I did, however, find evidence that SA genes are expressed throughout development.

*A subset of the analyses presented in this chapter were included in a manuscript, submitted to Nature Ecology and Evolution, with me as first author—see Appendix A.*

### **1.7.3 Chapter 4**

In this chapter, I sought to validate the candidate antagonistic SNPs identified in chapter 2 by performing an evolve-and-resequence experiment under sex-limited selection. I made use of a modified middle-class-neighbourhood design (Moorad and Hall 2009), which effectively eliminates selection in a population by constraining reproductive output of all individuals to the same number of offspring. I applied this design asymmetrically (to only a single sex) and created two replicate populations where only males were subject to selection (ML selection) and two where only females were under selection (FL

selection) (Morrow et al. 2008). I evolved these populations over three generations and sequenced them at both the start and the end of the experiment. From the allele frequency data I estimated selection coefficients for alleles at the candidate loci and a set of background non-candidate loci identified in chapter 2. Overall, I found that SA alleles responded as expected under FL selection, with putative female beneficial alleles increasing in frequency over the course of selection. However, the results were less conclusive under ML selection. Here, non-candidate loci responded more to selection than candidates. Moreover, female-beneficial alleles also increased in frequency under ML selection (contrary to expectations), although to a lesser extent than when under FL selection. Based on the data that I gathered, I also was able to define a set of highly supported candidate SNPs with selection coefficients that fell in the extreme of the distribution of antagonistic responses and that showed frequency changes in the expected direction under sex-limited selection.

#### **1.7.4 Chapter 5**

Chapter 5 contains a theoretical examination of the impact of sexually antagonistic selection on gene regulatory networks. Along with my collaborators Dr Alex Stewart and Dr Max Reuter, I combined a biologically realistic model of transcription factor binding with a population genetic analysis for the invasion and maintenance of SA alleles. This model was motivated by the key role that gene expression regulation plays in generating sexual dimorphism (Ellegren and Parsch 2007), as well as by the previous associations between sexual antagonism and gene regulation documented in this thesis and in other work (Roberts et al. 2009; Innocenti and Morrow 2010). We show that polymorphism can arise in our model under conditions that are not conducive to SA variation in the simple 2-allele models of sexual antagonism that have been studied previously. We further show that, in a regulatory cascade, polymorphism that initially arises at a gene directly under SA selection, is often displaced to genes higher up in the regulatory cascade.

*This work was initiated by myself and developed and conducted in collaboration with Dr Alex Stewart and Dr Max Reuter. Dr Stewart took the lead on developing the analytical model, I aided in the running and analysis of simulations. All three collaborators contributed to the interpretation of the results. A manuscript describing our findings is being prepared for submission to Nature Ecology and Evolution.*

### **1.7.5 Chapter 6**

The final chapter contains discussion of all the work contained within this thesis and provides broader context to my findings. I describe how the data from each of my thesis elements are related to each other and can be integrated to lead to new insights about the evolution of SA. I include an assessment of appropriate ways to extend my current findings and identify important questions about SA that remain a challenge for future research.

### **1.7.6 Appendix A**

This is a copy of a manuscript, with me as first author, which was submitted to Nature Ecology and Evolution. It contains some of the work documented in chapters 2 & 3. Here my analyses are combined with those of Filip Ruzicka, another PhD student in the Reuter laboratory. We show elevated signatures of balancing selection at candidate loci across the *D. melanogaster* distribution range. This suggests that the antagonism I describe is both persistent and not specific to the LH<sub>M</sub> population.

### **1.7.7 Appendix B**

This appendix contains a copy of a research article published in Evolution to which I made a significant contribution in terms of data analysis. Specifically, I performed a number of important bioinformatic filtering procedures to prepare the genome-wide SNP data for downstream analysis and interpretation. The work documents a case of resolution of sexual antagonism in a replicate of the LH<sub>M</sub> population. We further used an  $F_{st}$  outlier approach to find those loci

associated with the resolution event.

### **1.7.8 Appendix C**

This appendix contains a copy of a Forum article published in Trends in Genetics. I contributed to discussion of ideas and writing of the paper. The piece describes a recent study by Yi and Dean (2016) where the authors show how phenotypic plasticity arises in a bacterial system. We used this Forum article to make a conceptual link between the evolution of plasticity in response to adaptive trade-offs imposed by fluctuating environments and the evolution of sexual dimorphism in response to contrasting sex-specific selection pressures. Furthermore, we highlighted the potential for antagonistic variation to arise across environments, just as sexual antagonism can result from sex-specific selection.

## Chapter 2

# Genome-wide identification of sexually antagonistic loci in *Drosophila melanogaster*

*Material from this chapter was included in a manuscript, submitted to Nature Ecology and Evolution, with me as first author—see Appendix A. All of the analyses presented in this chapter are included in the manuscript.*

## 2.1 Abstract

Males and females frequently have divergent phenotypic optima for homologous traits. However, responding to these differential selection pressures is hampered by a largely shared genome. In this situation, selection is expected to favour the invasion of genetic variants with opposing fitness consequences in each sex, so called 'sexually antagonistic (SA) alleles'. A wealth of study has now shown that large amounts of segregating fitness variation in both natural and laboratory populations is antagonistic; however, the actual identity of the underlying loci remains unknown. This is an important deficit, as without knowledge of the identity of SA loci we are unable to fully understand either the general biological processes encapsulated in sexual antagonism, or the evolutionary dynamics of SA variation. To address this, I perform the first genome-wide identification of SA SNPs using the *Drosophila melanogaster* model system. By sequencing haplotypes with contrasting sex-specific fitness profiles (high fitness in one sex and low fitness in the other) I identify 6,275 candidate antagonistic SNPs. I go on to show that the number of antagonistic SNPs identified is much greater than the null expectation and that these loci are non-randomly distributed across the *D. melanogaster* genome. Notably, and contrary to some longstanding predictions, I find that antagonistic SNPs are significantly underrepresented on the X chromosome. I further show that SA loci identified here have significant associations with previous analyses of sexual antagonism. The list of SA loci I describe constitutes a critical breakthrough and provides the foundation for elucidating the functional properties and evolutionary dynamics of SA loci.

## 2.2 Introduction

The different reproductive roles of males and females generate sexually antagonistic (SA) selection where opposing trait values are favoured in each sex. However, responding to these divergent selection pressures is constrained by a largely shared genome. This results in sexual antagonism, where, at a given locus, alternative alleles are favoured in each sex (Bonduriansky and Chenoweth 2009; Cox and Calsbeek 2009; Van Doorn 2009; Pennell and Morrow 2013). This can ultimately prevent either sex from reaching their respective phenotypic optima (Lande and Kirkpatrick 1988).

A wealth of quantitative genetic studies has convincingly shown that large amounts of SA genetic variation is segregating in wild and laboratory populations across taxa (see Cox and Calsbeek 2009, for review), including mammals (Mokkonen et al. 2011), birds (Tarka et al. 2014), reptiles (Svensson et al. 2009), insects (Rice 1992; 1998; Berger et al. 2014) fish (Roberts et al. 2009; Barson et al. 2015) and plants (Delph et al. 2011). Documenting the presence of SA genetic variation can be achieved through a variety of quantitative genetic approaches. For example, in *D. melanogaster*, hemiclinal analysis, where individuals are sampled from a population and their genomes expressed in random genetic background, has been commonly used (Rice 1998; Prasad et al. 2007; Chippindale et al. 2001; Innocenti and Morrow 2010). By measuring the fitness of genomes in male and female genetic backgrounds it is possible to observe the effects of genome-wide genetic variation on sex-specific fitness. For non-laboratory organisms, an analogous approach is to demonstrate reduced fitness of opposite-sex offspring (Fedorka and Mousseau 2004). This shows that variants that produce high fitness in one sex have the opposite effect when expressed in the other. As well as methods that characterise standing genetic variation, sexual antagonism can also be documented in experimental evolution or artificial selection experiments. For example, Prasad et al. (2007) enforced male-limited transmission of a sampled haploid genome for 41 generations and measured the change in sex-specific fitness. They showed that males with the

evolved genome had higher fitness than control males. In contrast females with the evolved genome had lower fitness than control females. This is consistent with the accumulation of male-beneficial / female-detrimental alleles. In a more recent experiment Mokkonen et al. (2011) selected on testosterone level in male bank voles *Myodes glareolus*. The authors showed that artificial selection for increased testosterone levels increased mating rates in males but decreased female mating rates. Thus, they provide evidence that the production of testosterone is a SA trait in bank voles.

In light of the observed abundance of segregating SA variation, sexual antagonism is considered a significant constraint to sex-specific adaptation and a fundamental mechanism for maintaining fitness variation (Kidwell et al. 1977). More broadly, sexual antagonism is thought to be a key driver of sex chromosome evolution (Rice 1987; Charlesworth and Charlesworth 2005) and the evolution of sex determination (Haag and Doty 2005; Van Doorn 2009). In addition, sexual antagonism can erode ‘good gene’ benefits to sexual selection (Pischedda et al. 2006). This is because the benefits to female preference for honest signals of male quality are weakened by sexual antagonism because high fitness males can sire low fitness daughters. However, despite the documented abundance of SA genetic variation and its clear evolutionary importance, we still know almost nothing of the underlying loci.

This paucity of information on the identity of SA loci is a critical shortcoming. Because of this, we do not have a handle on the number of SA loci and whether the results from early quantitative genetic studies are driven by few loci with large effects or many loci with smaller individual effects. Similarly, we do not know how SA loci are distributed across the genome, an issue that has been the focus of much theoretical work (see below). Beyond questions of number and distribution, identifying the underlying loci will also enable progress towards understanding the biological processes encapsulated in sexual antagonism and help to elucidate the timescales over which we can expect sexual antagonism to persist, as well as the mechanisms by which it can be

resolved. In short, without information about the identity of antagonistic loci, we cannot hope to fully understand the adaptive limits to sexual dimorphism.

To date, empirical studies which identify SA alleles remain rare and most only characterise individual SA loci (Roberts et al. 2009; Smith et al. 2011; Barson et al. 2015). For example, Roberts et al. (2009) identified the genetic basis of the orange-blotch (OB) colour pattern phenotype in Lake Malawi Cichlids. The OB colour pattern provides camouflage benefits to females against the lake bed, thus increasing their fitness, but disrupts male nuptial pigmentation patterns, resulting in decreased male fitness. The trait was mapped to a cis-regulatory mutation near the *pax7* gene. Interestingly, this gene was found to be in tight linkage with a dominant sex-determining locus. The OB phenotype is almost exclusively expressed in females, suggesting that sexual antagonism is mainly resolved for this trait. Colouration is also sexually antagonistic in Guppies (Houde and Endler 1990; Kemp et al. 2009), where brightly coloured males are more attractive to females but suffer increased predation. In females, these bright colours are deleterious, as they only incur the costs of increased predation without providing any other fitness benefit. Much like the sex-linkage of the OB phenotype in Lake Malawi Cichlids, colouration in guppies is tightly sex-linked and mostly maps to the Y-chromosome (Wright et al. 2017). The consequence is that expression of this trait is largely restricted to males, again reflecting predominant resolution of conflict. As well as these colouration traits in fishes, several sexually antagonistic traits in other taxa have been characterised. For example, the DDT-R (DDT resistance) allele in *D. melanogaster* has also been shown to be SA in the absence of the pesticide DDT (dichlorodiphenyltrichloroethane) (Smith et al. 2011), conferring increased fecundity to females while reducing male fitness. In this system resistance to DDT is the result of the insertion of a single transposable element into the promoter region of the *Cyp6g1* gene (Daborn et al. 2002). Taken together, these multiple findings across species constitute interesting case-studies, but with each only characterising individual antagonistic loci, they are not infor-

mative about the overall number nor the genomic distribution of SA loci.

On a genome-wide scale, one previous transcriptomic study has associated antagonistic fitness effects with the patterns of gene expression in *D. melanogaster* (Innocenti and Morrow 2010). This study used the LH<sub>M</sub> laboratory population and measured the fitness of a suite of hemiclinal genomes when expressed in males and females. The authors then took ten of these haplotypes with the most extreme sex-specific fitness effects (five male-beneficial / female-detrimental and five female-beneficial / male detrimental) as well as five with intermediate fitness profiles (haplotypes with average fitness in both sexes) and performed a microarray gene expression analysis. By combining fitness with expression data, the authors were able to identify transcripts with SA expression patterns. These were defined as those transcripts where significant variation in expression was explained by an interaction between fitness and sex. Using this approach, Innocenti and Morrow (2010) identified 1,292 genes with SA patterns of expression. These genes were non-randomly distributed across the genome and particularly enriched on the X chromosome. However, while this approach was the first genome-wide identification of antagonistic genes in any organism, it is limited because it only characterises antagonism in terms of gene expression. Thus, while this does correlate patterns of gene expression with sexually antagonistic effects, it cannot distinguish between causal antagonistic loci and their downstream regulatory targets i.e., it is unclear whether these SA expression patterns are driven by individual, sexually antagonistic cis-regulatory variants at each of the candidate genes, or a small number of trans-acting SA polymorphisms in transcription factors that regulate the genes identified.

In the absence of knowledge of their identity, the genomic distribution of SA loci has also been a longstanding question. A number of theoretical studies have generated predictions about the expected genomic distribution of SA alleles between sex chromosomes and autosomes. Early population genetic theory suggested that the X chromosome may be a hotspot for the accumu-

lation of SA alleles (Rice 1984). This prediction was based on the fact that X-linked alleles reside in females 2/3 of the time and only 1/3 of their time in males. Thus, X-linked, female-beneficial, dominant alleles can increase in frequency even when they are more costly to males than they are beneficial to females. Likewise, X-linked, recessive male-beneficial alleles are shielded from selection in females, meaning they can increase in frequency even when they are more costly to females than they are beneficial to males. However, this prediction of X chromosome enrichment only holds when assuming that the dominance of SA alleles is the same in each sex. When this assumption is relaxed, SA polymorphism is supported over a greater range of parameter space on autosomes than on the X chromosome (Fry 2010; Patten and Haig 2009; Crispin and Charlesworth 2012).

In line with these opposing predictions, empirical studies have failed to provide a consistent picture of chromosomal enrichment of SA variation. Several suggest that the X chromosome harbours an disproportionate amount of SA genetic variation (e.g. Chippindale et al. (2001); Gibson et al. (2002); Innocenti and Morrow (2010)), while others point to autosomal enrichment (Fedorka and Mousseau 2004; Calsbeek and Sinervo 2004; Delcourt et al. 2009). However, these studies rely on quantitative genetic approaches and subsequently cannot differentiate the number of loci from their effect size. As a result, these patterns could be driven by a few loci of large effect rather than reflecting the overall distribution of SA variation. Overall, there is little consensus in theoretical expectations or empirical findings as to whether SA loci will preferentially accumulate on the X / Z chromosomes or autosomes. Given this uncertainty, studies which explicitly identify genome-wide causal SA variants are required to ascertain the true genomic distribution of SA alleles.

To reduce the shortfall in our understanding of sexual antagonism, I here identify the first genome-wide putative causal SA SNPs in any organism. To do so, I compare the genomic sequences of hemiclinal fly lines derived from a laboratory population of *D. melanogaster* (originally from Innocenti and Morrow

(2010)) that exhibited extreme male-beneficial/female-detrimental ( $N_{\text{MBFD}} = 5$ ) and female-beneficial/male-detrimental ( $N_{\text{FBMD}} = 4$ ) fitness effects. Out of 1,052,882 informative SNPs, 6,275 variants have a pattern of perfect segregation, where the two fitness classes of genomes were fixed for opposing alleles. I show that: i) the number of candidate SA SNPs identified far exceeds the null expectation, ii) that these loci are non-randomly distributed across the genome and particularly depauperate on the X chromosome, and iii) that candidate loci are significantly associated with previous analyses of sexual antagonism, supporting their credibility. My results constitute the first information on the identity and characteristics of causal SA loci and provide a novel and robust foundation for future studies to build on.

## 2.3 Materials and Methods

### 2.3.1 Hemiclonal haplotypes

I sequenced the genomes of the set of most antagonistic genotypes that had been identified in a previous study (Innocenti and Morrow 2010). These genotypes were extracted from the  $\text{LH}_M$  population, a large, outbred population in which sexual antagonism has been previously studied (Rice 1992; 1998; Chipindale et al. 2001; Prasad et al. 2007; Innocenti and Morrow 2010). Specifically, 5 male-beneficial/female-detrimental (MBFD) genotypes and 4 female-beneficial/male-detrimental (FBMD) genotypes (a fifth FBMD had been lost prior to this study) had been maintained as ‘hemiclones’, i.e., intact unrecombined haploid sets of chromosomes X, 2 and 3, by back-crossing males to ‘clone-generator’ females [C(1)DX, y, f; T(2;3) rdgC st in ri pP bwD]. In order to obtain the genomic sequences of the haploid hemiclones, I expressed the haploid hemiclonal genomes in three different genetic backgrounds that could then be used to infer the genome sequence of interest with certainty (see section 2.3.3). The three genotypes sequenced for each hemiclonal genome were (i) females in which the hemiclonal genome was complemented with chromosomes from the *D. melanogaster* reference strain iso-1 (y[1]; Gr22b[iso-1] Gr22d[iso-

1] cn[1] CG33964[iso-1] bw[1] sp[1]; MstProx[iso-1] GstD5[iso-1] Rh6[1]), (ii) females in which the hemiclinal genome was complemented with chromosomes from the Canton-S strain, and (iii) males in which the hemiclinal genome was complemented with chromosomes from the clone-generator strain.

### **2.3.2 DNA extraction, sequencing and initial processing of haplotype sequencing reads**

10-25 adult individuals were collected for each of the 27 samples (9 hemiclones, 3 genetic backgrounds per hemiclone). I extracted total genomic DNA using DNeasy Blood and Tissue Kit (Qiagen) according to the manufacturer's protocol and purified DNA samples using Agencourt AMPure XP beads (Beckman Coulter). Paired-end Nextera libraries were prepared using a Nextera DNA sample preparation kit (Illumina). Completed libraries were pooled in equimolar amounts and fragments between 450 and 650bp were collected using the Pippin Prep DNA size selection system (Sage Scientific). Size-selected pools were purified using Agencourt AMPure XP beads. Library preparation and sequencing (on 4 lanes of an Illumina HiSeq 2000) were performed at the Center for Genomic Research, University of Liverpool.

Basecalling and de-multiplexing of the indexed sequencing reads was performed using CASAVA version 1.8.2 (Illumina). The raw fastq files were first trimmed using Cutadapt version 1.2.12 (Martin 2011) to remove Illumina adapter sequences. The reads were then further trimmed to remove low quality bases (minimum window score of 20) and very short reads (<10bp) with Sickle version 1.200 ([github.com/najoshi/sickle](http://github.com/najoshi/sickle)). Read pairs were then aligned to the *D. melanogaster* reference sequence (BDGP 5.5), obtained from the FlyBase online database (<http://flybase.org/>), using Bowtie2 version 2.1.03 in 'local' alignment mode (Langmead and Salzberg 2012). To avoid false positive SNP calls resulting from misalignment around indels, reads were locally realigned using the Genome Analysis Toolkit (GATK) version 2.1.13 (McKenna et al. 2010; DePristo et al. 2011). Duplicate reads, arising from PCR amplification during library construction were removed using Picard version 1.85 ([43](http://</a></p></div><div data-bbox=)

sourceforge.net/projects/picard/). The alignment results were visually inspected using the Integrative Genomics Viewer (Robinson et al. 2011) SNP calling was performed using the GATK ‘UnifiedGenotyper’ package (McKenna et al. 2010) with heterozygosity set to 0.14 (to more closely reflect the average heterozygosity of *D. melanogaster*). Identified SNPs were then filtered to remove SNPs with low confidence and low coverage (<10 reads) using the GATK ‘VariantFiltration’ package (McKenna et al. 2010).

### **2.3.3 Identification of informative and candidate SNPs**

To identify informative SNPs from the hemiclinal genomes, I exploited the fact that their DNA was present in each of three crosses and that in one of the crosses, they were complemented with chromosomes of the reference strain. Thus, for a given chromosomal position with sufficient coverage in the sequencing of all three crosses, I inferred the hemiclinal variant to be an alternative (non-reference) variant if an identical alternative variant was detected in all three crosses. If this condition was not fulfilled, then the variant was assumed to be the reference variant. Once variants for all nine hemiclinal genomes were identified in this way, I identified a set of informative SNPs where variants were polymorphic across the nine hemiclinal genomes. Candidate SA SNPs were then defined as those ‘perfectly segregating’ SNPs where all MBFD hemiclinal genomes were fixed for one variant and all FBMD hemiclinal genomes were fixed for the other variant). This rule-based approach to identifying candidate SA SNPs is appropriate given the small number of hemiclinal genotypes analysed and is analogous to applying locus-specific  $\chi^2$  contingency table tests to compare allele counts across the two fitness classes, where only ‘perfectly segregating’ patterns yield significant P-values. One option to generate a greater range of P-values would have been to calculate the probability of observing a pattern of segregation given the population allele frequencies. However, this would have unduly penalised loci with even allele frequencies because the probability of achieving a perfectly segregating pattern is higher with higher minor allele frequencies. Given that SA loci are expected to be under balancing

selection (Gavrilets and Rice 2006; Mullon et al. 2012; Connallon and Clark 2014), this approach would have been biased against many of the loci that are of greatest interest.

### **2.3.4 Distribution of candidate loci**

To examine the clustering of candidate SNPs across chromosome arms, I calculated the median distance between all pairs of adjacent candidate SNPs (ignoring interspersed non-candidate SNPs). I did this separately for the autosomes and the X chromosome, to accommodate for the lower SNP density on the X chromosome. I then designed a permutation test to determine the significance of the observed clustering. Candidate/non-candidate status was permuted among all informative SNPs, distances recalculated as before between adjacent SNPs labelled as ‘candidates’ after permutation and the median distance recorded. This process was repeated 1,000 times in order to generate a null distribution of median distances. Significance was calculated as the proportion of median distances in the null distribution that were lower than or equal to the true median distance.

To examine the relative representation of antagonistic SNPs on autosomes and the X chromosome, I compared the proportion of antagonistic SNPs to the proportion of all informative SNPs that mapped to each chromosomal compartment. I did this for each chromosomal compartment in turn, using Z-tests. The under- or over-representation of antagonistic SNPs in each compartment therefore took into account the general differences in SNP density between chromosome arms and, in particular, lower polymorphism on the X chromosome.

### **2.3.5 Assessing the contribution of false positives to the number of SA SNPs**

I implemented two independent tests to assess whether the number of candidate SNPs detected with our approach was greater than expected by chance and estimate the false positive rate: (i) a resampling test based on population

allele frequencies, and (ii) a permutation test that shuffled hemiclinal haplotypes among fitness classes (MB and FB). In a first resampling approach, I merged our dataset with high quality genome-wide allele frequency data generated from the same  $LH_M$  population (data from (Collet et al. 2016)). I then used binomial sampling to generate allelic samples for each SNP according to the population allele frequencies and recalculated the number of perfectly segregating sites ('pseudo-candidate SNPs'). This procedure was repeated 1,000 times and the null distribution of the number of pseudo-candidate SNPs was compared to the observed number of true antagonistic SNPs (Figure 2.4A). Significance was determined by calculating the proportion of instances where the number of pseudo-candidates was greater than or equal to the number of true candidate SNPs. The false positive rate was estimated as the median number of pseudo-candidates across the permuted datasets, divided by the total number of true candidate SNPs covered in the population genomic data. In a second permutation approach, I produced all possible permutations of hemiclinal haplotypes among the two fitness classes and for each permutation I recalculated the numbers of perfectly segregating sites. Here, the false positive rate was estimated by dividing the total number of true candidate SNPs by the median number of pseudo-candidates from the most permuted datasets i.e., those where the arrangement of haplotypes across fitness classes was most dissimilar to the true data (in the case where two haplotypes had been swapped between fitness classes).

### **2.3.6 Characterisation of sexually antagonistic loci**

As well as the quantitative assessments described above, I additionally examined my candidates for non-random patterns of functional enrichment, which would further support their credibility. I used the variant effect predictor (Ensembl, VEP (McLaren et al. 2010)) to map SNPs to genes and infer their genetic consequences. In accordance with the VEP default settings, I included extended gene regions ( $\pm$  5kb of gene coordinates) in my definition of candidate genes. To gain preliminary insights into the functions of antagonistic

genes I used the Gorilla Gene Ontology tool (Eden et al. 2009), and applied a false discovery rate (FDR) to correct for multiple testing across many GO terms. Here, all of the genes covered in our entire SNP dataset (informative SNPs) were used as the background set.

To assess the degree of overlap between antagonistic genes identified here and those associated with SA expression patterns in a previous study (Innocenti and Morrow 2010) (Figure 2.5), I included only genes covered in both datasets, and only those genes in both datasets that were adult-expressed. To determine whether genes were adult expressed I used the *Drosophila* gene expression atlas (FlyAtlas, Chintapalli et al. 2007). Conservatively, I defined a gene as ‘adult expressed’ if its transcript was detected as present in at least one library of one adult-derived sample. I then used a  $\chi^2$  test to assess the degree of overlap between the datasets. I removed non-adult expressed genes for this test as the Innocenti and Morrow (2010) study only characterised adult gene expression, meaning that genes expressed exclusively in pre-adult stages could never be characterised as SA and thus do not constitute a suitable background set.

### **2.3.7 Statistical analysis and plotting**

All statistical analyses were conducted in R version 3.2.3. Plots were produced with the ggplot2 (Wickham 2009), and VennDiagram (Chen and Boutros 2011) packages.

## **2.4 Results**

### **2.4.1 Identification and distribution of sexually antagonistic candidate SNPs**

Haplotype sequencing identified a total of 1,052,882 high quality and informative SNPs. These SNPs were non-randomly distributed across chromosome arms ( $\chi_4^2=188160$ ,  $P < 0.001$ ), with autosomal chromosome arms enriched for polymorphisms and the X chromosome severely depauperate for polymorphic

sites. This pattern of reduced polymorphism on the X chromosome is expected owing to the smaller effective population size  $N_e$  of the X chromosome relative to autosomes (Charlesworth et al. 1987).

SA SNP loci were defined as those informative SNPs where the two alleles segregated perfectly between fitness classes, meaning all FBMD haplotypes were fixed for one allele and all MBFD haplotypes fixed for the other allele. As the 4th chromosome is not isolated in the generation of the hemiclinal haplotypes, results are presented for chromosomes II, III and the X. With this approach I identified 6,275 candidate antagonistic SNPs across the *D. melanogaster* genome. The distribution of candidate SNPs across chromosome arms was non-random ( $\chi_4^2=193$ ,  $P < 0.001$ ), with candidate SNPs depauperate on chromosome arm 2R and the X chromosome and enriched on chromosome arms 3L and 3R (Figure 2.2). Importantly, grouping chromosomes together, the number of autosomal candidate SNPs was no greater than expected ( $P=0.16$ ) but the number of X-linked SA candidate SNPs was substantially lower than the random expectation ( $P < 0.001$ ), after accounting for the lower SNP density of the X chromosome.

Candidate SNPs were tightly clustered along chromosome arms with median distances between autosomal and X-linked candidate SNPs of 187bp and 6,980bp, respectively. The large difference in the median distance between candidate SNPs on the autosomes and the X chromosome reflects the very small number of X-linked candidates ( $N = 50$ ). To visualize the distribution of candidate SNPs across chromosome arms I performed a sliding-window analysis. Shown in Figure 2.3, is the percentage of all informative SNPs in a window that are antagonistic across the length of each chromosome arm. In line with the clear clustering of antagonistic variants across individual chromosome arms, a permutation test confirmed a statistically significant clustering of candidate SNPs along autosomes (range of median distances between autosomal pseudo-candidate SNPs = 8,644bp — 9,670bp,  $P < 0.001$ ) as well as along the X chromosome (range of median distances between X-linked pseudo-candidate SNPs

= 146106bp — 494424bp,  $P < 0.001$ ). The results of the permutation test are presented in Figures 2.1A (autosomes) and 2.1B (X chromosome) where the observed median distances between candidate SNPs are substantially lower than the distributions of median distances between pseudo-candidate SNPs.

## 2.4.2 Characteristics of SA loci

The credibility of candidate loci would be supported by a non-random distribution across functional categories. Accordingly, to ascertain whether there was any functional enrichment among candidate loci I first used the Variant Effect Predictor (VEP) to characterise the genetic consequences of all SNPs covered in the haplotype sequencing. Relative to all informative SNPs, candidate antagonistic SNPs were significantly enriched for upstream ( $Z = 2.91$ ,  $P = 0.004$ ), downstream ( $Z = 6.00$ ,  $P < 0.001$ ), and 3-prime UTR variants ( $Z = 2.07$ ,  $P = 0.039$ ) whilst being underrepresented in intronic ( $Z = -9.84$ ,  $P < 0.001$ ) and intergenic ( $Z = -3.28$ ,  $P = 0.001$ ) regions. I also assessed whether candidate genes were non-randomly associated with different biological functions annotated in the Gene Ontology (GO). I defined candidate genes from the SNP data by considering genes to be SA if they contained 1 or more candidate SNPs within 5kb up- or down-stream of the gene start coordinates (in accordance with VEP default settings), thus identifying 1,949 candidate genes. Using GO analysis, I found that these genes were enriched for several processes relating to development, morphogenesis, metabolism and development (for full details and further interpretation see chapter 3). These patterns of functional enrichment, taken together with the clear excess of observed candidate SNPs and their non-random genomic distribution, support the credibility of the candidate SNPs identified here.

If the loci I identify here are credible then I would also expect those loci to overlap significantly with loci identified in previous analyses of sexual antagonism. To test this, I utilised publicly available data from two previous studies, (i) a study which examined SA gene expression in the same haplotypes used here (Innocenti and Morrow 2010), and (ii) a study that associated

genomic regions with the resolution of sexual antagonism in a replicate of the LH<sub>M</sub> population (Collet et al. 2016). I found significant overlap in the antagonistic candidate genes identified here and those of Innocenti and Morrow (2010) (observed overlap = 202, expected overlap = 153,  $\chi_1^2 = 19.9$ ,  $P < 0.001$ , Figure 2.5). Innocenti and Morrow (2010) identified genes with sexually antagonistic expression patterns so the significant overlap between their and my findings means that genes containing antagonistic SNPs are also more likely to have SA expression patterns. I also found significant overlap between the antagonistic candidate SNPs and candidate genes (defined as above as genes with 1 candidate SNP) identified here and those from a previous study (Collet et al. 2016) that identified regions associated with the resolution of sexual antagonism (SNPs: observed overlap = 31, expected overlap = 21,  $\chi_1^2 = 4.8$ ,  $P = 0.028$  ; genes: observed overlap = 183, expected overlap = 147,  $\chi_1^2 = 10.5$ ,  $P = 0.001$ , Figure 2.5).

## 2.5 Discussion

Despite the ubiquity of sexual antagonism across animal and plant species (Rice 1992; Chippindale et al. 2001; Cox and Calsbeek 2009; Roberts et al. 2009; Svensson et al. 2009; Mokkonen et al. 2011; Berger et al. 2014; Tarka et al. 2014; Delph et al. 2011) and the clear evolutionary importance of this phenomenon (Rice 1992; Charlesworth and Charlesworth 2005; Pischedda et al. 2006; Van Doorn 2009; Pennell and Morrow 2013), we know almost nothing about the underlying genetic loci (Cox and Calsbeek 2009; Pennell and Morrow 2013). Here, I have addressed this shortcoming and identified, for the first time, putative SA SNPs across the *D. melanogaster* genome. A critical aspect of the interpretation of my data is to ascertain the credibility of the candidate loci and to assess what proportion of causal SA loci my approach is likely to have captured. Below, I examine the qualitative evidence which supports the credibility of the candidate loci and subsequently consider the contribution of type I (false positives) and type II (false negatives) errors to the number of

candidate loci that I describe. In this way, I can comment on the polygenicity of sexual antagonism in fruitflies.

My analyses have provided several lines of evidence to support the credibility of the candidate loci that I describe. First, both of the Monte Carlo approaches consistently revealed a significant excess of observed candidate loci, whose number far exceeds the expectation from the null distribution. Second, the candidate loci showed a number of non-random patterns of functional enrichment. Specifically, candidate SNPs were enriched in upstream, downstream and 3'UTR regions but depauperate in intergenic and intronic regions. Previous empirical work in *Drosophila* suggests that a large proportion of non-coding regions are functionally important and subject to strong purifying selection (Andolfatto 2005). Interestingly in the context of my findings 3'UTR regions were among those with the strongest signatures of purifying selection, whereas intronic and intergenic regions were much less strongly selected. In addition, candidate genes also showed functional enrichment, with several enriched GO terms.

These patterns of enrichment, documented at the level of both individual SNPs and genes, would not be expected if the candidates were just randomly associated with sexual antagonism, rather it suggests they are responding to selection. This is further supported by findings documented in appendix A. Here, we showed elevated signatures of balancing selection at the SA loci identified here across multiple independent populations. Finally, there is a level of independent validation for the candidate loci that I identify from their overlap with previous analyses of sexual antagonism. Namely, there is significant overlap between candidate genes and genes with sexually antagonistic expression patterns (Innocenti and Morrow 2010), as well as between candidate loci (both SNPs and genes) and regions associated with the resolution of sexual antagonism (Collet et al. 2016).

The qualitative evidence discussed above suggests that the candidate loci that I describe are highly credible and likely to underlie the antagonism that

has previously been described at the phenotypic level (Rice 1992; 1998; Chipindale et al. 2001; Innocenti and Morrow 2010). However, a question remains as to the degree to which the loci that we identify do reflect the true number of loci at which SA alleles segregate in the LH<sub>M</sub> population. In order to address this question, one must assess to what extent both type I error (false positives) and type II error (false negatives) contribute to the quantitative identification / misidentification of SA loci. The false positive rate estimated from the two Monte-Carlo approaches indicates that the vast majority of the candidates are true positives and are informative about the genetic basis of the SA fitness effects that characterise the hemiclones. However, while I expect that the vast majority of the 6,275 candidate loci are not false positives in a statistical sense, linkage effects may contribute substantially to this number. This is because linkage disequilibrium (LD) can cause neutral variants close to the causal loci to be falsely associated with the trait of interest. Indeed, the first Monte Carlo approach makes the assumption that draws of alleles from adjacent SNPs are independent, which may not be the case if there is strong linkage disequilibrium (LD) between SNPs along the chromosome. However, this concern is addressed by the second Monte-Carlo permutation approach. Here, haplotypes were permuted across the fitness classes, thus breaking the associations between phenotypic fitness class and genotype, whilst preserving haplotypic structure (e.g. Linkage disequilibrium). A further approach which accounts for linkage structure in the LH<sub>M</sub> population is to resample whole genomes (Appendix A). Gilks et al. (2016) provides whole genome sequence data for 220 individual genomes across the LH<sub>M</sub> population. By resampling sets of 9 genomes, assigning them to one of the two fitness classes (FBMD & MBFD) and counting the number of loci where the two fitness classes are fixed for alternative alleles it is possible to generate a null distribution of the number of false positive candidate SNPs, accounting for linkage structure. This approach provides an estimate for the false positive rate at 17.4%, in line with the two approaches detailed in this study. Taken together, the relatively con-

sistent false positive estimates from three independent approaches suggest that LD does not substantially inflate the number of false positives.

In order to get a better estimate of the true number of causal SA polymorphisms, one can estimate the number of independent SNP clusters. This can be done by quantifying the clusters of SNPs based on LD decay in the population, where all SNPs within a cluster are in strong LD with each other but not in LD with any SNP from a different cluster. This approach defines 798 isolated SNP clusters which capture 5,852 of the total 6,275 candidate SA SNPs (Filip Ruzicka, personal communication). This figure of 798 independent clusters constitutes a lower bound estimate of the true number of causal SA loci in this sample of the LH<sub>M</sub> population because it assumes that only one SNP of each cluster is causally linked to SA and all others are simply associated through linkage effects. This assumption, however, may be too restrictive given that previous theoretical work (Patten et al. 2010) predicts that LD between causal SA loci will be favorable for the invasion and maintenance of individual SA alleles. Thus, selection coefficients that would otherwise result in fixation of one allele at a SA locus can maintain polymorphism if that locus is in LD with a second SA locus of similar fitness effect. Consistent with this, in Appendix A we show that the SA alleles (defined here) tend to co-segregate with other SA alleles with concordant fitness effects (i.e. they form local haplotypes of MBFD alleles linked with other MBFD alleles and *vice versa*). Moreover, it was found that LD is elevated between pairs of candidate SNPs compared to pairs of non-candidates and mismatched pairs of candidate and non-candidate SNPs (Appendix A). Taken together, these findings suggest that rather than each cluster simply containing a single causal antagonistic locus, many of the clusters likely contain multiple, linked, causally antagonistic loci. Overall, this places the estimate of the number of causally antagonistic loci among all candidates described here between 798 and 4,706 (total - expected number of false positives). It is beyond the scope of the current study to offer any greater resolution to the likely number of true positive antagonistic loci among the

candidates. However, this could be addressed with further empirical studies which test the fitness consequences of candidate loci, thus providing independent validation (see chapter 4).

As well as estimating the number of true causal SA loci among all candidates, a further question remains as to how many of the total SA variants segregating in the  $LH_M$  population were missed with my approach (false negative rate). The power to detect causal SA variants (which is the complement of the false negative rate) is primarily limited by the number of genotypes that were originally sampled from the population (in this case 100), the number of genotypes with extreme sex-specific fitness phenotypes ( $N = 9$ ) that are compared, and the effect size of SA alleles (Xing and Xing 2009). Quantitative genetic simulations built to mirror the experimental design used here suggest that power (calculated as the percentage of simulated loci that are captured) is relatively low for reasonable effect sizes ( $< 5\%$  of the phenotypic variation), although increases in power are observed when considering nearby polymorphisms that can act as markers for true causal SA loci, (2-16%, Max Reuter, personal communication). While these simulations do not consider more complex effects that could potentially increase power (e.g. synergistic epistasis between SA alleles) they do suggest that my approach is likely to miss a significant number and provide a minimum estimate for the number of true causal SA loci. In contrast, one would expect that the loci identified by the experiments are those with the strongest SA fitness effects (Mackay et al. 2009). Thus, these candidates constitute an invaluable resource to better understand functional roles and evolutionary dynamics of SA loci.

The relatively high estimated number of causal SA loci that I identify, combined with the implication that there are potentially a significant additional number segregating within the population that I could not detect, make it clear that the genetic basis of sexual antagonism is highly polygenic. This polygenicity is unsurprising given that measures of fitness that originally characterised the hemiclinal haplotypes sequenced here (Innocenti and Morrow

2010) are a compound of many contributory traits. Indeed, this also fits with the general findings of two decades of QTL (quantitative trait loci) mapping studies, which show genetic variation for quantitative traits is predominantly due to many loci with individually small effects, rather than few loci with larger effects (see Mackay 2001; Mackay et al. 2009, for review).

The genomic distribution of SA loci has been a longstanding question in the field. While classical models suggested that the X chromosome is a hotspot for the accumulation of SA alleles (Rice 1984), this prediction rested critically on the assumption of equal dominance of each allele in each sex (Fry 2010). When this assumption is relaxed, as in more recent models (Patten and Haig 2009; Crispin and Charlesworth 2012), and unequal dominance is considered, SA polymorphism at autosomal loci is supported over a broader range of sex-specific selection coefficients compared to that supported for X-linked SA polymorphism. The reason for this is that dominance reversal, i.e., dominance of the beneficial allele in each sex, effectively increases the average relative fitness of heterozygotes, thereby generating strong balancing selection and maintaining polymorphism. Thus, the low prevalence of X-linked SA polymorphisms that I report here fits well with the more recent theory and also suggests that sex-dependent dominance may well be a common feature of SA variants. Although there is currently a shortage of empirical data to support this, a recent study (Barson et al. 2015) reported that sex-dependent dominance at a SA locus maintains variation in age at maturity in Salmon. In addition, loci underlying sexually dimorphic traits in mice have greater between-sex differences in dominance than those underlying non-dimorphic traits (Hager et al. 2008). Beyond these few studies which have examined specific loci and their patterns of sex-dependent dominance, there is evidence that fitness traits have high degrees of dominance and that the two sexes have contrasting levels of dominance for many adult fitness traits (Spencer and Priest 2016).

While the lack of X-linked SA polymorphisms fits with recent theoretical

work it is somewhat at odds with previous empirical findings from quantitative genetic studies in *D. melanogaster*. Such studies in the LH<sub>M</sub> (Gibson et al. 2002; Pischedda et al. 2006) and other laboratory populations (Connallon and Jakubowski 2009) suggested that the X chromosome is a hotspot for the accumulation of SA alleles. For example, Gibson et al. (2002) measured the fitness of 20 X chromosomes, randomly sampled from the LH<sub>M</sub> population, in male and female genetic backgrounds. They estimated that the X chromosome contributes  $\approx 45\%$  of the genome-wide adult fitness variation and  $\approx 97\%$  of the SA fitness variation. However, these estimates have relative large standard deviations owing to the modest number of X chromosomes sampled. Moreover, quantitative genetic approaches are unable to disentangle the number of loci from their phenotypic effects. Thus, these findings may be the result of a few large-effect loci on the X chromosome and therefore not reflect the real genomic distribution of all SA loci. This issue of effect size may help to reconcile the apparent lack of X-linked SA loci identified here and the abundance of SA fitness variation explained by the X chromosome in quantitative genetic studies. In addition, it is possible that other classes of variants, not quantified here (i.e. large insertions / deletions, structural variants), might account for a great deal of the variation. Although estimating the effect size of individual SA candidate loci is beyond the scope of the current study, follow-up experiments could track the evolution of SA alleles. This would allow one to estimate selection coefficients at candidate loci across the genome. Another approach would be to utilise modern sequence editing technologies (e.g. CRISPR-cas9) to test the phenotypic effects of individual SA candidates in a standardised genetic background.

The study which originally isolated the hemiclinal lines sequenced here (Innocenti and Morrow 2010) also found the X chromosome to be enriched for genes with sexually antagonistic expression patterns. Thus, within the hemiclinal lines used here there is a large discrepancy between the number of genes with sexually antagonistic expression patterns and the number of SA

SNPs that map to the X-chromosome. There are two, non-mutually exclusive, scenarios that could help to explain this pattern: i) there are a few causal loci on the X chromosome that regulate a large number of the genes with antagonistic expression profiles, and ii) many of the X-linked genes with antagonistic expression patterns are regulated by causal trans-regulatory variants located on other chromosomes. These constitute interesting questions that warrant further investigation. Testing whether any of the X-linked candidate loci have large and local regulatory effects should be possible with modern sequence editing approaches given the modest number of such candidates. However, elucidating the trans-regulatory roles of candidate loci is a more challenging prospect. This is mainly because they can reside anywhere in the genome relative to the target gene unlike cis-regulatory variants. Moreover, trans-regulatory variants typically have smaller effect sizes than do cis-regulatory variants (Schadt et al. 2003; Metzger et al. 2016).

In conclusion, this study documents the first genome-wide identification of SA SNPs in any organism. The credible list of SA loci that is defined here has allowed me to begin testing longstanding predictions from previous empirical and theoretical work. Building upon this foundation, future studies will be able to characterise the functional properties of SA loci and to explore their evolutionary dynamics. Indeed, Chapter 3 of this thesis takes the candidates defined here and examines their functional properties in greater depth. Furthermore, it is important that the candidate loci identified in this genome-wide scan are validated with follow up experiments. As a first step towards this, Chapter 4 describes the results of an experiment that examines the evolution of SA alleles under sex-limited selection. Finally, studies can start to leverage ever cheaper sequencing pipelines in order to perform much larger screens for SA loci than the one performed here, in multiple populations and species. Doing so would shed light on whether antagonistic alleles are largely population specific and short-lived or deeply conserved.

## 2.6 Tables and Figures

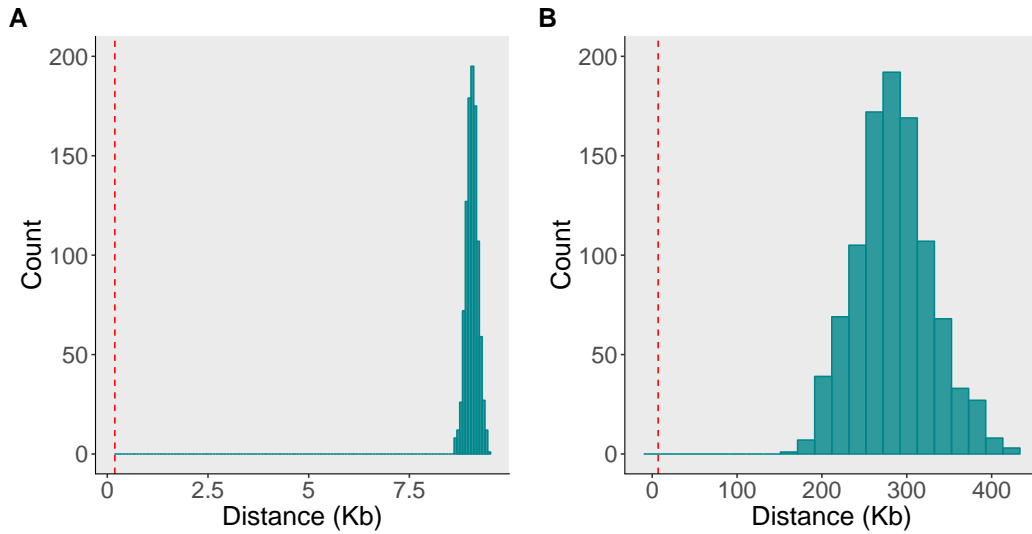


**Figure 2.1: Clustering analysis of candidate antagonistic SNPs along chromosomes.** **A**, Null distribution of genetic distances between candidate SNPs on autosomal chromosome arms (median distance between pseudo-candidates = 9055bp). The dashed red line indicates the observed median distance between autosomal candidate SNPs (187bp). **B**, Null distribution of genetic distances between candidate SNPs on the X chromosome (median distance between pseudo-candidates = 285036bp). The dashed red line indicates the observed median distance between X-linked candidate SNPs (6980bp).

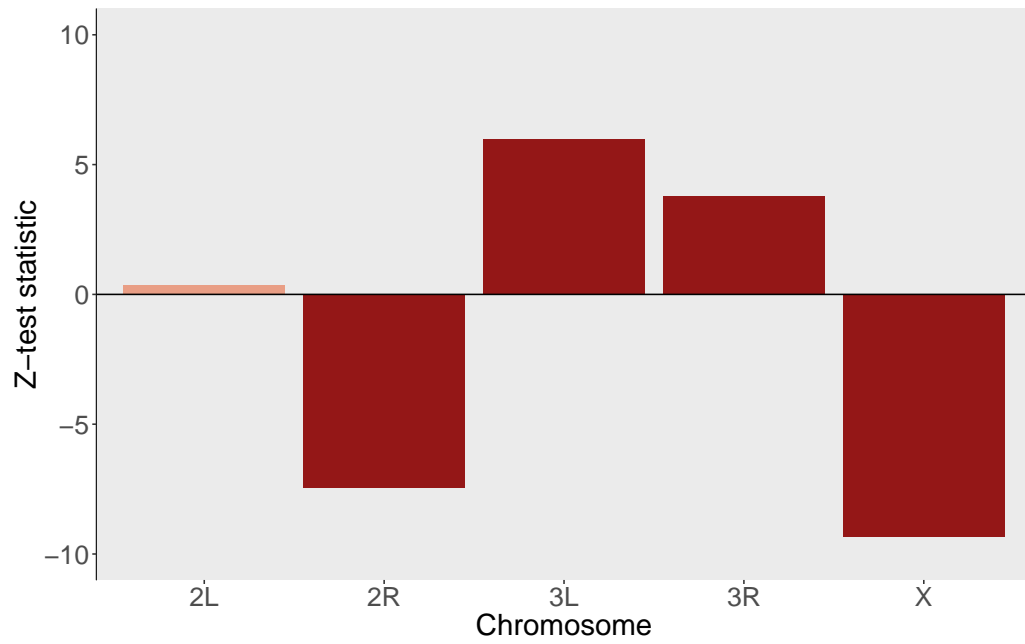


**Figure 2.2: Relative distribution of antagonistic candidate SNPs across the genome.** Z-test statistics summarising the representation of antagonistic candidate SNPs, relative to all informative SNPs, for each major chromosome arm. Dark red bars indicate statistically significant over-/under- representation, lighter red bars  $P > 0.05$ .

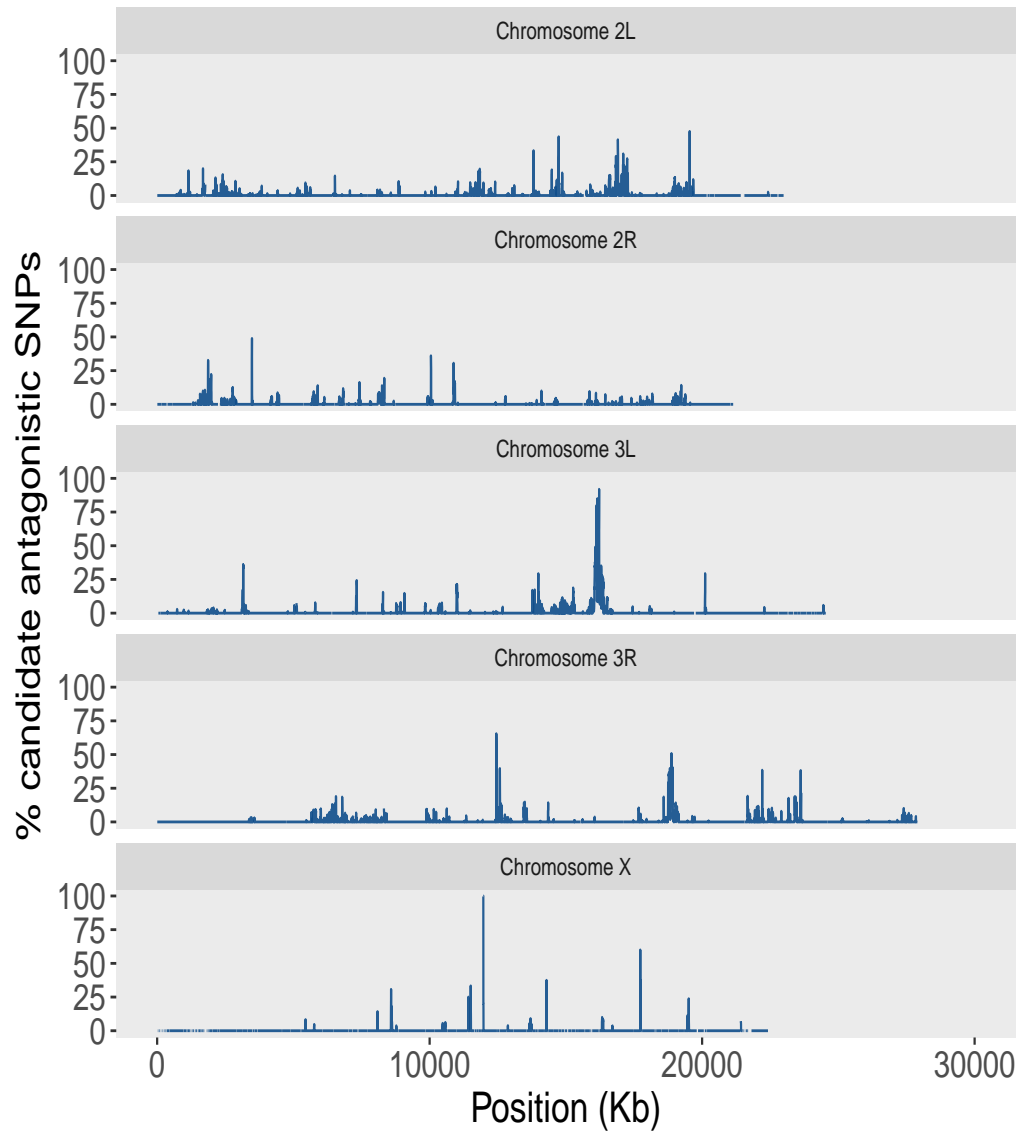


**Figure 2.3: Distributions of antagonistic candidate SNPs across major chromosome arms.** Sliding-window plots (window size=10000bp, step size=2500bp) showing the percentage of informative SNPs in each window that are antagonistic candidates for each major chromosome arm.

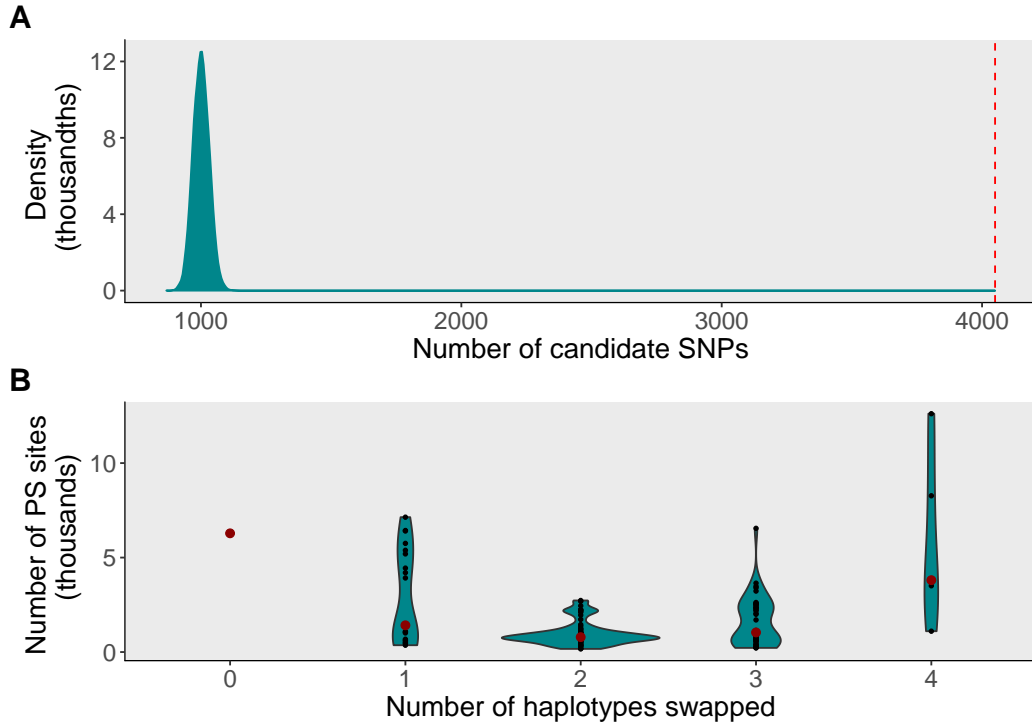


**Figure 2.4: Comparison of the number of antagonistic candidate SNPs to the null expectation.** **A**, Null distribution of the expected number of candidate SNPs from simulated sampling of alleles according to their frequency in the LH<sub>M</sub> population (green surface). The median number of pseudo-candidates across permuted datasets was equal to 1000. The dashed red line indicates the observed number of candidate antagonistic SNPs that are covered in the population genomic data used for simulated sampling (N=4071). **B**, Distributions of the number of perfectly segregating (PS) sites as a function of the number of haplotypes swapped between fitness classes (0 = original fitness classes). The red points depict the median number of PS sites for each swapped category.

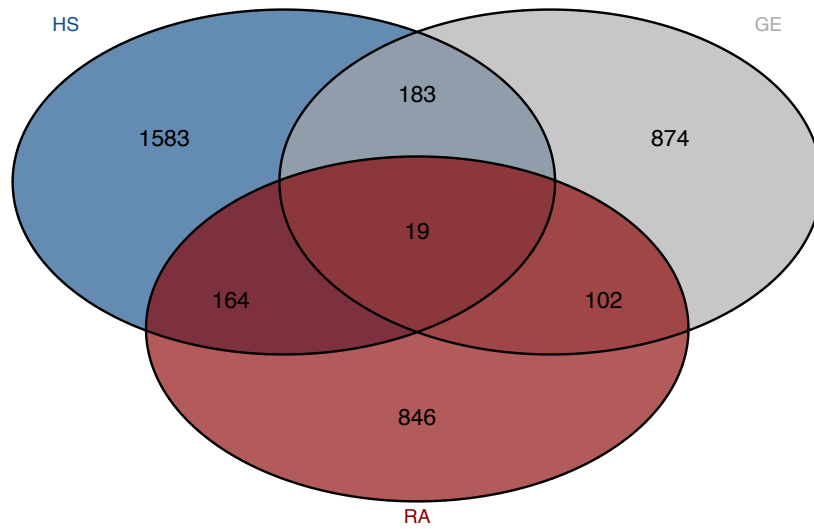


**Figure 2.5: Association of candidate genes with previous analyses of sexual antagonism.** Overlap in the number of sexually antagonistic genes identified here through haplotype sequencing (HS, blue), a previous analysis of antagonistic gene expression (GE, grey, Innocenti and Morrow (2010)), and a previous association of genes with the resolution of sexual antagonism (RA, red, Collet et al. (2016)).

## Chapter 3

# Elucidating the functional properties of sexually antagonistic loci in *Drosophila melanogaster*

*A subset of the analyses presented in this chapter were included in a manuscript, submitted to Nature Ecology and Evolution, with me as first author—see Appendix A.*

### 3.1 Abstract

Sex-specific adaptation towards divergent phenotypic optima is hindered by the shared genome of males and females. In this situation selection favours the invasion of sexually antagonistic alleles, with opposing fitness consequences in each sex. Despite the broad taxonomic distribution and evolutionary importance of sexual antagonism, we still have little knowledge of the basic biological processes that underlie it. Fundamentally, it is still unknown whether sexual antagonism is mainly rooted in coding or regulatory sequence variation. To address this, I here use the sexually antagonistic loci, that I identified in the preceding chapter (chapter 2), in combination with publicly available data to perform a series of bioinformatic analyses. I present evidence that is consistent with a predominantly regulatory basis to sexual antagonism. I find that sexually antagonistic SNPs are enriched up- and down-stream of genes and in 3' UTR regions. In addition, I find several lines of evidence that antagonism is associated with specific branches of the regulatory network. Thus, upstream regions of antagonistic genes are enriched for binding sites of specific transcription factors, and sexually antagonistic SNPs are preferentially located within a number of specific TF binding motifs. Interestingly, there are also a number of specific associations with the sex-determination / sexual differentiation cascade. Taken together, my results place gene regulation at the core of sexual antagonism and suggest that the biggest hurdle to the resolution of antagonism is the need to acquire sex-specific regulation.

## 3.2 Introduction

The shared genome of males and females hinders sex-specific adaptation towards divergent phenotypic optima for homologous traits. In this situation, selection favours the invasion of sexually antagonistic (SA) alleles, which have opposing fitness consequences in each sex, effectively moving one sex closer toward its phenotypic optimum while further displacing the other (Rice 1984; Bonduriansky and Chenoweth 2009; Van Doorn 2009; Connallon and Clark 2011). SA variation has now been documented across a broad range of species including: mammals (Mokkonen et al. 2011), birds (Tarka et al. 2014), reptiles (Svensson et al. 2009), insects (Rice 1992; 1998; Berger et al. 2014) fish (Roberts et al. 2009; Barson et al. 2015) and plants (Delph et al. 2011). However, despite this apparent ubiquity, we still have little idea of the biological processes that underlie it.

One fundamental question that remains unaddressed concerns the relative contributions of coding and regulatory sequence variants to antagonistic polymorphism. Indeed, the relative importance of coding and regulatory changes for fitness variation and adaptive evolution in general has been the subject of much debate (King and Wilson 1975; Hoekstra and Coyne 2007). Results from a series of genetic mapping experiments offer contrasting views, with some supporting a dominant role of regulatory variation (e.g. Carroll 2005; Wray 2007; Jones et al. 2012) and others refuting this idea (see Hoekstra and Coyne (2007), for review).

These fundamental properties have important implications for the evolutionary dynamics of sexual antagonism, and in particular the mechanisms that decouple intersexual genetic correlations ( $r_{MF}$ ) and resolve the conflict. Theoretically, sexual antagonism could be mitigated by a number of mechanisms including the duplication and subsequent sex-specific regulation of the antagonistic genes (Connallon and Clark 2011), sex-specific splicing (Pennell and Morrow 2013), genomic imprinting (Day and Bonduriansky 2004), and sex-dependent dominance (Kidwell et al. 1977; Barson et al. 2015). The biological

properties of SA alleles will have a bearing on which of these mechanisms, if any, are likely to be effective in resolving conflict. For example, the resolution of sexual antagonism over protein-coding sequence (where alternative protein isoforms are favoured in each sex) would require both gene duplication or the addition of a novel alternative splice site, as well as the subsequent evolution of sex-specific regulation (Stewart et al. 2010). In contrast, conflict over gene expression may be easier to resolve, here the major limit to resolution will be the acquisition of sex-specific regulation and thus fewer mutational steps may be required (Stewart et al. 2010).

While the resolution of conflict over gene expression may require fewer mutational steps, additional biological properties could also play an important role in determining the timescale over which this conflict is likely to persist. For example, pleiotropic interactions could hinder the resolution of sexual antagonism because resolving conflict over one function of a gene may negatively impact upon another function (Ellegren and Parsch 2007; Mank et al. 2008). This has received some empirical attention. Mank et al. (2008) examined sex-biased expression and tissue-specificity of genes across mouse and chicken genomes. They found a consistent trend whereby the most broadly expressed genes (indicative of the greatest levels of pleiotropy) were those which also had relatively unbiased expression across the sexes. In this study the authors used unbiased expression profiles as a proxy for ongoing sexual antagonism. This is because mechanisms which up- or down-regulate genes according to the sex in which they are expressed in would enable expression levels to better match sex-specific optima and thus reduce sexual conflict. Accordingly, we expect genes with the strongest ongoing antagonism to have relatively equivalent expression levels in each sex. However, unbiased patterns of expression could also simply reflect a lack of divergent selection and thus not be tied to sexual antagonism at all. Additional empirical work is needed to establish a more direct link between sexual antagonism and pleiotropy.

The differential role of genes throughout development also introduces a

potential source of constraint on the resolution of sexual antagonism (Pennell and Morrow 2013). This is because genetic changes that mitigate conflict at one life stage may have deleterious consequences at other life stages. Overall, the question of how sexual antagonism plays out throughout development remains understudied. It has been suggested that sexual antagonism should be predominantly manifested at adult life stages, where sex roles truly diverge (Chippindale et al. 2001; Cox and Calsbeek 2009). This is supported by some studies which find no evidence for sexual antagonism in *Drosophila* larvae (e.g. Long and Rice 2007). However, sex-specific processes are known to occur at various developmental stages (Pennell and Morrow 2013) and pre-adult developmental processes can have fitness consequences at later life stages. Moreover, a recent experiment found evidence for SA expression patterns at pre-adult life stages (Ingleby et al. 2016).

As well as questions over the functional properties of SA alleles, we also have limited knowledge of the general traits involved in sexual antagonism. This is for two key reasons. First, many studies examine global patterns of male and female fitness variation and thus do not capture the action of specific individual traits, just their collective impact on fitness (Chippindale et al. 2001; Foerster et al. 2007). For example, Chippindale et al. (2001) sampled 40 haploid genomes from a laboratory adapted *D. melanogaster* population and measured their fitness in both male and female genetic backgrounds. They found genotypes that conferred high fitness in one sex usually conferred low fitness in the other. While this provides convincing evidence for substantial SA fitness variation, it cannot partition this variation across specific traits.

Second, studies that do take a trait-focused approach can only be informative about the specific trait examined and not others. For example, a series of studies have now characterised a number of individual SA traits, including colouration in fish (Roberts et al. 2009), immune response in lizards (Svensson et al. 2009) and locomotory activity in fruitflies (Long and Rice 2007). While these and other studies have been important in advancing our knowl-

edge of which phenotypic traits contribute to SA variation, there are some important caveats to note. Firstly, to convincingly show that a trait is under sexually antagonistic selection requires reliable measures of both fitness and trait variation. This means that those traits that have been characterised represent those that are reliably measured in species/populations where fitness is relatively tractable. Overall, this means that we likely have an incomplete and potentially biased view of the diversity of traits that could contribute to SA variation for fitness. Secondly, by characterising only a single trait, one likely only captures a small proportion of the total amount of SA variation segregating within a population.

Having identified genome-wide putative causal SA loci in chapter 2 now allows me to address some of the questions detailed above. The breadth of this dataset enables a general evaluation of the biological mechanisms that underlie a large proportion of the SA genetic variation within the  $LH_M$  population, generating insight into the general functional properties of SA loci as well as the biological processes encapsulated in sexual antagonism. My results suggest that sexual antagonism is rooted in developmental regulation and associated with a number of specific cis-regulatory elements. Interestingly, I find multiple associations with sexual differentiation, the most notable of which was a number of SNPs mapping to *fruitless*, a gene at the core of sex-specific development. I find little evidence to support pleiotropy as an important mechanism for maintaining SA variation. I did, however, find evidence that SA genes are expressed throughout development. Taken together, these results suggest the rate at which sex-specific regulation can evolve is the major limiting factor to the evolution of sexual dimorphism.

## **3.3 Materials and Methods**

### **3.3.1 Sexually antagonistic SNP data**

The SA loci characterised here were previously identified in Chapter 2. Briefly, I sequenced hemiclinal lines with opposing sex-specific fitness profiles, 5 male-

beneficial/female-detrimental (MBFD) and 4 female-beneficial/male detrimental (FBMD). Informative SNPs were identified as those loci where variants were polymorphic across the nine hemiclinal genomes. SA SNPs were then defined as those informative SNPs where all MBFD hemiclinal genomes were fixed for one allele and all FBMD hemiclinal genomes were fixed for the other allele ('perfectly segregating'). Full details are given in section 2.3. Analyses of the SA SNPs revealed that I identified many more than expected by chance (FDR 15-20%). Furthermore, they showed a number of non-random properties that support their credibility as SA candidates. Namely, they were significantly clustered along chromosome arms, enriched in genic regions, and overlapped significantly with previous analyses of sexual antagonism.

### **3.3.2 Functional roles of SA loci**

I used the Variant Effect Predictor (Ensembl VEP, McLaren et al. (2010)) to infer the genetic consequences of informative SNPs. To assess the relative representation of each genetic consequence among SA SNPs I compared the number of occurrences of each consequence among SA SNPs to the total number across all informative SNPs. From this I used one sample Z-tests to determine the significance of over-/underrepresentation of individual variant consequences.

I also used the VEP to map informative SNPs to genes. In accordance with the VEP default settings, I included extended gene regions ( $\pm 5$ kb of gene coordinates) in my gene definitions. To gain preliminary insights into the functions of antagonistic genes I used the Gorilla (Eden et al. 2009) Gene Ontology tool, and applied false discovery rate (FDR) to correct for multiple testing across many GO terms. Here, all genes covered in the full informative SNP dataset were used as the background set.

### **3.3.3 Regulatory functions of SA loci**

To compare the number of antagonistic and non-antagonistic transcription factor genes, I annotated all genes in my dataset that encode transcription

factors, using the supervised regulatory network data from Marbach et al. (2012), which defines 617 putative transcription factors. I further mapped SNPs to cis-regulatory modules (CRMs) annotated on REDfly (Gallo et al. 2011) and compared the number of candidate and non-candidate SNPs falling within CRMs. In both cases  $\chi^2$  tests were used to determine significance of the observed overlap.

To assess antagonistic genes for signatures of shared regulation I used the Motif Enrichment Tool (Blatti and Sinha 2014) with default settings, to search regions 5kb upstream of the transcription start sites for enriched motifs. Here again, all genes covered in my SNP dataset were used for the background set. I applied FDR corrections to P-values to account for the testing of multiple motifs. To test for motif enrichment close ( $\pm 20$ bp) to antagonistic SNPs, I used the Centrimo tool from MEMESuite (Bailey et al. 2009) with default settings. I generated the input FASTA files using bedtools (Quinlan and Hall 2010) and extracted the sequences ( $\pm 20$ bp) flanking the SNPs in my dataset from the *D. melanogaster* reference genome (BDGP 5.5). I used flanking sequences for all informative SNPs to generate the background model and the flanking sequences of antagonistic SNPs as the target set.

### **3.3.4 Sex-biased gene expression**

To examine the relationship between antagonistic genes and sex-biased gene expression I used the Sebida online database (Gnad and Parsch 2006) to annotate genes covered in my SNP dataset as having either sex-biased or unbiased expression status, based on the meta-class identifier. I then used a  $\chi^2$  test to compare the sex-biased expression status of antagonistic and non-antagonistic genes. To test how the quantitative degree of sex-bias in expression differs between candidate and non-candidate genes, I took the absolute values of the log-transformed male/female sex ratio score, thereby summarising male and female bias into a single variable. I then tested how variation in this bias variable is explained by candidate status using a general linear model (glm) with Gaussian error structure and square-root transformed response variable

to improve model fit.

### 3.3.5 Expression of genes across tissues and developmental stages

I compared expression breadth (a proxy for pleiotropy McShea 2000) between candidate and non-candidate genes using the tissue-specificity index ( $\tau$ ). I used FlyAtlas (Chintapalli et al. 2007) expression data after removing gonadal tissues (to ensure that only tissues that are present in both sexes contributed to the measures of  $\tau$ ) to get average expression values for each tissue and then calculated  $\tau$  as:

$$\tau = \frac{\sum_{i=1}^n (1 - \hat{x}_i)}{n - 1},$$

where  $\hat{x}_i = \frac{x_i}{\max(x_i)}$  is the proportional expression level of the gene in tissue  $i$  and  $n$  is the number of tissues. Once values of  $\tau$  had been calculated for all genes covered in the main dataset I compared  $\tau$  for candidate and non-candidate genes using a Wilcoxon rank-sum test.

As an additional proxy for pleiotropy I examined the number of protein-protein interactions (PPIs) between candidate and non-candidate genes. I used the physical interactions table from FlyBase (Gramates et al. 2017) to summarise the total number of PPIs for all genes covered in the haplotype sequencing and then compared candidate and non-candidate genes using a general linear model with quasipoisson error structure to account for overdispersion.

I compared expression of candidate and non-candidate genes across developmental stages by calculating a life stage specificity index (LSI). This index was calculated in a way analogous to the calculation of  $\tau$ . Here, I used data from the modENCODE project (Celniker et al. 2009) to obtain expression values for each gene at each developmental stage and then calculated  $LSI$  as:

$$LSI = \frac{\sum_{i=1}^n (1 - \hat{x}_i)}{n - 1},$$

where  $\hat{x}_i = \frac{x_i}{\max(x_i)}$  is the proportional expression level of the gene at developmental stage  $i$  (relative to its maximum expression level across all developmental stages) and  $n$  is the number of developmental stages. Once values of LSI had been calculated for all genes covered in the main dataset, I compared LSI for candidate and non-candidate genes using a Wilcoxon rank-sum test.

To test whether candidate and non-candidate genes were expressed differently over the course of development I first removed those genes with no expression across developmental stages. I then fitted a general linear model with Gaussian error structure to test how variation in gene expression (RPKM) was explained by the interaction between developmental stage and candidate status. I  $\log_2$  transformed the response variable to improve model fit.

### 3.3.6 Statistical analysis and plotting

All statistical analyses were conducted in R version 3.2.3. Plots were produced with the ggplot2 package (Wickham 2009).

## 3.4 Results

### 3.4.1 Functional roles of candidate loci

In order to gain insights into the general functions of antagonistic candidate genes, I performed a Gene Ontology (GO) analysis. Overall, the 1,949 candidate genes were enriched for processes relating to development, morphogenesis, and metabolism (Figure 3.1). As well as these term-by-term analyses I additionally examined functional clusters of gene ontology terms. Here, the top five annotation clusters were associated with, body morphogenesis, metabolic processes, cuticle development, enzyme catalysis, and regulation of development, respectively (Table 3.1).

To assess the relative contribution of coding and regulatory variation to

the generation of sexual antagonism, I examined the genetic consequences of candidate SA SNPs relative to all informative SNPs. In terms of absolute numbers, there were many more potential regulatory variants than there were missense variants (Table 3.2). Enrichment analyses further showed that SA SNPs did not cause missense changes more frequently than expected from the entire SNP dataset (if anything, they were marginally underrepresented), but SA SNPs were enriched in specific genic regions, in particular up-/downstream regions and 3'-untranslated regions (Figure 3.2). These regions are known to be associated with expression regulation, suggesting that antagonism predominantly arises owing to adaptive conflict over gene expression, rather than over coding sequence.

### 3.4.2 Regulatory functions of SA loci

To better resolve the potential regulatory functions of SA loci I examined their overlap with annotated trans- and cis-regulatory elements. First, I looked at the relative representation of transcription factor genes (TFs) among candidate SA genes. While there were more TFs than expected, the trend was not significant (observed number of candidate TFs = 86, expected number of candidate TFs = 75,  $\chi_1^2 = 1.6$ ,  $P = 0.202$ ). Thus, sexual antagonism does not appear to be preferentially associated with trans-regulatory effects. I next mapped all informative SNPs to cis-regulatory modules (CRMs) annotated on RedFly (Gallo et al. 2011). Here, the number of candidate SNPs mapping to CRMs was, again, greater than expected but marginally non-significant (observed number of SA SNPs in CRMs = 708, expected number of SA SNPs in CRMs = 662,  $\chi_1^2 = 3.5$ ,  $P = 0.061$ ), showing that SA variation was not generally enriched in cis-regulatory regions either.

While I failed to detect significant global enrichment of candidate loci in trans- and cis-regulatory elements, this does not mean that individual associations are unimportant. This is because some associations will have a greater functional impact than others. For example, SA polymorphisms at central positions in gene networks might have much larger fitness consequences than

those at the periphery. Here, the CRMs with the greatest abundance of SA SNPs are upstream of important TFs such as *Ultrabithorax* (*Ubx*, 18 SA SNPs), *abdominal-A* (*abd-A*, 9 SA SNPs), *Dichaete* (*D*, 9 SA SNPs) and *decapentaplegic* (*dpp*, 8 SA SNPs). This suggests that although globally SA loci are not enriched in trans- and cis- regulatory elements there are several important associations with potentially large effects on the expression of many downstream genes.

I also tested for significant associations with specific cis-regulatory functions. I first examined the upstream regions of candidate genes for enriched binding site motifs of known TFs. Here I found 114 binding sites, corresponding to 93 unique TFs, enriched upstream of antagonistic candidate genes (FDR $\leq$ 5%, Table 3.3). This analysis highlights that there are signatures of shared regulation among the candidate genes, with many genes responding to common upstream TFs. To more specifically place candidate SNPs among TF binding sites I next tested short flanking sequences (+/- 20bp) centered around candidate SNPs for significant enrichment of annotated binding sites. These flanking sequences were centrally enriched for the binding sites of 8 TFs (Table 3.4). This highlights key regions where SA SNPs are most likely to have an impact on gene regulation.

### 3.4.3 Sex-biased gene expression

To explore patterns of sex-biased gene expression I used publically available data from the Sebida database (Gnad and Parsch 2006). In line with prior expectations I found that sex-biased genes were marginally but significantly underrepresented among candidate genes (observed overlap between sex-biased and candidate genes= 950 , expected overlap= 1011 ,  $\chi_1^2= 11.6$ ,  $P<0.001$ ). This pattern is also observed when considering the degree of sex bias rather than just assigning genes qualitatively to categories of biased and unbiased expression. Thus, candidate genes have a subtle but significantly lower quantitative degree of sex bias (mean=0.619) compared to non-candidate genes (mean=0.644,  $F_{1,10600} = 4.82$ ,  $P=0.022$ , Figure 3.3). This means that even

when SA genes do have sex-biased expression profiles, they are less biased, on average, than non-candidate genes.

#### **3.4.4 Expression of genes across tissues and life stages**

To directly test the relationship between pleiotropy and antagonism, I compared SA candidate and non-SA candidate genes in terms of their breadth of expression across tissues, a proxy for the action of pleiotropy (McShea 2000). In contrast to prior empirical findings (Mank et al. 2008), antagonistic genes are, on average, more tissue-specific in their expression patterns than non-candidate genes ( $W=7837600$ ,  $P<0.001$ , Figure 3.4). This apparent lack of pleiotropy was confirmed when using protein-protein interactions (PPIs) as an alternative proxy for pleiotropy. Here, I found no difference in the number of PPIs between candidate and non-candidate genes ( $F=0.1695$ ,  $P=0.681$ ).

To examine the expression of SA genes across developmental stages I utilised the modENCODE dataset (Celniker et al. 2009). Overall, many of the candidate genes were expressed at pre-adult developmental stages. Interestingly however, the expression of candidate genes was more strongly concentrated on specific developmental stages than the expression of non-candidate genes ( $W=10029000$ ,  $P<0.001$ , Figure 3.5). Thus, candidate genes are more highly expressed than non-candidate genes during late embryonic development (18-20 hour embryo) ( $t=2.465$ ,  $P=0.014$ , Figure 3.6), while at other times during development candidate genes tend to be expressed at lower levels than non-candidates.

### **3.5 Discussion**

While the number of studies that identify individual SA traits across many species is ever increasing, a general understanding of the biological processes that generate antagonism is currently lacking. Identifying the first genome-wide list of SA candidate SNPs in chapter 2 allowed me to address this by characterising the biological properties of the genome-wide SA genetic variation in a laboratory adapted population of *D. melanogaster*. Below I discuss,

in turn, the major findings of the work contained within this chapter.

Previous work has made explicit links between expression regulation and sexual dimorphism (Ellegren and Parsch 2007) and there have also been associations between expression variation and sex-specific fitness in *D. melanogaster* (Innocenti and Morrow 2010). However, until now it has been unclear whether sexual antagonism is primarily rooted in regulatory or coding variation, a question that has been discussed more widely in the context of phenotypic evolution (King and Wilson 1975; Hoekstra and Coyne 2007). Here, I was able to show that SA SNPs did not cause missense changes more often than expected. Instead, SA SNPs were enriched up- and downstream of genes and within 3'-UTR regions, suggesting a prominent role in gene regulation. Moreover, I detected a number of specific cis-regulatory associations that paint a picture of sexual antagonism clustering in specific branches of regulatory cascades.

In chapter 2 I discussed the potential shortcomings of a previous genome-wide approach to identifying sexually antagonistic genes in *D. melanogaster* (Innocenti and Morrow 2010). This was on the basis that that study could not differentiate between causal antagonistic loci and loci that were simply responding to upstream regulators which themselves really harboured the causal polymorphism. In the light of my findings of a significant regulatory basis to sexual antagonism, it is likely that their approach has in fact succeeded in capturing a proportion of the total sexual antagonism for adult fitness in the LH<sub>M</sub> population. This is supported by the significant overlap that I reported in chapter 2 between the candidate genes that were identified in their and my approaches. It is also notable, however, that while many genes did overlap there were also a significant amount of genes which did not do so. This could be for a number of (non-mutually exclusive) reasons. For example, the large number of genes they identify as having antagonistic expression patterns but which are not identified as harbouring antagonistic variation here could suggest that much of the causal SA variation might segregate upstream, in the regulators of the genes that exhibit SA expression patterns. In addition, I

found enriched developmental GO terms as well as greater expression of SA genes than other genes at specific developmental stages. This suggests that by focussing specifically on adult gene expression, Innocenti and Morrow (2010) may have missed developmental SA genes that operate during pre-adult life stages. The importance of developmental regulation in SA that I report also introduces another possible confounding effect in the previous expression analysis, namely that some of the expression differences that Innocenti and Morrow (2010) document could be generated by differences in anatomy. Thus, the size of the tissues, influenced by pre-adult developmental processes, where these genes are expressed could confound the analysis.

Having found a prominent regulatory basis to sexual antagonism in this *D. melanogaster* laboratory population, an obvious question arises as to how general this association is likely to be. Given the absence of equivalent genome-wide analyses in other species, one indirect way to assess this is to re-examine previously identified sexually antagonistic traits. Although there are only a few cases where the genetic basis of an SA trait has been mapped these are informative in the light of my new findings. For example, Roberts et al. (2009) mapped the genetic basis of a SA colouration trait in Lake Malawi Cichlids. They found that the causal locus was a cis-regulatory variant upstream of the *pax7* gene (see section 1.6 for more information). Another example comes from *D. melanogaster*, where resistance to DDT (dichlorodiphenyltrichloroethane) is SA when in the absence of the pesticide. Here, resistance is attributed to single transposable elements insertion in the promoter region of the gene *cyp6g1* (Daborn et al. 2002) (see Section 1.6 for more information). Unlike the previous two examples, another study (Barson et al. 2015) found that a large proportion of the variation in age at maturity in Salmon was explained by a missense SNP at the *VGLL3* locus. Age at maturity in Salmon is under opposing selection in each sex with earlier maturation favoured in females than males. Taken together, although the list of SA traits is necessarily biased by ease of study, many of them are likely have a major regulatory component,

consistent with the regulatory bias observed here. This suggests that the present findings are not just artefactual outcomes in a single species but likely correspond to general features of sexual antagonism across species and taxa.

Unfortunately, assessing the relative role of cis- and trans- regulatory variants to the generation of sexual antagonism is beyond the scope of this study. In general, trans-regulatory elements are more poorly characterised than cis-regulatory elements in *Drosophila* (Gallo et al. 2011). Furthermore, the topologies of gene regulatory networks in *Drosophila* are still poorly understood, making it difficult to empirically investigate where SA really sits in regulatory cascades. Indeed, we currently do not even have a theoretical expectation of when and where SA polymorphisms will invade and be maintained within gene regulatory networks, whether in cis-, at a gene directly under SA selection, or further up in the regulatory hierarchy. These questions are addressed in chapter 5 of this thesis.

My analyses suggest that regulatory variation is dominant in generating sexual antagonism, with no global enrichment of missense changes. However, it is highly improbable that there is no conflict at all over coding sequence. Indeed, a total 241 SA SNPs were characterised as causing missense changes, corresponding to 150 genes. Although there was no overall enrichment of specific GO terms among these genes, several contained multiple SA missense SNPs. Those containing the greatest concentration of SA missense SNPs were: *mutagen-sensitive 312* (*mus312*, 12 SA missense SNPs), *CG3502* (7 SA missense SNPs), *Tequila* (*Teq*, 6 SA missense SNPs), *lame duck* (*lmd*, 5 SA missense SNPs), and *Hemolectin* (*Hml*, 5 SA missense SNPs). Interestingly two of these, *Teq* and *Hml* are both important for chitin binding, recapitulating the enrichment for chitin process GO terms in the full SA gene set.

Overall, functional terms relating to body morphogenesis and chitin / cuticle development were heavily enriched among the candidate genes and individual associations were also present among genes containing multiple missense variants (e.g. *Teq*) and binding sites enriched for SA SNPs (e.g. *Mes2*). Infer-

ring more specific traits from an enrichment of cuticle development GO terms is difficult. However, one interesting possibility is that pigmentation traits may be involved in sexual antagonism in *Drosophila*. Indeed, it is known that pigmentation is highly sexually dimorphic in *Drosophila* (Kopp et al. 2000). This could imply that the current levels of sexual dimorphism in pigmentation do not represent males and females at their respective optima but instead are an example of ongoing antagonism. This constitutes an interesting hypothesis to test with future empirical study. As a very first step towards this it would be possible to examine haplotypes with similar antagonistic fitness effects to those sequenced here and quantify variation in various pigmentation traits. If the variation in pigmentation could be explained by the sex-specific fitness profiles of the haplotypes this could provide strong evidence that pigmentation plays a role in generating sexual antagonism.

I also find numerous functional associations for terms in the context of nutrient processing. SA genes are enriched for the GO terms ‘aminoglycan metabolic process’, ‘amino sugar metabolic process’, and ‘carbohydrate derivate metabolic process’. In addition, SA SNPs are centrally enriched in the binding sites for two TFs important for nutrient processing (*Ets at 97D* and *slow border cells*). This association of sexual antagonism and aspects of nutrient processing fits well with previous empirical studies that show that males and females have divergent nutritional requirements but suffer from genetic constraint on the evolution of sex-specific dietary choice (Maklakov et al. 2008; Reddiex et al. 2013; Jensen et al. 2015). For example, Maklakov et al. (2008) measured male and female reproductive performance in field crickets *Teleogryllus commodus* when reared on diets containing differing ratios of carbohydrate and protein. They found that fitness was maximised in very different regions of the nutritional landscape in each sex and that although there was some degree of dimorphism in dietary preference, this did not allow the sexes to simultaneously reach their respective nutritional optima.

The narrower expression patterns of SA genes compared to non-SA genes

in terms of the number of tissues that they are expressed in contrasts with previous work suggesting that the resolution of sexual antagonism is impeded by pleiotropy (Mank et al. 2008). However, there are two important caveats to consider with this previous association. First, antagonism was indirectly inferred by the lack of sex-biased gene expression. However, this is not a reliable proxy for antagonism, because unbiased patterns of expression could also simply reflect a lack of divergent selection and thus not be tied to sexual antagonism at all. Second, using  $\tau$  as a measure of pleiotropy can be unreliable in isolation. The use of breadth of expression as a proxy for pleiotropy postulates that those genes expressed in a greater number of tissues are more pleiotropic, owing to a higher likelihood of having multiple functions. Of course this may not always or even often be the case, meaning that a non-pleiotropic gene may be broadly expressed across tissues, performing the same function in each of them. Here, I avoided both of these shortcomings. I was able to analyse true SA candidate genes, rather than inferring antagonism indirectly from (the lack of) sex-biased expression. In addition, I used more than one proxy for pleiotropy, expression breadth and the number of protein-protein interactions of candidate and non-candidate genes, in order to increase the robustness of my conclusions. Doing so, I found no significant difference between the two gene classes. My analyses therefore provide little or no evidence that pleiotropy is an important mechanism to maintain SA genetic variation.

To date most research on sexual antagonism has focused on conflict at adult life stages. Indeed, one might expect that sexual antagonism should be greatest at these life stages as this is when sex-roles are most divergent. In line with this idea, Chippindale et al. (2001) documented a significant negative  $r_{mf}$  for fitness in *D. melanogaster* adults, reflecting sexual antagonism. However, when they calculated  $r_{mf}$  for larval fitness they found it to be significantly positive, suggesting that at larval life stages the fitness optima of the two sexes are aligned. Prasad et al. (2007) used a different approach and performed sex-limited experimental evolution whereby hemiclinal genomes were

exclusively paternally inherited. Their results on adult fitness matched those of Chippindale et al. (2001), after 25 generations of selection males carrying the evolved genomes (ML-genomes) had increased fitness whereas the fitness of females carrying the same genomes had decreased relative to the controls. Interestingly however, they also found concordant changes in pre-adult growth rates. Specifically, they found that flies (both males and females) carrying ML-genomes had significantly longer developmental times than those with control genomes - a shift towards the male optimum. To what extent the findings of these two studies are comparable is questionable, however, owing to the largely different proxies of juvenile fitness employed. Chippindale et al. (2001) used egg-to-adult viability as a measure of juvenile fitness while Prasad et al. (2007) used larval growth rates. While viability is expected to capture a large amount of total fitness variation, it omits aspects of condition upon eclosion which may have dramatic fitness consequences. In accordance with the findings of Prasad et al. (2007), I found that many SA genes were expressed throughout pre-adult life stages. The widespread expression of SA genes throughout development suggests that developmental pleiotropy may be a significant source of constraints that prevent the resolution of sexual antagonism. Moreover, the patterns of expression for candidate and non-candidate genes were significantly different. In particular, candidate genes were expressed more highly than non-candidate genes during late embryonic development (18-20hr old embryo). While it is not possible to differentiate between scenarios where sexual antagonism is generated over larval performance or where these expression patterns reflect developmental processes that affect adult phenotypes, these findings underscore the importance for future studies of reconsidering the importance of sexual antagonism throughout development.

Interestingly, I found a number of associations between antagonistic SNPs and regulatory elements involved in sexual differentiation. Thus, in terms of cis-regulation, the binding targets for 5 SD genes were enriched upstream of SA genes, including *hermaphrodite*, and *anterior open*. Further, SA SNPs were

centrally enriched in binding sites for *cut*. Candidate TF genes include several that relate to sexual differentiation (SD), notably: *abdominal A*, *Abdominal B*, *bric a brac 2*, and again *anterior open*. Of particular note among these associations is *fruitless*, a direct target of the *Drosophila* sex determination cascade which plays an essential role in physiology and behaviour as well as specifying a sexually dimorphic nervous system (Kimura et al. 2005; Vilella and Hall 2008). Multiple SA SNPs were clustered around the *fruitless* P1 promoter from which sex-specific isoforms of FRU are produced (Neville et al. 2014). In *D. melanogaster* a total of three different male-specific FRU isoforms are produced. Male-specific *fru* transcripts help to specify a sexually dimorphic nervous system and are expressed in approximately 3% of central-nervous-system neurons, helping to promote male sexual behaviour (Neville et al. 2014). Unlike male-specific FRU isoforms, female-specific *fru* transcripts are not translated so that no functional protein is produced (Usui-Aoki et al. 2000). It is, however, possible that female-specific transcripts of *fru* have hitherto uncharacterised regulatory functions. The abundance of SA SNPs near the P1 promoter suggests that if these are causal variants at *fru* then they operate by modulating promoter activity, effectively altering the expression of the sex-specific transcripts.

The possibility that some of the adaptive conflict between males and females is generated by variation in key regulators of sexual differentiation has been previously suggested (Collet et al. 2016). My study provides additional support for this hypothesis and further suggests that SA variation could reach the very top of the sexual differentiation regulatory cascade. Overall, this suggests that the major constraint on the evolution of sexual dimorphism is the speed at which genes can acquire sex-specific regulation. This idea is consistent with the twin observations of the lower incidence and smaller absolute levels of sex-biased expression of SA genes, compared to the rest of the genome. The constraint of the speed of acquisition of sex-specific regulation of genes could then drive the invasion of SA alleles across developmental regulatory cascades,

enabling them to permeate to central positions of the network, as in the case of *fruitless*. At one level the idea that SA alleles can invade regions subject to strong purifying selection is somewhat surprising. However, given that mutations in these regions can impact many aspects of both male and female phenotypes simultaneously, it is clear that those locations are where SA alleles can generate the large and balanced fitness effects characteristic of long lived antagonistic polymorphisms (Connallon and Clark 2012; Mullon et al. 2012).

In conclusion, the results presented here constitute important advances in our understanding of the functional genetic basis of sexual antagonism and subsequently help us to understand the evolutionary dynamics of SA alleles. They place gene regulation at the core of sexual antagonism and also suggest that the biggest hurdle to the resolution of antagonism is the need to acquire sex-specific regulation. In addition, these results highlight that antagonism unfolds throughout development rather than being confined purely to the adult life-history stage. Finally, these results also serve as a useful guide for future validation attempts. In particular, they suggest that approaches which manipulate expression levels of candidate SA genes could be an effective means of validation.

## 3.6 Tables and Figures

**Table 3.1:** Results from GO cluster analysis. Shown are top five annotation clusters.

Cluster	Category	Term	P-value
1	GOTERM_BP_DIRECT	GO:0010171_body morphogenesis	2.80E-07
1	GOTERM_MF_DIRECT	GO:0005214_structural constituent of chitin—based cuticle	1.38E-06
1	GOTERM_CC_DIRECT	GO:0005578_proteinaceous extracellular matrix	2.41E-06
2	GOTERM_BP_DIRECT	GO:0006520_cellular amino acid metabolic process	2.86E-05
2	GOTERM_MF_DIRECT	GO:0070573_metalloprotease activity	6.76E-04
2	GOTERM_MF_DIRECT	GO:0004046_aminoacylase activity	6.76E-04
2	GOTERM_BP_DIRECT	GO:0043171_peptide catabolic process	0.080
3	GOTERM_BP_DIRECT	GO:0040003_chitin—based cuticle development	2.68E-06
3	GOTERM_MF_DIRECT	GO:0008010_structural constituent of chitin—based larval cuticle	0.100
3	GOTERM_MF_DIRECT	GO:0042302_structural constituent of cuticle	0.310
3	GOTERM_CC_DIRECT	GO:0031012_extracellular matrix	0.480
4	GOTERM_MF_DIRECT	GO:0004058_aromatic—L—amino—acid decarboxylase activity	0.001
4	GOTERM_MF_DIRECT	GO:0016831_carboxy—lyase activity	0.054
4	GOTERM_MF_DIRECT	GO:0030170_pyridoxal phosphate binding	0.072
5	GOTERM_BP_DIRECT	GO:0045570_regulation of imaginal disc growth	0.021
5	GOTERM_BP_DIRECT	GO:0048636_positive regulation of muscle organ development	0.034
5	GOTERM_BP_DIRECT	GO:0061327_anterior Malpighian tubule development	0.064

**Table 3.2:** Frequency of different variant consequences for all SNPs covered in the haplotype sequencing.

Consequence	Total frequency	Candidate frequency
3_prime_UTR_variant	44078	329
5_prime_UTR_variant	28269	194
downstream_gene_variant	734429	5310
initiator_codon_variant	54	1
intergenic_variant	122727	723
intron_variant	519734	2882
intron_variant,non_coding_transcript_variant	4071	41
missense_variant	39123	241
missense_variant,splice_region_variant	317	3
non_coding_transcript_exon_variant,non_coding_transcript_variant	5403	44
splice_region_variant,5_prime_UTR_variant	304	3
splice_region_variant,intron_variant	7810	62
splice_region_variant,synonymous_variant	916	4
stop_gained	201	1
synonymous_variant	115632	754
upstream_gene_variant	792114	5485

**Table 3.3:** Enriched motifs upstream of candidate genes

Motif name	Associated gene	FDR q-value
fkh_NAR_FBgn0000659	FBgn0000659	0.003776376
sv_SOLEXA_5_FBgn0005561	FBgn0005561	0.003776376
Exd_Cell_FBgn0000611	FBgn0000611	0.003776376
sug_SOLEXA_5_FBgn0033782	FBgn0033782	0.003776376
Achi_SOLEXA_FBgn0033749	FBgn0033749	0.003776376

klu_SOLEXA_5_FBgn0013469	FBgn0013469	0.003776376
Vis_SOLEXA_FBgn0033748	FBgn0033748	0.003776376
Lag1_Cell_FBgn0040918	FBgn0040918	0.003776376
Ets97D_SANGER_10_FBgn0004510	FBgn0004510	0.005398254
run_Bgb_NBT_FBgn0003300	FBgn0003300	0.005931458
Exd_SOLEXA_FBgn0000611	FBgn0000611	0.005931458
tup_SOLEXA_10_FBgn0003896	FBgn0003896	0.005931458
run_Bgb_NBT_FBgn0013753	FBgn0013753	0.005931458
slp2_SANGER_5_FBgn0004567	FBgn0004567	0.008626561
Eve_SOLEXA_FBgn0000606	FBgn0000606	0.009333028
CG3407_SANGER_2.5_FBgn0031573	FBgn0031573	0.009333028
dl_FlyReg_FBgn0000462	FBgn0000462	0.009333028
Mes2_SANGER_5_FBgn0037207	FBgn0037207	0.009333028
Achi_Cell_FBgn0033749	FBgn0033749	0.009333028
Eip74EF_SANGER_5_FBgn0000567	FBgn0000567	0.009333028
lmd_SOLEXA_5_FBgn0039039	FBgn0039039	0.012376919
gl_SOLEXA_5_FBgn0004618	FBgn0004618	0.012376919
slp1_NAR_FBgn0003430	FBgn0003430	0.012376919
Bsh_Cell_FBgn0000529	FBgn0000529	0.015298444
shn-F1-2_SANGER_5_FBgn0003396	FBgn0003396	0.015298444
Fer1_SANGER_5_FBgn0037475	FBgn0037475	0.015298444
Vnd_Cell_FBgn0003986	FBgn0003986	0.015298444
pad_SANGER_5_FBgn0038418	FBgn0038418	0.015298444
Lag1_SOLEXA_FBgn0040918	FBgn0040918	0.017665347
lola_PK_SANGER_5_FBgn0005630	FBgn0005630	0.017665347
tgo_ss_SANGER_5_FBgn0015014	FBgn0015014	0.017665347
tgo_ss_SANGER_5_FBgn0003513	FBgn0003513	0.017665347
CG3919_SANGER_5_FBgn0036423	FBgn0036423	0.017665347
nub_NAR_FBgn0085424	FBgn0085424	0.017665347
rn_SANGER_10_FBgn0259172	FBgn0259172	0.017665347

hth_SOLEXA_2_FBgn0001235	FBgn0001235	0.017665347
klu_SANGER_10_FBgn0013469	FBgn0013469	0.022178295
CG5953_SANGER_5_FBgn0032587	FBgn0032587	0.022178295
Ftz_Cell_FBgn0001077	FBgn0001077	0.022178295
CG12236-PB_SANGER_2.5_FBgn0029822	FBgn0029822	0.022178295
CG33980_Cell_FBgn0053980	FBgn0053980	0.022178295
pnt_SANGER_5_FBgn0003118	FBgn0003118	0.022178295
jim_F1-9_SOLEXA_2.5_FBgn0027339	FBgn0027339	0.025884571
Hsf_FlyReg_FBgn0001222	FBgn0001222	0.025884571
onecut_SOLEXA_FBgn0028996	FBgn0028996	0.025884571
bin_SANGER_5_FBgn0045759	FBgn0045759	0.025884571
Odsh_Cell_FBgn0026058	FBgn0026058	0.025884571
Hmx_SOLEXA_FBgn0085448	FBgn0085448	0.025884571
CrebA_SANGER_5_FBgn0004396	FBgn0004396	0.025884571
En_Cell_FBgn0000577	FBgn0000577	0.025884571
BH2_Cell_FBgn0004854	FBgn0004854	0.025884571
Her_SANGER_5_FBgn0030899	FBgn0030899	0.025884571
lola-PA_SANGER_5_FBgn0005630	FBgn0005630	0.028216244
Rx_Cell_FBgn0020617	FBgn0020617	0.028216244
Al_SOLEXA_FBgn0000061	FBgn0000061	0.028216244
CG11085_Cell_FBgn0030408	FBgn0030408	0.028216244
Ro_Cell_FBgn0003267	FBgn0003267	0.028216244
CG12768_SANGER_5_FBgn0037206	FBgn0037206	0.028216244
CG31670_SANGER_5_FBgn0031375	FBgn0031375	0.028216244
pfk_SANGER_5_FBgn0035405	FBgn0035405	0.028216244
lola-PU_SANGER_5_FBgn0005630	FBgn0005630	0.028216244
Ets96B_SANGER_5_FBgn0039225	FBgn0039225	0.028216244
Hth_SOLEXA_FBgn0001235	FBgn0001235	0.028216244
inv_SOLEXA_2_FBgn0001269	FBgn0001269	0.028216244
odd_NAR_FBgn0002985	FBgn0002985	0.028216244

Mitf_SANGER_5_FBgn0263112	FBgn0263112	0.028216244
Ind_Cell_FBgn0025776	FBgn0025776	0.028216244
Six4_SOLEXA_2_FBgn0027364	FBgn0027364	0.028216244
en_SOLEXA_2_FBgn0000577	FBgn0000577	0.034152852
Ap_Cell_FBgn0000099	FBgn0000099	0.034152852
CG10904_SANGER_5_FBgn0034945	FBgn0034945	0.034152852
Trl_FlyReg_FBgn0013263	FBgn0013263	0.034152852
aop_SANGER_10_FBgn0000097	FBgn0000097	0.034152852
gsb-n_SOLEXA_5_FBgn0001147	FBgn0001147	0.034152852
exd_SOLEXA_2_FBgn0000611	FBgn0000611	0.034152852
peb-F1-3_SANGER_2.5_FBgn0003053	FBgn0003053	0.034152852
vfl_SOLEXA_5_FBgn0259789	FBgn0259789	0.034152852
Hth_Cell_FBgn0001235	FBgn0001235	0.034152852
Unpg_Cell_FBgn0015561	FBgn0015561	0.034152852
Tup_SOLEXA_FBgn0003896	FBgn0003896	0.038985135
Vis_Cell_FBgn0033748	FBgn0033748	0.038985135
Hmx_Cell_FBgn0085448	FBgn0085448	0.038985135
Kr_NAR_FBgn0001325	FBgn0001325	0.038985135
Clk_cyc_SANGER_5_FBgn0023094	FBgn0023094	0.038985135
lola-PO_SANGER_5_FBgn0005630	FBgn0005630	0.038985135
CG3407_SOLEXA_2.5_FBgn0031573	FBgn0031573	0.038985135
Clk_cyc_SANGER_5_FBgn0023076	FBgn0023076	0.038985135
bin_FlyReg_FBgn0045759	FBgn0045759	0.038985135
Opa_SANGER_5_FBgn0003002	FBgn0003002	0.038985135
Sox14_SANGER_10_FBgn0005612	FBgn0005612	0.038985135
CG14962_SOLEXA_5_FBgn0035407	FBgn0035407	0.038985135
ttk-PA_SANGER_5_FBgn0003870	FBgn0003870	0.038985135
chinmo_SOLEXA_15_FBgn0086758	FBgn0086758	0.038985135
Scr_Cell_FBgn0003339	FBgn0003339	0.038985135
Hey_SANGER_5_FBgn0027788	FBgn0027788	0.038985135

dl_NBT_FBgn0000462	FBgn0000462	0.038985135
Aef1_SANGER_5_FBgn0005694	FBgn0005694	0.044920357
l1sc_da_SANGER_5_FBgn0002561	FBgn0002561	0.044920357
sd_FlyReg_FBgn0003345	FBgn0003345	0.044920357
Fer1_da_SANGER_10_FBgn0037475	FBgn0037475	0.044920357
opa_NAR_FBgn0003002	FBgn0003002	0.044920357
Deaf1_FlyReg_FBgn0013799	FBgn0013799	0.044920357
her_SANGER_10_FBgn0001185	FBgn0001185	0.044920357
HLHmgamma_SANGER_5_2_FBgn0002735	FBgn0002735	0.044920357
pnr_SANGER_5_FBgn0003117	FBgn0003117	0.044920357
l1sc_da_SANGER_5_FBgn0000413	FBgn0000413	0.044920357
Ets21c_SANGER_5_FBgn0005660	FBgn0005660	0.044920357
Fer1_da_SANGER_10_FBgn0000413	FBgn0000413	0.044920357
Zen_SOLEXA_FBgn0004053	FBgn0004053	0.044920357
Dfd_SOLEXA_FBgn0000439	FBgn0000439	0.044920357
Rel_SANGER_5_FBgn0014018	FBgn0014018	0.044920357
Six4_Cell_FBgn0027364	FBgn0027364	0.044920357
pho_SANGER_10_FBgn0002521	FBgn0002521	0.044920357
Hr83_SANGER_5_FBgn0037436	FBgn0037436	0.044920357

**Table 3.4:** Enriched motifs in sequences flanking (+/- 20bp) candidate SNPs.

Motif name	Associated gene	Adjusted P-value
Mes2_SANGER_5	FBgn0037207	1.80E-04
CG12236-PB_SOLEXA	FBgn0029822	2.50E-04
slbo_FlyReg	FBgn0005638	9.40E-04
peb-F5-7_SOLEXA	FBgn0003053	1.10E-03
odd_NBT_5	FBgn0002985	1.70E-03
Ct_Cell	FBgn0004198	6.10E-03
Eip74EF_FlyReg	FBgn0000567	6.30E-03
Ets97D_SANGER_10	FBgn0004510	6.70E-03

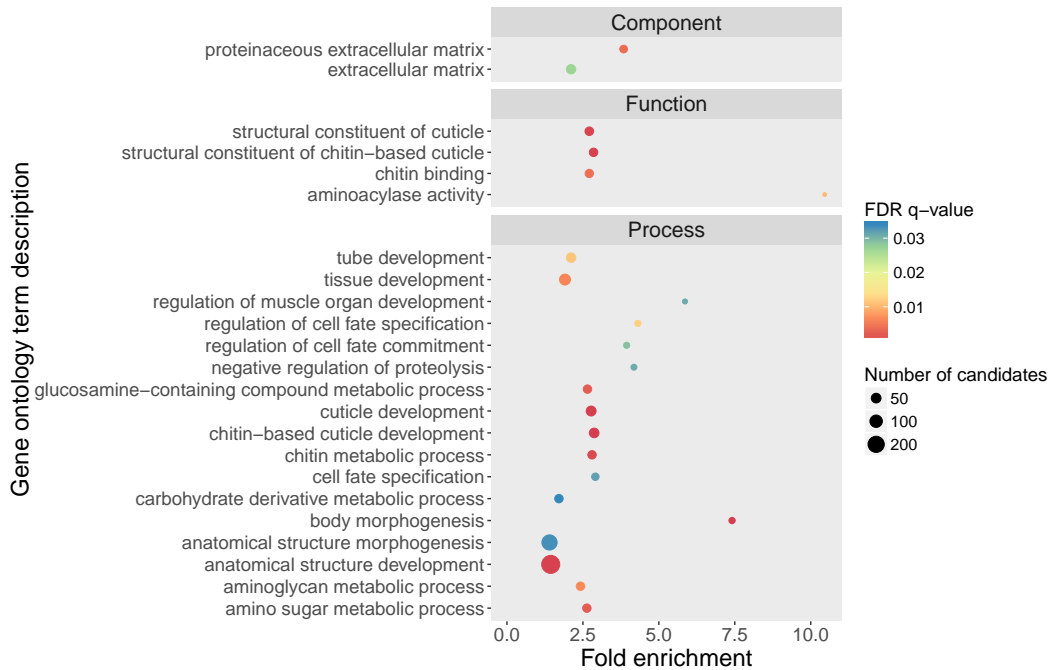


**Figure 3.1: Enriched Gene Ontology terms of candidate genes.** Depicts all of the enriched Gene Ontology (GO) component, function, and process terms of SA genes (FDR  $\leq 5\%$ ). Fold enrichment for each term is shown along the x-axis. Colour of points indicate the FDR q-values for each individual term with warmer-colours indicating more significant associations. Size of points show how many individual candidate genes were associated with each GO term.

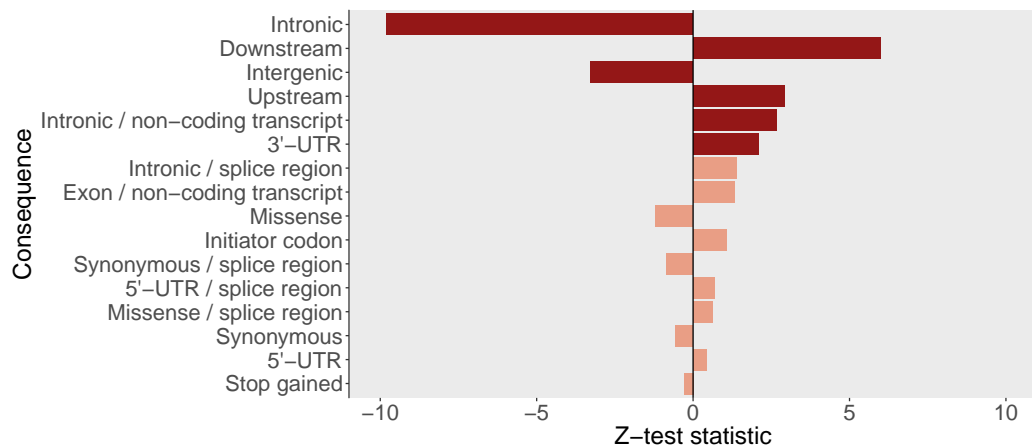


**Figure 3.2: Genetic consequences of antagonistic candidate SNPs.** Predicted variant effects of sexually antagonistic candidate SNPs relative to all SNPs covered in the haplotype sequencing. Dark red bars indicate statistically significant over-/under-representation, lighter red bars  $P > 0.05$

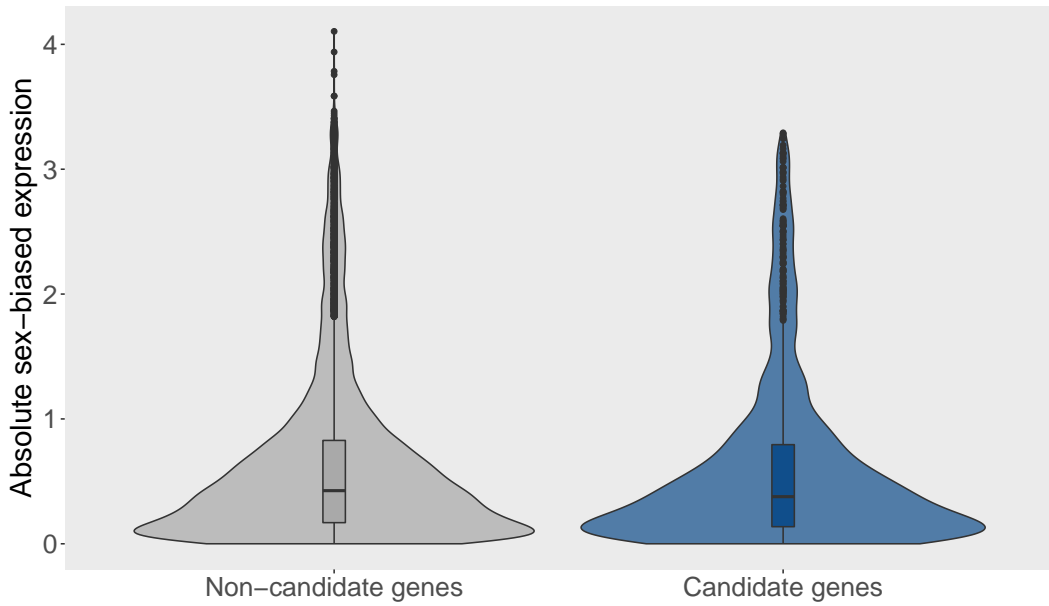


**Figure 3.3: Expression bias of non-candidate and candidate genes.** Absolute sex-biased expression of non-candidate (grey) and candidate (blue) genes. Higher values indicate increasingly sex-biased expression.

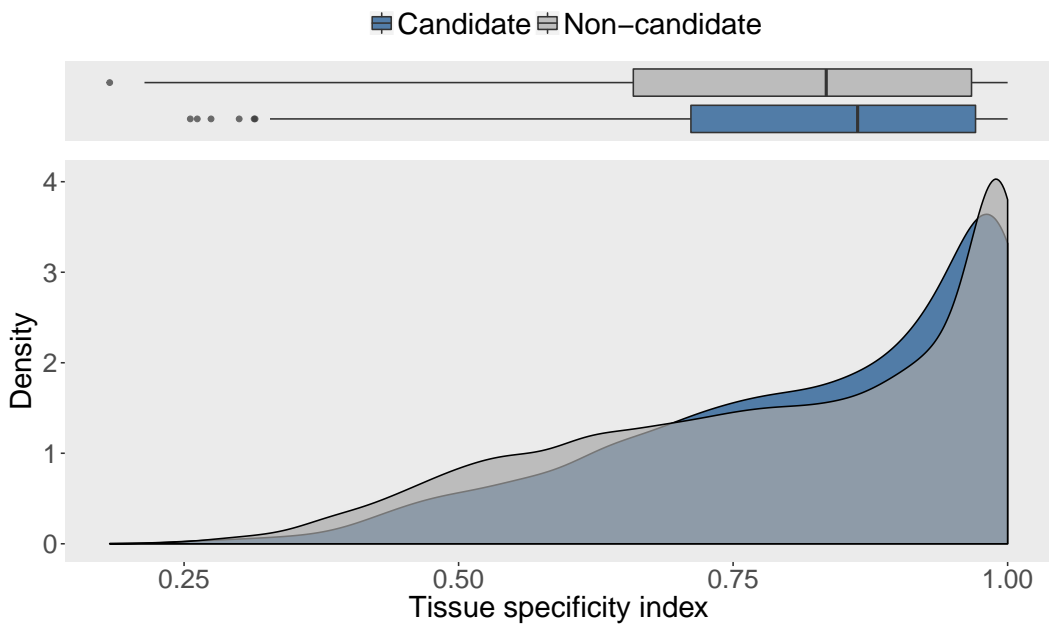


**Figure 3.4: Expression specificity of non-candidate and candidate genes across tissues.** Density surfaces show the distributions of the tissue specificity index ( $\tau$ ) for candidate (blue) and non-candidate (grey) genes. Lower values of ( $\tau$ ) are indicative of broader expression across tissue types.

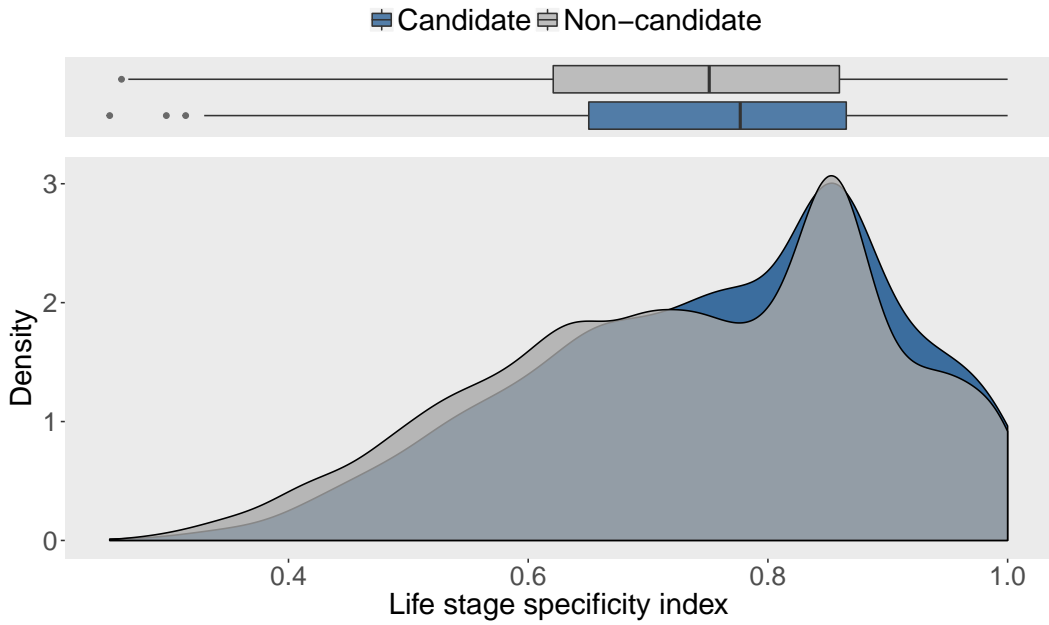


**Figure 3.5: Expression specificity of non-candidate and candidate genes across life stages.** Density surfaces show the distributions of the life stage specificity index (*LSI*, see 3.3.5) for candidate (blue) and non-candidate (grey) genes. Lower values of (*LSI*) are indicative of broader expression across developmental stages.

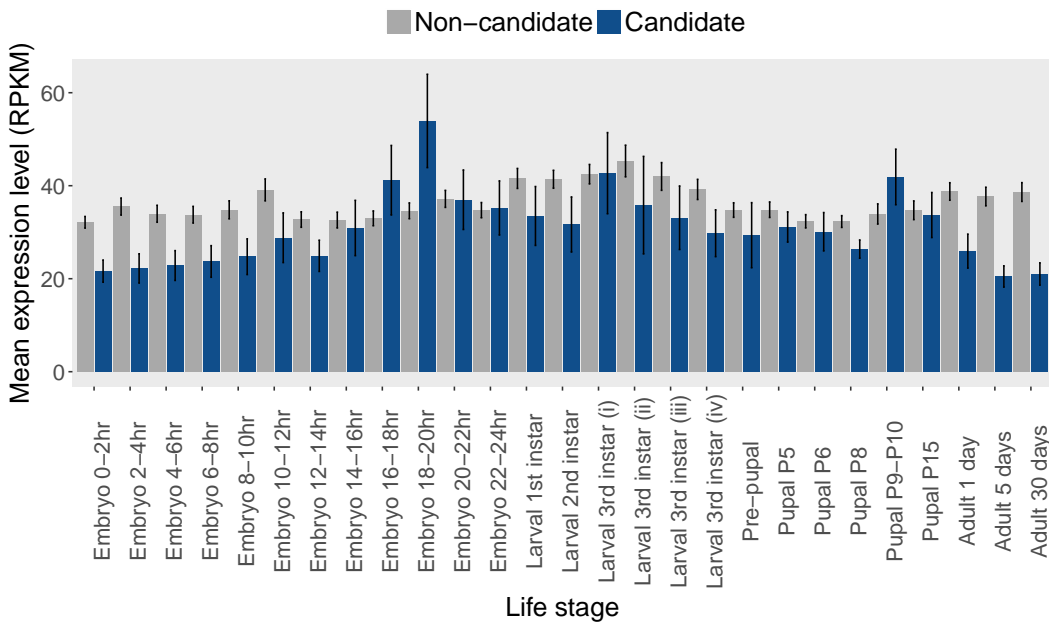


**Figure 3.6: Expression of non-candidate and candidate genes across life stages.** Mean expression level (RPKM - reads per kilobase of transcript per million mapped reads) of non-candidate (grey) and candidate (blue) genes across life stages in *D. melanogaster*. Expression data from modEncode. Error bars show standard error of the mean.

## Chapter 4

# Verifying putative sexually antagonistic loci using experimental sex-limited selection

## 4.1 Abstract

Several decades of research have firmly established sexually antagonistic genetic variation as a pervasive feature of sexual species. In chapter 2 I identified a large number of credible sexually antagonistic SNPs in the *Drosophila melanogaster* LH<sub>M</sub> laboratory population. Building on this, an important next step is to independently verify these SNPs and generate a more definitive list of causal SA variants. Here, I use experimental evolution under sex-limited selection to test the fitness effects of candidate SA loci on a genome-wide scale. By limiting selection to a single sex, SA alleles beneficial to the selected sex are able to freely increase in frequency, owing to the lack of counter-selection from the other sex. I show that over the course of only 3 generations under female-limited selection, alleles at SA SNPs responded more to the selection treatment than did alleles at non-antagonistic background sites. Moreover, female-beneficial alleles have significant and positive selection coefficients under FL selection. These results suggest that many of the putative antagonistic alleles responded in the manner that would be expected from the previously inferred antagonistic fitness effects. However, the expected corresponding mirror-effect under male-limited selection is not observed, possibly owing to there being greater variance in male reproductive success. Nevertheless, by generating a null distribution of antagonistic selection coefficients, I am able to individually validate a number of candidate SNPs. These are valuable because they will serve as prime targets for future study to obtain finer-grained mechanistic detail of the action of sexually antagonistic variants.

## 4.2 Introduction

Several decades of quantitative genetic research have established sexually antagonistic (SA) variation as a pervasive feature of sexual species (Cox and Calsbeek 2009; Van Doorn 2009; Bonduriansky and Chenoweth 2009; Pennell and Morrow 2013). This widespread variation, where alleles have opposing fitness consequences in each sex, reflects a major constraint to sex-specific adaptation. Given the previous lack of knowledge on the underlying loci, I identified and characterised candidate SA for the first time in chapters 2 and 3. My results suggest that the genetic basis of sexual antagonism is highly complex, with a large number of underlying causal variants. Furthermore, these loci appear to play a predominant role in gene expression regulation.

A series of initial analyses documented in chapter 2 supported the credibility of the candidates. Thus, there were many more than expected by chance, they had non-random functional properties and overlapped significantly with loci associated with sexual antagonism in previous studies (Innocenti and Morrow 2010; Collet et al. 2016). However, while this list of candidates is highly credible and has allowed me to produce the first general insights into the functional basis of sexual antagonism (chapter 3), independently validating these loci is an important next step in generating a more definitive list of causal SA variants.

Validating candidate loci underlying relatively simple traits, where few loci of large effect explain much of the variance, can often be accomplished through various single-locus validation approaches. For example, quantitative complementation (Long et al. 1996; Geiger-Thornsberry and Mackay 2004a), allows for very detailed dissection of the role individual variants play in shaping phenotypes. Quantitative complementation tests have been successfully used to validate loci associated with a number of quantitative traits such as lifespan (Geiger-Thornsberry and Mackay 2004b) and bristle number (Long et al. 1996) in *Drosophila melanogaster*, and obesity in mice (Yang et al. 2009). The basic approach that underlies quantitative complementation tests is to sys-

tematically contrast the effects of mutant alleles (loss-of-function mutants) of a candidate gene with those of naturally occurring allelic variation. If the impact of a mutant allele is different when paired against alternative natural alleles it is defined as 'failing to complement' and suggests that the region in question is causally associated with the trait of interest.

RNA interference (RNAi) is another commonly used method of validation. RNAi is a biological process whereby RNA molecules inhibit gene expression by preventing translation of mRNA molecules (Agrawal et al. 2003). If the causal variants that influence a trait do so by modifying gene expression, then using targeted RNAi to reduce expression of the candidate genes allows one to directly observe the relationship between expression and trait variation. Similarly, gene knockouts can be used to entirely prevent transcription of a target gene and measure the resulting change to trait variation (e.g., Liu et al. 2013; Vonesch et al. 2016).

While validation approaches that test individual loci separately are possible and appropriate in some cases, many traits have a highly complex genetic basis, making validation much more difficult. This is because the majority of the causal loci will individually have small phenotypic effects, making them difficult to detect in downstream functional studies. In this situation, approaches that seek to validate implicated loci on a larger, genome-wide scale offer a promising alternative (Schlötterer et al. 2014). Genome-wide approaches accrue benefits from testing many loci simultaneously, capturing global effects, at the cost of providing weaker evidence for a causal role for each individual locus.

One way to examine the wider genetic basis underlying quantitative traits is to use an evolve and resequence (E&R) framework. E&R studies use experimental selection protocols and combine this with deep sequencing of populations / individuals before and after a period of selection to track the resulting allele frequency changes and identify loci under selection. For example, Turner and Miller (2012) conducted an E&R experiment whereby they selected on the

interpulse interval (IPI) of male courtship song in opposing directions for 14 generations (Turner and Miller 2012). They associated a large number of SNPs ( $N=13,343$ ) with male IPI with high confidence (FDR=0.005). Interestingly, in a previous genome-wide association study (GWAS) Turner et al. (2011) failed to detect any significant associations with male IPI. Indeed, E&R experiments are considered to be a powerful means of detecting loci under selection (Kofler and Schlötterer 2014).

Given the complex genetic basis of sexual antagonism revealed in chapter 2, I conduct an E&R experiment in order to test the fitness effects of a large number of candidate loci simultaneously. Specifically, I used a sex-specific selection regime, where selection is limited to a single sex. By limiting selection to a single sex, SA alleles that are beneficial to the selected sex are free to increase in frequency, owing to the lack of counter-selection from the other sex. This approach has previously been used to demonstrate the presence of sexual antagonism in the LH<sub>M</sub> population. Morrow et al. (2008) established 4 replicate populations, 2 of which experienced male-limited (ML) selection and 2 of which experienced female-limited (FL) selection for 26 generations. Limiting selection to a single sex can be achieved through the application of a modified middle-class-neighbourhood (MCN) design. The traditional MCN is a mutation accumulation protocol whereby purifying selection is almost entirely eliminated within a population by constraining reproductive output of all individuals to the same number of offspring, thus removing all variance in fitness (Moorad and Hall 2009). By here constraining the reproductive output of a single sex instead of both sexes this modified protocol renders it possible for populations to evolve when only one sex is exposed to selection.

Morrow et al.'s (2008) experiments showed that, as expected, the fitness of the unselected sex decreased relative to the selected sex over the course of selection. However, the fitness of the selected sex also decreased relative to the control population. The general decline in fitness associated with the asymmetric application of the MCN design suggests that mutations with dele-

terious fitness consequences in both sexes accumulated during the course of the experiment. This is unsurprising, given that restricting selection to one sex effectively halves the strength of selection on mutations with concordant deleterious effects, leading to an accumulation of such mutations over the course of the 26 generations that the experiment was run (Morrow et al. 2008). Despite this influx of unconditionally deleterious mutations, the greater relative fitness decline of the unselected sex relative to the selected sex suggests substantial standing SA genetic variation and/or the accumulation of many mutations with SA fitness effects. Taken together these findings show that sex-limited selection can effectively uncover the effects of sexually antagonistic variation segregating within a population. But, they also suggest that running this type of experimental evolution experiment for an extended period is problematic, owing to mutation accumulation.

A number of studies have shown short-term selection experiments to be effective in uncovering loci under selection. Indeed, even single generation resequencing experiments have been successful in detecting candidate variants. For example, Gompert et al. (2014) transplanted wild stick insects onto native and novel host plants and measured genome-wide allele frequency changes across a single generation. While many of the frequency changes could be attributed to drift, they did detect significant evidence of selection at 116 loci and could further link this response to known colour-pattern traits. Another study used a single-generation selection experiment to examine evolutionary change during ocean acidification (Pespeni et al. 2013). Specifically, the authors measured genome-wide allele frequency changes over 6 days of development in purple sea urchin larvae that had been exposed to increased carbon-dioxide concentrations. 30 out of 19,493 tested SNPs showed significant allele frequency changes in the experimental populations compared to control populations. Also, the genes with highest allele frequency changes were enriched for specific functional processes.

Building on the experimental design of Morrow et al.'s (2008) study, I

imposed sex-limited selection on 4 replicate populations (2x FL and 2x ML), established from the LH<sub>M</sub> population. I sequenced pools of individuals from the initial populations and subsequently resequenced them following a short period (3 generations) of selection. I then used the frequency change of alleles over the course of selection to infer selection coefficients at candidate and non-candidate SNPs and to examine the fitness effects of putative SA alleles that I identified in chapter 2. Overall, I found that SA alleles responded as expected under FL selection, with putative female beneficial alleles increasing in frequency over the course of selection. However, the results were less conclusive under ML selection. Here, non-candidate loci responded more to selection than candidates. Moreover, even when under ML selection putative female-beneficial alleles increased in frequency (contrary to expectations), although to a lesser extent than when under FL selection. Based on the data that I gathered, I also was able to define a set of highly supported candidate SNPs with selection coefficients that fell in the extreme of the distribution of antagonistic responses and that showed frequency changes in the expected direction under sex-limited selection.

## 4.3 Materials and Methods

### 4.3.1 Experimental evolution protocol

To evolve populations under sex-limited selection, I used a modified middle-class-neighbourhood design (Moorad and Hall 2009). This design removes fitness variance in a population by constraining the reproductive output of all individuals to be the same number of offspring, thereby effectively eliminating selection. By applying this design asymmetrically—to one sex—it is possible to create populations where only males or only females experience selection (Morrow et al. 2008). As counter-selection from the unselected sex is removed in this design, sexually antagonistic alleles are not subject to elimination and are free to accumulate and/or rapidly increase in frequency. I applied sex-limited selection to males and females in this way in independent lineages,

establishing two replicate populations for each selection treatment. I allowed all four experimental populations to evolve for 3 generations. The number of replicate populations chosen was a compromise between statistical power and logistical constraints.

Each population of the male-limited selection (ML) treatment was composed of 120 mating groups of 4 males and 1 female (600 flies in total), sampled as virgins from the LH<sub>M</sub> stock population. After interacting for two days in ‘adult competition’ vials, each group of flies was transferred to new ‘oviposition vials’ for 18h before being discarded. After 9 days of development, 5 virgin adults (4 males, 1 female) were collected from each vial, ensuring that each female in the population had produced an identical number of offspring (4 males, 1 female) while male fitness varied according to mating success. After aging for 3 days the virgin flies of the next generation were pooled and re-distributed among a new set of 120 adult competition vials, maintaining the 4:1 ratio of male:female (Figure 4.1). This procedure was repeated for two more generations (total number of generations = 3). Evolution under female-limited selection was performed in an equivalent way, but using mating groups of 4 females and 1 male (Figure 4.1). Both the male- (ML) and female-limited (FL) selection regimes were designed to closely follow the standard rearing regime of the LH<sub>M</sub> base population (Rice et al. 2005). The number of flies per vial was chosen to maximise the selective pressure (with the skewed sex ratio allowing for stronger selection) while still being feasible in terms of the required scale of virgin collections and the losses due to mortality of experimental flies (mainly owing to male harassment of females flies in the ML treatment) throughout the experiment.

### **4.3.2 DNA extraction and sequencing of the experimental populations**

I collected flies from each experimental population at the start (all 600 founder parents in the first generation) and the end of the experiment (2000+ offspring collected after the last round of selection), yielding a total of 8 pooled

samples. I extracted total genomic DNA from each of these samples using a CTAB/DTAB extraction method, and further purified the DNA samples using Agencourt AMPure XP beads (Beckman Coulter). Paired-end Nextera libraries were prepared using a Nextera DNA sample preparation kit (Illumina) and sequenced on an Illumina HiSeq 2000 at the UCL Institute of Child Health.

Basecalling and de-multiplexing of the indexed sequencing reads was performed using CASAVA version 1.8.2 (Illumina), producing fastq files from the sequenced libraries. The raw fastq files were first trimmed using Cutadapt version 1.2.12 to remove Illumina adapter sequences. The reads were then further trimmed to remove low quality bases (requiring a minimum window quality score of 20) and very short reads (<10bp) with Sickle version 1.200 ([github.com/najoshi/sickle](http://github.com/najoshi/sickle)). Read pairs were then aligned to the *Drosophila melanogaster* reference sequence (BDGP 5.5), obtained from the FlyBase online database (<http://flybase.org/>), using Bowtie2 version 2.1.03. To avoid false positive SNP calls resulting from misalignment around indels, reads were locally realigned using the Genome Analysis Toolkit (GATK) version 2.1.134.5. Duplicate reads, arising from PCR amplification during library construction were removed using Picard version 1.85 (<http://sourceforge.net/projects/picard/>). The alignments were visually inspected using the Integrative Genomics Viewer (Robinson et al. 2011).

I called SNPs separately for each population using the SNVer tool (Wei et al. 2011). SNVer tests for the significant presence of an alternative allele rather than polymorphism *per se*. In order to correct for this, I re-ran the tool against a modified reference genome where the reference allele had been swapped for the alternative allele detected in the initial run. I considered a site to be a SNP if both tests were significant. All *P*-values were corrected for the false discovery rate using the q-value package (<http://www.bioconductor.org>). I then used the filtered SNVer output (minimum read depth = 100, maximum read depth = 2x mean coverage) to ascertain allele frequencies at SNPs

identified across the 8 samples.

### **4.3.3 Inferring selection coefficients from the evolve-and-resequence data**

To estimate selection coefficients, I used ApproxWF (Ferrer-Admetlla et al. 2016), which approximates the Wright-Fisher process using a Markov model. I analysed allele frequency data for all autosomal candidate SNPs covered in the sequencing of the experimental evolution experiment ( $N=2,721$ ). I excluded X-linked SNPs from the analysis because the lack of father-to-son transmission of the X chromosome makes male-limited selection less efficient on this chromosome and the lower census size of X-chromosomes (which are hemizygous in males) generally reduces the efficacy of selection on X-linked variants.

In addition to generating selection coefficient data for candidate SNPs I generated data from background non-antagonistic sites ( $N=91,271$ ). I took all autosomal SNPs that conformed to any 4/5 pattern across the hemiclonal lines and were sufficiently covered (minimum read depth = 100) in the E&R sequencing. That is, there were 4 copies of one allele and 5 copies of an alternative allele, but unlike at perfectly segregating sites the pattern of segregation was not structured by sex-specific fitness. This allowed me to construct a null distribution of selection coefficients under sex-limited selection. In both FL and ML cases the selection coefficients were estimated for the reference allele.

To examine selection coefficients at background and candidate sites under FL and ML selection, I fitted a GLM with Gaussian error structure to model how the variation in absolute selection coefficients was explained by selection regime, candidate status, and their interaction. To improve the model fit the response variable (absolute selection coefficient) was square-root transformed. Qualitatively these results were also obtained with non-parametric Wilcoxon Rank-sum tests.

#### **4.3.4 Selection on female-beneficial alleles under sex-limited selection**

To examine the direction of change at candidate antagonistic SNPs under ML and FL selection, I assigned the reference and alternative alleles to either female-beneficial or male-beneficial classes based on the haplotype sequencing and then tracked the assigned female-beneficial alleles. The direction of polarisation here is arbitrary, with the results of polarising for male-beneficial alleles simply a mirror of those when polarising for female-beneficial alleles. In this case, a positive selection coefficient indicates selection in favour of the female-beneficial allele/against the male-beneficial allele and a negative selection coefficient indicates selection in favour of the male-beneficial allele/against the female-beneficial allele. To compare selection coefficients for female-beneficial alleles under ML and FL selection, I fitted a GLM with Gaussian error structure to model how variation in selection coefficients was explained by selection regime. Qualitatively these results were also obtained with non-parametric Wilcoxon Rank-sum tests.

#### **4.3.5 Selection response index**

To generate a null distribution for the expected change under sex-limited selection, I calculated a 'selection response index'. This index reflects whether and to what degree allele frequency change occurred in the same direction under ML and FL selection. Specifically, negative values indicate antagonistic change whereby the reference allele increased in frequency in one selection regime and decreased in the other. Positive values indicate concordant patterns of change. The index is calculated as the sum of the absolute selection coefficients under FL and ML selection at each locus. This raw value is then signed such that concordant changes are positive and antagonistic changes are negative.

#### **4.3.6 Estimating effective population size**

The inference of selection requires information about the intensity of genetic drift, and hence the effective population size ( $N_e$ ). I parameterised the Ap-

proxWF runs with the theoretical expectation for  $N_e$  based on the experimental design. I calculated  $N_e$  from the numbers of males and females and the (co)variances in male and female mating success using Equation 2 of Nomura (2002):

$$\frac{1}{N_e} = \frac{1}{16N_m} \left( 2 + \sigma_{mm}^2 + 2 \frac{N_m}{N_f} \sigma_{mm,mf} + \left( \frac{N_m}{N_f} \right)^2 \sigma_{mf}^2 \right) + \frac{1}{16N_f} \left( 2 + \sigma_{ff}^2 + 2 \frac{N_f}{N_m} \sigma_{mf,ff} + \left( \frac{N_f}{N_m} \right)^2 \sigma_{fm}^2 \right),$$

where  $N_m$  and  $N_f$  are the number of males and females,  $\sigma_{ij}^2$  is the variance in the number of offspring of sex  $j$  produced by a parent of sex  $i$  and  $\sigma_{ij,ik}$  is the covariance between the number of offspring of sexes  $j$  and  $k$  produced by a parent of sex  $i$ . All variances are equal to zero for the sex that is not under selection, as all individuals of that sex produce the same number of male and female offspring. Reproductive variances for the selected sex are non-zero and  $N_e$  increases with decreasing reproductive variances, i.e., with a more even sharing of reproduction between competitors. In order to be conservative, I calculated  $N_e$  for the worst-case scenario where reproductive variance is maximal and only a single individual of the selected sex reproduces in each mating group. In this case,  $\sigma_{ij}^2 = \frac{1}{4}(4-1)^2 + \frac{3}{4}(0-1)^2$  for  $i = j$  (e.g., paternal variance in the production of sons in the male-limited treatment) and  $\sigma_{ij}^2 = \frac{1}{4}(1-\frac{1}{4})^2 + \frac{3}{4}(0-\frac{1}{4})^2$  for  $i \neq j$  and  $\sigma_{ij,ik} = \frac{1}{4}(4-1)(1-\frac{1}{4}) + \frac{3}{4}(0-1)(0-\frac{1}{4})$  for the covariance between offspring of sexes  $j$  and  $k$  in the selected sex  $i = j$ . The theoretical effective population size in this case is  $N_e=291$ .

### 4.3.7 Statistical analysis and plotting

All statistical analyses were conducted in R version 3.2.3. Plots were produced with the ggplot2 package.

## 4.4 Results

### 4.4.1 Overall response to sex-limited selection

To establish whether sex-limited selection over 3 generations generated the expected evolutionary response at candidate loci, I first compared absolute (unsigned) selection coefficients under both FL and ML selection at candidate and non-candidate background SNPs. The mean absolute selection coefficients at candidate loci under FL and ML selection were  $\bar{s}_{FL} = 0.030$  and  $\bar{s}_{ML} = 0.026$  respectively (range FL:  $1.04 \times 10^{-8} - 1.97 \times 10^{-1}$ ; range ML:  $2.55 \times 10^{-5} - 1.77 \times 10^{-1}$ ). Overall, the variation in selection coefficients was explained by the interaction between selection regime and candidate status ( $F_{1,187966}=23.05$ ,  $P<0.001$ ), meaning that candidate loci responded differently under FL and ML selection. To better understand this difference between selection regimes I analysed the two regimes separately. These analyses suggest that under FL selection the candidate sites were under stronger selection, on average, than the background sites ( $F_{1,93983}=18.73$ ,  $P<0.001$ ), whereas under ML selection this pattern was reversed and candidate sites were under weaker selection, on average, than background sites ( $F_{1,93983}=5.95$ ,  $P=0.015$ ).

In order to test whether any of the individual candidate sites responded more antagonistically than expected by chance, I calculated a 'site response index' (SRI). The SRI reflects the degree to which the reference allele at a SNP responded antagonistically (in different directions under ML and FL selection) or concordantly (in the same direction under FL and ML selection). Thus, negative values indicate an antagonistic response to selection whereas positive values indicate a concordant response. Overall, the distribution of the SRI at candidate and non-candidate sites was significantly different ( $W=126940000$ ,  $P=0.027$ , Figure 4.2), although the direction of this trend was not as expected, with mean SRI for candidate sites (mean SRI = 0.006) being marginally greater than that for non-candidate sites (mean SRI = 0.004). I used the distribution of the SRI at non-antagonistic sites to define a null distribution for the response to sex-limited selection. To examine whether any of the candidate

SNPs had a more antagonistic response than expected by chance, I identified those candidate antagonistic SNPs which fell into the extreme 5% of the most antagonistic responses among the background sites. The 5% significance cut-off in this case identified candidate SNPs with an SRI  $\leq -0.117$  (Figure 4.2). In total 83 candidate SNPs fell within this range.

#### 4.4.2 Selection on female-beneficial alleles under sex-limited selection

While the previous analyses identify how the overall response of candidate and non-candidate sites differed under sex-limited selection they do not differentiate between male-beneficial and female-beneficial effects of candidate SA alleles. Accordingly, they do not assess whether the alleles inferred from the haplotype sequencing data to be beneficial to a specific sex responded in the correct direction under sex-limited selection. To address this, I polarised the data, such that I could calculate selection coefficients specifically for female-beneficial alleles, as inferred from the haplotype sequencing data. Overall, the distribution of selection coefficients for female-beneficial alleles ( $N=2,721$ ) strongly differed under the two sex-limited regimes ( $F_{1,5441}=73.10$ ,  $P<0.001$ , Figure 4.3A). Specifically, selection coefficients of female-beneficial alleles under FL selection were positive and significantly different from zero ( $t_{1,5441}=15.3$ ,  $P<0.001$ , Figure 4.3A & B). Female beneficial alleles under ML selection were also positive and significantly different from zero, but to a much smaller extent than under FL selection ( $t_{1,5441}=3.21$ ,  $P=0.001$ , Figure 4.3A & B).

I next examined how the SRI correlated with the direction of change based on the polarised allele data. Reassuringly, there was a significant negative correlation between the antagonistic SRI (SRI  $<0$ ) and the proportion of responses in the expected direction ( $F_{1,17}=7.54$ ,  $P=0.014$ , Figure 4.4). This means that the more extreme antagonistic changes are more likely to have occurred in the expected direction than weaker antagonistic responses. I further re-examined the 83 SNPs with significant values of the SRI in light of allelic

effects (Figure 4.5). Of the 83 SNPs, 58 (70%) responded as expected based on the fitness effects determined by the haplotype sequencing data. That is, the inferred female-beneficial allele had a positive selection coefficient in the FL treatment and a negative selection coefficient in the ML treatment. The 58 SNPs which responded in the correct direction constitute those with the highest independent support for a causal association with the sexually antagonistic fitness effects that characterise the hemiclinal lines. Hereafter, I will refer to these sites as validated SA SNPs.

### 4.4.3 Properties of validated SA SNPs

To better inform future validation strategies I characterised the 58 validated SA SNPs in terms of their genetic consequences and their associated genes. Overall, these 58 variants correspond to 70 unique genes including 4 transcription factors: *tailup*, CG15812, *Chronologically inappropriate morphogenesis*, and *apterous*. In the context of my findings from chapter 3, it is relevant that these transcription factors are primarily involved in developmental morphogenesis, with *Chronologically inappropriate morphogenesis* playing a role in male sex-determination. In addition, there are two characterised cis-regulatory modules (CRM) which contain validated candidate SA SNPs, namely CRMs associated with *derailed* and *Odorant receptor 88a*, two genes that play important roles in olfactory response. Owing to the small number of validated loci, I have not performed any statistical tests of functional enrichment, as these would lack sufficient discriminatory power.

## 4.5 Discussion

In the experiments described here, I restricted selection to a single sex in order to release SA alleles from counter-selection in the unselected sex and allow them to increase in frequency (Morrow et al. 2008). In line with this rationale, I found that over the course of only 3 generations under FL selection, alleles at previously defined antagonistic loci (described in chapter 2) responded more to the selection treatment than did alleles at non-antagonistic background

sites. Moreover, female-beneficial alleles had significant and positive selection coefficients under FL selection. These results suggest that many of the putative antagonistic alleles responded in line with their presumed fitness effects. However, the response to ML selection was somewhat different and not as expected. Here, the response at candidate loci was lower, on average, than at non-antagonistic background loci. In addition, female-beneficial alleles also had significantly positive selection coefficients under ML selection, the inverse of what was expected.

The selection coefficients inferred under female-limited selection suggest that I captured a number of causal antagonistic loci in the haplotype sequencing, despite the unexpected response of candidate loci under male-limited selection. In terms of individual loci, I was further able to show that 83 candidate SNPs had significant antagonistic responses to the selection treatments. Of these, 58 responded in the direction expected. Therefore, these 58 loci are those that have the strongest support, across two independent studies, for playing a causal role in the generation of sexually antagonistic fitness effects.

My estimates of selection coefficients also show that, overall, putative antagonistic SNPs were under reasonably strong selection over the course of the experiment, with mean absolute selection coefficients of  $\bar{s}_{FL} = 0.030$  and  $\bar{s}_{ML} = 0.026$  respectively. Indeed, some of the SA loci were inferred to be under very strong selection with selection coefficients of up to 0.19. To put these values in to context, Bersaglieri et al. (2004) estimated selection coefficients of 0.09 — 0.19 associated with carrying at least one copy of a lactase-persistence allele (allele that allows adults to digest lactose contained in milk) in a Scandinavian human population. This strong selection for lactase-persistence was inferred to have occurred within the past 5,000 — 10,000 years, consistent with the arrival of dairy farming. These selection coefficients are among the highest yet observed for any gene in the human genome.

Due to the small number of validated SA SNPs, statistical tests of functional enrichment such as those conducted in chapter 3 are not possible. How-

ever, the functional properties of individual validated SNPs are useful for informing future downstream validation approaches. For example, the validated SNPs that fall within annotated CRMs would be good candidates to follow up with nucleotide editing approaches to assess the impact of these variants on the expression of the associated genes. The TFs detected among the validated loci predominately play roles in developmental morphogenesis, a pattern consistent with the findings in chapter 3. Moreover, one of the TFs *Chronologically inappropriate morphogenesis* is involved in male somatic sex determination and this association fits well with a number of the observed associations with sexual differentiation that I documented in chapter 3. In addition, both of the CRMs containing validated SA SNPs are associated with genes which play important roles in olfactory responses. To date there has been no direct association of olfactory response with sexual antagonism; however, substantial sexual dimorphism in antennal lobe (the region of the brain where olfactory signals are initially processed) anatomy has been described in *D. melanogaster* (Cachero et al. 2010). In addition, studies in mice have revealed sexual dimorphism in neural responses to olfactory cues (Stowers and Logan 2010). The association documented here, along with previous empirical studies revealing sexual dimorphism in olfactory traits, raises the possibility that olfaction could play an important role in generating sexual antagonism. It would be valuable in the future to investigate further the potential link of olfaction to sexual antagonism.

While I was able to verify a number of putative SA loci, the unexpected response under ML selection reduces the overall power of my experiment. A potential explanation for this unexpected response in the ML treatment is that greater stochasticity in fitness variance may have swamped the effect of the selection treatment over the short number of generations of the experiment. It is well established that males of sexual species typically have greater variance in reproductive success than females (Clutton-Brock 1991; Andersson 1994). The reason is that in most sexual species males invest in a large

number of cheap gametes, whereas females invest in fewer, more expensive gametes (Trivers 1972). This means that male reproductive success is primarily limited by the number of matings, while female reproductive success is mainly limited by the production of eggs. The present study was a short-term E&R experiment conducted over just 3 generations. Provided that the variance in male reproductive success was sufficiently high then the phenotypic effects of sexually antagonistic loci could be masked, with the consequence that I would fail to detect the expected effect of negative selection coefficients for female beneficial alleles.

Another unexpected observation was that the majority of antagonistic loci responded concordantly to the two selection regimes (Figure 4.2). This could mean that the majority of the tested candidate loci do not have antagonistic fitness effects and were detected in chapter 2 owing to linkage with true antagonistic variants. However, as detailed in chapter 2, the resampling tests I performed along with those in appendix A suggest that linkage effects do not contribute substantially to the number of false positives. A further, non-mutually exclusive possibility is that, despite my best efforts to match the highly standardised rearing conditions of the LH<sub>M</sub> population (Rice et al. 2005), I may have inadvertently generated novel selection pressures to adapt to the conditions of the sex-limited selection protocol. Perhaps the largest difference between the standardised rearing regime of the LH<sub>M</sub> population and the sex-limited design used here is that flies are selected over a much narrower time window post-emergence (all flies collected as virgins on a single day). This selection on emergence time, which penalises early and late eclosions relative to the standardised rearing conditions, may have negated some components of fitness, important in the standard conditions. In addition, larval densities would be much lower throughout initial development in the selection lines relative to the standard conditions (owing to fewer ovipositing females in each vial). The more benign larval environment could similarly shift selection pressures.

Although not entirely applicable to the issues raised above, results from

previous empirical studies show that sex-specific selection gradients and genetic correlations between male and female fitness components can be altered in response to environmental changes (Delcourt et al. 2009; Delph et al. 2011; Long et al. 2012; Berger et al. 2014; Punzalan et al. 2014). In many cases, novel environmental conditions aligned the direction of selection on each sex, alleviating, at least temporarily, sexually antagonistic constraints on adaptation (Long et al. 2012; Berger et al. 2014) (but see Delcourt et al. (2009)). For example, Berger et al. (2014) compared the intersexual genetic correlation ( $r_{MF}$ ) for fitness in two populations of seed beetle. They calculated  $r_{MF}$  in both the standard benign laboratory conditions and again at a novel stressful temperature. Under benign conditions  $r_{MF}$  was significantly negative (-0.51), indicative of substantial sexual antagonism. However, in the novel temperature treatment this trend reversed and a positive  $r_{MF}$  was observed (0.21). Connallon and Hall (2016) developed a theoretical model to explore this further. Their results support the idea that environmental changes should often align the direction of selection between the sexes even when male and female optima are highly divergent. Thus, the shift from the standard rearing regime to the novel experimental set-up used here could have been sufficiently different to cause sex-specific phenotypic optima to shift in similar directions at many of the antagonistic loci, explaining the observation of a large number of concordant changes at putative antagonistic loci over the course of selection.

One thing that could potentially help to alleviate issues associated with higher male reproductive variance and concordant responses to novel rearing conditions is to run the experiment over a greater number of generations. A longer experiment would more reliably differentiate the effects of genetic drift and selection (Kofler and Schlötterer 2014). Similarly, increasing the number of time points would allow for more accurate tracking of allele frequency changes and thus improve inference of selection. However, simply increasing the length of the experiment may not be entirely effective. This is because long-term sex-specific selection regimes are subject to heightened effects of deleterious

mutations. As noted by Morrow et al. (2008), by halving total selection one is effectively doubling the mutational load. This means that incoming deleterious mutations are less effectively purged by selection and can accumulate. Over the 26 generations of selection in their study, Morrow et al. (2008) found that both sex-limited treatments resulted in a reduction in fitness compared to the control population. By using a small number of generations I hoped to minimise the accumulation of new mutations that could have otherwise influenced the selection experiment. In addition, while imposing selection over a greater number of generations is expected to increase the power of a study to detect the targets of selection, this effect is predominantly driven by the increase in power for detecting weakly selected sites (Kofler and Schlötterer 2014). In the present study, those loci with the strongest antagonistic effects should increase / decrease in frequency rapidly, meaning that I would only additionally recover weakly selected sites over longer time periods.

As well as the number of generations, an additional factor that is an important determinant of the power of an E&R experiment is the effective population size ( $N_e$ ). Lower effective population sizes increase the intensity of genetic drift making it more difficult to differentiate true targets of selection. Here, I estimated the effective population size of the experimental populations at  $N_e=291$ . This was estimated based on the case of maximal reproductive skew whereby only a single individual of the selected sex reproduced in each mating group. While this is most likely a significant underestimate, even with minimal reproductive variance the effective population sizes of the populations in this study are relatively modest.

Overall, this study has successfully validated a small number of the candidate SA loci that were first described in chapter 2. This group of validated loci serves as an important future resource and can be informative for additional targeted validation approaches for individual loci. However, the power of this E&R study was somewhat compromised by an unexpected response to ML selection. In view of that response, future studies that exploit sex-

limited selection should pay special care to the higher reproductive variance expected under ML selection and adjust their experimental designs accordingly. Nonetheless, E&R constitutes a powerful way to validate candidate loci on a genome-wide scale and is a valuable tool for future research.

## 4.6 Tables and Figures

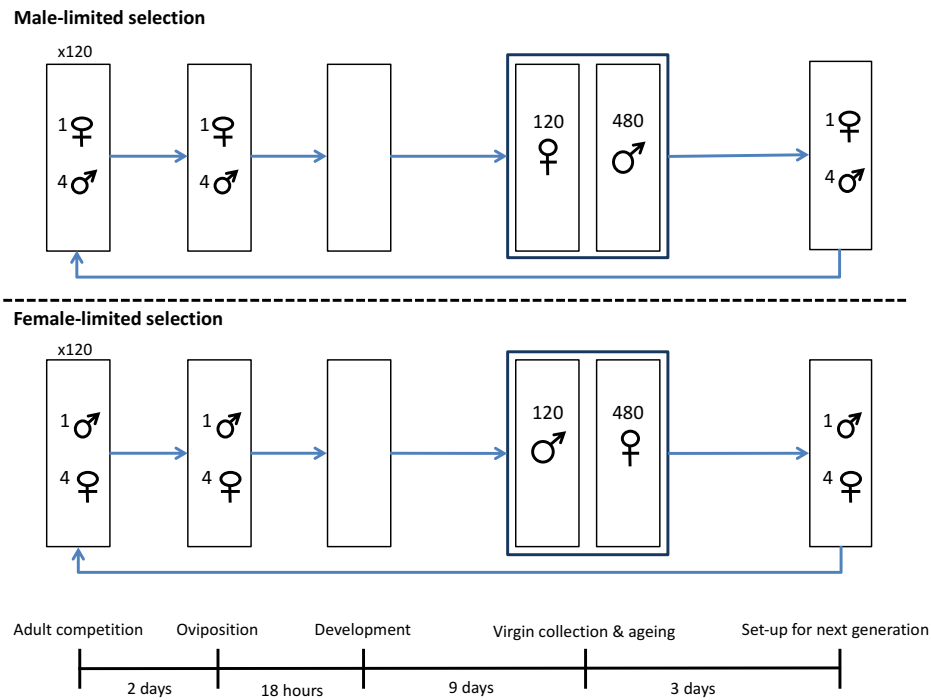


**Figure 4.1: Experimental design used to restrict selection to a single sex.** In the male-limited (ML) selection regime (upper element of figure) 1 female and 4 males are placed in each adult competition vial (x120) for two days before being transferred to oviposition vials. After 18h adult flies are removed and the oviposition vials are kept at 25°C for 9 days while offspring develop. On day 9 newly eclosed adult virgin flies are collected from each vial. To enforce the sex-limited selection, each vial contributes exactly 1 female and 4 males to the next generation. Virgins are kept in same-sex groups for 2 days to age, as per the standard rearing conditions before being mixed and redistributed across 120 new vials, each containing 1 female and 4 males. In female-limited (FL) selection (lower element of figure) the same regime was enforced but each vial contains a single male and 4 females.

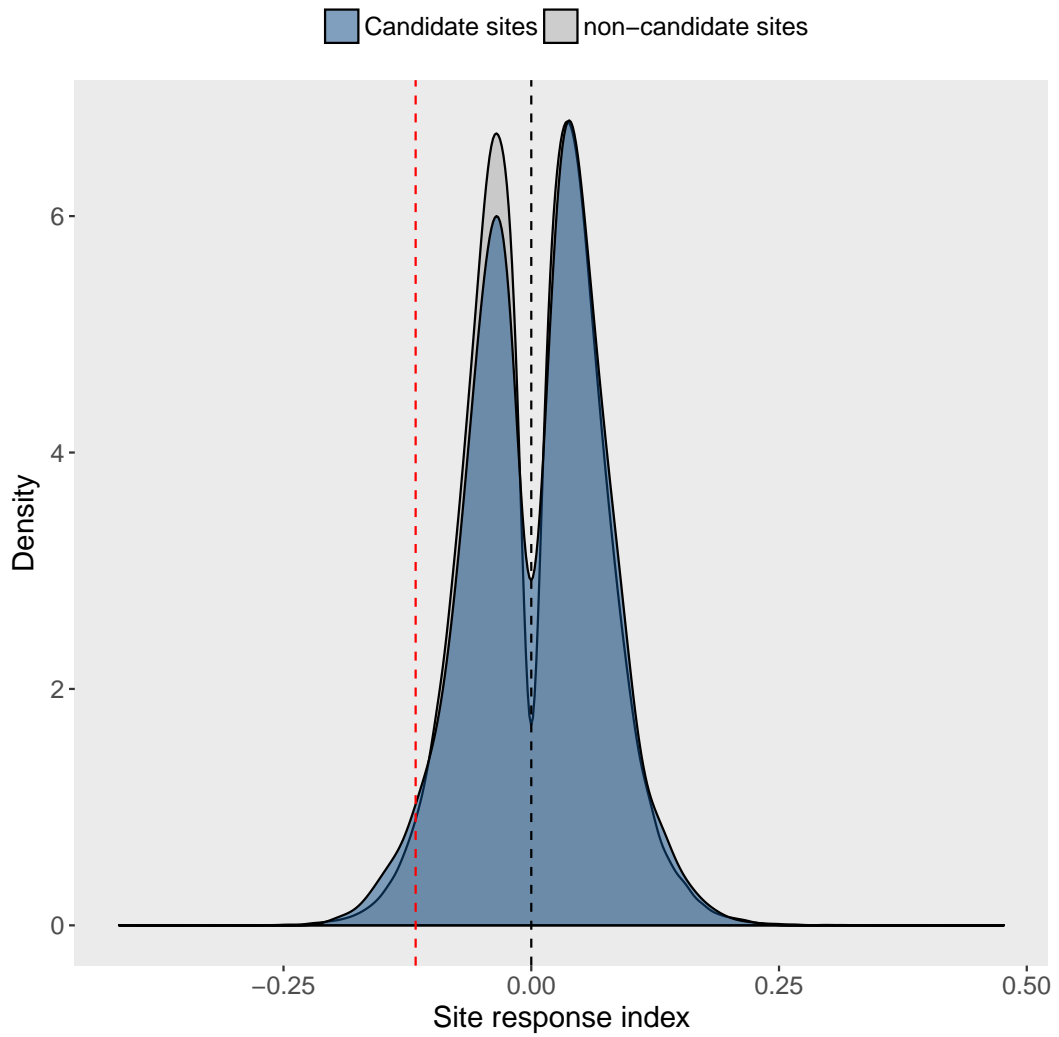


**Figure 4.2: Distribution of the site response index.** Distribution of the site response index (SRI) for candidate (blue) and non-candidate (grey) SNPs. Positive values of the SRI indicate concordant response to selection in the two selection regimes while negative values indicate an antagonistic response. Values of SRI to the left of the red dashed red line ( $y$ -intercept = -0.117) fall within the most extreme proportion (5%) of antagonistic responses to sex-limited selection among non-candidate sites. Antagonistic SNPs falling into this region ( $N=83$ ) are those deemed to have responded more than expected by chance to sex-limited selection.

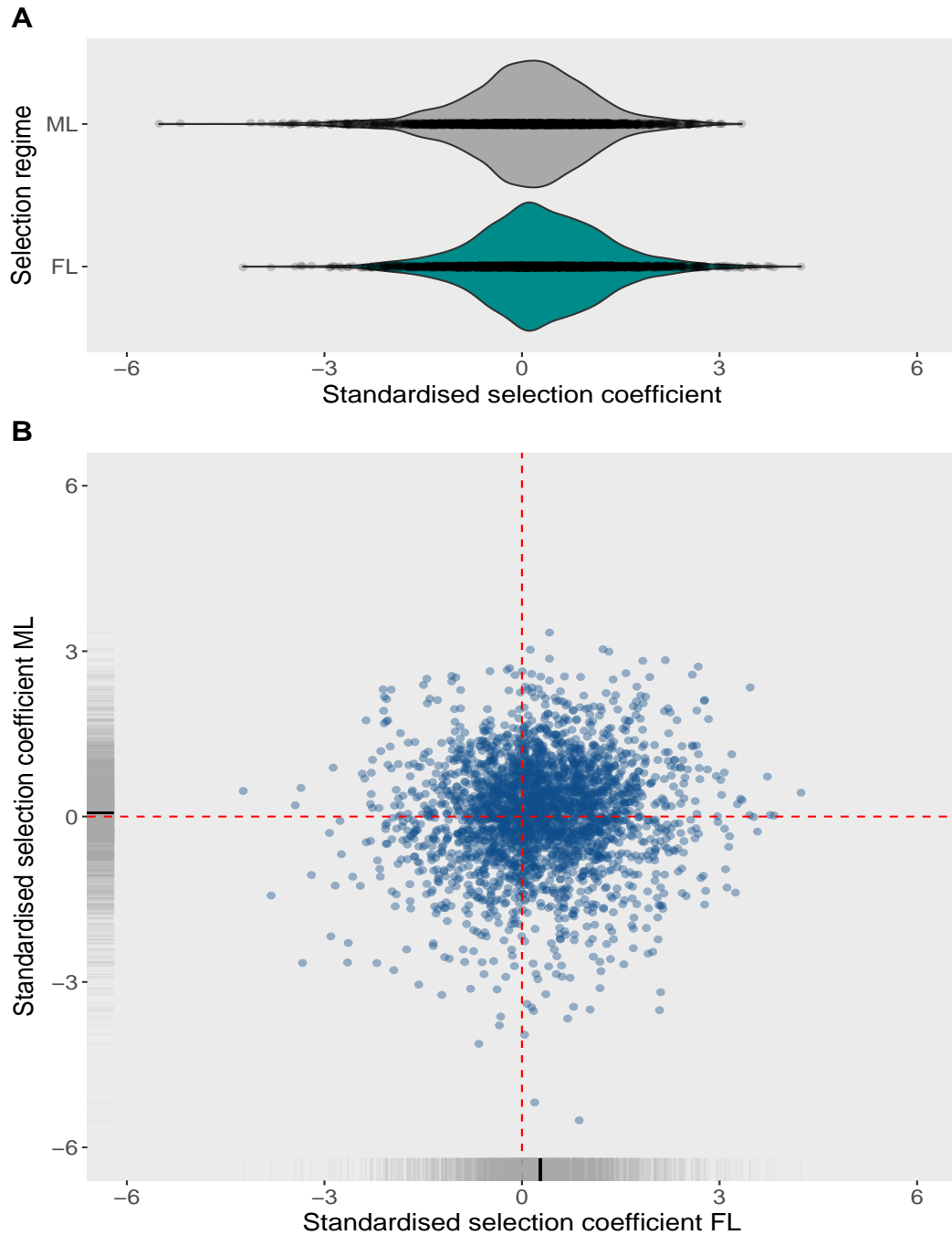


**Figure 4.3: Selection on autosomal female-beneficial variants under sex-limited selection.** **A**, Standardised selection coefficients of female-beneficial variants (as inferred from the haplotype sequencing data) under female- (FL, turquoise) and male-limited (ML, grey) selection for all autosomal antagonistic SNPs in the evolve-and-resequence data. **B**, Relationship between selection coefficients of female-beneficial alleles under male-limited and female-limited selection. The black line in each axis ribbon denotes mean standardised selection coefficient under FL and ML selection.

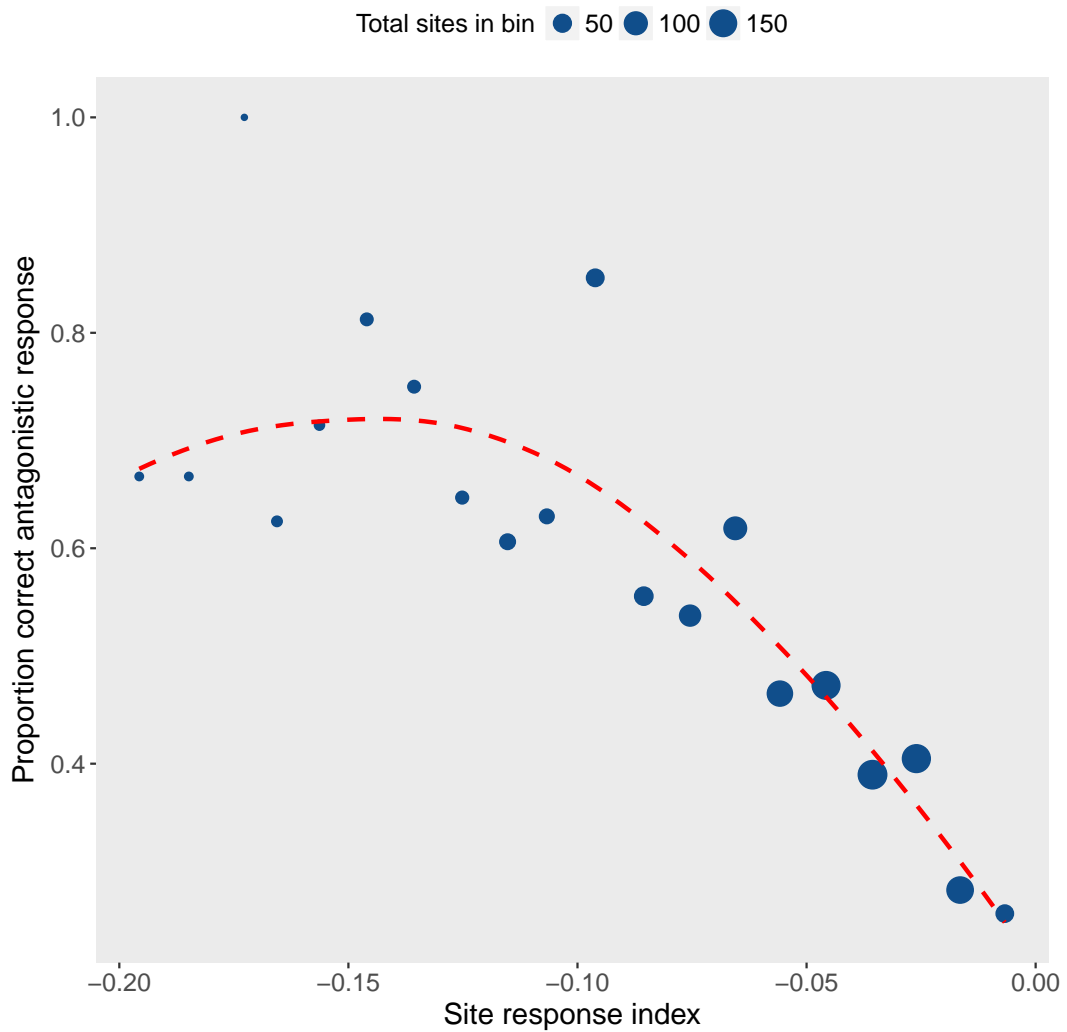


**Figure 4.4: Direction of antagonistic response as a function of the site response index.** Results of an analysis where the antagonistic site response index (site response index  $< 0$ ) was binned (number of bins = 20) and the proportion of responses in the direction expected from the polarised allele analysis was calculated. Expected responses are those where female beneficial alleles increased in frequency under FL selection and decreased in frequency under ML selection. The size of the points corresponds to the total number of SNPs in each bin. The dashed red line is the fitted line from a loess regression, weighted by the number of sites in each bin.

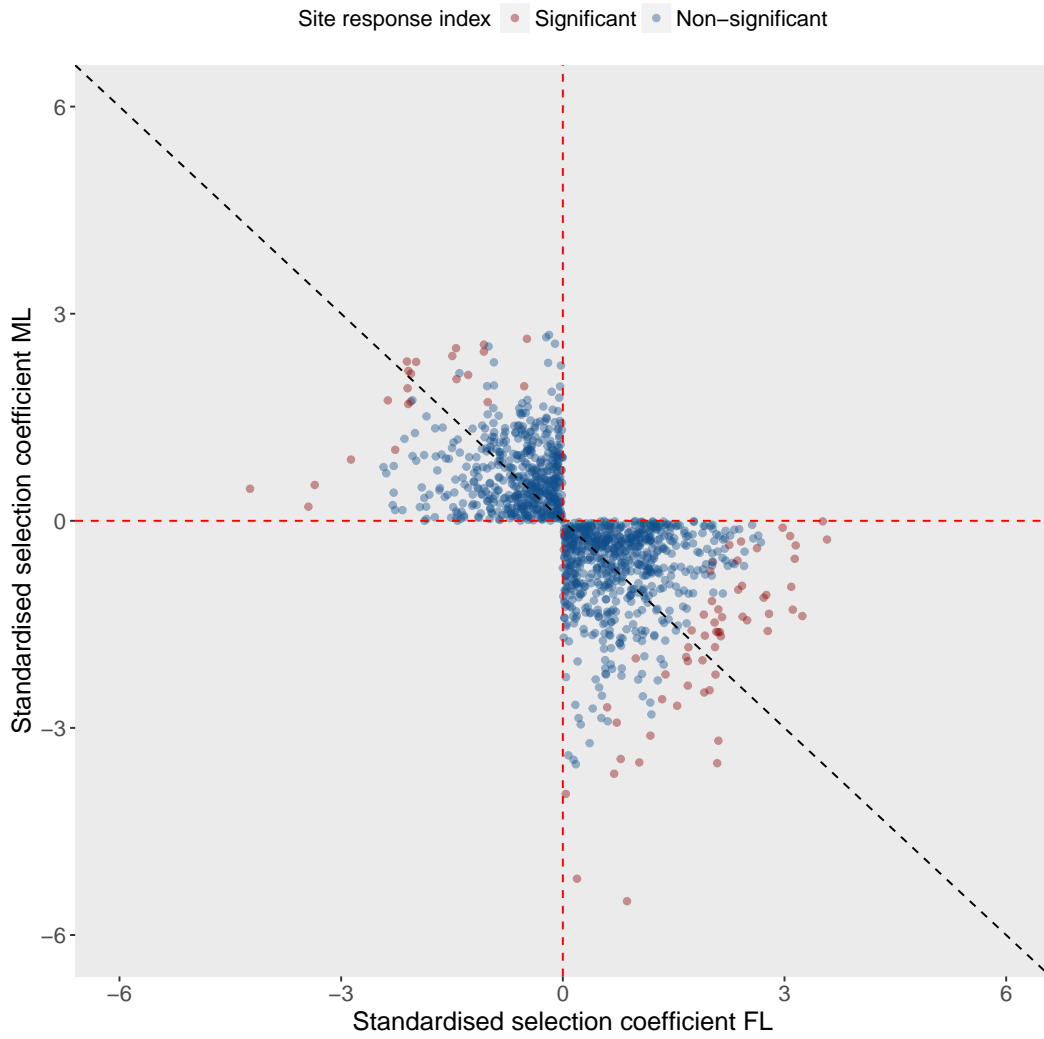


**Figure 4.5: Antagonistic axis of allele frequency change.** Relationship between ML and FL selection coefficients for female-beneficial alleles along the antagonistic axis of allele frequency change (black dashed line). Red points denote those sites which exceed the nominal significance cut-off and fall within the most extreme 5% of the SRI null distribution. Blue dots are those sites which do not fall within the most extreme 5% of the null distribution.

## Chapter 5

# Sexual antagonism and displaced polymorphism in gene regulatory cascades

*This work was initiated by myself and developed and conducted in collaboration with Dr Alex Stewart and Dr Max Reuter. Dr Stewart took the lead on developing the analytical model, I aided in the running and analysis of simulations. All three collaborators contributed to the interpretation of the results. A manuscript describing our findings is being prepared for submission to Nature Ecology and Evolution.*

## 5.1 Abstract

Sexual antagonism, where selection at a locus favours different alleles in each sex, is widespread in populations of animals and plants. Yet, while we have a general understanding of the conditions which favour the presence of sexually antagonistic (SA) alleles, exactly how the biological details of real systems shape these responses to SA selection remains unknown. Here, we address this question for the evolution of gene expression, which is known to contribute to sexual antagonism. By combining a biophysically explicit model of transcription-factor binding with a population genetic analysis of SA polymorphism, we explore the action of SA selection binding site variants evolving on realistic fitness landscapes. We show that the conditions under which polymorphisms will arise at a focal binding site are not adequately captured by a simple 2-allele model of sexual antagonism, analogous to those that have been previously studied. We further show that, when binding sites are part of a wider regulatory cascade, polymorphism that initially arises at a gene directly under SA selection is often later displaced to genes higher up in the regulatory cascade.

## 5.2 Introduction

Males and females are often subject to divergent selection pressures on shared traits, owing to fundamentally different reproductive roles. However, responses to divergent selection are hampered by a largely shared genome, which slows or even prevents the evolution of sexual dimorphism where the two sexes reach their respective phenotypic optima. In this situation, selection can favour the invasion of ‘sexually antagonistic’ (SA) alleles that move the trait value of one sex closer to its optimum, while the value in the other sex is further displaced (Rice 1984; Bonduriansky and Chenoweth 2009; Cox and Calsbeek 2009; Pennell and Morrow 2013).

Sexual antagonism is increasingly recognised to be a taxonomically widespread and important evolutionary phenomenon. A wealth of empirical studies has now documented substantial SA fitness variation across a wide range of animal and plant species (Mokkonen et al. 2011; Tarka et al. 2014; Svensson et al. 2009; Rice 1992; Berger et al. 2014; Barson et al. 2015; Delph et al. 2011). The balancing selection generated by sexual antagonism in these species helps to maintain surprisingly large amounts of heritable fitness variation (Patten et al. 2010). More broadly, sexual antagonism is thought to be a key driver of sex chromosome evolution (Rice 1987; Charlesworth and Charlesworth 2005) and the evolution of sex determination (Haag and Doty 2005; Van Doorn 2009). In addition, sexual antagonism can erode ‘good gene’ benefits to sexual selection (Pischedda et al. 2006).

Classic population genetic theory informs us about the general conditions in which SA alleles can invade and remain polymorphic (Rice 1984; Gavrilets and Rice 2006; Fry 2010). These models have explored the effects of selection and drift on frequency change (Mullon et al. 2012; Connallon and Clark 2012), but in the absence of knowledge about the functional basis of antagonism they have remained purposefully general and do not account for specific properties that arise from the functions of SA variants. Indeed, a number of recent computational and empirical studies show that real evolutionary trajectories are

critically determined by biological properties such as the regulatory architecture (Friedlander et al. 2017) and the patterns of epistasis in the genotype-phenotype map (Wu et al. 2016; Sailer and Harms 2017) associated with genes and the traits they encode. Accordingly, if we are to fully understand the role of SA selection in fundamental evolutionary processes, we must address this problem and characterise SA in the context of realistic and biologically motivated fitness landscapes.

To this end, here we begin to incorporate greater biological context into models of SA selection by creating a realistic model of antagonism in transcription regulation. The focus on gene regulation is motivated by prior empirical work (Ellegren and Parsch 2007; Innocenti and Morrow 2010) as well as the findings of chapter 3. Here, I presented evidence consistent with a largely regulatory basis to sexual antagonism and showed that the binding sites for several transcription factors (TFs) were centrally enriched within short sequences flanking SA SNPs. Thus, we have prior empirical evidence that SA variants do segregate within binding sites. However, what we do not yet know is how easily SA alleles can invade in these regulatory regions and where in regulatory cascades we should expect to find SA polymorphism.

Our model incorporates a realistic description of transcription regulation, built on the biophysical properties of interactions between transcription factors and their DNA binding sites (Gerland and Hwa 2002; Buchler et al. 2003; Bintu et al. 2005; Mustonen et al. 2008). We combine this with a population genetic analysis of the conditions for the invasion and maintenance of SA variants (Rice 1984; Kidwell et al. 1977; Fry 2010; Gavrillets and Rice 2006; Mullon et al. 2012) in finite populations, with regulatory binding sites evolving under weak mutation (Moses et al. 2003; Berg et al. 2004; Sella and Hirsh 2005). Our approach takes into account the action of genetic drift on the evolution of regulatory binding sites and allows for a variety of SA fitness landscapes at the level of gene expression, including those displaying both synergistic and antagonistic epistasis.

Our results show that the details of regulatory architecture fundamentally influence both when and where SA polymorphism will arise. In particular, the conditions for when polymorphisms will arise cannot be adequately captured by a simple 2-allele model of SA, such as those that have been studied previously (Rice 1984; Gavrillets and Rice 2006). We further found that where polymorphism will arise in a gene regulatory cascade is not fixed over time, with polymorphisms that initially arise at genes directly under SA selection frequently undergoing later displacement to other genes higher up in a regulatory cascade.

## 5.3 Methods

### 5.3.1 Biophysical model of transcription factor binding

To model the evolution of binding sites under SA selection we employ a mechanistic model that captures the biophysics of transcription factor binding (Gerland and Hwa 2002; Buchler et al. 2003; Bintu et al. 2005; Mustonen et al. 2008). In this model, transcription factor binding sites are composed of a contiguous region of  $n$  nucleotides. There is one correct binding site sequence (also called the consensus sequence) that provides minimal binding energy between the chromosomal DNA and the transcription factor. Binding energy depends on the binding site sequence in such a way that at each position a “correct” nucleotide will decrease the total binding energy, while an “incorrect” nucleotide will increase it. We make the assumption that each position contributes equally ( $1/n$ ) and independently to the site’s binding energy. Thus, binding energy will decrease linearly (maximum energy to zero) with the number of correct nucleotides, irrespectively of which positions in the binding site sequence are correctly matched.

Under this model the probability that a binding site is bound by a transcription factor (TF) to produce transcript depends on the binding energy and

is given by

$$\pi_i = \frac{P}{P + \exp[\epsilon(n - i)]}. \quad (5.1)$$

Thus, binding depends on the number of TF proteins  $P$  available to bind, the binding site length  $n$  (number of nucleotides), the number of nucleotides  $i$  that match the consensus sequence, and a constant  $\epsilon$  which describes the increase in binding energy for each additional mismatch between the binding site and the consensus sequence (found empirically to be  $\sim 1 - 3k_B T$  (Gerland and Hwa 2002; Lässig 2007)).

This model adequately captures the biophysics of transcription factor binding (Lässig 2007) and generates a probability of binding that is sigmoidal in the number of nucleotides in a binding site that match the consensus sequence. In reality, the assumption that each nucleotide position contributes equally and independently to binding energy does not necessarily hold (Lässig 2007; Santolini et al. 2014), however this simplified model is useful for capturing the evolutionary dynamics of gene regulation (Stewart and Plotkin 2012).

Under our simplified model, any of the three mismatching incorrect nucleotides at a position in the binding site produces a functionally equivalent non-binding state. The important consideration is therefore not which nucleotide occurs at a given position but only whether the nucleotide matches the consensus sequence. We can use this degeneracy to reduce the number of different alleles associated with a given site from  $4^n$ —the number of distinct genotypes that can occur—to  $n + 1$ , the number of possible correctly matched nucleotides at the site (ranging from 0, 1, 2, to  $n$ ). A binding site is thus characterized by a single number  $i$  which is the number of positions that match the consensus sequence.

### 5.3.2 Gene regulation under weak mutation

Mutations in the binding site occur through single nucleotide substitutions which increase,  $\mu^+$ , or decrease,  $\mu^-$  the number of matches. Across the entire binding site, the rates of these mutations are

$$\begin{aligned}\mu_i^+ &= \mu \frac{n-i}{3n} \\ \mu_i^- &= \mu \frac{i}{n}\end{aligned}\tag{5.2}$$

where  $\mu$  is the per-nucleotide rate of substitution. What is immediately clear from Equation (5.2) is that mutation rates are asymmetrical and, more importantly, vary with genotype (specifically, they depend on the number of current matches  $i$ ). This latter property violates the assumption of constant mutation rate that is commonly made in general population genetic models (including those of sexual antagonism) and complicates analyses whenever mutations occur in polymorphic populations (because the genetic background of a new mutation is not random). We can avoid these complications by treating the evolution of binding sites in the weak mutation limit, i.e., in a case where mutations are sufficiently rare for one mutation to either be lost or go to fixation before the next one arrives. This assumption requires that the product of effective population size and mutation rate be small,  $2n\mu N_e \ll 1$ . This is justified here, because we are considering mutation rates at the level of nucleotide substitutions which are typically low (between  $10^{-9} - 10^{-7}$ , Nachman and Crowell 2000) and therefore fulfil the weak mutation condition for reasonably large effective population sizes.

In the weak mutation limit without SA selection, evolutionary dynamics are well approximated by the diffusion process (Sella and Hirsh 2005). If we write  $\pi_i^t$  for the probability that the population has a binding site with  $i$  matched nucleotides at time  $t$  then we can write

$$\pi_i^{t+1} = \pi_i^t(1 - \mu_i^+ \rho_{i \rightarrow i+1} - \mu_i^- \rho_{i \rightarrow i-1}) + \pi_{i+1}^t \mu_{i+1}^- \rho_{i+1 \rightarrow i} + \pi_{i-1}^t \mu_{i-1}^+ \rho_{i-1 \rightarrow i} \quad (5.3)$$

where  $\rho_{i \rightarrow j}$  is the probability that a mutant with  $j$  matched nucleotides fixes in a population where an allele with  $i$  matches is resident. For a given pair of alleles in the absence of SA, the fixation probabilities  $\rho$  can be calculated based Kimura's classic expression (Kimura 1962). This can then be used in an equilibrium condition obtained by detailed balance

$$\pi_i \mu_i^- \rho_{i \rightarrow i-1} = \pi_{i-1} \mu_{i-1}^+ \rho_{i-1 \rightarrow i} \quad (5.4)$$

which can be solved numerically.

### 5.3.3 Sexual antagonism and weak mutation

When we are dealing with SA selection, this weak mutation treatment breaks down. The main reason is that in the presence of SA as a source of potentially balancing selection, the population can no longer be assumed to be monomorphic. Furthermore, with opposing sex-specific selection pressures the evolutionary dynamics of an invading allele are different between males and females. However, this limitation can also be dealt with. Thus, when selection is weak, polymorphism cannot typically be maintained under SA selection and evolutionary dynamics are well approximated by assuming that an allele under antagonistic selection is at the same frequency among males and females (Charlesworth et al. 1987; Connallon and Clark 2011). We can then use Equation (5.4) to gain insights into the evolutionary dynamics of sexual antagonism at a binding site under weak selection.

To define SA fitness landscapes (and determine the values of  $\rho$  in Equation (5.4)) we use the biophysical model of TF binding detailed above to calculate

the expression level  $E$  as a function of the number of matches  $i$ . We assume diploidy (two binding sites) and the expression level  $E$  of a focal gene is then given by the sum of expression across two alleles:

$$E = \frac{P}{P + \exp[\epsilon(n - i_1)]} + \frac{P}{P + \exp[\epsilon(n - i_2)]} \quad (5.5)$$

We then need to convert expression levels into fitness values. We assume, without loss of generality, that selection favours high expression in males and low expression in females. This generates a fitness landscape where fitness in males ( $w_m$ ) monotonically increases with increasing expression and fitness in females ( $w_f$ ) monotonically decreases with increasing expression. Fitness is determined by the strength of selection ( $\sigma$ ), the total expression ( $E$ ), and the curvature of the fitness landscape ( $c$ ), such that

$$\begin{aligned} w_m &= A_m [1 + \sigma_m E]^{c_m} \\ w_f &= A_f [1 + \sigma_f (1 - E)]^{c_f} \end{aligned} \quad (5.6)$$

where the constant  $A$  scales absolute fitness to a maximum of 1.

### 5.3.4 Evolutionary dynamics of a binding site under SA selection

In order to analyse the evolutionary dynamics of a binding site under SA selection in the weak-mutation weak-selection limit, first recall Kimura's expression for the fixation probability of a mutation with relative fitness  $1 + s$  (in the homozygote state) against a resident with relative fitness 1 (Kimura 1962):

$$\rho = \frac{1 - \exp[-2s]}{1 - \exp[-4Ns]}, \quad (5.7)$$

where weak selection requires  $2Ns \ll 1$ . We then use Equation (5.5) to calculate the average fitness effect  $s$  of a mutation that changes the number of nucleotide matches  $i$  in a binding site by  $\pm 1$ :

$$s \approx \frac{w_m(i) + w_f(i)}{w_m(i+1) + w_f(i+1)} - 1 \quad (5.8)$$

where  $w_l(i)$  is the fitness of an individual of sex  $l$  that is homozygote for binding site sequences with  $i$  nucleotide matches. Substituting this expression of  $s$  into Equation (5.4) we can calculate the ratio of transition probabilities for mutations that increase or decrease nucleotide matches

$$\phi_i = \frac{(n-i)\rho_{i \rightarrow i+1}}{3(i+1)\rho_{i+1 \rightarrow i}} \quad (5.9)$$

If  $\phi_i > 1$ , the number of nucleotide matches tends to increase whereas when  $\phi_i < 1$ , the number of nucleotide matches tends to decrease. This is used to describe the evolutionary dynamics as shown in Figure 5.3 (described in the results 5.4.1).

### 5.3.5 Conditions for polymorphism

SA can lead to polymorphism where a given pair of alleles may be simultaneously maintained in the population for long periods of time. This is especially true when we move outside of the weak selection limit, where balancing selection becomes stronger relative to genetic drift (Connallon and Clark 2012;

Mullon et al. 2012). In this case, the condition for a pair of alleles to be maintained is given by (Connallon and Clark 2012)

$$\frac{s_m(1 - h_m)}{h_f(1 - s_m)} > s_f > \frac{s_m h_m}{1 - h_f + h_m s_m}. \quad (5.10)$$

We can now calculate  $h$  and  $s$  as follows

$$\begin{aligned} s_m &= \frac{w_m(i)}{w_m(i+1)} - 1 \\ s_f &= \frac{w_f(i)}{w_f(i+1)} - 1 \\ h_m &= \frac{\frac{w_m(i)}{w_m(i,i+1)} - 1}{\frac{w_m(i)}{w_m(i+1)} - 1} \\ h_f &= \frac{\frac{w_f(i)}{w_f(i,i+1)} - 1}{\frac{w_f(i)}{w_f(i+1)} - 1} \end{aligned} \quad (5.11)$$

where  $w(i, i+1)$  is a heterozygote consisting of alleles with  $i$  and  $i+1$  nucleotide matches. Substituting Equation (5.11) into Equation (5.10) we recover the regions in which polymorphism can arise, as shown in Figure 5.3 (described in the results 5.4.1).

### 5.3.6 Simulations

We carried out evolutionary simulations using the model for transcription factor binding as described above. This allowed us to relax the somewhat restrictive assumptions we made for the analytical approximations. Furthermore, we could extend our model from a single gene to a multi-gene cascade. We simulated populations composed of  $N/2$  males and  $N/2$  females evolving under the diploid Moran model. This model captures the case of a fixed population

size with overlapping generations. The model consists of birth-death events, in which in each timestep a pair of one male and one female are randomly drawn from the population, with probabilities weighted by the individuals' fitness. The chosen pair then produces one offspring which replaces another member of the population chosen at random. At each locus, the offspring receives one allele from its mother and one from its father. These alleles, both potentially altered by mutation, determine the binding at this particular binding site in the offspring.

We used individual-based simulations to track the evolution of simple, hierarchical gene regulatory cascades of up to three genes, each with an evolving transcription factor binding site. The top gene is an initial TF that receives a fixed input (equal in males and females). This TF regulates the second gene in the cascade, an intermediary TF, which in turn regulates the terminal target gene. Only the expression level of the terminal target gene is directly subjected to SA selection. (the cascade is illustrated on the right-hand side of Figure 5.4). We calculated the expression level of each gene in the cascade according to our model of TF binding, which then gave the fitness of the individual based on the expression level of the terminal gene (Equation (5.6)). We simulated populations of  $N$  individuals with a per nucleotide mutation rate of  $\mu = 0.1/(2Nn)$  to ensure weak mutation.

## 5.4 Results

In order to study when and where polymorphism due to SA selection will arise in a gene network, we develop a population genetic model that captures the evolutionary dynamics of binding site mutations while explicitly taking into account the biophysical properties of transcription factor binding (Figure 5.1). We explore the model via a combination of analytical approximation and individual-based simulations.

### 5.4.1 Polymorphism at a single binding site

Using the framework described above we examine the conditions that lead to polymorphism arising at a binding site regulating a gene under SA selection for expression levels. We first explore this question analytically, in order to gain an understanding of the evolutionary dynamics of binding sites under sexually antagonistic selection. Specifically, we examine, in the weak selection weak mutation limit, the equilibrium number of binding site matches  $i$ , as a function of the curvature of the fitness landscape  $c$  upon which the binding site evolves. Low values of  $c$  describe a fitness landscape where a population monomorphic for intermediate binding (and hence expression level) achieves greater average fitness across males and females than a polymorphic population with strong binding (high expression) and weak binding (low expression) (Figure 5.1c - left). In contrast, high values of  $c$  capture a scenario where average fitness across males and females is greater with polymorphism (high and low expression) than with monomorphic intermediate expression (Figure 5.1c - right).

Figure 5.3 shows that for low values of  $c$ , there is a single stable equilibrium number of binding site matches  $i \approx 5$ , defining selection for a monomorphic, intermediate strength binding site. As  $c$  increases the population moves to a state where there are two stable equilibria, separated by a single unstable equilibrium (light blue line in the figure), describing disruptive selection for binding site matches. The grey region of the plot shows the conditions when polymorphism between pairs of alleles can initially arise, and the arrows the tendency for evolution to result in increased or decreased numbers of binding site matches ( $i$ ). Thus, in order for SA polymorphism to arise, a pair of alleles must fall either side of the unstable equilibrium in the (grey) area of the parameter space that supports polymorphism.

Having established the general conditions for the invasion of SA polymorphism at a single binding site under weak selection, we next relax our restrictive assumptions in individual-based simulations to explore the emer-

gence of SA polymorphism as a function of the binding site length ( $n$ ). Given the critical importance of the landscape curvature revealed in the analytical approximations, we simulate on two contrasting fitness landscapes. (i) a ‘synergistic’ fitness landscape with  $c = 0.5$ , and (ii) an ‘antagonistic’ fitness landscape with  $c = 2$ , to capture the range of landscape space. These landscapes are shown in Figure 5.1c.

We find that as the binding site length increases from the 2-allele case (which is equivalent to a binding site length of 1) to more realistic values ( $n=10$ ), we move from a situation where polymorphism is common for both synergistic and antagonistic landscapes to one where polymorphism can only persist in antagonistic fitness landscapes (Figure 5.2a). To investigate how robust this result is in the face of genetic drift we simulated for a binding site of length  $n=10$  under a range of population sizes ( $N = 100 - 2000$ ). As can be seen in Figure 5.2b, we find that for binding sites of length  $n=10$ , polymorphism at binding sites on an antagonistic fitness landscape arises across the scale of population sizes, whereas it is never appreciable at binding sites on a synergistic fitness landscape.

### 5.4.2 Polymorphism in a gene regulatory cascade

Having established the conditions under which polymorphism will arise at an individual binding site under SA selection, we now incorporate a broader regulatory context to ask where polymorphism will arise and persist in a gene regulatory cascade. We consider the evolution of gene expression from this regulatory cascade on an antagonistic fitness landscape. Figure 5.4, shows a typical time series tracking polymorphism across the regulatory cascade over time. The traces illustrate that polymorphism quickly arises at the binding site of the terminal gene in the cascade, shown by the branching of the population to binding sites with four and seven matches, respectively. Interestingly, however, this polymorphism is not stable over time. Rather, after  $\approx 3,500$  generations, polymorphism is lost at the terminal gene with the population becoming fixed for increased binding (eight matches). At the same time, we

observe the invasion of SA polymorphism at the initial gene at the top of the regulatory cascade. Thus, we observe displacement of SA polymorphism from the base of the regulatory cascade to the top. Further simulations show that the displacement of SA polymorphism from the terminal gene to those further upstream is a general phenomenon and across simulation runs, the frequency of polymorphism observed at the intermediate or top genes increases steadily over the course of the generations simulated (Figure 5.5).

## 5.5 Discussion

Previous empirical work has made a strong link between expression regulation and sexual antagonism (Innocenti and Morrow 2010, chapter 3). But, until now we did not have a solid theoretical understanding of the conditions that allow SA polymorphism to invade at TF binding sites of genes subject to opposing sex-specific selection on gene expression. Moreover, it was not known where in gene regulatory cascades we should expect to find such polymorphism.

To address these questions, we first examined the conditions necessary for polymorphism at a single binding site under SA selection. We showed that when SA polymorphism arises is not accurately captured by a general two-allele model, such as those that have been previously studied (e.g., Rice 1984; Gavrilets and Rice 2006). Accordingly, polymorphism could arise under both synergistic and antagonistic landscapes in the two-allele model, whereas with more realistic binding site lengths ( $n > 1$ , Stewart and Plotkin 2012) polymorphism could only persist in antagonistic fitness landscapes.

To understand this discrepancy, we need to consider the interaction between the fitness landscape and the genetic encoding of binding. In synergistic fitness landscapes, selection will favour a monomorphic state of intermediate binding (and hence intermediate expression) because in this state the average fitness across males and females is greater than that achieved in a polymorphic population with strong binding (high expression) and weak binding (low expression). Our more explicit binding site model makes reaching this evolu-

tionary optimum possible, because intermediate binding can be achieved via an intermediate number of matching nucleotides, and accordingly predicts no polymorphism in this case. The two-allele model, however, effectively imposes a binding site of length one, thereby making intermediate binding impossible and forcing the population into a polymorphic state.

We next investigated where in a regulatory cascade polymorphism is expected to segregate. We showed that the location of polymorphism is not necessarily fixed over time. Thus, polymorphism that initially arises at a terminal gene of a regulatory cascade can later undergo displacement to genes higher up in the regulatory chain. This result can be understood by considering the compensatory mechanisms that occur in gene regulatory networks. The multiple layers of regulatory interactions that characterise gene regulatory cascades allow for variation in expression of upstream TFs to be buffered (MacNeil and Walhout 2011), reducing the variance felt at the terminal gene. This means that the waiting time for successful invasion of SA polymorphism at the terminal gene is much lower than that for invasion at the initial gene in the regulatory cascade, because mutations here can much more easily generate expression variance than those occurring further up in the cascade.

However, although it is easier for polymorphism to initially arise at the terminal gene, higher heterozygote fitness is associated with polymorphism higher up in the regulatory cascade. This is because a heterozygote with one strong binding allele and one weak binding allele at the terminal gene will yield intermediate expression levels, which in an antagonistic fitness landscape is, on average, worse than homozygous strong or weak binding. In contrast, a heterozygote at the initial gene in the cascade can still generate a pattern of high or low expression of the terminal gene owing to the compensatory buffering effect of regulatory interactions. This means that, overall, population fitness is highest with antagonistic polymorphism at the top of a regulatory cascade. Consequently, we see a pattern of SA alleles first invading at the terminal gene in a regulatory cascade and the later gain of SA polymorphism

at upstream genes over time (Figure 5.5).

In this study we simulated a simple linear regulatory cascade of three genes. In reality, gene regulatory networks can have more complicated topologies. Questions therefore remain as to how general we can expect the displacement of SA polymorphism across regulatory networks to be and what level of the regulatory hierarchy it can reach.

A major factor affecting the displacement of SA polymorphism in a regulatory network will be pleiotropy, where upstream TFs regulate more than one terminal gene. This is common in real networks, which often feature genes that serve as highly connected regulatory hubs, and where regulation is organised in a modular fashion (MacNeil and Walhout 2011). Whether an upward displacement of SA polymorphism will occur in this situation is likely to depend largely on how SA selection is distributed across transcriptional modules. For example, consider a case where a regulatory cascade has  $>1$  terminal genes, all of which are under SA selection. If selection is aligned across the genes of this module, i.e. high expression is favoured in males for all the genes and *vice versa*, this will effectively increase the strength of selection and most likely result in quicker displacement of polymorphism towards upper layers of the regulatory hierarchy. In contrast, non-symmetric fitness effects, where either SA selection pressures are reversed between co-regulated genes or a module contains genes under both SA and sexually concordant selection, would be expected to slow or preclude the invasion of upstream SA polymorphism. These expectations were supported by exploratory simulations, not detailed here. Taken together, this means that we can consider the probability that SA polymorphism ascends a regulatory cascade as a function of the modularity of SA phenotypes. Thus, the causal loci for highly modular SA phenotypes (where the trait is encoded by a relatively discrete regulatory cascade) may be more likely to map to upstream TFs than those for non-modular phenotypes.

The level in the regulatory hierarchy that SA polymorphism can reach will also be influenced by the level of redundancy. Redundancy can confer

phenotypic robustness, whereby a network can produce a given pattern of expression in the face of perturbation (for example from incoming mutation) (MacNeil and Walhout 2011). Redundancy can arise through several mechanisms. For example, multiple TFs from the same family could bind the same cis-regulatory sequence (e.g., Hollenhorst et al. 2007; Ow et al. 2008), or there could be several binding sites each bound by different TFs clustered together in a cis-regulatory module that collectively regulate a target gene (e.g., Small et al. 1992; Halfon et al. 2000).

Previous work in yeast suggests that different layers in the hierarchy of gene regulatory cascades can display quite striking differences, particularly in terms of the number of regulatory interactions. An emerging trend is that TFs at the top and bottom of the hierarchy regulate fewer target genes than those in the core layers (Maslov and Sneppen 2005; Farkas et al. 2006; Jothi et al. 2009). This suggests that there is a high level of redundancy at core levels of regulatory networks. In the context of our findings this means that if polymorphism is displaced from a target gene under SA selection it could bypass the intermediate tiers of regulators and jump further up the regulatory hierarchy. This is because SA target gene expression will be more sensitive to changes at the top of the regulatory cascade than to those at the core.

Our finding that SA polymorphism can ascend regulatory cascades over time is of great significance for how we interpret SA alleles identified in empirical studies. It suggests that when we observe SA alleles at genes at the base of regulatory cascades these are possibly much younger than those segregating among the upper echelons (see chapter 6 for more extensive discussion). The time taken for displacement will be largely sensitive to factors such as pleiotropy and mutation rate. Indeed, here we only allow for single nucleotide substitutions, but invasion of indels would likely speed up the process. As such, estimates of displacement time will likely have to be considered on a case-by-case basis. Overall, however, we expect it to be a relatively slow process.

The findings documented here are also of relevance to the resolution of sexual antagonism. In cases where SA alleles are distributed across the base of regulatory cascades, large-scale resolution will be relatively inefficient as it will require numerous independent mutations that allow for sex-specific regulation on a gene-by-gene basis. In contrast, if several genes under SA selection are arranged as a module and regulated by a TF segregating for SA alleles, then module-wide resolution can be achieved via the evolution of a single instance of sex-specific regulation of the upstream TF. The timescale over which resolution occurs following the invasion of SA polymorphism will likely be substantial in both cases. In the first case, gaining sex-specific regulation of multiple genes independently will be very slow. In the second case, the timescale is mainly determined by the rate at which SA polymorphism ascends a regulatory cascade, which is again expected to be slow.

Previous empirical work (Appendix B, Collet et al. 2016) has suggested that sexual antagonism may be characterised by long periods of stasis, followed by punctuated bursts of large-scale resolution. The upwards propagation of SA in regulatory cascades that we describe fits well with this hypothesis. Thus, periods of stasis are determined by the time it takes for ascension to occur. Once polymorphism has reached the upper levels of a regulatory cascade it would only take a single innovation, engendering sex-specific regulation, to resolve conflict at a large number of genes, and cause potentially large shifts in sex-specific fitness within a population. The extent to which SA alleles are clustered in the same regulatory cascades remains to be tested empirically but is currently difficult to assess given the low resolution of regulatory network annotation in *D. melanogaster*, the only species where we currently have a list of genome-wide putative SA alleles (chapter 2).

The model we present here specifically considers the action of SA selection. But, our framework could be extended to investigate other forms of antagonistic selection. Indeed, the movement of alleles through the two sexes over successive generations is analogous to experiencing alternating external

environments (Appendix C). Thus, in cases where there is selection for opposing levels of gene expression in different contexts we might expect similar patterns of evolutionary branching in regulatory networks. However, there are some caveats to consider when drawing parallels between sex-specific and environment-specific selection pressures. Principally among these is that the constancy of sex-specific selection pressures is likely much higher than the constancy of fluctuations in external selection pressures.

To conclude, we have shown that the invasion of SA polymorphism at binding sites under SA selection will depend critically on the shape of the fitness landscape. In some cases, owing to the multi-allele nature of TF binding, a monomorphic state yielding intermediate expression levels will be favoured above SA polymorphism. We have further shown that the location of SA polymorphism in a regulatory cascade is not fixed and can ascend up towards the top-level regulators over extended time periods. Once here, the resolution of SA may be more efficient as the incorporation of a single sex signal could allow resolution across many downstream antagonistic genes.

## 5.6 Tables and Figures

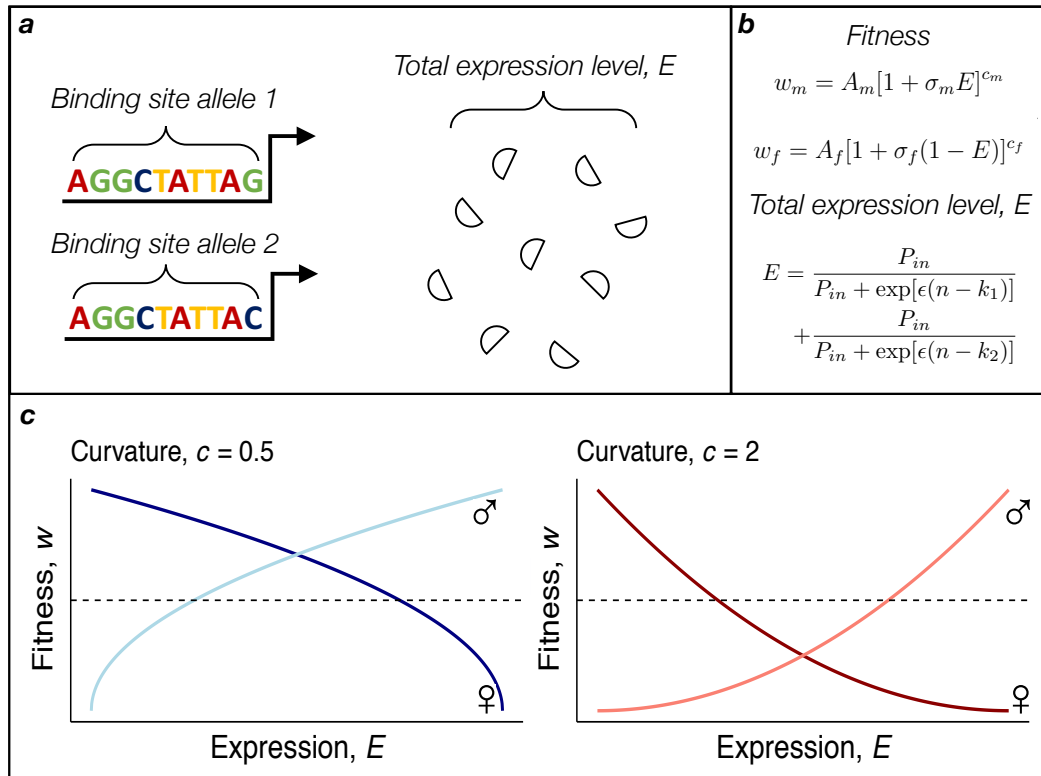


**Figure 5.1:** We study the impact of sexual antagonism on the evolution of gene regulatory networks (a) under which transcription factor binding sites modulate gene expression. We consider selection to act directly on expression (b) such that males have higher fitness if the gene under selection is highly expressed while females have higher fitness if the gene has low expression. This results in a fitness landscape (c) in which fitness is monotonically increasing (males) or decreasing (females) with increasing gene expression level. Depending on the curvature of the landscape  $c$ , the landscape is either antagonistic (right) such that the average fitness of males and females with an intermediately expressed gene is less than the average fitness due to having a polymorphism with both highly and lowly expressed genes (black line) or else a synergistic landscape (left) where the converse relationship is true.

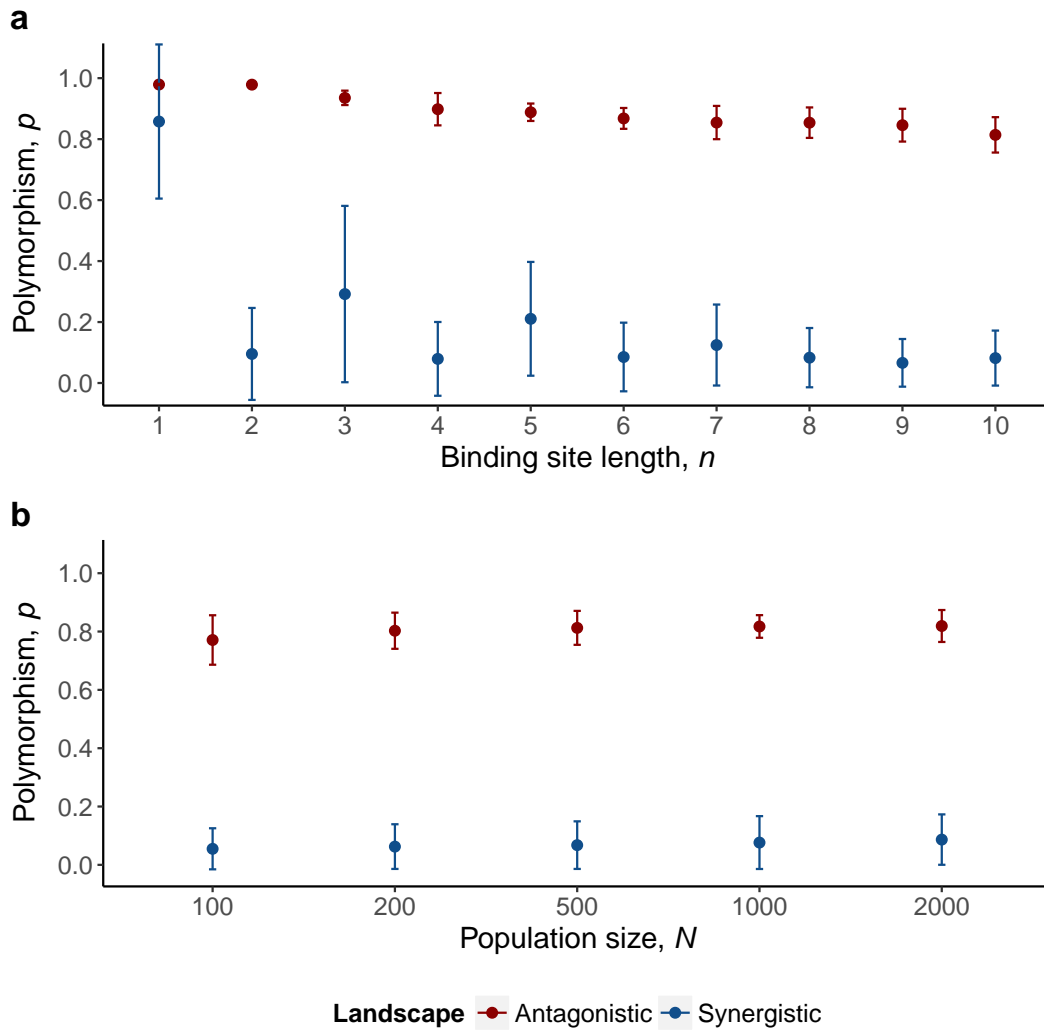


**Figure 5.2: Polymorphism as a function of binding site length and population size.** **a**, Results of individual-based simulations showing the amount of polymorphism ( $p$ ) as a function of the binding site length ( $n$ ) for antagonistic (red) and synergistic (blue) fitness landscapes. **b**, Results of individual-based simulations showing the amount of polymorphism ( $p$ ) as a function of the population size ( $N$ ) for antagonistic (red) and synergistic (blue) fitness landscapes.

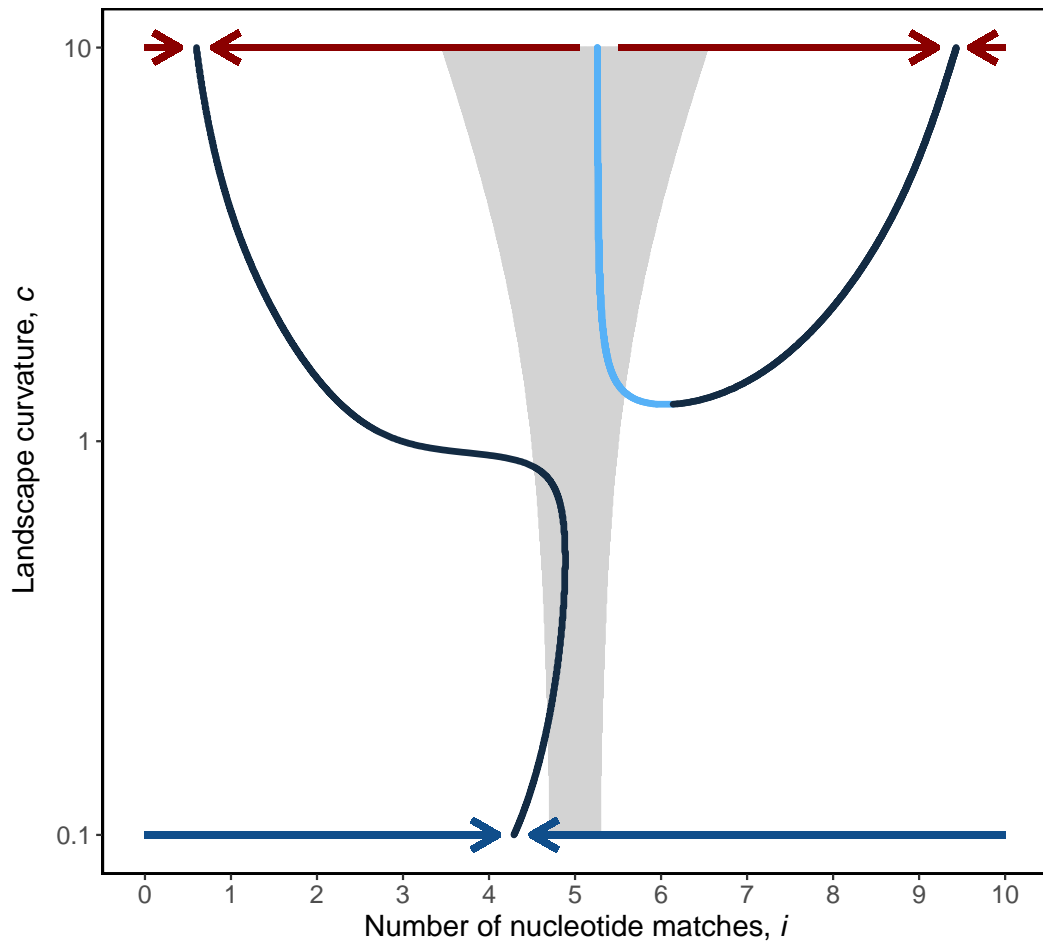


**Figure 5.3: Pairwise mutation-selection plot for an evolving binding site.** Solid lines show the equilibrium values of nucleotide matches ( $i$ ) as a function of the landscape curvature ( $c$ ). The colour of the solid lines indicate whether equilibria are stable (dark blue) or unstable (light blue). The grey region indicates values of  $i$  and  $c$  for which selection favours polymorphism between pairs of alleles. Finally, the arrows indicate the tendency for evolution to result in either increased or decreased values of  $i$  for antagonistic (red) and synergistic (blue) landscapes.

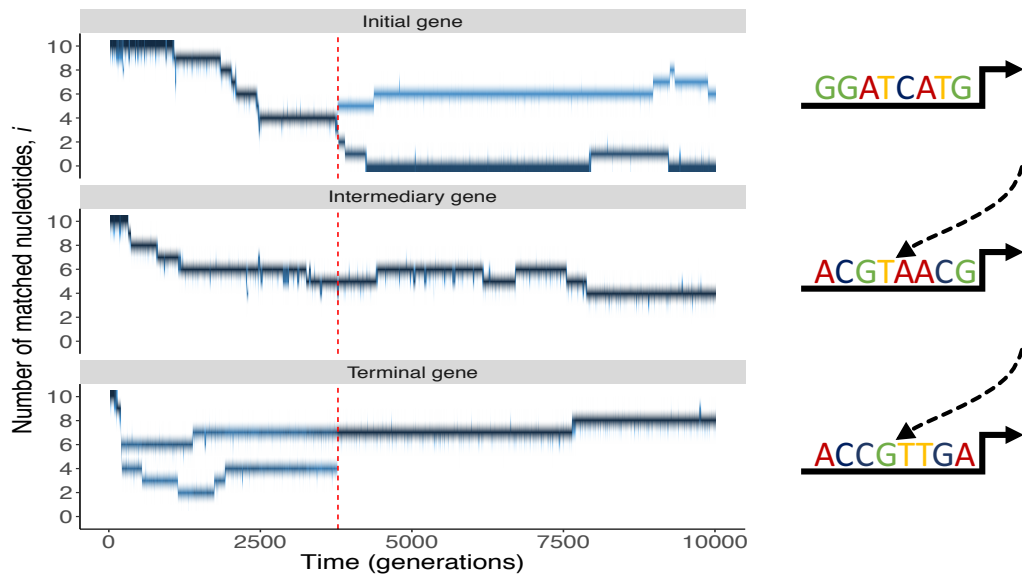


**Figure 5.4: Antagonistic polymorphism across a regulatory network.** Results from individual-based simulations showing the number of matched nucleotides ( $i$ ), across the population, as a function of time (number of generations). Colour of trace lines indicates the proportion of the population with a given value of  $i$ , darker blue represents higher density. The dashed red line delineates the time point at which displacement of polymorphism from the terminal gene (the gene directly under sexually antagonistic selection) to the initial gene, at the top of the regulatory cascade, occurs.

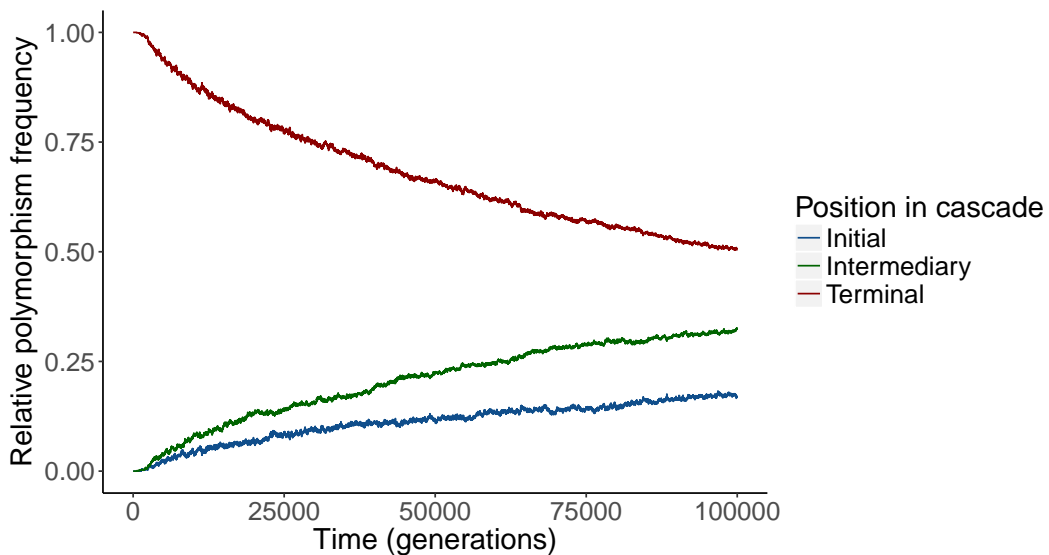


**Figure 5.5: General displacement of polymorphism over time.** Results from individual-based simulations showing the relative polymorphism frequency at each gene in the regulatory cascade, as a function of time (number of generations). Trace lines represent the average over 1,000 time series.

## Chapter 6

# General Discussion

## 6.1 Overview

Gaining a comprehensive understanding of the limits on the evolution of sexual dimorphism and sex-specific adaptation requires that we understand the genetic constraints that act on such adaptation. This includes elucidating the functional basis and the evolutionary dynamics of SA variation, which directly reflect the nature of adaptive constraint on the sexes. Until now, a major barrier to this has been an almost complete lack of information on the identity and characteristics of SA loci. In this thesis I have described the first genome-wide identification of SA loci in any species (chapter 2). Following on from the initial identification, I characterised the biological properties of these loci (chapter 3) and provided some independent validation (chapter 4). Finally, building on the insights gained throughout the preceding chapters and from previous work I explored the invasion and maintenance of SA alleles in gene regulatory networks (chapter 5). Here, I recapitulate and integrate the principal findings of this thesis and comment on promising directions for future research. In particular, I focus on what the current results tell us about the functional basis of sexual antagonism and how they help us to better understand its evolutionary dynamics.

In chapter 2, I focused on identifying putative SA SNPs across the *D. melanogaster* genome. For this I sequenced a set of nine haplotypes with strongly opposing sex-specific fitness profiles. Five of the haplotypes had male-beneficial / female-detrimental fitness effects and four had female-beneficial / male-detrimental fitness effects. Comparing these two sets of haplotypes allowed me to identify those regions that were associated with SA fitness effects. The large number of credible candidate SA SNPs identified fits with our expectations of a polygenic basis to sex-specific fitness, and hence sexual antagonism, which is affected by a diversity of biological processes and traits. One of the most striking findings from this study was the paucity of X-linked SA SNPs, far fewer than expected by chance. The lack of X-linked SA loci is somewhat at odds with classic population genetic theory that predicted the X chromosome

would be a 'hot-spot' for the accumulation of SA alleles (Rice 1984). However, the finding fits well with more recent theory that takes account of the impact of sex-dependent dominance and suggests a predominantly autosomal basis to sexual antagonism (Patten and Haig 2009; Fry 2010; Crispin and Charlesworth 2012).

In chapter 3, I used the list of SA variants that I defined in chapter 2 to elucidate the functional properties and biological roles of SA loci. I conducted a series of bioinformatic analyses using publicly available data. I found a prominent role of gene regulation in the generation of sexual antagonism, with SNPs being enriched up- and downstream of genes and in 3' UTR regions. In addition, I found several lines of evidence that antagonism is associated with specific branches of the regulatory network. Thus, I found that upstream regions of antagonistic genes and were enriched for binding sites of specific transcription factors, and SA SNPs were preferentially located within a number of specific TF binding motifs. Interestingly, there were also a number of specific associations with the sex-determination / sexual differentiation cascade. Finally, I showed that candidate genes are expressed throughout development, highlighting that antagonism unfolds throughout the entire life course rather than specifically arising in adulthood. Taken together, these findings suggest that the ability to acquire sex-specific gene regulation sits at the core of sexual antagonism and represents the biggest hurdle to its resolution.

In chapter 4, I used experimental evolution under sex-limited selection to validate the SA loci identified in chapter 2. I was able to show that over the course of only 3 generations of female-limited selection, alleles at SA loci (those identified in chapter 2) responded more to the selection treatment than did alleles at non-antagonistic background sites. Moreover, female-beneficial alleles had significantly positive selection coefficients under FL selection. These results suggest that many of the putative antagonistic alleles responded in the manner that would be expected from the previously inferred antagonistic fitness effects. However, the expected corresponding mirror-effect under

male-limited selection was not observed, possibly owing to there being greater variance in male reproductive success. Nevertheless, by generating a null distribution of antagonistic selection coefficients, I was able to individually validate a number of candidate SNPs. These serve as prime targets for future study to dissect their molecular function in greater detail.

Finally, and motivated by the findings in chapter 3 and previous studies (Ellegren and Parsch 2007; Innocenti and Morrow 2010), chapter 5 presents a population genetic analysis of SA in transcription factor binding sites that I developed in collaboration with Dr Alexander Stewart and Dr Max Reuter. The major finding here was SA polymorphism located in a regulatory cascade is not fixed over time. Rather, polymorphism often initially arises at the terminal gene in a regulatory cascade but often undergoes later displacement to genes higher up the regulatory hierarchy. The timescale over which displacement occurs is expected to be relatively long, fitting with the idea that sexual antagonism is characterised by long periods of stasis, where sexual antagonism generates substantial maladaptation, followed by periods of rapid evolution in sex-specific fitness on the back of resolution mechanisms.

## 6.2 Functional basis of sexual antagonism

One of the major outstanding questions, described at the outset of this thesis, concerned the functional basis of sexual antagonism. At a fundamental level, we still did not know whether sexual antagonism was predominantly generated over coding sequence or regulatory variation. Furthermore, we also have limited knowledge of the general traits involved in sexual antagonism. This is because studies to date either characterise global patterns of male and female fitness variation, or only characterise specific, individual traits. The former cannot compartmentalise SA variation across traits, and the latter may generate a biased view of which traits tend to be SA.

The analyses detailed in chapter 3 point to a largely regulatory basis to sexual antagonism in *D. melanogaster*. The lack of analogous genome-wide

SA loci in other populations and species makes it difficult to comment on the generality of this association. However, we know from previous empirical work that expression regulation plays a dominant role in generating sexual dimorphism (Ellegren and Parsch 2007) and has previously been associated with SA fitness effects (Innocenti and Morrow 2010). Moreover, some of the few SA traits that have so far been mapped do have a regulatory basis (Daborn et al. 2002; Roberts et al. 2009). For example, Roberts et al. (2009) mapped the genetic basis of the orange-blotch phenotype in Lake Malawi Cichlids. This is a SA trait which provides a fitness benefit to females owing to greater camouflage against predators and a fitness cost to males through disruption of nuptial pigmentation patterns. They found that the causal locus was a cis-regulatory variant upstream of the *pax7* gene.

Motivated by this finding, I, along with collaborators, developed a model for the action of SA selection on gene expression (chapter 5). One of the major findings from this work was that SA polymorphism will often initially invade at terminal output genes, but later be shifted upwards in the regulatory hierarchy. This tendency for upward displacement of SA polymorphism would be expected to be even stronger whenever the genes underlying antagonistic traits are organized into regulatory modules, where a single transcription factor regulates many genes that are subject to similar antagonistic selection pressures.

It is interesting to consider these predictions in light of the regulatory roles of antagonistic polymorphisms that I identified in chapter 2. There, I was able to associate SA SNPs with a number of potential cis- and trans-regulatory roles. Unfortunately, the current annotation of regulatory interactions in *D. melanogaster* is far from complete. As a consequence, I cannot place the candidates within a regulatory hierarchy in order to directly test for the findings of chapter 5. Nevertheless, I can comment on specific associations I detected. Of major note was the presence of multiple candidate SA SNPs at the *fruitless* locus. *fruitless* is a direct target of the *Drosophila* sex de-

termination cascade (Salz and Erickson 2010) and helps to specify a sexually dimorphic nervous system (Neville et al. 2014). In addition, it is important for both behaviour and physiology (Kimura et al. 2005; Vilella and Hall 2008). While we do not have a fully characterised cascade of sexual differentiation in *Drosophila*, *fruitless* is known to target multiple downstream genes in order to help regulate sex-specific development (Neville et al. 2014). Thus, we have strong evidence that SA alleles can indeed arise and persist at the top levels of regulatory cascades.

In terms of gaining a better understanding of the types of traits involved in sexual antagonism, the results of gene ontology analyses in chapter 3 point to a dominant involvement of genes relating to body morphogenesis, chitin / cuticle development, and metabolic processes / nutrient processing. While it is difficult to interpret these general associations in the light of more specific traits the association of SA and aspects nutrient processing has been previously established in *D. melanogaster* (Reddiex et al. 2013; Jensen et al. 2015) and other species (Maklakov et al. 2008). Interestingly, in the context of cuticle-related traits, pigmentation is known to be highly sexually dimorphic in *Drosophila* (Kopp et al. 2000). This could imply that the current levels of sexual dimorphism in pigmentation do not represent males and females at their respective optima but instead are an example of ongoing antagonism.

I additionally found some specific associations when looking at the verified SA SNPs documented in chapter 4. For example, there were CRMs containing verified SA SNPs, both of which were associated with genes important for olfactory responses. This has not previously been associated with sexual antagonism, so this constitutes a novel association worthy of future study.

### **6.3 Evolutionary dynamics of sexual antagonism**

Sexually antagonistic selection favours the invasion of alleles with opposing fitness consequences in each sex (Rice 1984; Gavrilets and Rice 2006). But,

we also expect selection for mechanisms that break down intersexual genetic correlations ( $r_{MF}$ ), allowing male and female phenotypes to emerge and sexual dimorphism to evolve (Stewart et al. 2010; Pennell and Morrow 2013). To date, several potential mechanisms of resolution have been suggested, including gene duplication and subsequent sex-specific regulation of the paralogues (Connallon and Clark 2011), sex-specific splicing (Pennell and Morrow 2013), genomic imprinting (Day and Bonduriansky 2004), and sex-dependent dominance (Kidwell et al. 1977; Barson et al. 2015). However, the absence of knowledge of the identity and general properties of SA loci has so far made it difficult to assess which mechanisms are likely to be effective and the timescales over which we can expect SA genetic variation to persist.

Here I provided evidence that sexual antagonism is mainly rooted in regulatory variation. Compared to conflict over coding sequence, resolution of sexual antagonism over gene expression likely requires fewer mutational steps. For example, protein divergence between the sexes might first require gene duplication, in order to provide redundancy, followed by paralogue divergence and eventually the acquisition of sex-specific regulation of the paralogues (Ellegren and Parsch 2007; Bonduriansky and Chenoweth 2009; Stewart et al. 2010; Connallon and Clark 2011). In contrast, resolving conflict over expression need only require the acquisition of sex-specific regulation. This means that we might expect resolution of conflict over expression to occur over shorter timescales than antagonism rooted in coding sequence.

Evolving novel sex-specific regulation can be achieved via the evolution of a regulatory sequence which can integrate a sex signal into the regulation of an antagonistic gene, either via a signaling cascade triggered by sex hormones or from a genetic sex-specific signal (Stewart et al. 2010). The latter is the case in *Drosophila*, a species with cell-autonomous sex determination. Here, regulatory information about sexual identity is provided by two top-level transcription factors, *doublesex* and *fruitless*, which are under direct control of the primary sex-determining gene *Sex-lethal* and its target *transformer* (see Salz

and Erickson 2010, for review).

A recent study provides an example of a transition from monomorphic to dimorphic expression of a gene via the evolution of a novel binding site for a sex-determining gene. Shirangi et al. (2009) traced the evolution of *desatF*, across fruitfly species. *desatF* is critical for the production of long-chained hydrocarbons that are important for female attractiveness to males. They found that a transition between monomorphic (equivalent in each sex) to dimorphic (female-specific) expression of *desatF* was achieved via the gain of a single binding site for DSF<sup>F</sup> in an upstream cis-regulatory element.

Although we have a general understanding of how, mechanistically, resolution of conflict over expression might proceed, a question remains as to the expected timescale. Overall, resolution is expected to proceed relatively slowly (Stewart et al. 2010). Indeed, in line with this, in Appendix A, we showed that signatures of balancing selection at the loci identified in chapter 2 were found across the species distribution range. Notably, this includes a population from Zambia, in the ancestral distribution range of the species. This suggests that much of the SA variation identified in the LH<sub>M</sub> population has been present since before the species range expansion out of Africa more than 10,000 years ago, and that conflict resolution has been largely absent over this period of time. In line with the apparent lack of resolution over 10,000 years, estimates for the waiting time for a novel binding site to evolve in *D. melanogaster*, assuming a mutation rate  $u \approx 2 \times 10^{-9}$ , a population size  $N \approx 10^6$ , and appreciable selection coefficients  $s \approx 10^{-3}$ , are of the order of  $10^6$  generations or  $10^5$  years (Berg et al. 2004). To contextualise this, the time since *D. melanogaster* split from its sister species *D. simulans* is estimated at  $2.5 \times 10^6$  years.

We recently documented a case of a rapid and large-scale resolution event over the course of  $\approx 200$  generations in a replicate of the LH<sub>M</sub> population (appendix B, Collet et al. 2016). The lack of antagonism in this replicate population (inferred by a positive  $r_{MF}$  for fitness) contrasts with the repeated documentations of ongoing conflict in the LH<sub>M</sub> (e.g., Chippindale et al. 2001;

Innocenti and Morrow 2010). Taken together, the implication from these studies is that antagonism may be characterised by long period of stasis, punctuated by rapid bursts of large-scale resolution (Collet et al. 2016). However, a question remains as to what mechanism would allow for such a large and rapid shift in sex-specific fitness within a population.

My findings from chapter 5, could help to explain such a large-scale resolution event. Thus, if several genes under SA selection are regulated by a TF segregating for SA alleles, large-scale resolution could be quite efficient. Specifically, as a single innovation, engendering sex-specific regulation of the TF, might allow for the resolution of conflict at a large number of genes. This could then generate the positive population-specific intersexual genetic correlation for fitness that was observed in the Collet et al. (2016) study. It seems likely in this case that a key innovation occurred at a top-level regulator that already had the capacity to respond to a sex-signal. Thus, there were a number of sexual differentiation genes containing SNPs associated with the alleviation of antagonism, notably including *transformer 2* and *bric à brac*. The first is a direct target of *Sex-lethal* (Salz and Erickson 2010) and the latter a direct target of *doublesex* (Williams et al. 2008). These would be prime locations for such an alleviation event as described above.

While the resolution of antagonism at a large number of genes via sex-specific regulation of an upstream TF may offer a more efficient route to large-scale resolution, it is difficult to predict how long the process of initial displacement of polymorphism will take. This is because the estimate will depend largely on a number of parameters specific to individual cascades, such as the length or the regulatory cascade, the level of pleiotropy etc. However, at a crude level, given that displacement is the acquisition of a new binding site, we can use the same estimate as before of  $\approx 10^6$  generations. What this means is that as soon as there are more than  $\approx$  two SA genes regulated by an upstream TF, resolution for both of these genes will be quicker with initial displacement followed by the evolution of binding site that responds to a sex-

signal at the TF, than if you were to wait for two independent binding sites at the downstream SA genes to evolve.

## 6.4 Avenues for future research

The work contained within this thesis has addressed some important gaps in our knowledge of sexual antagonism. But, it also provides a starting point for further, detailed studies. Below I will discuss some particularly promising directions for future research.

First, it is of paramount importance that the loci I describe are further validated through detailed dissection of the fitness effects of putative SA alleles and their molecular function. In chapter 4 I performed an evolve-and-resequence experiment to begin validating the SA loci identified in chapter 2 on a genome-wide-scale. While there were some issues with this experiment, it was able to provide a general level of support and additionally identified a reduced list of candidate loci for further testing. Beyond this general support, future studies can now use functional information from chapter 3 as well as the reduced list of verified candidate loci from chapter 4 to direct further candidate-by-candidate validation approaches. These studies would allow unambiguous demonstrations of SA fitness effects and enable a more detailed dissection of mechanisms that generate sexual antagonism.

The functional properties of the SA loci that I describe in chapter 3 offer a means to find the candidates that are most amenable to certain methods of validation. For example, the association of SA loci with several key binding sites points to regulators that we can expect to play a large role in generating sexual antagonism. Manipulating the expression of these regulators or manipulating the binding sites themselves with CRISPR-Cas9 is a promising place to start. Similarly, I found associations with several basal regulators of sexual differentiation (e.g. *fruitless*). SA polymorphism at these loci is likely to generate large and balanced fitness effects as these loci can influence aspects of male and female phenotypes simultaneously. Larger fitness effects will be

much easier to detect in focused validation experiments. Accordingly, a new experiment currently underway in the Reuter laboratory (Filip Ruzicka, PhD student) aims to validate the fitness effects of SA allelic variation at *fruitless* using a combination of quantitative complementation and sex-specific fitness assays. This approach could be transferable to many other candidate loci.

Second, there is scope to extend the theoretical model detailed in chapter 5. Here we focused on characterising the conditions for invasion of SA alleles in regulatory networks but we could extend this framework to explore the broader consequences of SA selection. In particular, it would be interesting to examine if and how SA selection in gene regulatory cascades causes network rewiring. For example, in a hypothetical regulatory network consisting of two chains of regulators targeting genes under both antagonistic and non-antagonistic selection, there could be strong selection for the disassociation of the two regulatory chains. One chain would then regulate the antagonistic gene and the other would regulate the non-antagonistic gene, reducing the deleterious pleiotropic costs of invading SA variants.

Finally, the empirical work contained here has all been performed in a laboratory adapted population of *D. melanogaster*, LH<sub>M</sub>. So a question remains as to how transferable these results are to other populations and indeed other species. I expect the fundamental findings that sexual antagonism is polygenic and rooted in regulatory variation is very general and applicable across taxa. Indeed, many of the traits that have previously been associated with sexual antagonism in various species likely have a regulatory basis (see chapter 3 for more in-depth discussion). In terms of more specific associations and the variants themselves, in appendix A we show that much of the segregating SA variation in the LH<sub>M</sub> population is also present in another North American population (the DGRP) and an ancestral population from Zambia (DPGP3). These findings show that this variation is not population-specific. Moreover, we are accumulating an ever-increasing amount of high quality population genomic data, in particular from numerous *Drosophila* species. This means that

comparative studies will in the future be able to assess whether the SA loci I identify are specific to *D. melanogaster* or are more generally found across species.

## **6.5 Conclusion**

To conclude, I find that sexual antagonism has a highly polygenic basis and is predominantly rooted in regulatory variation. The biological processes that contribute to sexual antagonism are diverse but typically relate to development and morphogenesis. SA alleles are distributed across gene regulatory networks and, in some cases, sit at the very top of regulatory cascades. This is in line with theory developed here that predicts SA polymorphism can permeate upwards in regulatory cascades over time. Overall, my work documented in this thesis fills important and longstanding gaps in our knowledge and serves as a solid foundation upon which future studies of sexual antagonism can now proceed.

# References

- Abbott, J. K., Bedhomme, S., and Chippindale, A. K. 2010. Sexual conflict in wing size and shape in *Drosophila melanogaster*. *Journal of Evolutionary Biology* 23:1989–1997.
- Abbott, J. K. and Morrow, E. H. 2011. Obtaining snapshots of genetic variation using hemiclonal analysis. *Trends in Ecology and Evolution* 26:359–368.
- Agrawal, N., Dasaradhi, P. V. N., Mohammed, A., Malhotra, P., Bhatnagar, R. K., and Mukherjee, S. K. 2003. RNA interference: Biology, mechanism, and applications. *Microbiology and Molecular Biology Reviews* 67:657–685.
- Andersson, M. B., 1994. *Sexual selection*. Princeton University Press.
- Andolfatto, P. 2005. Adaptive evolution of non-coding DNA in *Drosophila*. *Nature* 437:1149–1152.
- Arnqvist, G., Vellnow, N., and Rowe, L. 2014. The effect of epistasis on sexually antagonistic genetic variation. *Proceedings of the Royal Society B: Biological Sciences* 281:20140489.
- Bailey, T. L., Boden, M., Buske, F. A., et al. 2009. MEME Suite: Tools for motif discovery and searching. *Nucleic Acids Research* 37:W202–W208.
- Barson, N. J., Aykanat, T., Hindar, K., et al. 2015. Sex-dependent dominance at a single locus maintains variation in age at maturity in Salmon. *Nature* 528:405–408.
- Bateman, A. J. 1948. Intra-sexual selection in *Drosophila*. *Heredity* 2:349–368.
- Berg, J., Willmann, S., and Lässig, M. 2004. Adaptive evolution of transcription factor binding sites. *BMC Evolutionary Biology* 4:42.

- Berger, D., Berg, E. C., Widegren, W., Arnqvist, G., and Maklakov, A. A. 2014. Multivariate intralocus sexual conflict in seed beetles. *Evolution* 68:3457–3469.
- Bersaglieri, T., Sabeti, P. C., Patterson, N., et al. 2004. Genetic signatures of strong recent positive selection at the lactase gene. *American Journal of Human Genetics* 74:1111–1120.
- Bintu, L., Buchler, N. E., Garcia, H. G., Gerland, U., Hwa, T., Kondev, J., and Phillips, R. 2005. Transcriptional regulation by the numbers: Models. *Current Opinion in Genetics and Development* 15:116–124.
- Blatti, C. and Sinha, S. 2014. Motif enrichment tool. *Nucleic Acids Research* 42:W20–W25.
- Bonduriansky, R. and Chenoweth, S. 2009. Intralocus sexual conflict. *Trends in Ecology and Evolution* 24:280–288.
- Buchler, N. E., Gerland, U., and Hwa, T. 2003. On schemes of combinatorial transcription logic. *Proceedings of the National Academy of Sciences of the United States of America* 100:5136–41.
- Cachero, S., Ostrovsky, A. D., Yu, J. Y., Dickson, B. J., and Jefferis, G. S. X. E. 2010. Sexual dimorphism in the fly brain. *Current Biology* 20:1589–1601.
- Calsbeek, R. and Sinervo, B. 2004. Within-clutch variation in offspring sex determined by differences in sire body size: Cryptic mate choice in the wild. *Journal of Evolutionary Biology* 17:464–470.
- Carroll, S. B. 2005. Evolution at two levels: On genes and form. *PLoS Biology* 3:1159–1166.
- Casarini, L. and Brigante, G. 2014. The polycystic ovary syndrome evolutionary paradox: A genome-wide association studies-based, in silico, evo-

- lutionary explanation. *Journal of Clinical Endocrinology and Metabolism* 99:E2412–E2420.
- Celniker, S. E., L Dillon, L. A., Gerstein, M. B., et al. 2009. Unlocking the secrets of the genome. *Nature* 18:927–930.
- Charlesworth, B., Coyne, J. A., and Barton, N. 1987. The relative rates of evolution of sex chromosomes and autosomes. *The American Naturalist* 130:113–146.
- Charlesworth, D. and Charlesworth, B. 2005. Sex chromosomes: evolution of the weird and wonderful. *Current Biology* 15:R129–R131.
- Chen, C.-Y., Lopes-Ramos, C. M., Kuijjer, M. L., et al. 2016. Sexual dimorphism in gene expression and regulatory networks across human tissues. *bioRxiv* .
- Chen, H. and Boutros, P. C. 2011. VennDiagram: a package for the generation of highly-customizable Venn and Euler diagrams in R. *BMC Bioinformatics* 12:35.
- Chintapalli, V. R., Wang, J., and Dow, J. A. T. 2007. Using FlyAtlas to identify better *Drosophila melanogaster* models of human disease. *Nature genetics* 39:715–20.
- Chippindale, A. K., Gibson, J. R., and Rice, W. R. 2001. Negative genetic correlation for adult fitness between sexes reveals ontogenetic conflict in *Drosophila*. *Proceedings of the National Academy of Sciences of the United States of America* 98:1671–1675.
- Clutton-Brock, T. H., 1991. *The evolution of parental care*. Princeton University Press.
- Collet, J. M., Fuentes, S., Hesketh, J., et al. 2016. Rapid evolution of the intersexual genetic correlation for fitness in *Drosophila melanogaster*. *Evolution* 70:781–795.

- Connallon, T. and Clark, A. G. 2011. The resolution of sexual antagonism by gene duplication. *Genetics* 187:919–937.
- Connallon, T. and Clark, A. G. 2012. A general population genetic framework for antagonistic selection that accounts for demography and recurrent mutation. *Genetics* 190:1477–1489.
- Connallon, T. and Clark, A. G. 2014. Evolutionary inevitability of sexual antagonism. *Proceedings of the Royal Society B: Biological Sciences* 281:20132123.
- Connallon, T. and Hall, M. D. 2016. Genetic correlations and sex-specific adaptation in changing environments. *Evolution* 70:2186–2198.
- Connallon, T. and Jakubowski, E. 2009. Association between sex ratio distortion and sexually antagonistic fitness consequences of female choice. *Evolution* 63:2179–2183.
- Cox, R. M. and Calsbeek, R. 2009. Sexually antagonistic selection, sexual dimorphism, and the resolution of intralocus sexual conflict. *The American Naturalist* 173:176–187.
- Crispin, J. and Charlesworth, D. 2012. The potential for sexually antagonistic polymorphism in different genome regions. *Evolution* 66:505–516.
- Daborn, P. J., Yen, J. L., Bogwitz, M. R., et al. 2002. A single P450 allele associated with insecticide resistance in *Drosophila*. *Science* 297:2253–2256.
- Day, T. and Bonduriansky, R. 2004. Intralocus sexual conflict can drive the evolution of genomic imprinting. *Genetics* 167:1537–1546.
- Delcourt, M., Blows, M. W., and Rundle, H. D. 2009. Sexually antagonistic genetic variance for fitness in an ancestral and a novel environment. *Proceedings of the Royal Society B: Biological Sciences* 276:2009–2014.

- Delph, L. F., Andicoechea, J., Steven, J. C., Herlihy, C. R., Scarpino, S. V., and Bell, D. L. 2011. Environment-dependent intralocus sexual conflict in a dioecious plant. *New Phytologist* 192:542–552.
- DePristo, M. A., Banks, E., Poplin, R., et al. 2011. A framework for variation discovery and genotyping using next-generation DNA sequencing data. *Nature Genetics* 43:491–498.
- Eden, E., Navon, R., Steinfeld, I., Lipson, D., and Yakhini, Z. 2009. GOrilla: a tool for discovery and visualization of enriched GO terms in ranked gene lists. *BMC Bioinformatics* 10:48.
- Ellegren, H. and Parsch, J. 2007. The evolution of sex-biased genes and sex-biased gene expression. *Nature Reviews Genetics* 8:689–698.
- Farkas, I. J., Wu, C., Chennubhotla, C., Bahar, I., and Oltvai, Z. N. 2006. Topological basis of signal integration in the transcriptional-regulatory network of the yeast, *Saccharomyces cerevisiae*. *BMC Bioinformatics* 7:478.
- Fedorka, K. M. and Mousseau, T. A. 2004. Female mating bias results in conflicting sex-specific offspring fitness. *Nature* 429:65–67.
- Ferrer-Admetlla, A., Leuenberger, C., Jensen, J. D., and Wegmann, D. 2016. An approximate markov model for the wrightfisher diffusion and its application to time series data. *Genetics* 203:831–846.
- Foerster, K., Coulson, T., Sheldon, B. C., Pemberton, J. M., Clutton-Brock, T. H., and Kruuk, L. E. B. 2007. Sexually antagonistic genetic variation for fitness in red deer. *Nature* 447:11071110.
- Friedlander, T., Prizak, R., Barton, N. H., and Tkačik, G. 2017. Evolution of new regulatory functions on biophysically realistic fitness landscapes. *Nature Communications* 8:216.
- Fry, J. D. 2010. The genomic location of sexually antagonistic variation: Some cautionary comments. *Evolution* 64:1510–1516.

- Gallo, S. M., Gerrard, D. T., Miner, D., Simich, M., Des Soye, B., Bergman, C. M., and Halfon, M. S. 2011. REDfly v3.0: Toward a comprehensive database of transcriptional regulatory elements in *Drosophila*. *Nucleic Acids Research* 39:D118–D123.
- Gavrilets, S. and Rice, W. R. 2006. Genetic models of homosexuality: generating testable predictions. *Proceedings of the Royal Society B: Biological Sciences* 273:3031–8.
- Geiger-Thornsberry, G. L. and Mackay, T. F. C. 2004a. Quantitative trait loci affecting natural variation in *Drosophila* longevity. *Mechanisms of Ageing and Development* 125:179–189.
- Geiger-Thornsberry, G. L. and Mackay, T. F. C. 2004b. Quantitative trait loci affecting natural variation in *Drosophila* longevity. *Mechanisms of Ageing and Development* 125:179–189.
- Gerland, U. and Hwa, T. 2002. On the selection and evolution of regulatory DNA motifs. *Journal of Molecular Evolution* 55:386–400.
- Gibson, J. R., Chippindale, A. K., and Rice, W. R. 2002. The X chromosome is a hot spot for sexually antagonistic fitness variation. *Proceedings of the Royal Society B: Biological Sciences* 269:499–505.
- Gilks, W. P., Abbott, J. K., and Morrow, E. H. 2014. Sex differences in disease genetics: Evidence, evolution, and detection. *Trends in Genetics* 30:453–463.
- Gilks, W. P., Pennell, T. M., Flis, I., Webster, M. T., and Morrow, E. H. 2016. Whole genome resequencing of a laboratory-adapted *Drosophila melanogaster* population sample. *F1000Research* 5:2644.
- Gnad, F. and Parsch, J. 2006. Sebida: a database for the functional and evolutionary analysis of genes with sex-biased expression. *Bioinformatics* 22:2577–2579.

- Gompert, Z., Comeault, A. A., Farkas, T. E., Feder, J. L., Parchman, T. L., Buerkle, C. A., and Nosil, P. 2014. Experimental evidence for ecological selection on genome variation in the wild. *Ecology Letters* 17:369–379.
- Gramates, L. S., Marygold, S. J., Dos Santos, G., et al. 2017. FlyBase at 25: Looking to the future. *Nucleic Acids Research* 45:D663–D671.
- Haag, E. S. and Doty, A. V. 2005. Sex determination across evolution: Connecting the dots. *PLoS Biology* 3:e21.
- Hager, R., Cheverud, J. M., Leamy, L. J., and Wolf, J. B. 2008. Sex dependent imprinting effects on complex traits in mice. *BMC Evolutionary Biology* 8:303.
- Halfon, M. S., Carmena, A., Gisselbrecht, S., Sackerson, C. M., Jiménez, F., Baylies, M. K., and Michelson, A. M. 2000. Ras pathway specificity is determined by the integration of multiple signal-activated and tissue-restricted transcription factors. *Cell* 103:63–74.
- Hill, W. G. and Zhang, X.-S., 2009. Maintaining genetic variation in fitness. Pages 59–81 *in* *Adaptation and fitness in animal populations*. Springer Netherlands, Dordrecht.
- Hoekstra, H. E. and Coyne, J. A. 2007. The locus of evolution: Evo devo and the genetics of adaptation. *Evolution* 61:995–1016.
- Hollenhorst, P. C., Shah, A. A., Hopkins, C., and Graves, B. J. 2007. Genome-wide analyses reveal properties of redundant and specific promoter occupancy within the ETS gene family. *Genes and Development* 21:1882–1894.
- Houde, A. and Endler, J. 1990. Correlated evolution of female mating preferences and male color patterns in the guppy *Poecilia reticulata*. *Science* 248:1405–1408.

- Ingleby, F. C., Webster, C. L., Pennell, T. M., Flis, I., and Morrow, E. H. 2016. Sex-biased gene expression in *Drosophila melanogaster* is constrained by ontogeny and genetic architecture. bioRxiv .
- Innocenti, P. and Morrow, E. H. 2010. The sexually antagonistic genes of *Drosophila melanogaster*. PLoS Biology 8:e1000335.
- Jensen, K., McClure, C., Priest, N. K., and Hunt, J. 2015. Sex-specific effects of protein and carbohydrate intake on reproduction but not lifespan in *Drosophila melanogaster*. Aging Cell 14:605–615.
- Jones, F. C., Grabherr, M. G., Chan, Y. F., et al. 2012. The genomic basis of adaptive evolution in threespine sticklebacks. Nature 484:55–61.
- Jothi, R., Balaji, S., Wuster, A., et al. 2009. Genomic analysis reveals a tight link between transcription factor dynamics and regulatory network architecture. Molecular Systems Biology 5:294.
- Kemp, D. J., Reznick, D. N., Grether, G. F., and Endler, J. A. 2009. Predicting the direction of ornament evolution in Trinidadian guppies (*Poecilia reticulata*). Proceedings of the Royal Society B: Biological Sciences 276:4335–4343.
- Kidwell, J. F., Clegg, M. T., Stewart, F. M., and Prout, T. 1977. Regions of stable equilibria for models of differential selection in the two sexes under random mating. Genetics 85:171–183.
- Kimura, K. I., Ote, M., Tazawa, T., and Yamamoto, D. 2005. Fruitless specifies sexually dimorphic neural circuitry in the *Drosophila* brain. Nature 438:229–233.
- Kimura, M. 1962. On the probability of fixation of mutant genes in a population. Genetics 47:713–719.
- King, M.-c. C. and Wilson, A. C. 1975. Evolution at two levels in humans and chimpanzees. Science 188:107–116.

- Kofler, R. and Schlötterer, C. 2014. A guide for the design of evolve and resequencing studies. *Molecular Biology and Evolution* 31:474–483.
- Kokko, H. and Brooks, R. 2003. Sexy to die for? Sexual selection and the risk of extinction. *Annales Zoologici Fennici* 40:207–219.
- Kopp, A., Duncan, I., Godt, D., and Carroll, S. B. 2000. Genetic control and evolution of sexually dimorphic characters in *Drosophila*. *Nature* 408:553–559.
- Lande, R. 1980. Sexual dimorphism, sexual selection, and adaptation in polygenic characters. *Evolution* 34:292–305.
- Lande, R. and Kirkpatrick, M. 1988. Ecological speciation by sexual selection. *Journal of Theoretical Biology* 133:85–98.
- Langmead, B. and Salzberg, S. L. 2012. Fast gapped-read alignment with Bowtie 2. *Nature Methods* 9:357–359.
- Lässig, M. 2007. From biophysics to evolutionary genetics: statistical aspects of gene regulation. *BMC Bioinformatics* 8:S7.
- Liu, L. Y., Fox, C. S., North, T. E., and Goessling, W. 2013. Functional validation of GWAS gene candidates for abnormal liver function during zebrafish liver development. *Disease Models and Mechanisms* 6:1271–1278.
- Long, A. D., Mullaney, S. L., Mackay, T. F. C., and Langley, C. H. 1996. Genetic interactions between naturally occurring alleles at quantitative trait loci and mutant alleles at candidate loci affecting bristle number in *Drosophila melanogaster*. *Genetics* 144:1497–1510.
- Long, T. and Rice, W. R. 2007. Adult locomotory activity mediates intralocus sexual conflict in a laboratory-adapted population of *Drosophila melanogaster*. *Proceedings of the Royal Society B* 274:3105–3112.

- Long, T. A. F., Agrawal, A. F., and Rowe, L. 2012. The effect of sexual selection on offspring fitness depends on the nature of genetic variation. *Current Biology* 22:204–208.
- Mackay, T. F. 2001. Quantitative trait loci in *Drosophila*. *Nature reviews. Genetics* 2:11–20.
- Mackay, T. F. C., Stone, E. A., and Ayroles, J. F. 2009. The genetics of quantitative traits: challenges and prospects. *Nature Reviews Genetics* 10:565–577.
- MacNeil, L. T. and Walhout, A. J. M. 2011. Gene regulatory networks and the role of robustness and stochasticity in the control of gene expression. *Genome Research* 21:645–657.
- Mainguy, J., Cote, S. D., Festa-Bianchet, M., and Coltman, D. W. 2009. Father-offspring phenotypic correlations suggest intralocus sexual conflict for a fitness-linked trait in a wild sexually dimorphic mammal. *Proceedings of the Royal Society B: Biological Sciences* 276:4067–4075.
- Maklakov, A. A., Simpson, S. J., Zajitschek, F., et al. 2008. Sex-specific fitness effects of nutrient intake on reproduction and lifespan. *Current Biology* 18:1062–1066.
- Mank, J. E., Hultin-Rosenberg, L., Zwahlen, M., and Ellegren, H. 2008. Pleiotropic constraint hampers the resolution of sexual antagonism in vertebrate gene expression. *The American Naturalist* 171:35–43.
- Marbach, D., Roy, S., Ay, F., et al. 2012. Predictive regulatory models in *Drosophila melanogaster* by integrative inference of transcriptional networks. *Genome Research* 22:1334–1349.
- Martin, M. 2011. Cutadapt removes adapter sequences from high-throughput sequencing reads. *EMBnet.journal* 17:10.
- Maslov, S. and Sneppen, K. 2005. Computational architecture of the yeast regulatory network. *Phys. Biol* 2:94–100.

- McKenna, A., Hanna, M., Banks, E., et al. 2010. The genome analysis toolkit: A MapReduce framework for analyzing next-generation DNA sequencing data. *Genome Research* 20:1297–1303.
- McLaren, W., Pritchard, B., Rios, D., Chen, Y., Flicek, P., and Cunningham, F. 2010. Deriving the consequences of genomic variants with the Ensembl API and SNP Effect Predictor. *Bioinformatics* 26:2069–2070.
- McShea, D. W. 2000. Functional complexity in organisms: Parts as proxies. *Biology and Philosophy* 15:641–668.
- Metzger, B. P., Duveau, F., Yuan, D. C., Tryban, S., Yang, B., and Witkopp, P. J. 2016. Contrasting frequencies and effects of cis- and trans-regulatory mutations affecting gene expression. *Molecular Biology and Evolution* 33:1131–1146.
- Mokkonen, M. and Crespi, B. J. 2015. Genomic conflicts and sexual antagonism in human health: Insights from oxytocin and testosterone. *Evolutionary Applications* 8:307–325.
- Mokkonen, M., Kokko, H., Koskela, E., Lehtonen, J., Mappes, T., Martiskainen, H., and Mills, S. C. 2011. Negative frequency-dependent selection of sexually antagonistic alleles in *Myodes glareolus*. *Science* 334:972–974.
- Moorad, J. A. and Hall, D. W. 2009. Mutation accumulation, soft selection and the middle-class neighborhood. *Genetics* 182:1387–1389.
- Morrow, E. H. and Connallon, T. 2013. Implications of sex-specific selection for the genetic basis of disease. *Evolutionary Applications* 6:1208–1217.
- Morrow, E. H., Stewart, A. D., and Rice, W. R. 2008. Assessing the extent of genome-wide intralocus sexual conflict via experimentally enforced gender-limited selection. *Journal of Evolutionary Biology* 21:1046–1054.

- Moses, A. M., Chiang, D. Y., Kellis, M., Lander, E. S., and Eisen, M. B. 2003. Position specific variation in the rate of evolution in transcription factor binding sites. *BMC Evolutionary Biology* 3:19.
- Mullon, C., Pomiankowski, A., and Reuter, M. 2012. The effects of selection and genetic drift on the genomic distribution of sexually antagonistic alleles. *Evolution* 66:3743–3753.
- Mustonen, V., Kinney, J., Callan, C. G., and Lässig, M. 2008. Energy-dependent fitness: a quantitative model for the evolution of yeast transcription factor binding sites. *Proceedings of the National Academy of Sciences of the United States of America* 105:12376–12381.
- Nachman, M. W. and Crowell, S. L. 2000. Estimate of the mutation rate per nucleotide in humans. *Genetics* 156:297–304.
- Neville, M. C., Nojima, T., Ashley, E., et al. 2014. Male-specific fruitless isoforms target neurodevelopmental genes to specify a sexually dimorphic nervous system. *Current Biology* 24:229–241.
- Nomura, T. 2002. Effective size of populations with unequal sex ratio and variation in mating success. *Journal of Animal Breeding and Genetics* 119:297–310.
- Ow, M. C., Martinez, N. J., Olsen, P. H., et al. 2008. The FLYWCH transcription factors FLH-1, FLH-2, and FLH-3 repress embryonic expression of microRNA genes in *C. elegans*. *Genes and Development* 22:2520–2534.
- Partridge, L. and Farquhar, M. 1983. Lifetime mating success of male fruitflies (*Drosophila melanogaster*) is related to their size. *Animal Behaviour* 31:871–877.
- Patten, M. M. and Haig, D. 2009. Maintenance or loss of genetic variation under sexual and parental antagonism at a sex-linked locus. *Evolution* 63:2888–2895.

- Patten, M. M., Haig, D., and Úbeda, F. 2010. Fitness variation due to sexual antagonism and linkage disequilibrium. *Evolution* 64:3638–3642.
- Pennell, T. M. and Morrow, E. H. 2013. Two sexes, one genome: The evolutionary dynamics of intralocus sexual conflict. *Ecology and Evolution* 3:1819–1834.
- Pespeni, M., Sanford, E., Gaylord, B., et al. 2013. Evolutionary change during experimental ocean acidification. *Proceedings of the National Academy of Sciences* 110:6937–6942.
- Pischedda, A., Chippindale, A. K., Bangham, J., Rowe, L., and Gocayne, J. 2006. Intralocus sexual conflict diminishes the benefits of sexual selection. *PLoS Biology* 4:e356.
- Poissant, J., Wilson, A. J., and Coltman, D. W. 2010. Sex-specific genetic variance and the evolution of sexual dimorphism: A systematic review of cross-sex genetic correlations. *Evolution* 64:97–107.
- Prasad, N. G., Bedhomme, S., Day, T., and Chippindale, A. K. 2007. An evolutionary cost of separate genders revealed by male-limited evolution. *the American Naturalist* 169:29–37.
- Price, D. K. and Burley, N. T. 1993. Constraints on the evolution of attractive traits: genetic (co)variance of zebra finch bill colour. *Heredity* 71:405–412.
- Proulx, S. R. and Phillips, P. C. 2006. Allelic divergence precedes and promotes gene duplication. *Evolution* 60:881–892.
- Punzalan, D., Delcourt, M., and Rundle, H. 2014. Comparing the inter-sex genetic correlation for fitness across novel environments in the fruit fly, *Drosophila serrata*. *Heredity* 112:143–148.
- Quinlan, A. R. and Hall, I. M. 2010. BEDTools: A flexible suite of utilities for comparing genomic features. *Bioinformatics* 26:841–842.

- Reddiex, A. J., Gosden, T. P., Bonduriansky, R., and Chenoweth, S. F. 2013. Sex-specific fitness consequences of nutrient intake and the evolvability of diet preferences. *The American Naturalist* 182:91–102.
- Rice, W. R. 1984. Sex chromosomes and the evolution of sexual dimorphism. *Evolution* 38:735–742.
- Rice, W. R. 1987. The accumulation of sexually antagonistic genes as a selective agent promoting the evolution of reduced recombination between primitive sex chromosomes. *Evolution* 41:9–11.
- Rice, W. R. 1992. Sexually antagonistic genes: experimental evidence. *Science* 256:1436–1439.
- Rice, W. R. 1998. Male fitness increases when females are eliminated from gene pool: implications for the Y chromosome. *Proceedings of the National Academy of Sciences of the United States of America* 95:6217–6221.
- Rice, W. R. and Chippindale, A. K. 2002. The evolution of hybrid infertility: Perpetual coevolution between gender-specific and sexually antagonistic genes. *Genetics* 116:179–188.
- Rice, W. R., Linder, J. E., Friberg, U., Lew, T. A., Morrow, E. H., and Stewart, A. D. 2005. Inter-locus antagonistic coevolution as an engine of speciation: assessment with hemiclinal analysis. *Proceedings of the National Academy of Sciences of the United States of America* 102:6527–6534.
- Roberts, R. B., Ser, J. R., and Kocher, T. D. 2009. Sexual conflict resolved by invasion of a novel sex determiner in Lake Malawi cichlid fishes. *Science* 326:998–1001.
- Robinson, J. T., Thorvaldsdóttir, H., Winckler, W., Guttman, M., Lander, E. S., Getz, G., and Mesirov, J. P. 2011. Integrative genomics viewer. *Nature Biotechnology* 29:24–26.

- Robinson, M. R., Pilkington, J. G., Clutton-Brock, T. H., Pemberton, J. M., and Kruuk, L. E. B. 2006. Live fast, die young: trade-offs between fitness components and sexually antagonistic selection on weaponry in Soay sheep. *Evolution* 60:2168–2181.
- Rowe, L. and Day, T. 2006. Detecting sexual conflict and sexually antagonistic coevolution. *Philosophical Transactions of the Royal Society B: Biological Sciences* 361:277–285.
- Sailer, Z. R. and Harms, M. J. 2017. High-order epistasis shapes evolutionary trajectories. *PLoS Computational Biology* 13:e1005541.
- Salz, H. K. and Erickson, J. W. 2010. Sex determination in *Drosophila*: The view from the top. *Fly* 4:60–70.
- Santolini, M., Mora, T., and Hakim, V. 2014. A general pairwise interaction model provides an accurate description of in vivo transcription factor binding sites. *PLoS ONE* 9:e99015.
- Schadt, E. E., Monks, S. A., Drake, T. A., et al. 2003. Genetics of gene expression surveyed in maize, mouse and man. *Nature* 422:297–302.
- Schlötterer, C., Kofler, R., Versace, E., Tobler, R., and Franssen, S. U. 2014. Combining experimental evolution with next-generation sequencing: a powerful tool to study adaptation from standing genetic variation. *Heredity* 114:1–10.
- Sella, G. and Hirsh, A. E. 2005. The application of statistical physics to evolutionary biology. *Proceedings of the National Academy of Sciences of the United States of America* 102:9541–6.
- Shirangi, T. R., Dufour, H. D., Williams, T. M., and Carroll, S. B. 2009. Rapid evolution of sex pheromone-producing enzyme expression in *Drosophila*. *PLoS Biology* 7:e1000168.

- Small, S., Blair, A., and Levine, M. 1992. Regulation of even-skipped stripe 2 in the *Drosophila* embryo. *The EMBO journal* 11:4047–57.
- Smith, D. T., Hosken, D. J., Rostant, W. G., et al. 2011. DDT resistance, epistasis and male fitness in flies. *Journal of Evolutionary Biology* 24:1351–1362.
- Spencer, H. G. and Priest, N. K. 2016. The evolution of sex-specific dominance in response to sexually antagonistic selection. *The American Naturalist* 187:000–000.
- Stewart, A. D., Pischedda, A., and Rice, W. R. 2010. Resolving intralocus sexual conflict: Genetic mechanisms and time frame. *Journal of Heredity* 101:94–99.
- Stewart, A. J. and Plotkin, J. B. 2012. Why transcription factor binding sites are ten nucleotides long. *Genetics* 192:973–985.
- Stowers, L. and Logan, D. W. 2010. Sexual dimorphism in olfactory signaling. *Current Opinion in Neurobiology* 20:770–775.
- Svensson, E. I., McAdam, A. G., and Sinervo, B. 2009. Intralocus sexual conflict over immune defense, gender load, and sex-specific signaling in a natural lizard population. *Evolution* 63:3124–3135.
- Tarka, M., Åkesson, M., Hasselquist, D., Hansson, B., Akesson, M., Hasselquist, D., and Hansson, B. 2014. Intralocus sexual conflict over wing length in a wild migratory bird. *The American Naturalist* 183:62–73.
- Trivers, R. L., 1972. Parental investment and sexual selection. Pages 136–179 in *Sexual selection and the descent of man, 1871-1971*. Campbell B ed, Aldine, New York.
- Turelli, M. and Barton, N. H. 2004. Polygenic variation maintained by balancing selection: Pleiotropy, sex-dependent allelic effects and G x E interactions. *Genetics* 166:1053–1079.

- Turner, T. L. and Miller, P. M. 2012. Investigating natural variation in *Drosophila* courtship song by the evolve and resequence approach. *Genetics* 191:633–642.
- Turner, T. L., Stewart, A. D., Fields, A. T., Rice, W. R., and Tarone, A. M. 2011. Population-based resequencing of experimentally evolved populations reveals the genetic basis of body size variation in *Drosophila melanogaster*. *PLoS Genetics* 7:e1001336.
- Usui-Aoki, K., Ito, H., Ui-Tei, K., et al. 2000. Formation of the male-specific muscle in female *Drosophila* by ectopic fruitless expression. *Nature Cell Biology* 2:500–506.
- Van Doorn, G. S. 2009. Intralocus sexual conflict. *Annals of the New York Academy of Sciences* 1168:52–71.
- Villella, A. and Hall, J. C. 2008. Neurogenetics of courtship and mating in *Drosophila*. *Advances in Genetics* 62:67–184.
- Vonesch, S. C., Lamparter, D., Mackay, T. F. C., Bergmann, S., and Hafen, E. 2016. Genome-wide analysis reveals novel regulators of growth in *Drosophila melanogaster*. *PLOS Genetics* 12:e1005616.
- Wei, Z., Wang, W., Hu, P., Lyon, G. J., and Hakonarson, H. 2011. SNVer: A statistical tool for variant calling in analysis of pooled or individual next-generation sequencing data. *Nucleic Acids Research* 39:e132–e132.
- Wickham, H., 2009. *ggplot2: Elegant Graphics for Data Analysis*. Springer-Verlag New York. ISBN 978-0-387-98140-6.
- Williams, T. M., Selegue, J. E., Werner, T., Gompel, N., Kopp, A., and Carroll, S. B. 2008. The Regulation and Evolution of a Genetic Switch Controlling Sexually Dimorphic Traits in *Drosophila*. *Cell* 134:610–623.
- Wray, G. A. 2007. The evolutionary significance of cis-regulatory mutations. *Nature Reviews Genetics* 8:206–216.

- Wright, A., Darolti, I., Bloch, N., et al. 2017. Convergent recombination suppression suggests role of sexual selection in guppy sex chromosome formation. *Nature Communications* 8:14251.
- Wu, N. C., Dai, L., Olson, C. A., Lloyd-Smith, J. O., and Sun, R. 2016. Adaptation in protein fitness landscapes is facilitated by indirect paths. *eLife* 5:e16965.
- Wyman, M. J. and Wyman, M. C. 2013. Sex-specific recombination rates and allele frequencies affect the invasion of sexually antagonistic variation on autosomes. *Journal of Evolutionary Biology* 26:2428–2437.
- Xing, C. and Xing, G. 2009. Power of selective genotyping in genome-wide association studies of quantitative traits. *BMC Proceedings* 3:S23.
- Yang, X., Deignan, J. L., Qi, H., et al. 2009. Validation of candidate causal genes for obesity that affect shared metabolic pathways and networks. *Nature Genetics* 41:415–423.
- Yi, X. and Dean, A. M. 2016. Phenotypic plasticity as an adaptation to a functional trade-off. *eLife* 5:e19307.

## Appendix A

# Sexually antagonistic SNPs in the fruitfly reveal persistent constraints on sex-specific development

This is a copy of a manuscript, with me as first author, which was submitted to Nature Ecology and Evolution. It contains some of the work documented in chapters 2 & 3. Here my analyses are combined with those of Filip Ruzicka, another PhD student in the Reuter laboratory. We show elevated signatures of balancing selection at candidate loci across the *D. melanogaster* distribution range. This suggests that the antagonism I describe is both persistent and not specific to the LH<sub>M</sub> population.

# **Sexually antagonistic SNPs in the fruitfly reveal persistent constraints on sex-specific development**

Mark S. Hill<sup>1#</sup>, Filip Ruzicka<sup>1#</sup>, Sara Fuentes<sup>1</sup>, Julie M. Collet<sup>2</sup>, Edward H. Morrow<sup>3</sup>, Kevin Fowler<sup>1</sup>, & Max Reuter<sup>1\*</sup>

# Equal contribution

\* Corresponding author

<sup>1</sup> Research Department of Genetics, Evolution and Environment, University College London, London, UK

<sup>2</sup> Unité Mixte de Recherche, Centre de Biologie pour la Gestion des Populations, Institut National de la Recherche Agronomique, Avenue du Campus Agropolis, 34988 Montferrier-sur-Lez, France

<sup>3</sup> School of Life Sciences, University of Sussex, Brighton, UK

**The evolution of sexual dimorphism is constrained by a shared genome, leading to 'sexual antagonism' where different alleles at given loci are favoured in males and females. Despite its wide taxonomic incidence, we know virtually nothing about the evolutionary dynamics of sexually antagonistic sequence variants or the general biological processes underlying antagonism. Here we identify antagonistic SNPs across the genome of *D. melanogaster*. We show that antagonism generates signatures of balancing selection in populations across the *D. melanogaster* distribution range, indicating widespread and evolutionarily persistent (>10,000 years) genomic constraints. Contrary to longstanding predictions, antagonistic loci are significantly underrepresented on the X chromosome. Functionally, antagonism is rooted in the regulation of development and associated primarily with cis-regulatory elements. We also detect multiple associations with the sexual differentiation cascade, including the key regulator *fruitless*. These results demonstrate that conflict over sex-specific adaptation reaches to, and persists at, the core of sexual differentiation.**

The divergent reproductive roles of males and females favour different phenotypes<sup>1,2</sup>. However, responses to these selective pressures are constrained by a shared genome, leading to 'sexual antagonism' where different alleles at given loci are favoured in the two sexes<sup>1,3-5</sup>. A wealth of quantitative genetic studies has established sexual antagonism as near ubiquitous across a wide range of taxa, including mammals<sup>6</sup> birds<sup>7</sup>, reptiles<sup>8</sup>, insects<sup>9,10</sup>, fish<sup>11,12</sup> and plants<sup>13</sup>. Accordingly, sexual antagonism can be considered a major constraint on adaptation and an important mechanism for the maintenance of fitness variation within populations<sup>14</sup>. However, despite its evolutionary importance, we have little understanding of the biological mechanisms underlying this conflict and virtually no empirical data on the identity and evolutionary dynamics of antagonistic alleles<sup>12</sup>. While a small number of individual antagonistic loci have been identified<sup>11,12</sup>, these are of limited use for elucidating general properties of loci experiencing sexual antagonism. On a genome-wide scale, previous transcriptomic work has associated antagonistic fitness effects with patterns of gene expression<sup>15</sup>. But despite revealing some of the molecular correlates of antagonism, this approach cannot distinguish between causal antagonistic loci and their downstream regulatory targets. It is essential that we characterise causal antagonistic loci in order to understand the adaptive limits to sexual dimorphism and how mechanisms of conflict resolution might arise.

To address this shortcoming, we combined experimentation, population genomics and bioinformatics to identify causal antagonistic loci across the *D. melanogaster* genome. Building on previous studies, we assayed the LH<sub>M</sub> population in which sexually antagonistic fitness effects were first characterised<sup>9,16</sup>. LH<sub>M</sub> was established in 1991 from flies sampled in California and has since been maintained as a large, outbred laboratory population under a strict two-week rearing regime<sup>17</sup>. To identify causal sexually antagonistic SNPs, we compared the genomic sequences of hemiclonal fly lines<sup>15</sup> that exhibited extreme male-beneficial/female-detrimental (N<sub>MB</sub>=5) and female-beneficial/male-detrimental (N<sub>FB</sub>=4) fitness effects. Based on these, we defined putative sexually antagonistic SNPs as those where alleles ‘perfectly segregated’ between male- and female-beneficial hemiclonal genomes—that is, SNPs where the two fitness classes were fixed for different alleles (see Methods).

## Results

Out of 1,052,882 informative SNPs, 6,275 showed a pattern of perfect segregation. These SNPs constitute candidates for the underlying causal sexually antagonistic loci. A series of analyses support the credibility of our candidate sites. First, Monte-Carlo approaches demonstrated that the number of candidate SNPs detected in our screen far exceeded the random expectation. Simulated sampling of nine random genomes from a dataset of 220 individually sequenced whole genomes sampled from the same LH<sub>M</sub> population<sup>18</sup> returned significantly fewer incidences of perfectly segregating sites than the observed data, providing a false positive rate estimate of ~17% (Fig. 1A). This estimate was further corroborated by two additional, complementary approaches (Fig. S1)—the first using simulated sampling from genome-wide estimates of allele frequencies in LH<sub>M</sub><sup>19</sup>, the second permuting our nine genomes between fitness classes. In addition to the modest false-positive rates, the credibility of our candidates as functional sites under selection is supported by the fact that, compared to all informative SNPs, candidate SNPs were enriched in genic regions (including upstream, downstream, and 3'UTR regions) and depauperate in intergenic regions (Fig. 1B). Taken together, these results confirm that our approach detected a clear genetic signal of sexually antagonistic fitness effects. Our data are therefore well-suited to establish the general properties of causal sexually antagonistic variants on a genome-wide scale.

We examined the genomic distribution of antagonistic SNPs. The 6,275 antagonistic SNPs were significantly clustered along chromosome arms (Fig. 1C), with a median distance of 187bp and 6,980bp between adjacent antagonistic SNPs on the autosomes and the X, respectively. These distances were smaller than expected by chance (permutation test; autosomes: median distance between pseudo-antagonistic SNPs = 9,055bp,  $P < 0.001$ ; X chromosome: median distance = 285,036bp,  $P < 0.001$ ). Interestingly, we found that antagonistic sites were significantly underrepresented on the X chromosome compared to the autosomes (Fig. 1D). Approximately 2.7% non-antagonistic SNPs were X-linked, compared to ~0.8% antagonistic sites. This result contradicts classical theory which predicts that the X chromosome will be a hotspot for the accumulation of antagonistic variation<sup>3</sup>. The low prevalence of X-linked antagonistic polymorphisms is more in line with recent models<sup>20,21</sup> which have suggested that the emergence of autosomal variation is facilitated by sex-specific dominance of antagonistic variants (rather than equal dominance in the two sexes, as assumed by earlier models). Dominance of the beneficial allele in each sex increases the average fitness of heterozygotes and generates stronger balancing selection at autosomal loci than X-linked loci. This mechanism has been documented recently for a single sexually antagonistic polymorphism in salmon<sup>12</sup>, and may occur more generally.

We next investigated the population genetic effects of sexual antagonism. Models predict that the opposing sex-specific fitness effects of antagonistic alleles generate balancing selection, resulting in elevated levels of genetic polymorphism at antagonistic loci<sup>22-24</sup>. Our power to discern such a signal in the source population LH<sub>M</sub> is low, because considering SNPs that were polymorphic across nine antagonistic hemiclinal genomes imposes a strong ascertainment bias that elevates heterozygosity across all SNPs used and thereby masks differences between antagonistic and non-antagonistic SNPs. Despite this, we found a signal of balancing selection in LH<sub>M</sub>. Antagonistic SNPs were more likely to be detected as polymorphic in population genomic data from LH<sub>M</sub><sup>19</sup> than non-antagonistic SNPs (observed=4,049, expected=3,556,  $\chi^2=158.17$ ,  $P < 0.001$ ). Additionally, regional polymorphism—measured as Tajima’s D—was significantly higher in windows containing antagonistic SNPs than in windows containing only non-antagonistic SNPs (Fig. S2C). This shows that within LH<sub>M</sub>, the increased phenotypic variation in sex-specific fitness generated by sexual antagonism is mirrored by a signal of increased polymorphism at the underlying genetic loci.

A key, yet so far unresolved question is whether antagonistic polymorphisms are mainly short-lived and population-specific or persist over prolonged periods of time. The signature of balancing selection at antagonistic loci in LH<sub>M</sub> allowed us to address this question by looking for a matching signal in other populations. To do so, we analysed publicly available population genomic data from the *Drosophila* Genetics Reference Panel<sup>25,26</sup> (DGRP) and phase 3 of the *Drosophila* Population Genomics Project<sup>27</sup> (DPGP3). Each dataset provides information on whole-genome polymorphism from ~200 isogenic lines, with the DGRP constituting a sample from a recently introduced North American population (similar to LH<sub>M</sub>), while the DPGP3 was sampled in Zambia in *D. melanogaster*'s ancestral distribution range. Just as in LH<sub>M</sub>, we found that antagonism generated a clear signature of balancing selection in these two independent population samples. Antagonistic SNPs were significantly more likely to be polymorphic in the DGRP and DPGP3 populations compared to non-antagonistic SNPs (DGRP: observed=5,848, expected=5,404,  $\chi^2=270.64$ ,  $P<0.001$ ; DPGP3: observed=5,124, expected=4,641,  $\chi^2=210.96$ ,  $P<0.001$ ). Furthermore, of those SNPs that were detected in either population, antagonistic SNPs had significantly elevated heterozygosity compared to non-antagonistic SNPs (Fig. 2A). At a larger scale, antagonistic windows had significantly higher polymorphism (Tajima's D) than non-antagonistic windows (Fig. 2B), while also exhibiting lower population differentiation between the DGRP and DPGP3 (measured as  $\Phi_{ST}$ ; Fig. 2C). Importantly, these results also held after controlling for spatial autocorrelations in genomic properties, such as genome-wide variation in recombination rate and proximity to functional regions ('linked selection'<sup>28</sup>; see also further analyses in Fig. S3). Taken together, these comparative analyses demonstrate that the antagonistic allelic variation identified in LH<sub>M</sub> is neither recent nor specific to this population. To a significant degree, it has been conserved since before the extension of the species range beyond Africa >10,000 years ago<sup>29-32</sup>.

The population genomic whole-genome sequence data also revealed strong linkage between antagonistic SNP variants. Looking at clusters of antagonistic SNPs, we found that even in the DPGP3, the population most phylogenetically distant from LH<sub>M</sub>, alleles that were inferred to have concordant fitness effects in LH<sub>M</sub> frequently occurred as linked local haplotypes (i.e. male-benefit alleles linked with other male-benefit alleles, and vice-versa; see example in Fig. 2D). To assess whether this linkage was due to selection or due to low local

recombination rate (e.g. inversions), we compared local (<1000bp) linkage disequilibrium (LD) between three types of SNP pairs: antagonistic/antagonistic, non-antagonistic/non-antagonistic and antagonistic/non-antagonistic. We found that LD between pairs of antagonistic SNPs was significantly elevated compared to both ‘control’ pairs (Fig. 2E). Note that the antagonistic/antagonistic vs. antagonistic/non-antagonistic contrast only considers sites in proximity to antagonistic SNPs, effectively controlling for local variations in recombination rate. Thus, these results support the conclusion that elevated LD between adjacent antagonistic variants is maintained by selection and not by low local recombination rates. These observations are consistent with theory predicting that linkage disequilibrium between alleles with similar fitness effects helps to maintain antagonistic polymorphisms<sup>33</sup> because it effectively increases the strength of antagonistic selection acting on the haplotype as a whole.

Another fundamental knowledge gap concerns the biological processes that underlie sexual antagonism. Our data allow us to characterise these processes for the first time. At the most basic level, our results suggest that antagonism arises mainly due to adaptive conflict over gene expression, rather than over coding sequences. Thus, antagonistic SNP variants did not cause missense changes more often than expected but were enriched in genic regions that contribute to expression regulation (up- and down-stream, UTRs, Fig. 1B). In line with antagonistic selection on gene expression, we found that the 1,949 antagonistic genes defined by our SNP data (those containing one or more antagonistic SNPs within  $\pm 5$ kb of the gene coordinates) significantly overlapped with genes that were previously shown to have sexually antagonistic expression patterns (opposing relationships between expression level and fitness in males and females<sup>15</sup>, Fig. 3A). Furthermore, antagonistic genes showed a lower incidence of sex-biased expression than the genome in general (observed=950, expected=1,011,  $\chi^2=11.6$ ,  $P<0.001$ ). This is expected for antagonistic genes under divergent selection for expression, where differential expression between the sexes would contribute to the resolution of antagonism.

In terms of specific regulatory functions, we did not detect a global enrichment of transcription factors among antagonistic genes (*trans* regulation). However, we did find evidence for associations between antagonism and specific *cis*-regulatory functions. Thus, antagonistic genes were enriched for targets of specific regulators, with binding site motifs of

93 transcription factors being over-represented upstream of antagonistic genes (Fig. 3B, Tab. S1). Also, short sequence stretches immediately flanking antagonistic SNPs were centrally enriched for binding motifs for 8 transcription factors (Fig. 3C). These results suggest that antagonism tends to be clustered in specific branches of gene regulatory cascades.

The general biological functions performed by antagonistic genes tended to relate to development and morphogenesis (Gene Ontology analysis; Tabs S2-4). Interestingly, we found a number of associations with the sex-determination and differentiation pathway. Thus, among antagonistic genes were several genes that play important roles in sexual differentiation, including *abdominal A*, *Abdominal B*, *bric à brac 2* and *anterior open*. Of particular note is *fruitless*, a direct target of the *Drosophila* sex-determination cascade and an important regulatory component of sex-specific neuronal development, male courtship behaviour, and physiology<sup>34-36</sup>. Despite its fundamental and highly evolutionarily conserved role in sexual differentiation<sup>37</sup>, *fruitless* contained several clusters of antagonistic SNPs (Fig. S4). Significant associations between antagonism and sexual differentiation also appeared at the *cis*-regulatory level. Thus, antagonistic genes were enriched for targets of several sexual differentiation genes (Fig. 3B, Tab. S1), including *hermaphrodite*, and again *anterior open*. In addition, a binding motif for *cut* was centrally enriched in sequences flanking antagonistic SNPs (Fig. 3C).

## Discussion

Our characterisation of causal loci has provided unprecedented insights into the evolutionary dynamics and functional basis of sexual antagonism. Our data show that variation at antagonistic loci is stably maintained across *D. melanogaster* populations throughout the species' distribution range, aided by the long-term persistence of extended antagonistic haplotypes. Thus, signatures of balancing selection due to antagonism are evident across introduced New World and ancestral Old World populations, indicating that antagonistic polymorphisms have been conserved since before the extension of the species range beyond Africa >10,000 years ago<sup>29-32</sup>. The low turnover in antagonistic sequence variation implies that the phenotypic and genetic targets of sexually antagonistic selection have remained remarkably stable over time and space.

It also suggests that the evolutionary constraints on sexual dimorphism inherent in antagonism are difficult to resolve, possibly requiring complex genetic changes that are unlikely to arise in single mutational steps. The resolution of antagonism, and the evolution of dimorphism, is then likely to proceed in a punctuated, stepwise manner<sup>19</sup>. Recently, we have described a possible example of such a resolution event in a LH<sub>M</sub> stock population<sup>19</sup>, where we observed a significant reduction in antagonism at the phenotypic level and rapid, chromosomally localised frequency change at the sequence level. Interestingly, the loci affected there show significant overlap with the antagonistic loci identified here (genes: observed=183, expected=147,  $\chi^2=10.5$ , P=0.001; SNPs: observed=31, expected=21,  $\chi^2=4.8$ , P=0.028), corroborating the proposed model of long-term stasis and punctuated resolution.

The prevalence of antagonism among regulators of sexual differentiation suggests that the evolution of dimorphism is impeded by the rate with which genes can acquire sex-specific regulation. This is supported by the fact that antagonistic genes show a lower incidence of sex-biased expression than the genome at large (observed=950, expected=1,011,  $\chi^2=11.6$ , P<0.001). With this constraint in place, antagonism permeates across developmental regulatory cascades and up to their very top, as in the case of *fruitless*. Superficially, the association of antagonism with such a fundamental and tightly selected biological process might be surprising. However, the sexual differentiation cascade provides an effective regulatory lever whereby mutations can simultaneously affect many aspects of male and female phenotypes. This will allow them to generate the large and balanced fitness effects that characterise the antagonistic polymorphisms most likely to be maintained over prolonged periods of time<sup>23,38</sup>.

Having filled a longstanding and major gap in our understanding of sexual antagonism now provides a platform from which to further elucidate the origin and resolution of this important evolutionary phenomenon.

## Methods

### Hemiclonal haplotypes

We sequenced the genomes of the nine most antagonistic genotypes identified in a screen of 100 hemiclones conducted as part of a previous study<sup>15</sup>. 5 male-beneficial/female-detrimental (MB) genotypes and 4 female-beneficial/male-detrimental (FB) genotypes (a fifth FB had been lost prior to this study) had been maintained as ‘hemiclones’, i.e., intact haploid sets of chromosomes X, II and III, by back-crossing males to ‘clone-generator’ females [C(1)DX, y, f; T(2;3) rdgC st in ri pP bwD]. The fitness effects of the 100 lines used in the original screen were measured under tightly standardised conditions across a large number of replicate individuals, thus minimising environmental variance and maximising the power of inferring genetic effects on the measured phenotype. Additionally, the fitness effects of the nine antagonistic lines were measured again as part of a follow-up study<sup>19</sup>, and found to be consistent with the original experiment.

In order to obtain sequences of the nine haploid hemiclonal genomes, we expressed them in three different genetic backgrounds that could then be used to infer the genome sequence of interest with confidence (see section ‘Identification of informative and candidate SNPs’). The three genotypes sequenced for each hemiclonal genome were (i) females in which the hemiclonal genome was complemented with chromosomes from the *Drosophila melanogaster* reference strain iso-1 (y[1]; Gr22b[iso-1] Gr22d[iso-1] cn[1] CG33964[iso-1] bw[1] sp[1]; MstProx[iso-1] GstD5[iso-1] Rh6[1]), (ii) females in which the hemiclonal genome was complemented with chromosomes from the Canton-S strain, and (iii) males in which the hemiclonal genome was complemented with chromosomes from the clone-generator strain.

DNA extraction, sequencing and initial processing of haplotype sequencing reads 10-25 individuals were collected for each of the 27 samples in March 2012 (9 hemiclones, 3 genetic backgrounds per hemiclone). We extracted total genomic DNA using DNeasy<sup>®</sup> Blood and Tissue Kit (Qiagen) according to the manufacturer’s protocol and purified DNA samples using Agencourt<sup>®</sup> AMPure XP<sup>®</sup> beads (Beckman Coulter). Paired-end Nextera libraries were prepared using a Nextera DNA sample preparation kit (Illumina). Completed libraries were pooled in equimolar amounts and fragments between 450 and 650bp were collected using the Pippin Prep DNA size selection system (Sage Scientific). Size-selected pools were purified using Agencourt<sup>®</sup> AMPure XP beads. Sequencing was performed on 4

lanes of an Illumina HiSeq 2000 at the Center for Genomic Research, University of Liverpool.

Basecalling and de-multiplexing of the indexed sequencing reads was performed using CASAVA version 1.8.2 (Illumina). The raw fastq files were first trimmed using Cutadapt version 1.2.1<sup>39</sup> to remove Illumina adapter sequences. The reads were then further trimmed to remove low quality bases (minimum window score of 20) and very short reads (<10bp) with Sickle version 1.200 (github.com/najoshi/sickle). Read pairs were then aligned to the *D. melanogaster* reference sequence (BDGP 5.5), obtained from the FlyBase online database (<http://flybase.org/>), using Bowtie2 version 2.1.0<sup>40</sup> in '--local' alignment mode. To avoid false positive SNP calls resulting from misalignment around indels, reads were locally realigned using the Genome Analysis Toolkit (GATK) version 2.1.13<sup>41,42</sup>. Duplicate reads, arising from PCR amplification during library construction were removed using Picard version 1.85 ([http:// sourceforge.net/projects/picard/](http://sourceforge.net/projects/picard/)). The alignment results were visually inspected using the Integrative Genomics Viewer<sup>43</sup>. SNP calling was performed using the GATK 'UnifiedGenotyper' package with heterozygosity set to 0.14 (to more closely reflect heterozygosity of *D. melanogaster*). Identified SNPs were then filtered to remove SNPs with low confidence and low coverage (<10 reads) using the GATK 'VariantFiltration' package.

### **Identification of informative and candidate SNPs**

To identify informative SNPs from the hemiclinal genomes, we exploited the fact that their DNA was present in all three crosses and that in one of the crosses, they were complemented with chromosomes of the reference strain. Thus, for a given chromosomal position with sufficient coverage in the sequencing of all three crosses, we inferred the hemiclinal variant to be an alternative (non-reference) variant if an identical alternative variant was detected in all three crosses. The variant was assumed to be the reference variant if this condition was not fulfilled.

Once variants for all nine hemiclinal genomes were identified in this way, we defined a set of informative SNPs as variants which were polymorphic across the nine hemiclinal genomes. Candidates for sexually antagonistic SNPs were then defined as those SNPs where all MB hemiclinal genomes were fixed for one variant and all FB hemiclinal genomes were fixed for the other variant ('perfectly segregating').

Given the small number of hemiclones sequences, this rule-based approach for defining candidate antagonistic SNPs is the most appropriate. It is equivalent to applying locus-by-

locus contingency table tests to the counts of alleles in the two fitness classes, where only the ‘perfectly segregating’ pattern we use in the rule-based approach yields a significant P-value. A wider range of P-values could have been obtained by taking into account population allele frequencies to calculate the probability of an observed variant pattern at a focal SNP, given the population frequencies. However, this is not suitable when seeking to identify SNPs that are most likely under balancing selection, as is the case for sexually antagonistic loci. SNPs under balancing selection will have higher minor allele frequencies and would be unduly penalised in this approach because the probability of observing a perfectly segregating pattern is higher. This approach would therefore reject the very loci that are most likely to underlie antagonistic phenotypes.

### **Computational validation of candidate SNPs**

We implemented three independent tests to determine whether the number of candidate SNPs detected with our rule-based approach was greater than expected by chance, (i) a resampling test based on individually sequenced hemiclones from the LH<sub>M</sub> population<sup>18</sup>, (ii) a resampling test based on LH<sub>M</sub> population allele frequencies<sup>19</sup>, (iii) a permutation test that shuffled hemiclonal haplotypes among fitness classes (MB and FB).

In the first approach, we merged our dataset with individually sequenced genomes (N=220) from the LH<sub>M</sub> population<sup>18</sup>. We randomly sampled nine of the 220 whole-genome sequences and randomly assigned them to the two fitness classes (5x MB, 4x FB), before counting the number of perfectly segregating SNPs (‘pseudo-candidate SNPs’). This procedure was repeated 1,000 times to generate a null distribution of the number of pseudo-candidate SNPs (Fig. 1A). Significance was determined by calculating the proportion of instances where the number of pseudo-candidates was greater than or equal to the number of antagonistic SNPs observed in our original analysis of hemiclones with extreme fitness effects. This approach samples individual genomes rather than relying on population allele frequencies and so takes into account the exact linkage structure of the LH<sub>M</sub> population. Any underestimation of the false positive rate due to linkage between antagonistic sites is therefore obviated.

In a second, complementary approach, we merged our dataset with high quality genome-wide allele frequency data generated from the same LH<sub>M</sub> population<sup>19</sup>. This dataset was generated closer in time to the establishment of the nine extreme haplotypes than the genomic data by Gilks et al.<sup>18</sup> and thus provides a more accurate reflection of the

polymorphism at the time the hemiclones were established (but note that allele frequencies are also generally highly positively correlated between the two population genomic datasets). We then used binomial sampling to generate allelic samples ( $N=9$ ) for each SNP, with probabilities determined by population allele frequencies. The samples were randomly assigned to the two fitness classes (MB and FB). A null distribution of pseudo-candidate SNPs (Fig. S1A) and significance was determined as above.

In the third approach, we produced all possible permutations of the nine hemiclinal haplotypes among the two fitness classes and for each recalculated the numbers of perfectly segregating sites. We then presented these as a function of the number of genotypes that had been swapped between classes (Fig. S1B). If a true relationship between genotypes and phenotype (fitness effects) exists, we would expect to observe the lowest number of perfectly segregating sites in permutations where the association between fitness class and genotype is most ‘broken’ —i.e., where intermediate numbers of haplotypes are swapped (and this is observed).

### **Genomic distribution of antagonistic SNPs**

To examine the clustering of antagonistic SNPs across chromosome arms we calculated the median distance between all pairs of adjacent antagonistic SNPs (ignoring interspersed non-antagonistic SNPs). We did this separately for the autosomes and X chromosome, to accommodate for the lower SNP density on the X chromosome. We then designed a permutation test to determine the significance of the observed clustering. Antagonistic/non-antagonistic status was permuted among all informative SNPs, distances recalculated as before between adjacent SNPs labelled as ‘antagonistic’ after permutation and the median distance recorded. This process was repeated 1,000 times in order to generate a null distribution of median distances. Significance was calculated as the proportion of median distances in the null distribution that were lower than or equal to the true median distance. None of the permuted medians were lower or equal to the observed value, so  $P < 0.001$ .

To examine the relative representation of antagonistic SNPs on autosomes and the X chromosome, we compared the proportion of antagonistic SNPs to the proportion of all informative SNPs mapping to each chromosomal compartment. We did this for each chromosomal compartment in turn, using Z-tests. The under- or over-representation of antagonistic SNPs in each compartment therefore accounted for general differences in SNP density between chromosome arms and, in particular, lower diversity on the X chromosome.

### **LH<sub>M</sub>, DGRP and DPGP3 population genomic data**

We used population genomic data derived from pooled sequencing of 165 adult female individuals from the LH<sub>M</sub> population<sup>19</sup> to estimate polymorphism in the source population. We also used publicly available population genomic data from wild *D. melanogaster* populations in North America and Zambia. The North American data, from the *Drosophila* Genetic Reference Panel (DGRP<sup>25,26</sup>), consists of 205 whole-genome sequences derived from inbred lines established from flies caught in North Carolina (USA). The Zambian data, from phase 3 of the *Drosophila* Population Genomics Project (DPGP3<sup>27</sup>), consists of 197 whole-genome sequences derived from haploid embryos sampled from flies caught in a wild Zambian population. The two populations represent a range of divergence times from the LH<sub>M</sub> population. While DGRP flies, like those of LH<sub>M</sub>, are descendants of recent (~150 years<sup>32</sup>) colonisation of the USA, the DPGP3 was sampled in the ancestral range of *D. melanogaster*, and is separated from the American populations by ~19,000 years<sup>29,32,44</sup>. Genome sequences for the DGRP and DPGP3 were downloaded as FASTA files from <http://www.johnpool.net/genomes.html>. These sequence files have undergone standardised alignment and have been quality filtered<sup>27</sup>. SNP calling of the multiple sequence alignments was performed with *snp-sites*<sup>45</sup>. We further excluded SNPs that were covered in <100 genomes sequences, SNPs that segregated for more than two variants, SNPs where the minor allele was only present once (possible sequencing error), and SNPs where both variants did not match those detected among the antagonistic LH<sub>M</sub> hemiclinal haplotypes.

### **Balancing selection estimates in LH<sub>M</sub>, DGRP and DPGP3**

We performed genome-wide sliding window analyses (1,000bp windows, 500bp step size) to investigate regional signatures of balancing selection. Tajima's D, which compares SNP polymorphism (nucleotide diversity,  $\pi$ ) to SNP abundance (Watterson's estimator,  $\theta$ ), was compared for windows containing (i) one or more antagonistic SNPs and (ii) only non-antagonistic SNPs (Fig. 2B, Fig. S2). In the LH<sub>M</sub>, Tajima's D was calculated using *popoolation* (v. 1.2.2<sup>46</sup>; pool size=330, minimum quality=20, minimum count=2, minimum coverage=100, maximum coverage=290). In the DGRP and DPGP3, Tajima's D was calculated using the *PopGenome* package<sup>47</sup>. We incorporated estimates of linked selection<sup>48</sup> (estimated in 1,000bp windows) to account for genomic correlations between populations owing to factors unrelated to sexual antagonism, such as local recombination rate variation

and proximity to functional sequences. We used general linear models (GLMs) with Gaussian error structure to assess the effect of the number of antagonistic SNPs per window on Tajima's  $D$ , with estimates of linked selection included as covariates. Estimates of linked selection were not available on the X chromosome, so we used estimates of recombination rate as covariates instead<sup>49</sup>.

For the DGRP and DPGP3, we implemented SNP-level analyses by comparing expected heterozygosity between antagonistic and non-antagonistic SNPs (Fig. 2A). Expected heterozygosity was calculated as twice the product of the frequencies of the two alleles at a given SNP, and heterozygosities were compared between the two classes of SNPs using a Wilcoxon Rank-Sum test.

We tested whether balancing selection at the level of windows was associated with reduced population differentiation. Measures such as  $F_{ST}$  are sensitive to heterozygosity<sup>50</sup> and are less suitable for a window-based sequence comparison because they ignore the genetic distance between segregating haplotypic sequences. We therefore used the AMOVA framework<sup>51</sup> to calculate  $\Phi_{ST}$ , a measure of population differentiation that takes into account genetic distances (i.e., numbers of substitutions) between sequences when quantifying the proportion of genetic variation that occurs between vs within populations.  $\Phi_{ST}$  was calculated between the DGRP and the DPGP3 over sliding windows as above (1000bp windows, 500bp step) using the *poppr*<sup>52</sup> package. We did not include  $LH_M$  in this analysis because polymorphism data for this population is derived from pooled sequencing data where haplotype information is not available. Wilcoxon Rank-Sum tests were used to test for differences in  $\Phi_{ST}$  between windows with one or more antagonistic SNPs vs. windows with only non-antagonistic SNPs (Fig. 2C). To consider effects due to linked selection we re-ran Wilcoxon Rank-Sum tests and compared the residual  $\Phi_{ST}$  between window classes, once linked selection estimates (and recombination rate estimates, for the X chromosome) had been accounted for.

We considered the possibility that linked selection estimates do not fully capture genomic correlations driven by recombination rate and proximity to functional regions—i.e., that the antagonistic vs. non-antagonistic contrasts remain inflated by remaining linkage along chromosome arms which would lead to non-independence in the statistical tests applied to our data. In order to avoid such pseudo-replication, we repeatedly subsampled antagonistic and non-antagonistic windows (N=500 for each window class) while ensuring that these windows were sufficiently far apart (>10,000bp) to minimise spatial autocorrelations in

genomic properties. By repeating this subsampling procedure 1000 times and estimating the effect size (in a GLM, assuming Gaussian error structure) associated with the contrast of antagonistic vs. non-antagonistic windows, we generated an empirical distribution of effect sizes (Fig. S3).

### **Patterns of segregation between antagonistic SNPs**

We examined the extent to which antagonistic haplotypes are selectively maintained by investigating whether antagonistic SNPs commonly segregate as male- and female-benefit haplotypes (as inferred from  $LH_M$ ) in the DPGP3, the population that is most distant from  $LH_M$  and where such a signal would therefore be expected to be weakest. We used LD to quantify the extent to which SNPs segregate non-randomly as male- and female-benefit haplotypes – a pattern which should be reflected as a high  $r^2$  value. Thus, for all antagonistic SNPs situated within 1000bp of one another, we calculated pairwise LD between antagonistic SNPs. As a control set, we randomly sampled 100,000 non-antagonistic SNPs, and calculated pairwise LD between those situated within 1,000bp of each other. To test for significant differences in LD between ‘pair types’ (i.e. antagonistic/antagonistic pairs vs control/control pairs), we modelled variation in  $r^2$  as a declining exponential function of chromosomal distance, and assessed differences in residual  $r^2$  between groups (once distance was corrected for) using a Wilcoxon Rank-Sum test.

Genomic location can falsely inflate LD, if, for example, antagonistic SNPs are disproportionately situated in regions of low recombination (e.g. inversions). To correct for this, we additionally calculated LD between pairs where one SNP was antagonistic and one SNP was non-antagonistic. Contrasting previously calculated LD with this new pair type enabled us to disentangle the effect of selection and local recombination (Fig. 2E), since any local variations in recombination rate should affect both types of SNP pair equally. Significant differences in LD were assessed as above, using Wilcoxon Rank-Sum tests.

### **Functional analyses of antagonistic loci**

We used the variant effect predictor (Ensembl VEP<sup>53</sup>) to map SNPs to genes and infer their genetic consequences. In accordance with the VEP default settings, we included extended gene regions (+/- 5kb of gene coordinates) in our gene definition. To gain preliminary insights into the functions of antagonistic genes we used the Gorilla<sup>54</sup> Gene Ontology tool, and applied false discovery rate (FDR) to correct for multiple testing across many GO terms

(Tabs. S2-4). Here all genes covered in our entire SNP dataset were used as the background set.

To examine the relationship between antagonistic genes and sex-biased gene expression we used the Sebida online database<sup>55</sup> to annotate genes covered in our sequencing as having either sex-biased or unbiased expression profiles, based on the meta-class identifier. We then used a  $\chi^2$  test to compare the sex-biased expression status of antagonistic and non-antagonistic genes.

To assess the degree of overlap between antagonistic genes identified here and those associated with sexually antagonistic expression patterns in a previous study<sup>15</sup> (Fig. 3A), we included only genes covered in both datasets, and only those genes in both datasets that were adult-expressed. To determine whether genes were adult expressed we used the *Drosophila* gene expression atlas (FlyAtlas<sup>56</sup>). Conservatively, we considered a gene ‘adult expressed’ if its transcript was detected as present in at least one library of one adult-derived sample. We then used a  $\chi^2$  test to assess the degree of overlap between the datasets.

To compare the number of antagonistic and non-antagonistic transcription factor genes, we annotated all genes in our data that encode for transcription factors using the supervised regulatory network data from Marbach *et al.*<sup>57</sup>, which defines 617 putative transcription factors.

To assess antagonistic genes for signatures of shared regulation (Fig. 3B, Tab. S1) we used the Motif Enrichment Tool<sup>58</sup> with default settings, to search regions 5kb upstream of the transcription start sites for enriched motifs. Here again, all genes covered in our SNP dataset were used for the background set. We applied FDR corrections to P-values to account for the testing of multiple motifs.

To test for motif enrichment close to antagonistic SNPs (Fig. 3C), we used the Centrimo tool from MEMEsuite<sup>59</sup> with default settings. We generated the input FASTA files using bedtools<sup>60</sup> and extracted the sequences ( $\pm 20$ bp) flanking the SNPs in our dataset from the *D. melanogaster* reference genome (BDGP 5.5). We used flanking sequences for all informative SNPs to generate the background model and the flanking sequences of antagonistic SNPs as the target set.

## Statistical software

All statistical analyses were carried out in R (version 3.2.3, R Core Development Team 2016).

## Data availability

Pooled sequencing data from the LH<sub>M</sub> population is available at

<http://www.ebi.ac.uk/ena/data/view/PRJEB12822> under accession SAMEA3881048.

Population genomic data from the DGRP and DPGP3 is available at

<http://www.johnpool.net/genomes.html>.

Sequence data from this study will be made available at the European Nucleotide archive.

## Code availability

Analysis code is available on request.

## References

1. Bonduriansky, R. & Chenoweth, S. F. Intralocus sexual conflict. *Trends Ecol. Evol.* **24**, 280–8 (2009).
2. Van Doorn, G. S. Intralocus sexual conflict. *Ann. N. Y. Acad. Sci.* **1168**, 52–71 (2009).
3. Rice, W. R. Sex chromosomes and the evolution of sexual dimorphism. *Evolution.* **38**, 735–742 (1984).
4. Cox, R. M. & Calsbeek, R. Sexually Antagonistic Selection, Sexual Dimorphism, and the Resolution of Intralocus Sexual Conflict. *Am. Nat.* **173**, 176–187 (2009).
5. Pennell, T. M. & Morrow, E. H. Two sexes, one genome: The evolutionary dynamics of intralocus sexual conflict. *Ecol. Evol.* **3**, 1819–1834 (2013).
6. Mokkonen, M. *et al.* Negative Frequency-Dependent Selection of Sexually Antagonistic Alleles in *Myodes glareolus*. *Science.* **334**, 972–974 (2011).
7. Tarka, M. *et al.* Intralocus Sexual Conflict over Wing Length in a Wild Migratory Bird. *Am. Nat.* **183**, 62–73 (2014).
8. Svensson, E. I., McAdam, A. G. & Sinervo, B. Intralocus sexual conflict over immune defense, gender load, and sex-specific signaling in a natural lizard population. *Evolution.* **63**, 3124–3135 (2009).
9. Rice, W. R. Sexually antagonistic genes: experimental evidence. *Science.* **256**, 1436–1439 (1992).
10. Berger, D., Berg, E. C., Widegren, W., Arnqvist, G. & Maklakov, A. A. Multivariate intralocus sexual conflict in seed beetles. *Evolution.* **68**, 3457–3469 (2014).
11. Roberts, R. B., Ser, J. R. & Kocher, T. D. Sexual conflict resolved by invasion of a

- novel sex determiner in Lake Malawi Cichlid fishes. *Science* **326**, 998–1001 (2009).
12. Barson, N. J. *et al.* Sex-dependent dominance at a single locus maintains variation in age at maturity in salmon. *Nature* **528**, 405–408 (2015).
  13. Delph, L. F. *et al.* Environment-dependent intralocus sexual conflict in a dioecious plant. *New Phytol.* **192**, 542–552 (2011).
  14. Kidwell, J. F., Clegg, M. T., Stewart, F. M. & Prout, T. Regions of stable equilibria for models of differential selection in the two sexes under random mating. *Genetics* **85**, 171–183 (1977).
  15. Innocenti, P. & Morrow, E. H. The sexually antagonistic genes of *Drosophila melanogaster*. *PLoS Biol.* **8**, e1000335 (2010).
  16. Chippindale, A. K., Gibson, J. R. & Rice, W. R. Negative genetic correlation for adult fitness between sexes reveals ontogenetic conflict in *Drosophila*. *Proc. Natl. Acad. Sci. U. S. A.* **98**, 1671–1675 (2001).
  17. Rice, W. R. *et al.* Inter-locus antagonistic coevolution as an engine of speciation: assessment with hemiclonal analysis. *Proc. Natl. Acad. Sci. U. S. A.* **102**, 6527–6534 (2005).
  18. Gilks, W. P., Pennell, T. M., Flis, I., Webster, M. T. & Morrow, E. H. Whole genome resequencing of a laboratory-adapted *Drosophila melanogaster* population sample. *F1000Research* **5**, 2644 (2016).
  19. Collet, J. M. *et al.* Rapid evolution of the intersexual genetic correlation for fitness in *Drosophila melanogaster*. *Evolution.* **70**, 781–795 (2016).
  20. Fry, J. D. The genomic location of sexually antagonistic variation: some cautionary comments. *Evolution.* **64**, 1510–6 (2009).
  21. Jordan, C. Y. & Charlesworth, D. The potential for sexually antagonistic polymorphism in different genome regions. *Evolution.* **66**, 505–516 (2012).
  22. Gavrillets, S. & Rice, W. R. Genetic models of homosexuality: generating testable predictions. *Proc. R. Soc. B Biol. Sci.* **273**, 3031–8 (2006).
  23. Mullon, C., Pomiankowski, A. & Reuter, M. The effects of selection and genetic drift on the genomic distribution of sexually antagonistic alleles. *Evolution.* **66**, 3743–3753 (2012).
  24. Connallon, T. & Clark, A. G. Balancing selection in species with separate sexes: insights from Fisher’s geometric model. *Genetics* **197**, 991–1006 (2014).
  25. Mackay, T. F. C. *et al.* The *Drosophila melanogaster* Genetic Reference Panel. *Nature*

- 482**, 173–8 (2012).
26. Huang, W. *et al.* Natural variation in genome architecture among 205 *Drosophila melanogaster* Genetic Reference Panel lines. *Genome Res.* **24**, 1193–1208 (2014).
  27. Lack, J. B. *et al.* The *Drosophila* Genome Nexus: a population genomic resource of 623 *Drosophila melanogaster* genomes, including 197 from a single ancestral range population. *Genetics* **199**, 1229–1241 (2015).
  28. Elyashiv, E. *et al.* A Genomic Map of the Effects of Linked Selection in *Drosophila*. *PLOS Genet.* **12**, e1006130 (2016).
  29. Lachaise, D. *et al.* Historical biogeography of the *Drosophila melanogaster* species subgroup. *Evol. Biol.* **22**, 159–225 (1988).
  30. Li, H. & Stephan, W. Inferring the demographic history and rate of adaptive substitution in *Drosophila*. *PLoS Genet.* **2**, e166 (2006).
  31. Thornton, K. & Andolfatto, P. Approximate Bayesian inference reveals evidence for a recent, severe bottleneck in a Netherlands population of *Drosophila melanogaster*. *Genetics* **172**, 1607–1619 (2006).
  32. Duchon, P., Zivkovic, D., Hutter, S., Stephan, W. & Laurent, S. Demographic inference reveals African and European admixture in the North American *Drosophila melanogaster* population. *Genetics* **193**, 291–301 (2013).
  33. Patten, M. M., Haig, D. & Úbeda, F. Fitness variation due to sexual antagonism and linkage disequilibrium. *Evolution.* **64**, 3638–3642 (2010).
  34. Kimura, K. I., Ote, M., Tazawa, T. & Yamamoto, D. Fruitless specifies sexually dimorphic neural circuitry in the *Drosophila* brain. *Nature* **438**, 229–233 (2005).
  35. Vilella, A. & Hall, J. C. Neurogenetics of Courtship and Mating in *Drosophila*. *Advances in Genetics* **62**, 67–184 (2008).
  36. Neville, M. C. *et al.* Male-specific fruitless isoforms target neurodevelopmental genes to specify a sexually dimorphic nervous system. *Curr. Biol.* **24**, 229–241 (2014).
  37. Gailey, D. A. *et al.* Functional conservation of the fruitless male sex-determination gene across 250 Myr of insect evolution. *Mol. Biol. Evol.* **23**, 633–643 (2006).
  38. Connallon, T. & Clark, A. G. A general population genetic framework for antagonistic selection that accounts for demography and recurrent mutation. *Genetics* **190**, 1477–1489 (2012).
  39. Martin, M. Cutadapt removes adapter sequences from high-throughput sequencing reads. *EMBnet.journal* **17**, 10 (2011).

40. Langmead, B. & Salzberg, S. L. Fast gapped-read alignment with Bowtie 2. *Nat. Methods* **9**, 357–359 (2012).
41. McKenna, A. *et al.* The genome analysis toolkit: A MapReduce framework for analyzing next-generation DNA sequencing data. *Genome Res.* **20**, 1297–1303 (2010).
42. DePristo, M. A. *et al.* A framework for variation discovery and genotyping using next-generation DNA sequencing data. *Nat. Genet.* **43**, 491–498 (2011).
43. Robinson, J. T. *et al.* Integrative genomics viewer. *Nat. Biotechnol.* **29**, 24–26 (2011).
44. Pool, J. E. *et al.* Population Genomics of Sub-Saharan *Drosophila melanogaster*: African Diversity and Non-African Admixture. *PLoS Genet.* **8**, e1003080 (2012).
45. Keane, J. A. *et al.* SNP-sites: rapid efficient extraction of SNPs from multi-FASTA alignments. *Microb. Genomics* **2**, (2016).
46. Kofler, R. *et al.* PoPoolation: A Toolbox for Population Genetic Analysis of Next Generation Sequencing Data from Pooled Individuals. *PLoS One* **6**, e15925 (2011).
47. Pfeifer, B., Wittelsburger, U., Ramos-Onsins, S. E. & Lercher, M. J. PopGenome: An Efficient Swiss Army Knife for Population Genomic Analyses in R. *Mol. Biol. Evol.* **31**, 1929–1936 (2014).
48. Elyashiv, E. *et al.* A genomic map of the effects of linked selection in *Drosophila*. *PLoS Genet.* **12**, e1006130 (2016).
49. Comeron, J. M., Ratnappan, R., Bailin, S., Frith, M. & Grant, C. The Many Landscapes of Recombination in *Drosophila melanogaster*. *PLoS Genet.* **8**, e1002905 (2012).
50. Cruickshank, T. E. & Hahn, M. W. Reanalysis suggests that genomic islands of speciation are due to reduced diversity, not reduced gene flow. *Mol. Ecol.* **23**, 3133–3157 (2014).
51. Excoffier, L., Smouse, P. E. & Quattro, J. M. Analysis of molecular variance inferred from metric distances among DNA haplotypes: application to human mitochondrial DNA restriction data. *Genetics* **131**, 479–91 (1992).
52. Kamvar, Z. N., Tabima, J. F. & Grünwald, N. J. *Poppr* : an R package for genetic analysis of populations with clonal, partially clonal, and/or sexual reproduction. *PeerJ* **2**, e281 (2014).
53. McLaren, W. *et al.* Deriving the consequences of genomic variants with the Ensembl API and SNP Effect Predictor. *Bioinformatics* **26**, 2069–2070 (2010).
54. Eden, E., Navon, R., Steinfeld, I., Lipson, D. & Yakhini, Z. GOrilla: a tool for

- discovery and visualization of enriched GO terms in ranked gene lists. *BMC Bioinformatics* **10**, 48 (2009).
55. Gnad, F. & Parsch, J. Sebida: a database for the functional and evolutionary analysis of genes with sex-biased expression. *Bioinformatics* **22**, 2577–2579 (2006).
  56. Chintapalli, V. R., Wang, J. & Dow, J. A. T. Using FlyAtlas to identify better *Drosophila melanogaster* models of human disease. *Nat. Genet.* **39**, 715–20 (2007).
  57. Marbach, D. *et al.* Predictive regulatory models in *Drosophila melanogaster* by integrative inference of transcriptional networks. *Genome Res.* **22**, 1334–1349 (2012).
  58. Blatti, C. & Sinha, S. Motif enrichment tool. *Nucleic Acids Res.* **42**, W20–W25 (2014).
  59. Bailey, T. L. *et al.* MEME Suite: Tools for motif discovery and searching. *Nucleic Acids Res.* **37**, W202–W208 (2009).
  60. Quinlan, A. R. & Hall, I. M. BEDTools: a flexible suite of utilities for comparing genomic features. *Bioinformatics* **26**, 841–842 (2010).

## Acknowledgements

We thank the Centre for Genomic Research, University of Liverpool, and the Institute of Child Health, UCL, for assistance with high-throughput sequencing and Claire Fourcade for exploratory analyses of antagonistic gene regulatory effects. We are grateful to Laurent Keller, Andrew Pomiankowski and François Balloux for useful comments on the manuscript. MSH was funded by a UCL IMPACT PhD studentship, FR by a London NERC DTP PhD studentship, SF and JC by a NERC research grant (NE/G0189452/1) to MR and KF, and EHM by a European Research Council Grant (280632) and a Royal Society University Research Fellowship.

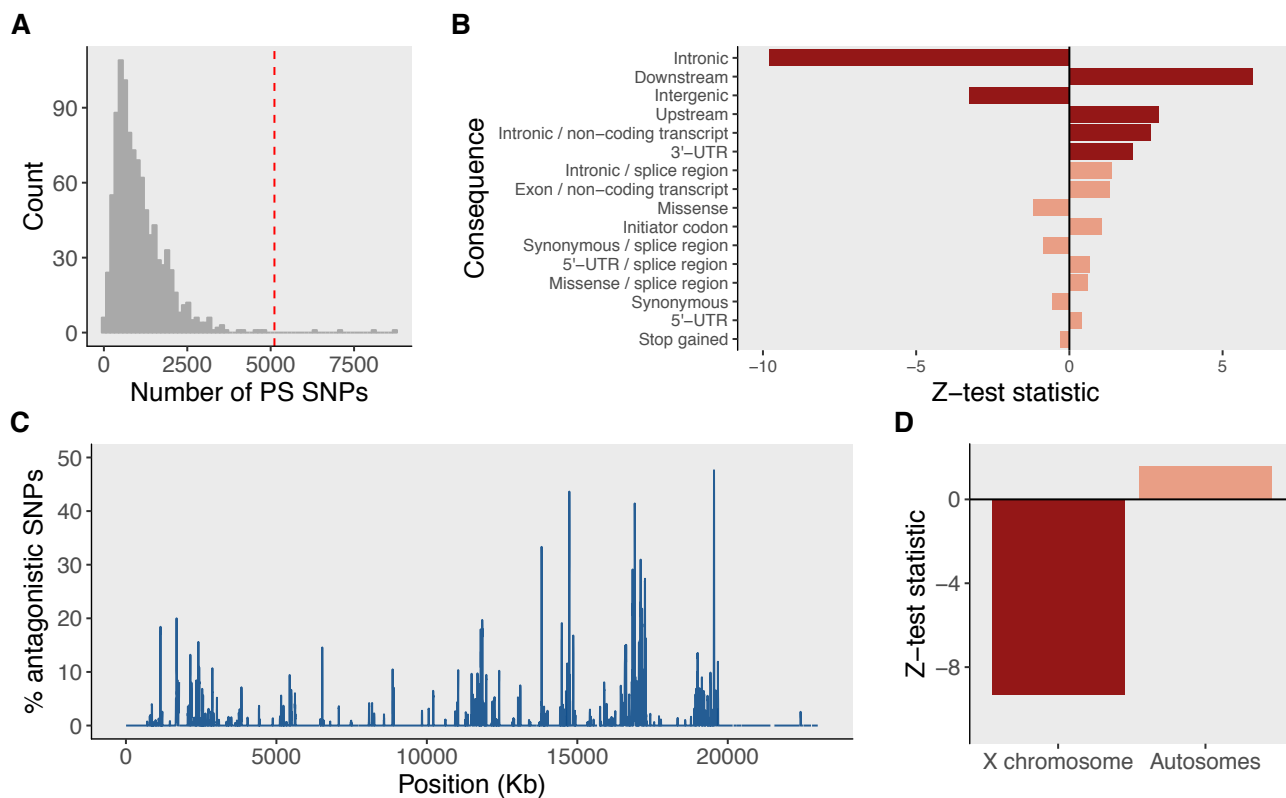
## Author contributions

MR and KF conceived the project. MSH, SF and JC conducted experiments. MSH, FR and MR analysed data. MSH, FR, KF and MR wrote the manuscript. TM contributed stocks and contributed to writing the manuscript.

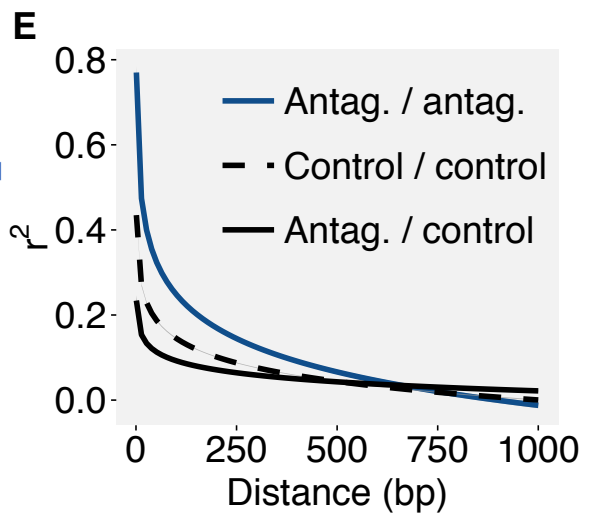
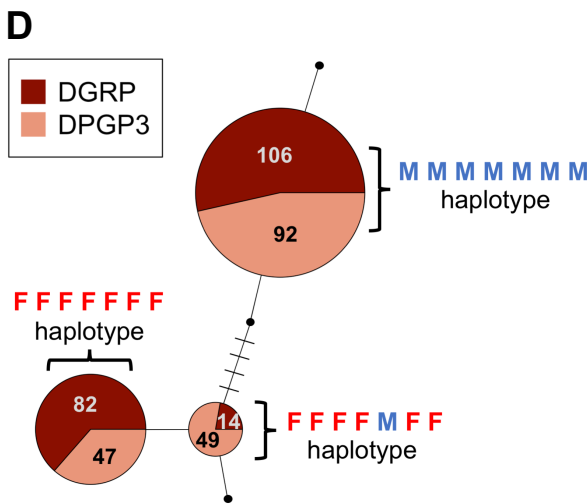
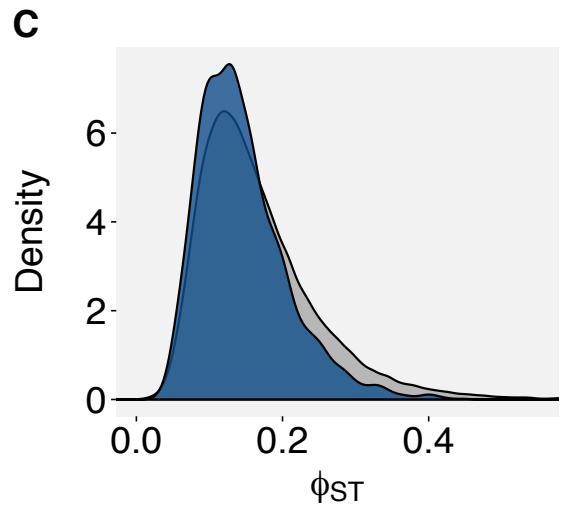
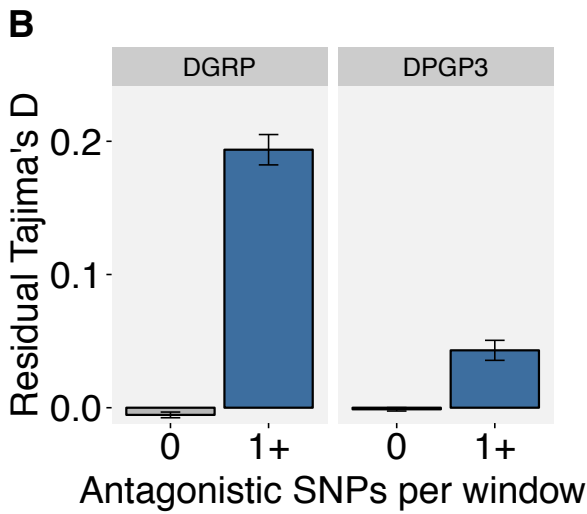
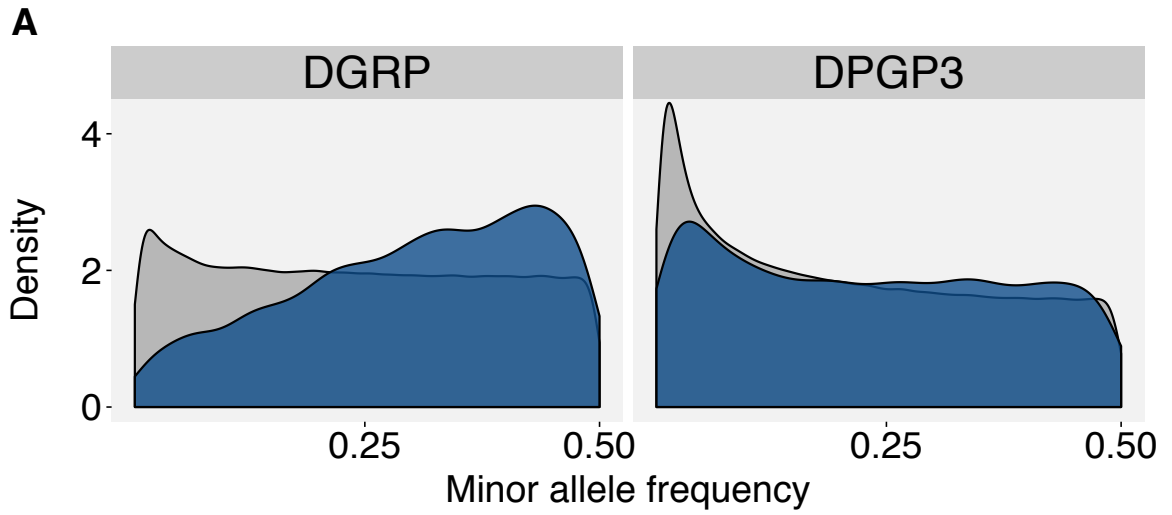
## Competing financial interests

The authors declare no competing financial interests.

# Figures

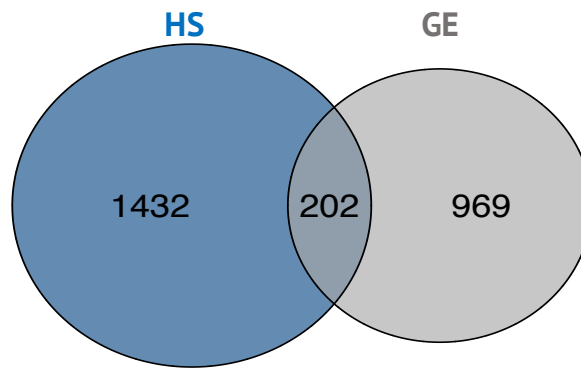


**Figure 1. Characteristics of candidate sexually antagonistic SNPs.** **A**, Null distribution of the expected number of perfectly segregating (PS) SNPs ('pseudo-candidates'), generated by randomly sampling 1,000 sets of 9 genomes from LH<sub>M</sub> whole-genome sequences (grey). The dashed red line indicates the observed number of candidate antagonistic SNPs that were covered in the genomic data used for sampling (N=5,113). The median number of pseudo-candidates across resampled datasets was equal to 888 (false positive rate = 17.3%). The overrepresentation of candidate SNPs in the observed data was statistically significant (P=0.004). **B**, Predicted variant effects of antagonistic candidate SNPs relative to all SNPs covered in the haplotype sequencing. Dark red bars indicate statistically significant over-/under-representation, lighter red bars P>0.05. **C**, Sliding window plot (window size=10,000bp, step size=2,500bp) of chromosome arm 2L showing the percentage of informative SNPs in each window that were antagonistic. **D**, Representation of antagonistic SNPs, relative to all informative SNPs, on autosomes and the X chromosome. Dark red bars indicate statistically significant over-/under- representation, lighter red bars P>0.05.



**Figure 2. Signatures of balancing selection generated by sexually antagonistic SNPs across *D. melanogaster* populations.**

**A**, Site frequency spectrum for highly covered (depth  $\geq 100$ ) SNPs in the DGRP and DPGP3 that our haplotype sequencing data identified as antagonistic (blue,  $N_{\text{DGRP}}=5,848$ ;  $N_{\text{DPGP3}}=5,124$ ) or non-antagonistic (grey,  $N_{\text{DGRP}}=894,798$ ;  $N_{\text{DPGP3}}=765,904$ ). Antagonistic SNPs had elevated minor allele frequencies, resulting in elevated heterozygosity (Wilcoxon test,  $P < 0.001$ ) in both populations. **B**, Mean  $\pm$  s.e.m. of Tajima's  $D$ , corrected for the effects of linked selection, in the DGRP and DPGP3. Blue bars indicate sliding windows (window size=1000bp, step size=500bp) containing one or more antagonistic SNPs ( $N_{\text{DGRP}}=2,693$ ;  $N_{\text{DPGP3}}=2,695$ ), grey bars indicate windows containing only non-antagonistic SNPs ( $N_{\text{DGRP}}=96,824$ ;  $N_{\text{DPGP3}}=97,282$ ). Antagonistic windows displayed elevated Tajima's  $D$  in both populations (DGRP:  $F_{1,99515}=252.2$ ,  $P < 0.001$ ; DPGP3:  $F_{1,99975}=79.02$ ,  $P < 0.001$ ). **C**, Population differentiation ( $\Phi_{\text{ST}}$ ) between the DGRP and DPGP3, calculated in sliding windows as above. Blue and grey density surfaces correspond to windows with ( $N=2,693$ ) or without ( $N=97,038$ ) antagonistic SNPs. Differentiation was significantly lower in windows containing antagonistic SNPs (Wilcoxon test,  $P < 0.001$ ). This remained true when accounting for linked selection (Wilcoxon test,  $P < 0.001$ ). **D**, Haplotype network for a cluster of seven antagonistic SNPs (M: male-beneficial allele; F: female-beneficial allele) situated in the gene *fruitless* (see also Fig. S4). Each circle represents a unique haplotype and is annotated with its frequency in each population; small black circles represent very infrequent haplotypes (0.5-2% of individuals). Notches indicate mutational steps between each haplotype. The two major haplotypes were identical to those identified as perfectly segregating in the  $\text{LH}_M$  population; recombinant haplotypes were comparatively infrequent ( $\sim 17\%$ ). **E**, Pairwise LD ( $r^2$ ) in the DPGP3 modelled as a declining exponential function of chromosomal distance between SNPs. Fitted LD curves are presented for three types of SNP pair: (i) pairs of antagonistic (antag.) SNPs (blue line), (ii) pairs of non-antagonistic (control) SNPs (dashed black line), (iii) pairs consisting of one antagonistic SNP and one non-antagonistic SNP (full black line). Antagonistic/antagonistic SNP pairs displayed significantly elevated  $r^2$  values relative to control/control (Wilcoxon test,  $P < 0.001$ ) and antagonistic/control (Wilcoxon test,  $P < 0.001$ ) pairs.

**A****B**

FBgn0000659	<i>fork head</i>
FBgn0005561	<i>shaven</i>
FBgn0000611	<i>extradenticle</i>
FBgn0033782	<i>sugarbabe</i>
FBgn0033749	<i>achintya</i>
FBgn0013469	<i>klumpfuss</i>
FBgn0033748	<i>vismay</i>
FBgn0040918	<i>schlank</i>
FBgn0004510	<i>Ets at 97D</i>
FBgn0003300	<i>runt</i>

**C**

FBgn0037207	<i>Mesoderm-expressed 2</i>
FBgn0029822	<i>CG12236</i>
FBgn0005638	<i>slow border cells</i>
FBgn0003053	<i>pebbled</i>
FBgn0002985	<i>odd skipped</i>
FBgn0004198	<i>cut</i>
FBgn0000567	<i>Ecdysone-induced protein 74EF</i>
FBgn0004510	<i>Ets at 97D</i>

**Figure 3. Functional properties of antagonistic loci.** **A**, Overlap of antagonistic genes identified in our study by haplotype sequencing (HS, blue) and antagonistically expressed genes identified in previous study of antagonistic gene expression<sup>15</sup> (GE, grey). The number of genes shared between the two studies was significantly greater than expected by chance (observed overlap=202, expected overlap=153,  $\chi^2=19.9$ ,  $P<0.001$ ). **B**, Top 10 genes associated with motifs enriched in upstream regions (5kb upstream of transcription start sites) of antagonistic genes. Upstream regions are denoted by the red bracket, antagonistic genes are shown in blue. **C**, Genes associated with motifs which were centrally enriched in short sequences flanking antagonistic SNPs (red nucleotide in the example sequence).

## Appendix B

# Rapid evolution of the inter-sexual genetic correlation for fitness in *Drosophila melanogaster*

This appendix contains a copy of a research article published in *Evolution* to which I made a significant contribution in terms of data analysis. Specifically, I performed a number of important bioinformatic filtering procedures to prepare the genome-wide SNP data for downstream analysis and interpretation. The work documents a case of resolution of sexual antagonism in a replicate of the LH<sub>M</sub> population. We further used an  $F_{st}$  outlier approach to find those loci associated with the resolution event.



# Rapid evolution of the intersexual genetic correlation for fitness in *Drosophila melanogaster*

Julie M. Collet,<sup>1,2,\*</sup> Sara Fuentes,<sup>1,\*</sup> Jack Hesketh,<sup>1</sup> Mark S. Hill,<sup>1</sup> Paolo Innocenti,<sup>3</sup> Edward H. Morrow,<sup>3,4</sup> Kevin Fowler,<sup>1</sup> and Max Reuter<sup>1,5</sup>

<sup>1</sup>Research Department of Genetics, Evolution and Environment, University College London, London, United Kingdom

<sup>2</sup>Current Address: School of Biological Sciences, University of Queensland, St. Lucia, QLD, Australia

<sup>3</sup>Department of Animal Ecology, Uppsala University, Uppsala, Sweden

<sup>4</sup>Current Address: School of Life Sciences, University of Sussex, Brighton, United Kingdom

<sup>5</sup>E-mail: m.reuter@ucl.ac.uk

Received November 23, 2014

Accepted February 17, 2016

Sexual antagonism (SA) arises when male and female phenotypes are under opposing selection, yet genetically correlated. Until resolved, antagonism limits evolution toward optimal sex-specific phenotypes. Despite its importance for sex-specific adaptation and existing theory, the dynamics of SA resolution are not well understood empirically. Here, we present data from *Drosophila melanogaster*, compatible with a resolution of SA. We compared two independent replicates of the “LH<sub>M</sub>” population in which SA had previously been described. Both had been maintained under identical, controlled conditions, and separated for around 200 generations. Although heritabilities of male and female fitness were similar, the intersexual genetic correlation differed significantly, being negative in one replicate (indicating SA) but close to zero in the other. Using population sequencing, we show that phenotypic differences were associated with population divergence in allele frequencies at nonrandom loci across the genome. Large frequency changes were more prevalent in the population without SA and were enriched at loci mapping to genes previously shown to have sexually antagonistic relationships between expression and fitness. Our data suggest that rapid evolution toward SA resolution has occurred in one of the populations and open avenues toward studying the genetics of SA and its resolution.

**KEY WORDS:** Adaptation, evolutionary genomics, fitness, population genetics, quantitative genetics, sexual conflict.

Due to their different reproductive roles, male and female adults are often selected for different optimal phenotypes. However, the response to this divergent selection is limited by the fact that the sexes share a large part of their genome and, thus, new mutations frequently affect the phenotype of males and females in a similar way. The combination of genetically correlated male and female phenotypes and divergent selection on the sexes sets the scene for intralocus sexual conflict or sexual antagonism (SA), where some alleles increase the fitness in one sex at the expense of the fitness in the other sex (Rice 1984; Bonduriansky and Chenoweth 2009;

Van Doorn 2009; Connallon and Clark 2014). Sexually antagonistic genetic variation has been shown to segregate in natural and laboratory populations of a wide range of organisms, including insects (Chippindale et al. 2001; Fedorka and Mousseau 2004; Lewis et al. 2011; Berg and Maklakov 2012), vertebrates (Brommer et al. 2007; Foerster et al. 2007; Mainguy et al. 2009; Mokkonen et al. 2011), and plants (Kohorn 1994; Scotti and Delph 2006; Delph et al. 2011). This growing body of evidence demonstrates that the common genetic basis of male and female phenotypes limits the adaptive evolution of sex-specific traits. The adaptive trade-offs inherent in sexually antagonistic allelic variation prevent both sexes from attaining their sex-specific optima

\*These authors contributed equally to this work.

and generate balancing selection that can maintain genetic variation at antagonistic loci. For this reason, sexual antagonism is also a powerful agent for the maintenance of genetic variation for fitness (Kidwell et al. 1977).

Despite being recognized as an important evolutionary force, the study of SA has so far focused mostly on characterizing antagonism as snapshots of particular populations at particular time-points and relatively little is known about its long-term dynamics (Stewart et al. 2010; Dean et al. 2012; Pennell and Morrow 2013). More specifically, it is currently unclear to what degree the intensity of antagonism changes over time, and over what timescale such changes occur. Similarly, there is scant information on whether individual antagonistic loci remain polymorphic over long periods of time and, if not, what mechanisms are involved in the fixation of one or the other allele. Answering these questions is vital for our understanding of ongoing conflicts over adaptation between the sexes, and of the evolution of sexual dimorphism.

Changes in the extent of SA can occur in response to variation in a population's environment as well as in its genetic composition. Experimental work in fruit flies has shown that the extent of SA varies between environmental conditions due to genotype-by-environment interactions (Delcourt et al. 2009; Punzalan et al. 2014). Large shifts in the environment might also eliminate antagonism (Long et al. 2012; Connallon and Clark 2014; Punzalan et al. 2014). This occurs if the change in conditions is large enough for the new selective optima of two sexes to both fall above (or below) their current trait values. This would then put both sexes under concordant directional selection and result in a positive genetic correlation between male and female fitness across genotypes.

The extent of SA can also vary in response to changes in the genetic composition of a population through mutation, drift, and selection. Mutations can increase the degree of antagonism if it generates similar phenotypic effects in the two sexes and hence increases their genetic correlation for traits under opposing selection (Connallon and Clark 2014). Genetic drift, in contrast, will result in a loss of genetic polymorphism at antagonistic loci, and hence can reduce the degree of SA observable within populations (Connallon and Clark 2012; Mullon et al. 2012; Hesketh et al. 2013). The rate at which this loss occurs depends on the effective population size at antagonistic loci, and thus will be faster in small populations, populations with large reproductive skew, and at loci under increased drift due to effects of chromosome dose (such as X or Z sex chromosomes) or selective interference between loci (Vicoso and Charlesworth 2009; Connallon and Clark 2012; Mullon et al. 2012).

Finally, and most importantly from an evolutionary point of view, the intensity of SA can be reduced through adaptive

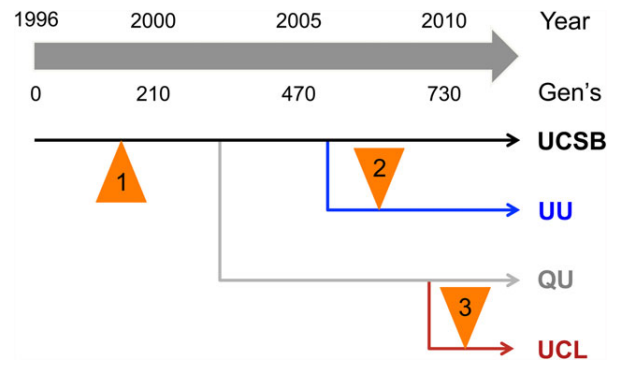


**Figure 1.** Schematic history of LH<sub>M</sub> populations. The relationship between the LH<sub>M</sub> populations used here, and the ancestral populations from which they were derived. The timeline is represented in calendar years and generations (approximate). For more details, refer to the Methods section of the main text. Orange triangles denote quantitative genetic studies of sex-specific fitness, 1: Chippindale et al. (2001), 2: Innocenti and Morrow (2010), 3: this study.

evolution. The trade-off between male and female fitness that underlies antagonism will create a selection pressure for mechanisms that diminish the deleterious fitness effects of the allele whenever it resides in the disfavored sex. These mechanisms are not well characterized empirically but could include sex-specific modifier loci (Rice 1984), sex-specific dominance (Kidwell et al. 1977; Barson et al. 2015), gene duplication followed by the evolution of sex-specific gene expression and adaptation in the two paralogs (Connallon and Clark 2011; Parsch and Ellegren 2013), genetic imprinting (Iwasa and Pomiankowski 1999, 2001; Day and Bonduriansky 2004) or sex-specific splicing (Pennell and Morrow 2013). Such adaptations will result in the long-term resolution of antagonism and allow both sexes to approach their phenotypic optima, thereby increasing the degree of sexual dimorphism (Lande 1980; Ellegren and Parsch 2007; Bonduriansky and Chenoweth 2009; Parsch and Ellegren 2013).

Understanding how antagonism evolves requires repeated measurements of SA at several time points. This can be achieved by monitoring SA in a single population through time or, alternatively, by measuring the extent of SA in different populations derived from a common ancestral population. Here, we present the results of such a comparative study investigating SA in two recently diverged replicate populations of the laboratory-adapted *D. melanogaster* stock LH<sub>M</sub>. Both replicates were derived from the original LH<sub>M</sub> population maintained by William Rice at the University of California, Santa Barbara, in which sexual antagonism had previously been documented (Chippindale et al. 2001). At the time of our analysis, they had been separated for about 200 generations but maintained according to the same strictly imposed rearing regime (see Methods, Fig. 1). Combining existing

data on the genetic architecture of male and female fitness in one population (LH<sub>M</sub>-UU, Innocenti and Morrow 2010) with newly collected data on the other (LH<sub>M</sub>-UCL), we show that the intersexual genetic correlation for fitness has diverged significantly between the two populations since they have been separated. While one population shows a negative genetic correlation between male and female fitness, indicative of antagonism, male and female fitness are not significantly correlated in the other, despite similar levels of heritable variation for fitness in the two sexes of both populations. Using a population genomic approach to compare allele frequencies at genome-wide SNP loci, we identify islands of significant differentiation between the populations, both on the X chromosome and the autosomes. We show that patterns of differentiation are biased toward frequency change in the population with reduced SA and enriched in genes with sexually antagonistic expression patterns. We argue that these results are unlikely to be due to environmental effects and compatible with the alleviation or resolution of sexual antagonism in one of the study populations. Given the increasing recognition of SA as a significant evolutionary force, our findings provide insights into the long-term evolutionary dynamics of SA and indicate future ways to elucidate the mechanistic basis of antagonism.

## Materials and Methods

### STUDY POPULATIONS

This study uses two replicate populations derived from the outbred laboratory stock LH<sub>M</sub> (here LH<sub>M</sub>-UCSB), maintained by W. Rice at the University of California, Santa Barbara (Fig. 1). LH<sub>M</sub>-UCL was established from a duplicate of LH<sub>M</sub>-UCSB that was taken to Queen's University by A. Chippindale in February 2002 and then transferred to the Reuter group in May 2009. Independently, a replicate of LH<sub>M</sub>-UCSB was taken to the Morrow group, University of Uppsala, in December 2005 to establish the other population, LH<sub>M</sub>-UU.

Starting with the establishment of LH<sub>M</sub>-UCSB in 1996, all LH<sub>M</sub> populations have been continuously maintained at a constant adult population size of 1792 individuals (896 males and 896 females) and under the same strictly regimented 14-day rearing regime (described in Rice et al. 2005). Therefore, neither LH<sub>M</sub>-UCL nor LH<sub>M</sub>-UU had experienced population bottlenecks or more than subtle environmental shifts. The rigorous two-week cycle further allowed us to estimate the number of generations of separation between the populations, dating back to the split between LH<sub>M</sub>-QU and in February 2002 (Fig. 1). At the time of sampling genotypes for fitness measurements in October 2007, LH<sub>M</sub>-UU had undergone approximately 145 generations from that branching point. In LH<sub>M</sub>-UCL, genotypes were sampled in June 2010, approximately 215 generations since the original split.

### HEMICLONAL ANALYSIS OF MALE AND FEMALE FITNESS

We used hemiclonal analysis to measure the effects of haploid genomes on male and female fitness (see Abbott and Morrow 2011 for a review of the approach). Hemiclonal individuals share a common copy of chromosomes X, 2, and 3, which amount to 99.5% of an identical haplotype (all genes except for the 0.5% of the genome located on the “dot” fourth chromosome). The quantitative genetic analysis captures additive genetic effects of the hemiclonal X, 2, and 3 chromosomes (as well as additive effects of epistatic interactions between alleles within the hemiclonal haplotype) but averages the effects of epistasis or dominance between the hemiclonal haplotype and the genetic background (Rice et al. 2005).

The quantitative genetic analysis of fitness used here was closely modeled on previous studies (Chippindale et al. 2001; Pischedda and Chippindale 2006; Innocenti and Morrow 2010; see Supplementary Material and the previously cited studies for details). To measure fitness in hemiclones, crosses were performed to generate males and females that carry an identical hemiclonal genome complemented with random genetic material from the corresponding source population. The fitness of these flies was then measured under conditions that closely mimic the LH<sub>M</sub> rearing regime and in competition with a standard competitor stock. The competitors provide a point of reference from which to calculate the relative fitness of different experimental genotypes. Their exact identity and genetic composition is not important for the results generated, as long as their fitness is similar to those of the experimental flies. The competitor flies used here carried a homozygous *brown* (*bw*) mutation in a variable, outbred LH<sub>M</sub> background, ensuring competitiveness while allowing us to assign paternity to experimental and competitor males. The competitor stock was maintained following exactly the same regime as the wild-type LH<sub>M</sub> population.

#### *Fitness measurements for the LH<sub>M</sub>-UCL population*

LH<sub>M</sub>-UCL hemiclonal lines were established in June 2010 and their fitness was measured between July 2010 and September 2011. For all lines, fitness was assayed three times in each sex in blocks that included one replicate of each hemiclonal line and alternately assayed male and female fitness. Complete fitness data were obtained for 113 lines. In order to assess potential genotype-by-laboratory effects, we also assessed the fitness of nine of the 10 most sexually antagonistic lines created in the LH<sub>M</sub>-UU population (Fig. 1 in Innocenti and Morrow 2010; see also section “Comparing fitness measures across laboratories” below and Fig. 2 and Fig. S1).

Fitness assays for LH<sub>M</sub>-UCL were conducted in groups of 60 flies per vial, including 10 focal flies, 20 standard *bw* competitors of the same sex and 30 standard *bw* flies of the opposite sex.

For male assays, the flies were allowed to interact for 66 hours (days 11–14, interaction and oviposition phases of the 14-day rearing cycle) and fitness was measured as the proportion of offspring produced by the females of an assay vial that were sired by the focal hemiclinal males. For female assays, flies were allowed to interact for the 48 hours of the competition phase of the rearing regime (days 11 and 12 of the 14-day cycle) and fitness was measured as the average number of eggs laid by the focal hemiclinal females over the following 19.5 hours (the oviposition phase of the rearing regime). The average fecundity of *bw* competitors was also measured and included in standardized fitness measures (see section “Transformation of fitness data”).

*Fitness measurements for the LH<sub>M</sub>-UU population*

The dataset for the LH<sub>M</sub>-UU population had been compiled as part of Innocenti and Morrow (2010) and comprised fitness measures obtained from 100 hemiclones extracted from LH<sub>M</sub>-UU in October 2007. Fitness data had been obtained in a similar manner to that described above for the UCL population. Small differences included that fitness trials were performed on 30 flies per competition vial (five target individuals in competition with 10 *bw* flies) and that flies in the male assay were allowed to interact for 48 hours (instead of 48 + 18) before females were isolated (more details in Innocenti and Morrow 2010). Six male assays and four female assays were performed in the LH<sub>M</sub>-UU population, thus testing fitness of a total of 30 individual males and 20 individual females per hemiclone (compared to 30 of each in the LH<sub>M</sub>-UCL dataset).

**STATISTICAL ANALYSIS OF FITNESS**

*Transformation of fitness data*

Before analysis, each set of fitnesses was standardized to remove block and vial effects. Thus, we defined fitness as the residuals of a linear model that decomposed raw individual fitness scores into a fixed effect of experimental block and random residual error (which includes the genotypic effect on fitness). For female fitness measures obtained for LH<sub>M</sub>-UCL, we further included a fixed effect describing the productivity of individual competition vials, as measured by the average number of offspring produced by *bw* competitor females. The residuals of these models were Z-transformed separately for each sex and population in order to obtain metrics of fitness that were comparable across sexes and populations.

*Comparing fitness measures across laboratories*

We used nine hemiclones from the LH<sub>M</sub>-UU sample to verify that fitness across populations was measured in a repeatable and comparable way. These hemiclones constitute the extremes of the fitness distribution of the LH<sub>M</sub>-UU sample (four with extremely female-beneficial/male detrimental and five with extremely male-

beneficial/female-detrimental effects) and had been maintained in the Uppsala laboratory. Complementing their fitness measures originally obtained in Uppsala, the fitness of these hemiclones was assayed again at UCL alongside those of the LH<sub>M</sub>-UCL sample, using exactly the same experimental protocol as that used for all other UCL hemiclones. To compare the fitness scores across laboratories, we performed correlation analyses, separately for each sex, between the standardized fitness scores obtained in the original analysis by Innocenti and Morrow (2010) and those obtained in the experiments at UCL. In addition, we applied analyses of variance, again separately for each sex, to the standardized fitness data from both laboratories, modeling fitness as a function of hemiclone (G), laboratory (E), and their interaction (GxE).

*Estimation and comparison of genetic variance components*

We used mixed models to estimate the contribution of additive genetic effects of hemiclones to the variation in male and female fitness, and the covariance between these genetic effects on fitness in males and females. Prior to analysis, we removed one outlier hemiclone from the UCL dataset that had a very low male and female fitness (Fig. 2), compatible with the effects of a strongly deleterious mutation affecting both males and females. Removing this outlier was conservative because, if included, it artificially increased the estimates of heritabilities and the intersexual genetic correlation in the UCL population.

We used WOMBAT (Meyer 2007) to fit the following multivariate animal model:

$$Y = Zu_Y + e_Y, \tag{1}$$

where **Y** is the vector of standardized fitness scores (hemiclones, sexes, and populations concatenated), **Z** is the incidence matrix defining the population-specific combination of sex and genotype for each fitness value, **u<sub>Y</sub>** is the vector of sex- and population-specific additive genetic effects for fitness and **e<sub>Y</sub>** is the vector of residual effects (Meyer 1991; Lynch and Walsh 1998).

We estimated a cross-population genetic (co)variance matrix

$$G = \begin{pmatrix} G_{mf_{UCL}} & 0 \\ 0 & G_{mf_{UU}} \end{pmatrix}.$$

In this matrix, **G<sub>mf<sub>UCL</sub></sub>** and **G<sub>mf<sub>UU</sub></sub>** are the population-specific additive genetic variance-covariance matrices,

$$G_{mf} = \begin{pmatrix} \sigma_{a,m}^2 & cov_{mf} \\ cov_{mf} & \sigma_{a,f}^2 \end{pmatrix},$$

where  $\sigma_{a,m}^2$  and  $\sigma_{a,f}^2$  are the additive genetic variances for fitness in males and females and  $cov_{mf}$  is the intersexual additive genetic covariance. Due to the standardization of our fitness data to a mean fitness of 0 and a standard deviation in fitness of 1 within each

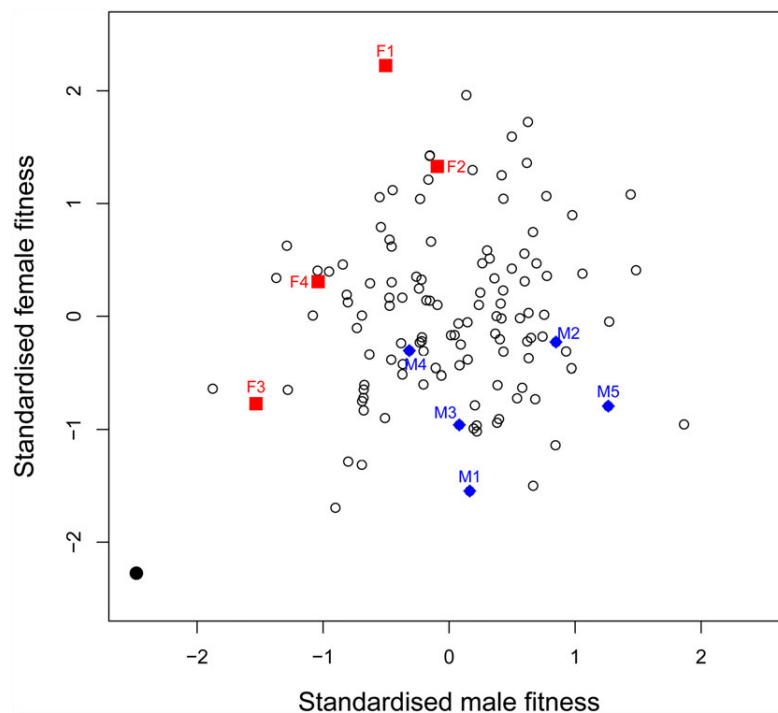


**Figure 2.** Male and female adult fitness across genotypes in the LHM-UCL population. Average male and female fitness across 113 hemiclones randomly extracted from LH<sub>M</sub>-UCL (open circles). One line (filled black circle) showed extremely low fitness in both sexes and was removed from further analyses. Fitness measures obtained at UCL for a set of hemiclones from LH<sub>M</sub>-UU previously assayed as part of Innocenti and Morrow (2010) are also shown. The blue diamonds and red squares show the UCL fitness estimates of the hemiclones from this set that were classed as male beneficial/female detrimental and female beneficial/male detrimental fitness lines, respectively, in that previous study. Labels identify individual hemiclones for comparison with their fitness values in the previous study, shown in Fig. S1.

sex and population, heritabilities are directly given by additive genetic variances,  $h_m^2 = \sigma_{a,m}^2$  and  $h_f^2 = \sigma_{a,f}^2$ . The intersexual genetic correlation for fitness can be calculated from the elements of the genetic variance-covariance matrix as  $r_{mf} = \frac{cov_{mf}}{\sqrt{\sigma_{a,m}^2} \sqrt{\sigma_{a,f}^2}}$ .

Estimation of genetic effects in the animal model relies on the numerator relationship matrix *A* that describes shared additive genetic effects between pairs of individuals. When defining this matrix, we considered hemiclones males and females as full-sibs ( $A_{ij} = 1/2$  for individuals *i* and *j* that are part of the same hemiclone line) and all other pairs as unrelated ( $A_{ij} = 0$  for pairs from different hemiclone lines). The model was fitted using Restricted Maximum Likelihood (REML) and parameters and their approximate sampling errors (sensu Meyer and Houle 2013; Houle and Meyer 2015) were estimated.

The significance of parameter estimates and their differences between populations were tested using Log-likelihood Ratio Tests (LRTs) based on the  $X^2$  distribution. These compared the full model (eq. 1) in which all parameters were freely estimated to simpler nested models in which specific parameters had been fixed to appropriate values (function FIXVAR in WOMBAT). Specifically, we tested for within-population differences between

the heritabilities  $h_m^2$  and  $h_f^2$  of fitness by comparing the full model to a model where genetic variances  $\sigma_{a,m}^2$  and  $\sigma_{a,f}^2$  were fixed to the average of their values estimated in the full model. To test whether the genetic covariance between male and female fitness  $cov_{mf}$  within a population was significantly different from 0, we compared the full model to a model where the covariance term for that population was fixed to 0. Similarly, to test for between-population differences in either the male or female fitness heritability or the covariance between male and female fitness, we compared the full model to models in which the values of these parameters in each population were fixed to their average between the UU and UCL estimates obtained in the full model.

**DNA extraction and sequencing**

We sampled 165 female adult flies from each of the populations in March 2012, about 260 generations after the separation of the two populations and about 46 and 115 generations after hemiclone genomes had been sampled from LH<sub>M</sub>-UCL and LH<sub>M</sub>-UU, respectively. We extracted total genomic DNA from homogenized flies pooled by population using DNeasyBlood and Tissue Kit (Qiagen) and purified it using Agencourt AMPure XP

beads (Beckman Coulter). One paired-end Illumina library (insert size <500 bp) was made from each pool using the Nextera DNA Sample Preparation Kit (Illumina). Libraries were sequenced on an Illumina HiSeq2000 machine at the Centre for Genomic Research, University of Liverpool. Sequencing reads were extracted using CASAVA (version 1.82). Paired reads were trimmed using Sickle (version 1.2, default settings) and deduplicated using Picard (version 1.77, <http://picard.sourceforge.net>) before being aligned to the *D. melanogaster* reference genome (BDGP5.25.60) using Bowtie2 (version 2.0.0-beta7, option -X 500). We removed regions flanking indels ( $\pm 5$ bp) with Popoolation (version 1.2.2, Kofler et al. 2011a) and used RepeatMasker (Smit et al. 2006, version 4.0.5 with option species = drosophila and flag no\_is) to mask interspersed repeats and low complexity regions. Finally, we applied a minimum read depth filter of 100 to ensure adequate precision of estimated allele frequencies, and a maximum read depth filter of 290 (about twice the average read depth of our sequencing runs, see Table S2), to avoid false-positive SNPs due to duplicated genomic regions.

### SNP detection and analysis

We called SNPs in each population separately using SNVer (Wei et al. 2011, version 0.4.1 release 4, function for pooled sequencing SNVerPool.jar with minimum read and mapping quality cutoffs  $m_q = 20$  and  $b_q = 20$ , haploid pool size  $n = 330$  and no filtering by minor allele frequency  $t = 0$ ). SNVer detects the significant presence of reads with the alternative allele (rather than polymorphism), so we reran the program on sites with high frequencies of the alternative allele, but using a reference genome sequence in which the corresponding positions were flipped to the alternative allele (i.e., testing for significant presence of the reference allele). We considered that a SNP was present if both polymorphism tests were significant. All  $P$ -values were corrected for false discovery rate ( $FDR < 0.05$ ) using the package  $q$ -value (<http://bioconductor.org>). For all SNPs identified in this way, allele frequencies were extracted from the SNVer output. Furthermore, we calculated  $F_{ST}$  as a measure of genetic differentiation between  $LH_M$ -UU and  $LH_M$ -UCL using PoPoolation2 (Kofler et al. 2011b).

In order to summarize the chromosomal distribution of candidate SNPs with significantly elevated  $F_{ST}$  (see Results), we calculated the median distance between all pairs of adjacent candidate SNPs, separately for the X chromosome and the autosomes. We tested for significant clustering of candidate SNP by randomly permuting “candidate” and “noncandidate” labels among SNP loci and recalculating the median distance among SNPs labeled “candidate.” Null distributions for the median distances between candidate SNPs were generated from 1000 such permutations (again, separately for X-linked, and autosomal markers). A  $P$ -value for significant clustering was calculated as the proportion

of median distances in the null distribution that was smaller or equal to the observed median distance.

### Functional characterization of selected SNPs

We used the Variant Effect Predictor tool from Ensembl (McLaren et al. 2010) to map all SNPs to annotated genes and infer the consequences of variants (such as synonymous or nonsynonymous coding sequence changes, splice variants, etc.). The tool uses extended gene regions that span 5 Kb up- and downstream of the gene coordinates. In line with this default setting, we considered genes with candidate SNPs in that range as candidate genes. Analyses ignoring up- and downstream variants in these extended regions provided qualitatively identical results.

To assess the overlap between candidate genes in our study and previously described genes with sexually antagonistic expression patterns, we matched the identifiers of candidate genes to the corresponding Affymetrix *Drosophila 2* probeset IDs. We then used the FlyAtlas data (Chintapalli et al. 2007) to consider only probesets that were expressed in adults, conservatively defined as those detected as “present” in at least one library of one FlyAtlas adult tissue sample. The list of adult-expressed probesets covered by our study was then matched to the list of genes with antagonistic expression from Innocenti and Morrow (2010, Table S1), retaining only those probesets in their study that were covered by our SNP data, and matches were back-translated into FlyBase gene identifiers.

We used Gene Ontology (GO) analysis implemented in DAVID (Huang et al. 2009a,b) to obtain insights into the functions of candidate genes. For enrichment analyses, we used all genes covered in our SNP dataset as the background set and applied a Benjamini–Hochberg correction for multiple testing to the  $P$ -values of individual tests. We further applied DAVID’s Functional Annotation Clustering (using the “high” stringency setting) to categorize enriched individual GO terms into groups of related annotations.

## Results

### HEMICLONAL FITNESS CAN BE MEASURED RELIABLY ACROSS LABORATORIES

A meaningful comparison between the genetic architecture of fitness across populations requires that the fitness of different genotypes be measured in a reliable and comparable way and in the absence of significant genotype-by-environment effects. Analyses of the fitness data from our nine reference hemiclones suggest that this is true here. First, we observed significant positive correlations between the sex-specific fitness measures obtained in the original experiments at the University of Uppsala and those obtained on the same hemiclones at UCL (females:  $r = 0.81$ ,  $t_7 = 3.67$ ,  $P = 0.008$ ; males:  $r = 0.73$ ,  $t_7 = 2.79$ ,  $P = 0.027$ , Fig. S2). Second, ANOVAs

performed on male and female fitness returned highly significant differences between hemiclones across laboratories, but no hemiclone-by-laboratory effects (females: hemiclone— $F_{8,45} = 11.42$ ,  $P < 0.0001$ , hemiclone-by-laboratory— $F_{8,45} = 1.19$ ,  $P = 0.33$ ; males: hemiclone— $F_{8,63} = 11.34$ ,  $P < 0.0001$ , hemiclone-by-laboratory— $F_{8,45} = 1.54$ ,  $P = 0.16$ ; laboratory term nonsignificant in both analyses, as expected for Z-transformed fitness data). Based on the (additive) Sums of Squares, these analyses also show that, in line with the nonsignificant effect, the total variance in the data attributable to hemiclone-by-laboratory interactions is low (females:  $SS_{\text{hemiclone-by-laboratory}}/SS_{\text{total}} = 0.065$ ; males:  $SS_{\text{hemiclone-by-laboratory}}/SS_{\text{total}} = 0.073$ ; see Table S1 for full ANOVA tables). These results indicate that the fitness variation between genotypes detected in our experiments is overwhelmingly due to genetic differences, rather than the interaction between genotypes and the specific assay and laboratory environments.

**THE INTERSEXUAL GENETIC CORRELATION FOR FITNESS DIFFERS BETWEEN POPULATIONS**

We evaluated whether the genetic architecture of fitness, and in particular the intersexual genetic correlation for fitness, differed between the two replicate LH<sub>M</sub> populations. Fitness heritabilities for LH<sub>M</sub>-UU were slightly higher than the estimates obtained in the earlier analysis of the UU dataset (Table 1 in Innocenti and Morrow 2010), in line with the fact that our approach accounted for the environmental effects of experimental assays. Our estimates confirmed that the heritability of male and female fitness differed in the LH<sub>M</sub>-UU population ( $X^2 = 12.2$ ,  $P = 0.0005$ , Table 1) while showing that LH<sub>M</sub>-UCL male and female heritabilities did not differ significantly ( $X^2 = 0.7$ ,  $P = 0.39$ ). Furthermore, male and female fitness heritabilities did not significantly differ across populations ( $X^2 = 2.6$ ,  $P = 0.11$  and  $X^2 = 0.4$ ,  $P = 0.52$ , respectively).

While both populations featured ample and comparable heritable fitness variance, they differed in their intersexual genetic correlation. The point estimate of  $r_{mfUU} = -0.41$  was significantly negative ( $X^2 = 4.5$ ,  $P = 0.03$ ) while the genetic correlation in LH<sub>M</sub>-UCL was positive ( $r_{mfUCL} = 0.21$ ) and not significantly dif-

ferent from 0 ( $X^2 = 1.2$ ,  $P = 0.27$ ). Further, the intersexual genetic correlations differed significantly between populations ( $X^2 = 5.1$ ,  $P = 0.02$ , Table 1, Fig. 2 and Fig. S1). This indicates that the sexual antagonism that was present in LH<sub>M</sub>-UU was absent in LH<sub>M</sub>-UCL.

**POPULATION GENOMICS REVEALED REGIONS OF SIGNIFICANT GENETIC DIVERGENCE BETWEEN THE POPULATIONS**

We performed genome-wide pooled sequencing of flies from LH<sub>M</sub>-UU and LH<sub>M</sub>-UCL in order to identify SNP loci with significant allele frequency differences between the populations (see Table S2 for general sequencing statistics). These loci would be candidates for regions potentially functionally related to the change in the genetics of fitness observed in the quantitative genetic analysis. Our sequencing approach covered the entire genome and for completeness we present results for all chromosomes, even though the contribution of the small 4th chromosome to fitness variation was not measured in our phenotypic assays.

Population sequencing identified more than 680,000 high-quality SNPs with significant allelic variation in at least one of the two populations. The density of SNP loci varied between chromosome arms ( $X^2_5 = 44997.1$ ,  $P < 0.0001$ ). Chromosome arms 2L, 2R, and 3L were enriched for SNP polymorphism, chromosome arm 3R had slightly fewer SNPs than expected, and chromosomes X and 4 were severely depleted for polymorphic sites (Table S3). The lower SNP densities on chromosomes X and 4 are expected based on the lower effective population sizes of these chromosomes, caused by the lower numerical population size of the X chromosome relative to the autosomes (Charlesworth et al. 1987; Mank et al. 2010) and selective interference along the virtually nonrecombining chromosome 4 (Jensen et al. 2002; Haddrill et al. 2007; Betancourt et al. 2009; Charlesworth et al. 2010).

Analysis of the SNP allele frequencies showed that LH<sub>M</sub>-UU was weakly, but significantly, more genetically diverse than LH<sub>M</sub>-UCL. This difference was reflected at two levels. First, the percentage of SNP loci that were variable in LH<sub>M</sub>-UU but fixed in LH<sub>M</sub>-UCL (12.3%; Table S3) was greater than the percentage that only segregated in LH<sub>M</sub>-UCL (8.8%; Proportion test:

**Table 1.** Heritabilities and genetic correlations for fitness in LH<sub>M</sub>-UU and LH<sub>M</sub>-UCL.

Population	Female $h^2$	Male $h^2$	$r_{mf}$
LH <sub>M</sub> -UU	0.71 (0.15)	0.19 (0.07)	-0.41 (0.18) <sup>1</sup>
LH <sub>M</sub> -UCL	0.58 (0.12)	0.41 (0.12)	0.21 (0.19) <sup>2</sup>
Difference between populations	$X^2_1 = 0.4$ , $P = 0.52$	$X^2_1 = 2.6$ , $P = 0.11$	$X^2_1 = 5.1$ , $P = 0.02$

The table provides estimates and, in parentheses, the approximate sampling error for the heritabilities of male and female fitness and the intersexual genetic correlation ( $r_{mf}$ ) for fitness in the two populations, as well as the results of likelihood ratio tests comparing estimates between populations (see Methods).

<sup>1</sup>Likelihood ratio test comparing the estimate to zero (see Methods):  $X^2_1 = 4.5$ ,  $P = 0.03$ .

<sup>2</sup>Likelihood ratio test comparing the estimate to zero (see Methods):  $X^2_1 = 1.2$ ,  $P = 0.27$ .

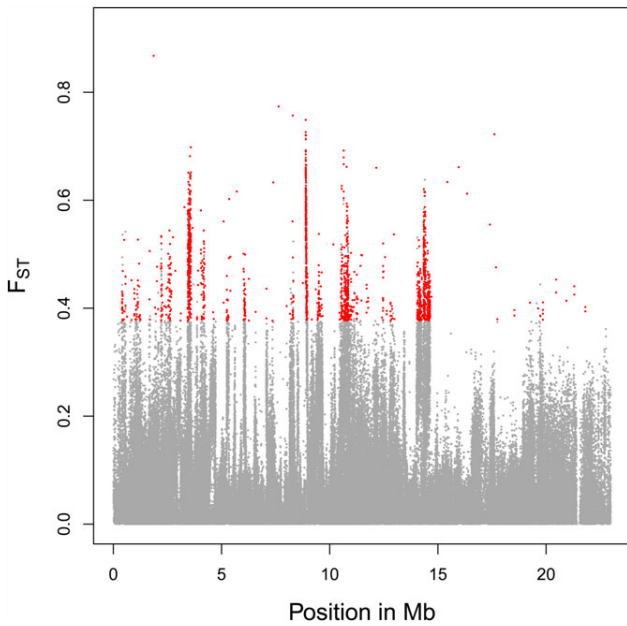


**Figure 3.**  $F_{ST}$  variation along SNPs in chromosome arm 2L. Gray dots indicate noncandidate loci, red dots candidate loci.

$X_1^2 = 4575.2$ ,  $P < 0.0001$ ). Second, expected heterozygosity ( $H_e$ ) was slightly higher in  $LH_M$ -UU than  $LH_M$ -UCL (Fig. S3), both for autosomal SNPs ( $H_{e\text{-auto,UU}} = 0.295 \pm 0.165$  mean  $\pm$  SD;  $H_{e\text{-auto,UCL}} = 0.278 \pm 0.173$ ; paired  $t$ -test:  $t_{61,3527} = 73.378$ ,  $P < 0.0001$ ) and for X-linked SNPs ( $H_{e\text{-X,UU}} = 0.284 \pm 0.166$ ;  $H_{e\text{-X,UCL}} = 0.264 \pm 0.176$ ; paired  $t$ -test:  $t_{69,303} = 26.350$ ,  $P < 0.0001$ ; note that these results are robust to corrections for possible nonindependence between sites, e.g., including only every 10th, 20th, or 50th SNP). These patterns also show again that X-linked variation was smaller than autosomal variation in both populations.

We estimated the genetic differentiation between the populations at each SNP locus by calculating the fixation index  $F_{ST}$  (Fig. 3 for chromosome arm 2L as an example, Fig. S4 for all chromosomes). The average level of differentiation across autosomal SNP loci was  $F_{ST} = 0.054 \pm 0.073$ , and that on the X chromosome was  $F_{ST} = 0.071 \pm 0.099$ . In order to identify SNP loci where genetic differentiation significantly exceeded the level expected from random genetic drift, we used the 105,851 SNPs causing synonymous variation (amino acid and stop codons). Synonymous allelic variation can be considered nearly neutral and used to establish an empirical null distribution of neutral background differentiation, against which sites under potential selection can be compared (e.g., McDonald and Kreitman 1991; Smith and Eyre-Walker 2002; Andolfatto 2005; Haddrill et al. 2010). We defined cut-off values for selective divergence between populations as  $F_{ST}$  values that exceeded the 99th quantile of the  $F_{ST}$  distribution across synonymous sites (Fig. S3). We did so sep-

**Table 2.** Distribution of candidate and noncandidate SNP loci across chromosomes.

Chr	Candidate		Noncandidate	
	Count	Percentage	Count	Percentage
X	717	16.00 <sup>+</sup>	68,587	10.11
2L	889	19.85 <sup>-</sup>	155,525	22.93
2R	634	14.16 <sup>-</sup>	144,559	21.31
3L	493	11.01 <sup>-</sup>	155,422	22.91
3R	1746	38.98 <sup>+</sup>	153,456	22.62
4	0	0	804	0.12
Autosomes	3762	84.00 <sup>-</sup>	609,766	89.89
Total	4479	100	678,353	100

Percentages of candidate SNPs on each chromosome were tested for significant over- or underrepresentation relative to noncandidate SNPs using one-sample Z-tests and  $P$ -values were Bonferroni-corrected for multiple testing. Fractions in *italics* are significantly over- (+) or underrepresented (-).

arately for the X chromosome and the autosomes, in order to accommodate the different intensities of genetic drift acting on these two genomic compartments. The cut-offs used were  $F_{ST} > 0.371$  for autosomes and  $F_{ST} > 0.453$  for the X chromosome. Applying these cut-offs to our entire SNP dataset (excluding the synonymous SNPs, which were used to define the cut-offs), 3762 autosomal and 717 X-linked SNP loci showed above-threshold levels of population differentiation (Fig. S5). The average absolute frequency difference between the two populations at these loci was  $0.666 \pm 0.091$  (median absolute difference 0.658). Independent verification using allele counts confirmed our  $F_{ST}$ -based definition of population differentiation, as allele frequencies differed significantly between the populations at all candidate loci, even when using a stringent Bonferroni correction (Fisher's Exact test on counts of reference and alternative alleles,  $P < 0.05/4479 = 1.12 \times 10^{-5}$  for all loci).

The distribution of the candidate SNPs was nonrandom across the chromosome arms and differed from that of noncandidate SNPs ( $X_3^2 = 1082.1$ ,  $P < 0.0001$ ). Specifically, candidate SNPs were overrepresented on the X chromosome and chromosome arm 3R and underrepresented elsewhere (Table 2). In addition to showing uneven distributions between chromosomes, candidate loci showed a clustered distribution along the chromosome arms and a large proportion of them fell within 100 bp from each other (Fig. S6). A permutation test (see Methods) confirmed statistically significant clustering and showed that the observed distance between candidate SNPs was much smaller than expected by chance (autosomes: observed median distance = 770 bp, range of median distances among 1000 sets of permuted loci = [12,998 bp–14,978 bp],  $P < 0.001$ ; X chromosome: observed median distance = 1292 bp, range of permuted median distances = [15,592 bp–20,567 bp],  $P < 0.001$ ).

The local clustering of candidate SNPs could indicate population differentiation in the frequency of chromosomal inversions, leading to parallel frequency changes of large numbers of alleles linked within the inverted part of the chromosome. Such effects have been observed in frequency clines among populations (Fabian et al. 2012) and frequency changes in response to laboratory selection (Kapun et al. 2014). In order to assess this possibility, we inspected patterns of polymorphism for diagnostic SNP alleles linked to seven cosmopolitan *D. melanogaster* inversions identified by Kapun et al. (2014). All but a few of these marker positions were well covered with high-quality reads in both samples (Table S4), but the data indicate that none of the inversions segregate in our populations. Only two of the inversion markers showed significant polymorphism in our samples (Table S4) and in both these cases the marker allele is the reference allele, suggesting either homoplasy (where the site on the inversion has convergently mutated back to the ancestral state) or an error in the inference of the marker allele.

#### CANDIDATE SNPS SHOW BIASED PATTERNS OF ALLELE FREQUENCY CHANGE

Population differentiation and elevated  $F_{ST}$  at candidate sites could arise due to allele frequency change in  $LH_M$ -UCL, in  $LH_M$ -UU or in both. In order to distinguish between these possibilities and infer the directionality of evolution at candidate SNPs, we used genotype data from the *Drosophila* Genetics Reference Panel (DGRP, Mackay et al. 2012; Huang et al. 2014). The DGRP constitutes an independent sample of genetic diversity derived, like the  $LH_M$ , from a wild North American population of *D. melanogaster*. In the absence of data on the ancestral  $LH_M$  population, it therefore provides a suitable external reference point to polarize frequency changes between  $LH_M$ -UCL and  $LH_M$ -UU. Focusing on the 636,924 SNPs that were shared and biallelic across the DGRP and  $LH_M$  samples, we found that levels of genetic differentiation between each of the  $LH_M$  populations and the DGRP differed markedly between noncandidate and candidate SNPs. For noncandidate SNPs,  $F_{ST}$  values between  $LH_M$ -UCL and the DGRP were of similar magnitude—although marginally (and significantly) higher—than those between  $LH_M$ -UU and the DGRP (autosomes:  $F_{ST, UCL-DGRP} = 0.099 \pm 0.127$  mean  $\pm$  SD,  $F_{ST, UU-DGRP} = 0.091 \pm 0.118$ , mean pairwise difference = 0.0073, CI = [0.0070, 0.0076],  $t_{568070} = 47.739$ ,  $P < 0.0001$ ; X chromosome:  $F_{ST, UCL-DGRP} = 0.105 \pm 0.126$ ,  $F_{ST, UU-DGRP} = 0.092 \pm 0.114$ , mean pairwise difference = 0.0128, CI = [0.0118, 0.0138],  $t_{64464} = 24.904$ ,  $P < 0.0001$ ). For candidate SNPs, in contrast, we observed a large excess of differentiation between  $LH_M$ -UCL and the DGRP, compared to that between  $LH_M$ -UU and the DGRP (autosomes:  $F_{ST, UCL-DGRP} = 0.270 \pm 0.224$ ,  $F_{ST, UU-DGRP} = 0.145 \pm 0.167$ , mean pairwise difference = 0.124, CI = [0.113, 0.136],  $t_{3634} = 21.348$ ,  $P < 0.0001$ ; X chromosome:  $F_{ST, UCL-DGRP} =$

$0.315 \pm 0.235$ ,  $F_{ST, UU-DGRP} = 0.142 \pm 0.154$ , mean pairwise difference = 0.173, CI = [0.146, 0.201],  $t_{707} = 12.548$ ,  $P < 0.0001$ ). Echoing these quantitative differences, a disproportionately large number of candidate loci showed greater  $F_{ST}$  between  $LH_M$ -UCL and the DGRP than between  $LH_M$ -UU and the DGRP (autosomes: 2327 of 3635 loci with  $F_{ST, UCL-DGRP} > F_{ST, UU-DGRP}$ ,  $X_1^2 = 202.660$ ,  $P < 0.0001$ ; X chromosome: 458 of 708 loci,  $X_1^2 = 34.168$ ,  $P < 0.0001$ ). These results show that differentiation between the two  $LH_M$  populations at candidate sites is disproportionately driven by allele frequency change in  $LH_M$ -UCL.

#### CANDIDATE SNPS HAVE NONRANDOM FUNCTIONS

To understand the functional relevance of the candidate SNPs, we used the Variant Effect Predictor tool to examine the genetic consequences of variants segregating at candidate and noncandidate sites. When compared to noncandidate SNPs, candidate SNPs were overrepresented among nonsynonymous coding polymorphisms (amino acid changes, loss and addition of translation start sites, stop codons; Table 3). In contrast, we observed an underrepresentation of candidate SNPs in intergenic regions (i.e., those further than 5 Kb away from any annotated gene). These nonrandom patterns of enrichment and depletion are indicative of a functional role for candidate polymorphisms.

Candidate SNPs mapped to a total of 1131 genes, 939 on the autosomes and 192 on the X chromosome. We performed GO term enrichment analyses to gain information on the biological processes in which these genes are involved and their molecular function. Term-by-term analyses revealed a strong association of candidate genes with biological processes related to growth, development, and differentiation (Table S5A). These trends were further highlighted in subsequent clustering of enriched GO terms, where eight out of the ten most enriched term groupings were related to development (Table S6). In terms of molecular function, we found significant enrichment for two terms, both related to transcription regulation (Table S5B; no clustering was performed due to the small number of significant terms).

To relate our results to previous analyses of sexual antagonism, we compared our list of candidate genes to genes previously shown to have sexually antagonistic expression patterns. Innocenti and Morrow (2010) used a combination of phenotypic fitness assays and whole-fly microarray expression analysis to identify genes that showed sex-differences in the relationship between expression level and fitness, mostly due to opposing associations of expression levels with male and female fitness (positive correlation between expression level and female fitness but negative correlation between expression level and male fitness, or vice versa). We observed a 30% excess of overlap between genes with candidate SNPs in our study and genes with such antagonistic expression patterns (147 overlapping genes to 112 expected,  $X_1^2 = 13.396$ ,  $P = 0.0003$ ). No excess overlap was seen between

**Table 3.** Comparison of genomic feature distributions between all SNPs, candidate SNPs, and noncandidate SNPs.

Functional category	All		Candidate		Noncandidate	
	Count	Percentage	Count	Percentage	Count	Percentage
UTR	42,706	6.25	312	6.97	42,394	7.41
Nonsynonymous	33,483	4.90	312	6.97 <sup>+</sup>	33,171	5.79
Synonymous	105,851	15.50	0	–	105,851	–
Splice site	6484	0.95	61	1.36	6423	1.12
Intron/noncoding exon	289,792	42.44	2286	51.04	287,506	50.22
Up-/downstream	135,364	19.82	1110	24.78	134,254	23.45
Intergenic	69,152	10.13	398	8.89 <sup>–</sup>	68,754	12.01

Proportional representations of functional categories were tested for significant over- or underrepresentation of candidate SNPs compared to noncandidate SNPs using one-sample Z-tests and *P*-values were Bonferroni-corrected for multiple testing. Categories in *italics* are significantly over- (+) or underrepresented (–). Synonymous polymorphisms were not considered while performing these tests, as they had been used to identify candidate SNPs and hence not tested here. For easier comparison, the synonymous variants were also excluded when calculating the percentages of candidate and noncandidate variants that fall into the different categories.

our candidates and Innocenti and Morrow's lists of genes showing expression levels that were only associated with male fitness ( $X_1^2 = 0.515$ ,  $P = 0.473$ ) or only with female fitness ( $X_1^2 = 1.821$ ,  $P = 0.177$ ). Thus, genes with antagonistic expression patterns were more likely to show large population differentiation in our study, but this association was not due to fitness-related genes being generally enriched among candidates in our study.

Finally, we investigated patterns of sex-biased gene expression among our candidate genes. Sex-biased expression is thought to be involved in the resolution of sexual antagonism. Accordingly, genes that show sex-biased expression should be less prone to antagonistic fitness effects and, inversely, genes with sexually antagonistic variation should have lower than average sex-biased expression. We compared our dataset to the Sebida database (Gnad and Parsch 2006) that classifies *D. melanogaster* genes as male-, female-, or unbiased, based on the integration of multiple expression datasets. Our candidate genes show an underrepresentation of sex-biased gene expression, relative to noncandidate genes. This is true when pooling male- and female-biased genes ( $X_1^2 = 22.241$ ,  $P < 0.0001$ ), and also when analyzing male- and female-biased genes separately (male-biased:  $X_1^2 = 6.397$ ,  $P = 0.0114$ ; female-biased:  $X_1^2 = 27.627$ ,  $P < 0.0001$ ). This suggests that candidate genes tend to be those where, if present, antagonism could be expected to be more pronounced, as it is not tempered by sex-biased expression.

## Discussion

Despite the well-documented prevalence of sexual antagonism in plant and animal populations (e.g., Kohorn 1994; Chippindale et al. 2001; Fedorka and Mousseau 2004; Scotti and Delph 2006; Brommer et al. 2007; Foerster et al. 2007; Delph et al. 2011; Lewis et al. 2011; Mokkonen et al. 2011; Berg and Maklakov 2012) we

know relatively little about its evolutionary dynamics (Cox and Calsbeek 2009; Stewart et al. 2010; Dean et al. 2012; Pennell and Morrow 2013). In this study, we document differences in intersexual genetic correlations of fitness ( $r_{MF}$ ) between two populations recently derived from the outbred laboratory stock LH<sub>M</sub> in which sexual antagonism had originally been documented. While we found a significantly negative genetic correlation between male and female fitness in LH<sub>M</sub>-UU, consistent with ongoing SA in this population,  $r_{MF}$  was not different from zero and antagonism absent in LH<sub>M</sub>-UCL. These differences in the genetic architecture of sex-specific fitness were associated with significant shifts in allele frequencies at SNPs across the genome. These frequency changes occurred more often than expected at loci linked to genes that had been previously and independently linked to SA and more strongly affected frequencies in LH<sub>M</sub>-UCL, the population with reduced SA. We argue that our data are suggestive of rapid evolution of  $r_{MF}$  and are, at the very least, compatible with recent partial resolution of SA in LH<sub>M</sub>-UCL.

An important first step to interpreting our data is to establish whether evolutionary change has in fact occurred between the two populations. While this is straightforward at the genetic level, where we directly demonstrate differences in allele frequencies between the populations, caution is required when interpreting the observed difference in the genetic fitness correlation  $r_{MF}$ . Gene-by-environment interactions are known to cause differences between estimates of genetic (co-)variances for male and female fitness obtained under different environmental conditions (Delcourt et al. 2009; Punzalan et al. 2014). Such effects could generate a spurious difference in  $r_{MF}$  here, because fitness measures for LH<sub>M</sub>-UU and LH<sub>M</sub>-UCL were obtained under conditions that—despite our efforts at standardization—cannot be assumed to have been completely identical. Importantly, however, our inclusion of a reference set of genotypes in experiments at both

Uppsala and UCL allowed us to rule out substantive genotype-by-laboratory effects. Comparison of fitness values between laboratories showed that the measures obtained at UCL correspond closely to those originally measured in Uppsala. Furthermore, the proportion of variation in male and female fitness that could be attributed to genotype-by-laboratory interactions was very small and not statistically significant. It therefore appears implausible that the observed differences in  $r_{MF}$  arose due to genotype-by-laboratory effects alone and can instead be assumed to reflect at least some evolutionary divergence in the genetic basis of fitness.

Several factors could have driven the evolutionary divergence between the populations. An important distinction is between neutral selective forces. Changes at the phenotypic ( $r_{MF}$ ) and allele frequency level can arise as a consequence of genetic drift during founding events or in populations of small effective size. Random fixation of antagonistic alleles can reduce the extent of SA or even render it undetectable. At the same time, however, such fixation events would result in a loss of heritable genetic variation in sex-specific fitness and a genetic homogenization at the sequence level. These hallmarks of genetic drift do not appear in LH<sub>M</sub>-UCL, where antagonism was absent. Although it is difficult to compare absolute levels of quantitative genetic variation between populations, heritable variation in male and female fitness was present in LH<sub>M</sub>-UCL and tended to be greater than in LH<sub>M</sub>-UU. Similarly, our molecular data are incompatible with the action of strong genetic drift in LH<sub>M</sub>-UCL. Although the average heterozygosity was slightly reduced in LH<sub>M</sub>-UCL compared to LH<sub>M</sub>-UU, both populations showed comparable levels of allelic variation. Most importantly, loci with particularly elevated frequency differences showed many aspects of nonrandomness in direction (divergence relative to the DGRP), position (clustering), and function (variant effects, association with antagonistic genes) that are incompatible with the action of random genetic drift. It therefore seems likely that the divergence between LH<sub>M</sub>-UU and LH<sub>M</sub>-UCL constitutes adaptive responses to selection pressures in one or both populations.

The most likely candidates for selection in these well-established laboratory populations are (i) differences in the micro-environment in which the populations were maintained, (ii) ongoing coevolutionary dynamics between the sexes (interlocus sexual conflict) occurring independently within each population, or (iii) differences in the response to selection to alleviate the gender load (Rice 1992) that is generated by the sex-specific deleterious effects of sexually antagonistic alleles segregating in the populations. Our results cannot unambiguously differentiate between these alternative adaptive scenarios but we can assess the plausibility of each selective force in the light of the data. Environmental adaptation appears the least plausible scenario. It is conceivable that different selective pressure in the two laboratories could drive genetic divergence and potentially shifts in  $r_{MF}$ , especially when

considering pathogens as part of the environment. Even though LH<sub>M</sub> stocks are superficially healthy, they are not maintained in sterile conditions and can be expected to undergo selection due to viral and/or bacterial pathogens. Interestingly, the evolution of immune resistance and disease tolerance shows sex-specific effects, where mutations altering resistance and tolerance can do so in opposing ways in males and females (Vincent and Sharp 2014). However, once again, divergent selection pressures deriving from any part of the environment in Uppsala and UCL would be expected to generate genotype-by-laboratory variation in fitness among our reference genotypes. In contrast, we found a positive correlation in their fitness across laboratories that implies that environmental selection pressures in the two laboratories were aligned, with the same genotypes (and hence phenotypes) having high (or low) fitness in both places. If environmental selection pressures occurred, their effect would have to be slight and unlikely to drive the population differentiation observed over the short timespans considered here.

Coevolutionary arms races between the sexes occur whenever males and females differ in their reproductive interests. The promiscuous mating system imposed by the LH<sub>M</sub> maintenance regime is expected to generate antagonistic interactions between males and females (“interlocus sexual conflict” or simply “sexual conflict,” Chapman et al. 2003; Arnqvist and Rowe 2005), often over mating rates (Pischedda and Rice 2012). The evolutionary arms race driven by sexual conflict can generate strong selection pressures, driving rapid divergence between populations (Rice and Holland 1997; Gavrillets 2000; Martin and Hosken 2003; Debelle et al. 2014). However, how this evolution would affect antagonistic variation is currently unclear. Potential links between male–female coevolution and sexual antagonism have been proposed (Pennell and Morrow 2013), but they await theoretical and empirical investigation. While we cannot rule out sexual conflict as a driver of evolution, certainly our data do not support that link. Many of the molecular phenotypes involved in the male contribution to the arms race (such as accessory gland proteins) are encoded by genes that show male-specific expression while our candidate SNPs are preferentially associated with genes that show unbiased expression in both sexes.

A more plausible scenario is that LH<sub>M</sub>-UCL adapted to selection generated by sexual antagonism. Sexually antagonistic variation can be stably maintained in populations under divergent selection on male and female traits (Gavrillets and Rice 2006), but any new variant that relieves the deleterious effect of antagonistic alleles in one sex while maintaining the benefit in the other is selectively favored (Rice 1984). The invasion of such variants will contribute to the resolution of antagonism and the evolution of further sexual dimorphism. Several aspects of our data are compatible with such change occurring in the LH<sub>M</sub>-UCL population. First, the evolutionary change that we observe at the

phenotypic and the genetic levels establish independent links to antagonism. This is obviously true for the phenotypes, where we directly assess SA. However, the population genomic analysis, which is unbiased with regard to the phenotypic measures, also invokes SA through the significant overlap of our candidates and genes previously shown to have antagonistic expression patterns (Innocenti and Morrow 2010). Second, the directionality of phenotypic and genetic evolution indicates adaptation in LH<sub>M</sub>-UCL, rather than symmetric divergence between the populations. The presence of SA and a negative  $r_{MF}$  is the ancestral state in the LH<sub>M</sub> population, demonstrated in the original stock population at UCSB (Chippindale et al. 2001) and then confirmed in LH<sub>M</sub>-UU (Innocenti and Morrow 2010). The absence of antagonism ( $r_{MF} \approx 0$ ) thus is a derived state toward which LH<sub>M</sub>-UCL evolved. The same directionality is reflected at the genomic level. Our analysis of allele frequencies across the two LH<sub>M</sub> populations and the DGRP show that frequency change at candidate loci consists disproportionately of LH<sub>M</sub>-UCL frequencies shifting away from those in LH<sub>M</sub>-UU. Phenotypic and genetic data thus paint mirror images of rapid change occurring mostly in LH<sub>M</sub>-UCL.

Our evidence in favor of a possible recent alleviation of antagonism in LH<sub>M</sub>-UCL contrasts with the repeated detections of antagonistic variation in LH<sub>M</sub> (Chippindale et al. 2001; Innocenti and Morrow 2010). This suggests that the recent rapid evolution of SA occurred following a long period of stasis, during which antagonistic variation was stably maintained for many generations. It implies that the alleviation of SA was caused by a key innovation decoupling male and female phenotypes, most likely relying on a rare mutational event, such as several epistatic variants arising more or less simultaneously. It seems implausible that the many loci across the genome at which we observe significant population divergence are causally involved in the alleviation of antagonism. Instead, the frequency change we observe at most loci is more likely a consequence, rather than the cause, of alleviation. An emergent mechanism of SA resolution would alter the sex-specific fitness effects of antagonistic alleles previously maintained in balanced polymorphism, leading to shifts in frequencies and potentially the fixation of the allele with the greater average fitness across the sexes (Rice 1984; Connallon and Clark 2012; Mullon et al. 2012).

Analyses to identify the causal genetic changes underlying an alleviation of SA and the specific mechanism(s) of resolution that they exploit are beyond the scope of this study. However, with the proviso that most of our candidate genes are associated with antagonism, our results are informative about the genetic basis of SA. Our data suggests an enrichment of loci on the X chromosome, in line with previous theoretical predictions (Rice 1984). It further suggests that the disproportionate contribution of the X chromosome to quantitative genetic variation in fitness previously observed in LH<sub>M</sub>-UCSB (Gibson et al. 2002) is at least in part

due to the number of X-linked antagonistic loci (rather than their phenotypic effects). Our data also provide a first glimpse of genes potentially involved in antagonism. At a general level, the prominent involvement in development of our candidate genes implies that many antagonistic fitness effects may be rooted in anatomical differences between the sexes. This fits with data showing how developmental processes allow the decoupling of male and female phenotypes (Gompel et al. 2005; Roberts et al. 2009; Khila et al. 2012). At the level of individual genes, our candidates include several genes known to be involved in male courtship behavior (*cacophony*, *period* and *Btk family kinase at 29A*) and loci related to sex determination and differentiation (*transformer 2*, *Wnt oncogene analog 2*, *doublesex-Mab related 93B*, *sister-of-Sex-lethal*, and *bric à brac*). While these manual screens are subjective, the presence of such genes raises the intriguing possibility that some of the adaptive trade-offs between males and females are caused by variation close to the top of the sex-specific regulatory cascade.

In conclusion, we have presented data indicating rapid evolutionary change in the genetic basis of fitness and consistent with a partial resolution of antagonism in LH<sub>M</sub>-UCL. Due to the enormous scale of the phenotypic assays that we report, our study only compares two populations and relied on combining existing and new data that were collected at different time-points. While the inclusion of phenotypic results from LH<sub>M</sub>-UCSC and the DGRP for genetic comparison add some depth and directionality, future work will need to expand our approach in order to establish patterns of SA and its resolution on a broader scale. Phenotypic measures will remain a limiting factor in this effort, due to the sheer amount of work they require and—in particular for wild populations—the uncertainty about how to measure fitness in a way that reflects the selection pressures under which such populations have evolved. However, a growing understanding of the genetic basis of SA will provide an interesting parallel avenue for enquiry, where patterns of diversity at antagonistic loci can be compared across populations to gain insights into the evolutionary dynamics of sexual antagonism. Building upon the results presented here, those efforts will allow us to gain a full understanding of the constraints acting on male and female traits and so elucidate the genomic innovations that allow populations to overcome constraints.

#### ACKNOWLEDGMENTS

We thank Chris Wheat and four anonymous reviewers, whose comments greatly improved that quality of our manuscript. We thank Jessica White, Rebecca Finlay, and Anja Schlott for technical assistance with data collection, Adam Chippindale for his input to planning the fitness assays and Steve Chenoweth, Julie Bertrand, Jacqueline Sztepanacz, and Jarrod Hadfield for their assistance with the quantitative genetic analyses. Steve Paterson and Ian Goodhead (Centre for Genomic Research, University of Liverpool) assisted with the initial treatment and quality-control of sequencing data. J.M.C. and S.F. were funded by a NERC research

grant (NE/G019452/1) to M.R. and K.F., J.H. by a BBSRC PhD studentship and MSH by a UCL IMPACT PhD studentship. P.I. and E.H.M. were funded by the Swedish Research Council (2004–2572, 2006–2848, 2008–5533), a European Research Council Grant (#280632) and a Royal Society University Research Fellowship.

#### DATA ARCHIVING

Dryad: doi:10.5061/dryad.18pk7 European Nucleotide Archive: <http://www.ebi.ac.uk/ena/data/view/PRJEB12822>.

#### LITERATURE CITED

- Abbott, J. K., and E. H. Morrow. 2011. Obtaining snapshots of genetic variation using hemiclinal analysis. *Trends Ecol. Evol.* 26:359–368.
- Andolfatto, P. 2005. Adaptive evolution of non-coding DNA in *Drosophila*. *Nature* 437:1149–1152.
- Arnqvist, G., and L. Rowe. 2005. *Sexual conflict*. Princeton Univ. Press, Princeton, NJ.
- Barson, N. J., T. Aykanat, K. Hindar, M. Baranski, G. H. Bolstad, P. Fiske, C. Jacq, A. J. Jensen, S. E. Johnston, S. Karlsson, et al. 2015. Sex-dependent dominance at a single locus maintains variation in age at maturity in salmon. *Nature*, 528:405–408.
- Berg, E. C., and A. A. Maklakov. 2012. Sexes suffer from suboptimal lifespan because of genetic conflict in a seed beetle. *Proc. R Soc. B* 279:4296–4302.
- Betancourt, A. J., J. J. Welch, and B. Charlesworth. 2009. Reduced effectiveness of selection caused by a lack of recombination. *Curr. Biol.* 19:655–660.
- Bonduriansky, R., and S. F. Chenoweth. 2009. Intralocus sexual conflict. *Trends Ecol. Evol.* 24:280–288.
- Brommer, J. E., M. Kirkpatrick, A. Qvarnström, and L. Gustafsson. 2007. The intersexual genetic correlation for lifetime fitness in the wild and its implications for sexual selection. *PLoS One* 2:e744.
- Chapman, T., G. Arnqvist, J. Bangham, and L. Rowe. 2003. Sexual conflict. *Trends Ecol. Evol.* 18:41–47.
- Charlesworth, B., A. J. Betancourt, V. B. Kaiser, and I. Gordo. 2010. Genetic recombination and molecular evolution. *Cold Spring Harb. Symp. Quant. Biol.* 74:177–186.
- Charlesworth, B., J. A. Coyne, and N. H. Barton. 1987. The relative rates of evolution of sex chromosomes and autosomes. *Am. Nat.* 130:113–146.
- Chintapalli, V. R., J. Wang, and J. A. T. Dow. 2007. Using FlyAtlas to identify better *Drosophila melanogaster* models of human disease. *Nat. Genet.* 39:715–720.
- Chippindale, A. K., J. R. Gibson, and W. R. Rice. 2001. Negative genetic correlation for adult fitness between sexes reveals ontogenetic conflict in *Drosophila*. *Proc. Natl. Acad. Sci. USA* 98:1671–1675.
- Connallon, T., and A. G. Clark. 2011. The resolution of sexual antagonism by gene duplication. *Genetics* 187:919–937.
- . 2012. A general population genetic framework for antagonistic selection that accounts for demography and recurrent mutation. *Genetics* 190:1477–1489.
- . 2014. Evolutionary inevitability of sexual antagonism. *Proc. R Soc. B* 281:20132123.
- Cox, R. M., and R. Calsbeek. 2009. Sexually antagonistic selection, sexual dimorphism, and the resolution of intralocus sexual conflict. *Am. Nat.* 173:176–187.
- Day, T., and R. Bonduriansky. 2004. Intralocus sexual conflict can drive the evolution of genomic imprinting. *Genetics* 167:1537–1546.
- Dean, R., J. C. Perry, T. Pizzari, J. E. Mank, and S. Wigby. 2012. Experimental evolution of a novel sexually antagonistic allele. *PLoS Genet.* 8:e1002917.
- Debelle, A., M. G. Ritchie, and R. R. Snook. 2014. Evolution of divergent female mating preference in response to experimental sexual selection. *Evolution* 68:2524–2533.
- Delcourt, M., M. W. Blows, and H. D. Rundle. 2009. Sexually antagonistic genetic variance for fitness in an ancestral and a novel environment. *Proc. R Soc. B* 276:2009–2014.
- Delph, L. F., J. Andicoechea, J. C. Steven, C. R. Herlihy, S. V. Scarpino, and D. L. Bell. 2011. Environment-dependent intralocus sexual conflict in a dioecious plant. *N. Phytol.* 192:542–552.
- Ellegren, H., and J. Parsch. 2007. The evolution of sex-biased genes and sex-biased gene expression. *Nat. Rev. Genet.* 8:689–698.
- Fabian, D. K., M. Kapun, V. Nolte, R. Kofler, P. S. Schmidt, C. Schlotterer, and T. Flatt. 2012. Genome-wide patterns of latitudinal differentiation among populations of *Drosophila melanogaster* from North America. *Mol. Ecol.* 21:4748–4769.
- Fedorka, K. M., and T. A. Mousseau. 2004. Female mating bias results in conflicting sex-specific offspring fitness. *Nature* 429:65–67.
- Foerster, K., T. Coulson, B. C. Sheldon, J. M. Pemberton, T. H. Clutton-Brock, and L. E. B. Kruuk. 2007. Sexually antagonistic genetic variation for fitness in red deer. *Nature* 447:1107–1110.
- Gavrilets, S. 2000. Rapid evolution of reproductive barriers driven by sexual conflict. *Nature* 403:886–889.
- Gavrilets, S., and W. R. Rice. 2006. Genetic models of homosexuality: generating testable predictions. *P R Soc B* 273:3031–3038.
- Gibson, J. R., A. K. Chippindale, and W. R. Rice. 2002. The X chromosome is a hot spot for sexually antagonistic fitness variation. *Proc. R. Soc. Lond. B* 269:499–505.
- Gnad, F., and J. Parsch. 2006. Sebida: a database for the functional and evolutionary analysis of genes with sex-biased expression. *Bioinformatics* 22:2577–2579.
- Gompel, N., B. Prud'homme, P. J. Wittkopp, V. A. Kassner, and S. B. Carroll. 2005. Chance caught on the wing: cis-regulatory evolution and the origin of pigment patterns in *Drosophila*. *Nature* 433:481–487.
- Haddrill, P. R., D. L. Halligan, D. Tomaras, and B. Charlesworth. 2007. Reduced efficacy of selection in regions of the *Drosophila* genome that lack crossing over. *Genome Biol.* 8:R18.
- Haddrill, P. R., L. Loewe, and B. Charlesworth. 2010. Estimating the parameters of selection on nonsynonymous mutations in *Drosophila pseudoobscura* and *D. miranda*. *Genetics* 185:1381–1396.
- Hesketh, J., K. Fowler, and M. Reuter. 2013. Genetic drift in antagonistic genes leads to divergence in sex-specific fitness between experimental populations of *Drosophila melanogaster*. *Evolution* 67:1503–1510.
- Houle, D., and K. Meyer. 2015. Estimating sampling error of evolutionary statistics based on genetic covariance matrices using maximum likelihood. *J. Evol. Biol.* 28:1542–1549.
- Huang, D. W., B. T. Sherman, and R. A. Lempicki. 2009a. Bioinformatics enrichment tools: paths toward the comprehensive functional analysis of large gene lists. *Nucleic Acids Res.* 37:1–13.
- . 2009b. Systematic and integrative analysis of large gene lists using DAVID bioinformatics resources. *Nat. Protoc.* 4:44–57.
- Huang, W., A. Massouras, Y. Inoue, J. Peiffer, M. Ramia, A. M. Tarone, L. Turlapati, T. Zichner, D. H. Zhu, R. F. Lyman, et al. 2014. Natural variation in genome architecture among 205 *Drosophila melanogaster* Genetic Reference Panel lines. *Genome Res.* 24:1193–1208.
- Innocenti, P., and E. H. Morrow. 2010. The sexually antagonistic genes of *Drosophila melanogaster*. *PLoS Biol.* 8:e1000335.
- Iwasa, Y., and A. Pomiankowski. 1999. Sex specific X chromosome expression caused by genomic imprinting. *J. Theor. Biol.* 197:487–495.
- . 2001. The evolution of X-linked genomic imprinting. *Genetics* 158:1801–1809.

- Jensen, M. A., B. Charlesworth, and M. Kreitman. 2002. Patterns of genetic variation at a chromosome 4 locus of *Drosophila melanogaster* and *D. simulans*. *Genetics* 160:493–507.
- Kapun, M., H. Van Schalkwyk, B. McAllister, T. Flatt, and C. Schlotterer. 2014. Inference of chromosomal inversion dynamics from Pool-Seq data in natural and laboratory populations of *Drosophila melanogaster*. *Mol. Ecol.* 23:1813–1827.
- Khila, A., E. Abouheif, and L. Rowe. 2012. Function, developmental genetics, and fitness consequences of a sexually antagonistic trait. *Science* 336:585–589.
- Kidwell, J. F., M. T. Clegg, F. M. Stewart, and T. Prout. 1977. Regions of stable equilibria for models of differential selection in 2 sexes under random mating. *Genetics* 85:171–183.
- Kofler, R., P. Orozco-terWengel, N. De Maio, R. V. Pandey, V. Nolte, A. Futschik, C. Kosiol, and C. Schlotterer. 2011a. PoPoolation: a toolbox for population genetic analysis of next generation sequencing data from pooled individuals. *PLoS One* 6:e15925.
- Kofler, R., R. V. Pandey, and C. Schlotterer. 2011b. PoPoolation2: identifying differentiation between populations using sequencing of pooled DNA samples (Pool-Seq). *Bioinformatics* 27:3435–3436.
- Kohorn, L. U. 1994. Shoot morphology and reproduction in Jojoba—advantages of sexual dimorphism. *Ecology* 75:2384–2394.
- Lande, R. 1980. Sexual dimorphism, sexual selection and adaptation in polygenic characters. *Evolution* 34:292–305.
- Lewis, Z., N. Wedell, and J. Hunt. 2011. Evidence for strong intralocus sexual conflict in the Indian meal moth, *Plodia interpunctella*. *Evolution* 65:2085–2097.
- Long, T. A. F., A. F. Agrawal, and L. Rowe. 2012. The effect of sexual selection on offspring fitness depends on the nature of genetic variation. *Curr. Biol.* 22:204–208.
- Lynch, M., and B. Walsh. 1998. *Genetics and analysis of quantitative traits*. Sinauer, Sunderland, MA.
- Mackay, T. F. C., S. Richards, E. A. Stone, A. Barbadilla, J. F. Ayroles, D. H. Zhu, S. Casillas, Y. Han, M. M. Magwire, J. M. Cridland, et al. 2012. The *Drosophila melanogaster* genetic reference panel. *Nature* 482:173–178.
- Mainguy, J., S. D. Cote, M. Festa-Bianchet, and D. W. Coltman. 2009. Father-offspring phenotypic correlations suggest intralocus sexual conflict for a fitness-linked trait in a wild sexually dimorphic mammal. *P R Soc B* 276:4067–4075.
- Mank, J. E., B. Vicoso, S. Berlin, and B. Charlesworth. 2010. Effective population size and the faster-X effect: empirical results and their interpretation. *Evolution* 64:663–674.
- Martin, O. Y., and D. J. Hosken. 2003. The evolution of reproductive isolation through sexual conflict. *Nature* 423:979–982.
- McDonald, J. H., and M. Kreitman. 1991. Adaptive protein evolution at the *Adh* locus in *Drosophila*. *Nature* 351:652–654.
- McLaren, W., B. Pritchard, D. Rios, Y. A. Chen, P. Flicek, and F. Cunningham. 2010. Deriving the consequences of genomic variants with the Ensembl API and SNP effect predictor. *Bioinformatics* 26:2069–2070.
- Meyer, K. 1991. Estimating variances and covariances for multivariate animal models by restricted maximum likelihood. *Genet. Sel. Evol.* 23:67–83.
- . 2007. WOMBAT—a tool for mixed model analyses in quantitative genetics by restricted maximum likelihood (REML). *J. Zhejiang Univ. Sci. B* 8:815–821.
- Meyer, K., and D. Houle. 2013. Sampling based approximation of confidence intervals for functions of genetic covariance matrices. *Proc. Assoc. Adv. Anim. Breed* 20:523–527.
- Mokkonen, M., H. Kokko, E. Koskela, J. Lehtonen, T. Mappes, H. Martiskainen, and S. C. Mills. 2011. Negative frequency-dependent selection of sexually antagonistic alleles in *Myodes glareolus*. *Science* 334:972–974.
- Mullon, C., A. Pomiankowski, and M. Reuter. 2012. The effects of selection and genetic drift on the genomic distribution of sexually antagonistic alleles. *Evolution* 66:3743–3753.
- Parsch, J., and H. Ellegren. 2013. The evolutionary causes and consequences of sex-biased gene expression. *Nat. Rev. Genet.* 14:83–87.
- Pennell, T. M., and E. H. Morrow. 2013. Two sexes, one genome: the evolutionary dynamics of intralocus sexual conflict. *Ecol. Evol.* 3:1819–1834.
- Pischedda, A., and A. K. Chippindale. 2006. Intralocus sexual conflict diminishes the benefits of sexual selection. *PLoS Biol.* 4:2099–2103.
- Pischedda, A., and W. R. Rice. 2012. Partitioning sexual selection into its mating success and fertilization success components. *Proc. Natl. Acad. Sci. USA* 109:2049–2053.
- Punzalan, D., M. Delcourt, and H. D. Rundle. 2014. Comparing the intersex genetic correlation for fitness across novel environments in the fruit fly, *Drosophila serrata*. *Heredity* 112:143–148.
- Rice, W. R. 1984. Sex chromosomes and the evolution of sexual dimorphism. *Evolution* 38:735–742.
- . 1992. Sexually antagonistic genes: experimental evidence. *Science* 256:1436–1439.
- Rice, W. R., and B. Holland. 1997. The enemies within: intergenomic conflict, interlocus contest evolution (ICE), and the intraspecific Red Queen. *Behav. Ecol. Sociobiol.* 41:1–10.
- Rice, W. R., J. E. Linder, U. Friberg, T. A. Lew, E. H. Morrow, and A. D. Stewart. 2005. Inter-locus antagonistic coevolution as an engine of speciation: assessment with hemiclinal analysis. *Proc. Natl. Acad. Sci. USA* 102:6527–6534.
- Roberts, R. B., J. R. Ser, and T. D. Kocher. 2009. Sexual conflict resolved by invasion of a novel sex determiner in Lake Malawi cichlid fishes. *Science* 326:998–1001.
- Scotti, I., and L. F. Delph. 2006. Selective trade-offs and sex-chromosome evolution in *Silene latifolia*. *Evolution* 60:1793–1800.
- Smit, A. F. A., R. Hubley, and P. Green. 2013–2015. RepeatMasker Open-4.0. <http://www.repeatmasker.org>.
- Smith, N. G. C., and A. Eyre-Walker. 2002. Adaptive protein evolution in *Drosophila*. *Nature* 415:1022–1024.
- Stewart, A. D., A. Pischedda, and W. R. Rice. 2010. Resolving intralocus sexual conflict: genetic mechanisms and time frame. *J. Hered.* 101:S94–S99.
- Van Doorn, G. S. 2009. Intralocus sexual conflict. *Ann. NY Acad. Sci.* 1168:52–71.
- Vicoso, B., and B. Charlesworth. 2009. Effective population size and the faster-X effect: an extended model. *Evolution* 63:2413–2426.
- Vincent, C. M., and N. P. Sharp. 2014. Sexual antagonism for resistance and tolerance to infection in *Drosophila melanogaster*. *P R Soc. B* 281:20140987.
- Wei, Z., W. Wang, P. Z. Hu, G. J. Lyon, and H. Hakonarson. 2011. SNVer: a statistical tool for variant calling in analysis of pooled or individual next-generation sequencing data. *Nucleic Acids Res.* 39:e132.

Associate Editor: C. Wheat  
Handling Editor: R. Shaw

## Supporting Information

Additional Supporting Information may be found in the online version of this article at the publisher's website:

**Table S1.** ANOVA tables for analyses of fitness across laboratories.

**Table S2.** Basic information on sequencing data from LH<sub>M</sub>-UU and LH<sub>M</sub>-UCL.

**Table S3.** Chromosomal distribution of SNP loci.

**Table S4.** Inversion markers in LH<sub>M</sub>-UU and LH<sub>M</sub>-UCL.

**Table S5.** Results of a Gene Ontology analysis on genes with candidate SNPs.

**Table S6.** Results of a clustering analysis of Gene Ontology terms associated with candidate genes.

**Figure S1.** Male and female adult fitness across genotypes in the LH<sub>M</sub>-UU population.

**Figure S2.** Relationship between fitness measures obtained across laboratories.

**Figure S3.** Difference in genetic polymorphism between LH<sub>M</sub>-UU and LH<sub>M</sub>-UCL.

**Figure S4.**  $F_{ST}$  at SNP loci along chromosome arms.

**Figure S5.** Distribution of  $F_{ST}$  among SNP loci.

**Figure S6.** Distribution of distances between neighbouring candidate SNPs.

## Appendix C

# Evolving plastic responses to external and genetic environments

This appendix contains a copy of a Forum article published in Trends in Genetics. I contributed to discussion of ideas and writing of the paper. The piece describes a recent study by Yi and Dean (2016) where the authors show how phenotypic plasticity arises in a bacterial system. We used this Forum article to make a conceptual link between the evolution of plasticity in response to adaptive trade-offs imposed by fluctuating environments and the evolution of sexual dimorphism in response to contrasting sex-specific selection pressures. Furthermore, we highlighted the potential for antagonistic variation to arise across environments, just as sexual antagonism can result from sex-specific selection.